https://ntrs.nasa.gov/search.jsp?R=19760025490 2020-03-22T13:37:28+00:00Z

A-139339
ASL-1

NASA CR-135036

1

DO NOT DESTROY
RETURN TO LIBRARY

PROOF TEST CRITERIA FOR THIN-WALLED 2219 ALUMINUM PRESSURE VESSELS

VOLUME I - PROGRAM SUMMARY AND DATA ANALYSIS

By
R. W. Finger

THE BOEING AEROSPACE COMPANY

Prepared For
NATIONAL AERONAUTICS AND SPACE ADMINISTRATION

8 OCT 1976
MCDONNELL DOUGLAS
RESEARCH & ENGINEERING LIBRARY
ST. LOUIS

NASA Lewis Research Center
Contract NAS3-18906
Gordon T. Smith, Project Manager

NASA-CR-135036

M76-16301

1. Report No	2. Government Accession No.	3. Recipient's Catalog No.
NASA CR-135036		

4. Title and Subtitle	5. Report Date
Proof Test Criteria For Thin Walled 2219 Aluminum Pressure Vessels Volume I - Program Summary and Data Analysis	August 1976
	6. Performing Organization Code
7. Author(s) R. W. Finger	8. Performing Organization Report No D180-20100-2
	10. Work Unit No.
9. Performing Organization Name and Address Boeing Aerospace Company Research and Engineering Division P. O. Box 3994 Seattle, Washington 98124	11. Contract or Grant No. NAS3-18906
12. Sponsoring Agency Name and Address National Aeronautics and Space Administration Lewis Research Center 21000 Brookpark Road Cleveland, Ohio 44135	13. Type of Report and Period Covered Contractor Report July 1974 - through Dec. 1975
	14. Sponsoring Agency Code

15. Supplementary Notes

Project Manager, Gordon T. Smith
Materials and Structures Division
NASA-LEWIS Research Center
Cleveland, Ohio 44135

16. Abstract

This experimental program was undertaken to investigate the crack growth behavior of deep surface flaws in 2219 aluminum. The program included tests of uniaxially loaded surface flaw and center crack panels at temperatures ranging from 20K (-423°F) to ambient. The tests were conducted on both the base metal and as-welded weld metal material. The program was designed to provide data on the mechanisms of failure by ligament penetration, and the residual cyclic life, after proof-testing, of a vessel which has been subjected to incipient penetration by the proof test. The results were compared and analyzed with previously developed data to develop guidelines for the proof testing of thin walled 2219 pressure vessels.

17. Key Words (Suggested by Author(s))		18. Distribution Statement
Surface Flow	Cyclic Flaw Growth	Unclassified, Unlimited
2219 Aluminum	Pressure Vessels	
Fracture Control	Stress Intensity	
Proof Testing	Crack Opening Displacement	

19. Security Classif. (of this report)	20. Security Classif. (of this page)	21. No. of Pages	22. Price*
Unclassified	Unclassified		

* For sale by the National Technical Information Service, Springfield, Virginia 22151

NASA-C-168 (Rev 6-71)

FOREWORD

This report describes an investigation of the flaw growth behavior, during proof testing, and the subsequent cyclic crack growth characteristics of deep surface flaws in the 2219-T87 aluminum alloy performed by the Boeing Aerospace Company from July 1974 through September 1975. The work was administered by Mr. Gordon T. Smith of the NASA-Lewis Research Center.

This program was conducted by the Research and Engineering Division of the Boeing Aerosapce Company, Seattle, Washington, under the supervision of Mr. H. W. Klopfenstein, Structures Research and Development Manager. The Program Leader was Mr. J. N. Masters, Supervisor, Failure Mechanisms Group. The Technical Leader was R. W. Finger; A. A. Ottlyk and H. M. Olden provided testing engineering support, and G. Buehler produced the technical illustration and art work. This technical report is also released as Boeing Document D180-20100-1.

TABLE OF CONTENTS

LIST OF FIGURES

LIST OF FIGURES (Cont.)

LIST OF FIGURES (Cont.)

LIST OF FIGURES (Cont.)

LIST OF TABLES

LIST OF TABLES (Cont.)

LIST OF TABLES (Cont.)

1.0 INTRODUCTION

A very high degree of reliability is essential for aerospace structures; therefore, much effort has been expended in developing analytical and experimental procedures for definition and better understanding of the associated fracture problem. Experience has shown the semi-elliptical surface flaw to be a realistic representation of common failure origins. Accordingly, this surface flaw model has been used extensively in the development of both the analytical procedures and experimental data for a description of the tank wall failure processes.

Initially the work was directed toward understanding the catastrophic (burst) failure problem. This situation occurs when the critical defect depth is less than the wall thickness; resulting in a failure mode which is fracture rather than a leak producing wall penetration. These studies have developed around the stress intensity factor solution for a semi-elliptical flaw in a finite thickness plate which was initially presented by Irwin. Multiplicative coefficients which are functions of the crack depth-to-thickness ratio and the crack depth-to-surface length ratio have been derived analytically and defined experimentally to extend the basic two-dimensional Green-Sneddon solution for an elliptical crack in an infinite solid to finite wall thicknesses representative of practical aerospace pressure vessel applications. Irwin estimated his original solution to be valid for surface flaws with depth to thickness ratios, a/t, of less than 0.5. Subsequent analytical and experimental efforts (1 through 7)* have provided "magnification factor" coefficients which extend the useability by accounting for effects of the stress free rear surface boundary condition and for limited plasticity about the crack tip. These developments were incorporated into a design methodology (8) which provided a well defined basis for utilizing nondestructive inspection and proof testing methods to verify that the design life could be realized in service operations.

Having recognized the factors causing failures of aerospace hardware, a gradual but marked change in design philosophy has occurred. The most prominent feature of this change has been the development and selection of materials which exhibit a high level of tolerance to crack-like defects inherent in either the raw material or manufacturing processes. An excellent example of this was the selection of 2219 aluminum, rather than the higher strength of 2014 aluminum alloy, for many of the space shuttle components.

---

* Numbers in parentheses refer to references at the end of the report.

The use of flaw tolerant materials does present some unique problems. These problems are a consequence of the defect size, which will cause failure (burst) during proof testing, being greater than the wall thickness. The procedures developed for assuring the service lives of vessels produced from brittle material are no longer directly applicable. Although the procedures for minimizing the chances of service failure are available for the "brittle" vessels, the probability of costly proof test failures and resultant schedule problems was sufficient impetus to cause the selection of the more flaw tolerant alloy. Although the selection of flaw tolerant materials could virtually eliminate the possibility of a catastrophic failure, deep flaws which survived the proof test cycle could grow through the thickness during service, thereby compromising mission objectives or possibly causing a total loss of the mission.

This program was directed toward developing a better understanding of the effect of proof testing a thin walled tank. The program was divided into two sections; the first was directed at determining the crack growth behavior of surface flaws during the application of a simulated proof test cycle, and the second was designed to evaluate the use of a proof test cycle in assuring subsequent service life. The program was an experimental effort which employed specimens fabricated from 2219-T87 aluminum - both base and weld metal. A variety of different surface flaw shapes were tested at temperatures ranging from $20^{o}K$ ($-423^{o}F$) to room temperature in specimen thicknesses from 3.18 mm to 9.53 mm (0.125 to 0.375 in).

The following sections of the report present a brief review of related background data, a description of the materials and experimental procedures, and a discussion of the results and a summary of the significant conclusions. Applicable data from other studies are incorporated into the analysis of the results.

2.0 BACKGROUND

Significant progress had been made in developing procedures for handling the shallow flaw problem when experimental work strictly devoted to the deep flaw problem was initiated in 1967. This work, published in Reference 1, involved static and cyclic tests of thick and thin gages of material, using a variety of different flaw shapes in order to bracket the problem. The resulting data were used to empirically derive deep flaw magnification terms to be applied to Irwin's surface flaw stress intensity solution. Instrumentation for determining whether breakthrough had occurred prior to fracture was not available during this program, although it was suspected that such behavior had occurred and influenced the results.

A subsequent experimental program (9) was undertaken to further explore the static and cyclic behavior of combinations of flaw depth, flaw shapes and thicknesses through that range where failure mode changed from "catastrophic failure" to leak-before-failure. Instrumentation was added to detect flaw breakthrough (leakage) prior to failure. The results from this program were used to establish the empirical formula

$$t - a = 0.10\ (K_{IE}/\sigma_{ys})^2 \qquad (1)$$

t = thickness
a = flaw depth

for determining the point where the failure mode changes from fracture to leak-before-fracture. Additionally, the results of this study indicated that K_{IE} values obtained from any of three available deep flaw solutions (1, 2, 3) can be used to describe fracture stress/flaw size loci for a wide range of thicknesses, flaw shapes, alloys, and stress loads. These ranges were:

a) - maximum failing stresses of about 0.90 σ_{ys}
b) - minimum thickness of about 0.25 $(K_{IE}/\sigma_{ys})^2$;
c) - ligament size greater than about 0.10 $(K_{IE}/\sigma_{ys})^2$;

For ligaments less than this value, leakage prior to failure would be expected. Final fracture strength is dependent on flaw length and the appropriate through crack toughness, K_{CN}.

Initial studies (1, 9, 10) had established that significant crack growth can occur during loading and had also determined the range of applicability of the available stress intensity solutions in determining the fracture stress/flaw size loci. Additionally, a criteria was presented to be used in determining the point at which the failure mode changes from fracture to leak-before-fracture. The primary emphasis of the initial studies was the fracture and cyclic flaw growth of aluminum and titanium base metal specimens.

A subsequent study, Reference 11, was performed to evaluate weldment flaw growth and fracture characteristics. 2219-T87 aluminum as-welded weldments and 6Al-4V STA titanium weldments were tested at room and cryogenic temperatures and on several thicknesses. K_{IE} values (for gross stress levels less than yield) were obtained only on the thicker/lower temperature combinations of the titanium specimens. Leakage occurred on several of these tests and substantiated the ligament restrictions developed in Reference 9. Validity of the ligament restriction could not be evaluated on the aluminum weldment tests because the surface flaw toughness is higher than can be measured in the thicknesses of interest. As expected, fracture prior to leakage was not observed except with small flaws which caused fracture well in excess of yield strength.

Cyclic tests on both proof loaded and non-proof loaded specimens were conducted under the Reference 11 study. Three major observations resulted from the analysis of the cyclic test data:

A) Cyclic lives of proof tested specimens always equalled or exceeded the lives of unproofed specimens. Although significant growth occurred during the proof loading, the subsequent cyclic growth was retarded due to the proof overload, and the resultant cyclic life was not adversely affected by the prior proof cycle.

B) The cyclic lives of the specimens increased with increasing initial flaw shape ratio (a/2c). For specimens of equal criticality (leakage) at proof, the stress intensity associated with the cyclic loading is less for the rounder flaws; therefore, the growth rate will be less and their subsequent cyclic life greater.

C) In tests of several dozen specimens which were proof tested to a point as close as possible to leakage, measurable subsequent cyclic life (at stresses of 85 percent of the proof stress) was realized. This observation was significant in that it provided confidence that safe life can be assured by proof testing of thin walled tankage fabricated from high toughness materials.

In addition to the published results presented above, a considerable amount of data has been generated at the Boeing Aerospace Company pertinent to the subcritical crack growth of surface flaws in 2219-T87 aluminum (base and weld metal) specimens. The key observations of the preceding discussion and the unpublished Boeing work pertinent to the subject report are:

- The failure stress-flaw size loci for surface flaw specimens can be divided into one or more of three regions,
  - Region I - inelastic range ($\sigma \geq 0.90\ \sigma_{ys}$)
  - Region II - elastic fracture
  - Region III - leakage prior to fracture.
- A complete description of the failure locus in Region I is not yet available; however, it appears that the failure locus lies along a relatively straight line extending from ultimate strength at zero flaw size to the point at about 0.90 σ_{ys}, where Region II begins.
- Region II can be described using available surface flaw stress intensity solutions (which account for a/t effects) up to the point where the initial ligament (t-a) is less than about 0.10 $(K_{IE}/\sigma_{ys})^2$, whereupon Region III begins.
- Final fracture strength in Region III can be described by consideration of original surface flaw length and the thru-crack toughness, K_{CN}, of the material (see Section 4.4 for K_{CN} calculation).
- There is very little stable flaw growth data available with which to perform in-depth resistance curve studies on surface flaws. Limited data which has been generated suggests that the resistance curve approach to analysis may prove to be quite useful.

- Flaw growth "damage" occurring during proof testing appears to be more than compensated for by subsequent retarded flaw growth rates.
- For equally critical long and short flaws surviving a given proof cycle, the long flaw has the shortest subsequent cyclic life.
- Considerable data is available to suggest that safe life (without leakage) can be assured by proper selection of relative proof and operating stress ratios.

The above points had a significant influence on the design of the experimental program reported herein. The results of this program are used to expand upon or modify several of the above points. These discussions are presented in the "discussion of results" section of this report.

3.0 MATERIALS

The test specimens were fabricated from 2219-T87 aluminum sheet and plate. The sheet material, 6.35 x 1219 x 2438 mm (0.25 x 48 x 96 in), was originally purchased for NAS3-17764 (Effect of Thermal Profile on Cyclic Flaw Growth in Aluminum) per Boeing Specification BMS7-105C (equivalent to Military Specification MIL-A-8920A). The plate material, 12.7 x 1219 x 3658 mm (0.50 x 48 x 144 in), was also purchased per Boeing Specification BMS 7-105C. The specification chemical compositions are presented in Table 1.

Welding was accomplished using a direct current straight polarity (DCSP) gas tungsten arc (GTA) welding process. A Merrick Power Supply and a Sciaky Boom Manipulator were used for the welding. The plate material was used to produce 12.7 mm (0.50 in) thick weld panels and the sheet was used to produce the 6.35 mm (0.25 in) panels. Weld wire (2319) was required on the 6.35 mm (0.25 in) panels only. The panel halves were prepared with a square butt edge preparation, then cleaned per BAC5765, wrapped and held for welding. Immediately prior to welding, the top and bottom surfaces, 1.0 inch back from the edges, were cleaned with a Scotch-Brite rotary wheel and the faying surfaces were hand-scraped to remove surface oxides. The weld panel halves were aligned on a hold-down tool and manually tack welded. Welding was then accomplished using the following parameters.

<u>0.50 in. Thick 2219-T87 Aluminum Panels</u>

Gas Tungsten Arc Weld, Square Butt, Two Pass (one per side)

<u>Pass #1 and #2</u>

Travel Speed - 127 mm/min (5 in/min)

Voltage - 13.5

Amperage - 245

Torch Gas - Helium at 2.5 m^3/hr (90 ft^3/hr)

Backup Gas - None used

Backup Bar - None used

Hold-Down Bar - None used - Panels restrained on outer edges (6 places)

Electrode 3.18 mm (0.125 in) diameter - 2% Thoriated

0.25 in Thick 2219-T87 Aluminum Panels

Gas Tungsten Arc Weld, Square Butt, Two Pass from One Side

Pass #1

Travel Speed - 180 mm/min (7 in/min)

Voltage - 13.2

Amperage - 195

Wire Speed - 500 mm/min

Torch Gas - Helium at 2.5 m^3/hr (90 ft^3/hr)

Backup Gas - None

Backup Bar - Copper

Hold-Down Bars - Copper, spaced 6.4 mm (0.25 in) each side of weld centerline

Electrode - 3.18 mm (0.125 in) diameter, 2% Thoriated

Pass #2

Travel - 180 mm/min (7 in/min)

Voltage - 15.4

Amperage - 180

Wire Speed - 635 mm/min (25 in/min)

Torch Gas - Helium at 2.5 m^3/hr (90 ft^3/hr)

Backup Gas - None

Backup Bar - Copper

Hold-Down Bars - Copper, spaced 6.4 mm (0.25 in) each

Electrode - 3.18 mm (0.125 in) diameter, 2% Thoriated.

NOTE: Amperage and voltage figures were measured through a calibrated 500 amp 50 MV shunt. Readout was made using a Fluke Differential Voltimeter; voltage figures were measured at the Merrick Control Unit.

After welding, all of the weldments were x-rayed to Boeing BAC 5935 Class A acceptance criteria. Areas in the weldments which did not meet the BAC 5935 Class A specifications were marked on the panels so they could be avoided during specimen fabrication.

4.0 PROCEDURES

4.1 Specimen Fabrication

The test specimens were machined using conventional milling techniques per the configuration presented in Figures 1 through 4. The specimen configurations were selected such that the test section widths would be sufficient to preclude any width effects. The specimens having a test section thickness of 9.53 mm (0.375 in) were machined from either the plate stock or the 12.7 mm (0.50 in) thick weld panels. The other specimens were machined from the 6.35 mm (0.25 in) sheet or weld panels. All of the specimens were removed from the parent material so that the loading would be applied perpendicular to the weld and/or rolling direction.

Fatigue crack starter slots were introduced into both the center crack and surface flaw specimens by Electric Discharge Machining (EDMing). The EDM electrodes were machined from 1.5 mm (0.06 in) packanite sheet. The starter slots terminated in a 30° included angle and a 0.08 mm (0.003 in) root radius. Low stress cyclic fatigue was used to produce fatigue cracks at the root of the starter slots. All of the surface flaw specimens having the same flaw size were precracked at the same stress level and cyclic frequency. The precracking frequency was 30 Hz for the center crack specimen, but varied from 15 to 30 Hz for the surface flawed specimens. The maximum stress level used for precracking the center crack specimens was 110 MN/m^2 (16 ksi) and 90 MN/m^2 (13 ksi) for the base and weld metal specimens, respectively. For the surface flawed specimens the maximum precracking stress levels were 83 MN/m^2 (12 ksi) and 70 MN/m^2 (10 ksi) for the base and weld metal, respectively. In general, 10,000 cycles were sufficient to produce the desired precrack. The precrack operation was monitored visually with the aid of a 30 power microscope.

4.2 Testing

During the course of the experimental program, three distinctly different types of tests were conducted (load/unload, fracture, cyclic). The load/unload tests consisted of monotonically loading to a predetermined load in approximately one minute and then unloading rapidly. The hold time at maximum load was essentially zero and the unloading time was generally less than

15 seconds. Fracture tests consisted of monotonically loading a specimen until it had fractured. The loading rate for the fracture tests was programmed so that fracture would occur in one to two minutes. Cyclic tests were conducted at room temperature and 78°K (-320°F) at a cyclic frequency of 60 or 1 cpm. The 60 cpm tests employed a sinusoidal loading profile, whereas the 1 cpm loading sequence was an equally segmented trapezoidal profile having 15 second rise, fall and hold (at maximum and minimum load) times. The 20°K (-423°F) cyclic tests employed either a 3 cpm sinusoidal profile or the 1 cpm trapezoidal profile. In all of the cyclic tests the minimum load was approximately zero; therefore, all of the cyclic test results are for an R ratio of zero. The cryogenic temperatures were maintained by surrounding the entire test section with either liquid nitrogen or liquid hydrogen. The liquid hydrogen level was monitored by liquid level sensors inside the cryostat. The fluid level within the liquid nitrogen cryostat was monitored visually. The minimum soak time of 30 minutes, after the entire test section had been covered, was used in all of the cryogenic tests.

4.3 Instrumentation

An Electrical Deflection Indicator (EDI) clip gage was used on all specimens, both center cracked and surface flawed, in order that a continuous record of crack opening displacement could be obtained. Additionally, the surface flaw specimens were equipped with pressure cups for determination of breakthrough (i.e., the flaw penetrating through the rear surface) and the center crack panels had crack propagation gages (CPG). The CPG gages (Type TK-090CPC03-003) consist of 20 parallel grid lines spaced at 2.03 mm (0.08 in) in a 39.6 x 19.1 mm (1.56 x 0.75 in) frame. Crack propagation through a grid line results in the failure of that line and is denoted by a stepwise change in resistance of the gage. The stress crack length relationship can be obtained by recording load versus gage resistance on an X-Y plotter. For determination of crack breakthrough, pressure cups are placed symmetrically on the specimen, one directly over and one behind the flaw. The front cup (i.e., the one over the flaw) is pressurized with helium and the pressure in the rear cup is plotted versus the applied load on an X-Y plotter. Breakthrough is denoted by an abrupt increase in pressure in the rear cup. Immediately prior to the application of any load, the rear cup is vented so that any pressure differential can be relieved. This is especially important for the cryogenic tests since a slight vacuum exists in the rear cup as a result of the cooldown cycle. Failure to vent the cup could therefore result in an erroneous breakthrough indication from seal leakage. The crack opening displacement gage was attached to the specimen by spring loading the gage arms against knife edges as illustrated in Figure 5. Integrally machined knife edges were used on the two thicker gages tested and the clip gage brackets were used for the remaining 6.35 mm (0.125 in) thick specimens. During fracture or load/unload testing, the crack opening displacement was recorded versus load on an X-Y plotter. For the cyclic tests, the COD was recorded versus time on a strip chart recorder.

The determination of the flaw dimensions were made directly from the fracture faces. The measurements were made with the aid of a 30 power microscope and polarized light. A load sequence technique was employed throughout the experimental portion of the program so that the flaw size measurements could be made from the fracture faces. The crack opening displacement records were used as guidelines and to provide further substantiation of the visual measurements.

4.4 Stress Intensity Solutions

Surface Flawed Specimens

The surface flaw stress intensity values reported in the tables were calculated using the Irwin Surface Flaw equation presented in Reference 7, modified with the deep flaw magnification term presented in Reference 1. The resulting equation is:

$$K_I = 1.1\ (\pi a/Q)^{1/2}\ M_K \sigma \qquad (2)$$

where K_I = surface flaw stress intensity at maximum flaw depth

σ = applied gross area stress

a = maximum flaw depth

Q = shape parameter (presented in Figure 6)

M_K = deep flaw magnification factor (presented in Figure 7)

Center Cracked Stress Intensity

The stress intensity values presented for the center crack specimens were calculated using the following formula:

$$K_{CN} = Y \frac{P(c)^{1/2}}{BW} \tag{3}$$

where K_{CN} = stress intensity

P = maximum load

c = one half the total initial crack length (2c)

B = specimen thickness

W = specimen width

Y = width correction factor presented in Figure 8 (from Reference 12).

5.0 RESULTS AND DISCUSSION

5.1 Mechanical Property Tests

The tensile properties of the 2219-T87 aluminum alloy, both parent and weld metal, are presented in Tables 2 and 4. The tests were conducted at room temperature, $75^{\circ}K$ ($-320^{\circ}F$) and $20^{\circ}K$ ($-423^{\circ}F$). The effect of temperature on yield strength, ultimate strength, Poisson's Ratio and elongation are presented in Figures 9, 10 and 11. The uniaxial yield strength values reported were calculated using the 0.2% offset method. A 50.8 mm (2.00 inch) gage length was used in determining the yield strength.

Poisson's Ratio was determined from continuous strain gage recordings of both longitudinal strain (E_L) and transverse strain (E_T). The elastic Poisson's Ratios were then calculated using the following formula:

$$\mu = \frac{dE_T}{dP} \div \frac{dE_L}{dP} \qquad (4)$$

where μ is Poisson's Ratio and P is the load.

5.2 Center Crack Panel Tests

Static fracture tests were conducted on center crack panels at room temperature, $75^{\circ}K$ ($-320^{\circ}F$) and $20^{\circ}K$ ($-423^{\circ}F$). All the specimens were monotonically loaded to failure in approximately one minute. The results of these tests have been summarized and are presented in Tables 5 through 12. All of the specimens were instrumented to provide a continuous record of both the crack opening displacement (COD) and crack length. The crack opening displacement record was obtained from an EDI clip gage. Crack propagation gages were used to monitor the crack length of each specimen.

Although crack propagation gages were applied to all of the specimens, valid outputs were not obtained from the weld metal specimens. This was a consequence of the extremely low yield strength of the weld nugget. The gages are capable of withstanding a 1.5% strain; for the weld nugget this only represents a stress of 22 ksi (at R.T.). Therefore, it was not possible to determine whether the gage output was an indication of crack extension or a result of yielding of the weld nugget. Local yielding was not a problem with the base metal specimens because a strain of 1.5% at room temperature represents a stress of 462 MN/m^2 (67 ksi). Although the room temperature 0.2% offset yield strength of the base metal material is 379 MN/m^2 (55 ksi) a strain of 1.5% corresponds to a stress of 462 MN/m^2 (67 ksi). For the base metal specimens the stresses at the start of crack extension and the critical crack length (i.e., crack length at instability) were determined from the crack propagation gages. An X-Y recorder was used to plot load versus CPG resistance. The instability crack length was the minimum crack length at maximum load as determined from the record load versus CPG resistance. Quite possibly the use of high-speed cameras or other more sophisticated crack length monitoring methods would have resulted in different crack lengths being defined as the critical ones. If the critical crack length is considered to be the point at which the crack propagation changes from a stable mode to an unstable mode, then the determination of the critical crack length is going to be highly dependent upon the manner in which crack length is monitored. For the alloy/temperature/gage combinations tested under the subject program, crack growth continues at an increasingly higher velocity from initiation to final fracture. The methods employed in the program cannot detect changes in crack length at crack growth velocity greater than approximately 300 mm/sec (1 Fps). This is orders of magnitude slower than velocities associated with dynamically propagating cracks. However, for most structural applications, crack propagation velocities of 300 min/sec (1 Fps) will be sufficient to insure failure of the component unless crack arrestment procedures are employed.

The base metal center crack panel data is presented in terms of gross section failure stress versus initial crack length in Figures 12 and 13. At net section levels in excess of 80% of the yield strength of the material (as determined from the mechanical property tests) there is a reduction in the apparent K_{CN} of the material. This apparent reduction in K_{CN} at high stress levels is commonly encountered and is consistent with the reduction in apparent K_{IE} value from surface flawed specimens when the net section stress exceeds 90% of yield. At net section stress below 80% of yield, the majority of the data falls within a $\pm10\%$ scatter band. There is a minor layering tendency throughout the data with the thinnest gages having the highest failure stresses. This tendency is most pronounced at the lower failure stresses and could be construed to be a shift in failure mode from plane stress toward plane strain. Observation of the fracture surfaces did indicate a shift from full shear to mixed mode as thickness increased. Note that thicknesses in excess of 25 mm (1.0 inch) are necessary if the plane strain thickness requirement $B = 2.5\ (K_{Ic}/\sigma_{ys})^2$ is to be met. The layering tendency was not affected by test temperature over the range tested. Although the majority of the data fell within a $\pm10\%$ scatter band, which is typical for this type of testing, the variation in gage thickness did exert a slight influence on the failure stress.

The base metal data is also presented in Figures 14 and 15 in terms of gross section stress at the start of crack growth versus initial crack length. The initiation of crack growth was determined from the CPG records. Constant stress intensity lines have been drawn on the figures so that a comparison of the stress intensity associated with the initiation of crack growth can be made with the K_{CN} values presented in previous figures. The layering tendency present in previous figures is not present here. Stable crack growth initiates at a stress intensity of approximately 53 $MN/m^{3/2}$ (48 ksi $\sqrt{in}$) regardless of gage thickness or test temperature over the range of variables tested. This stress intensity value is roughly 75% of the K_{CN} values obtained previously. A plot of initial crack length versus critical crack length is presented in Figure 16. The relationship between the initial and critical crack lengths for the base metal specimens can be approximated by a straight line defined by:

$$(2C)_{cr} = 1.24\ (2C)_i + B \qquad (5)$$

where: 2C = total crack length (see Figure 8)

cr = critical

i = initial

B = 14.7 mm (0.58 inch)

The extent of stable crack growth (i.e., critical crack length minus initial crack length) is insensitive to both gage thickness and temperature over the ranges tested. The stable crack growth between the initial and critical crack lengths was a uniform process in which the crack tip velocity increased monotonically from initial to critical crack length. A constant loading rate was employed in all of the center crack testing. Typical relationships between load and crack length are presented in Figure 17. As previously stated, the fracture process for the center crack panels consisted of a crack advancing across the specimen width at steadily increasing velocity. It was not possible to identify an instability point at which the crack velocity instantaneously increased to one which would be associated with a dynamically propagating crack.

Results of the weld metal center crack panels are presented in Figures 18 and 19. The data is presented in terms of gross section failure stress versus initial crack length. Resistance curve data presentation is not made because it was not possible to identify whether the change in resistance was related to crack extension or a consequence of the gage wires failing due to general yielding of the weld nugget. None of the weld metal specimens failed at net section stresses below their yield strength as determined by the mechanical property tests conducted at Boeing. The minor thickness effect experienced by the base metal specimen was not noticed in the weld metal panels. Lines of constant stress intensity are not presented in the figures because the linear elastic stress intensity concept has been shown to be inappropriate for correlating failure stresses significantly in excess of yield. From the figures it can be seen that for a 2219-T87 aluminum welded structure having 2 to 1 weld lands, the initial through-crack length ratio which will cause failure will be roughly 3 to 1 between the weld metal and base metal, respectively. Although the crack growth could not be determined from the CPG instrumentation, it is safe to assume that the failure mechanism of the weld metal panels was similar to the base metal panels. Results from the surface flaw specimen tests which will be discussed later (Section 5.3), suggest that crack growth may have initiated at a lower percentage of fracture load for the weld metal panels than for the base metal. There was, however, absolutely no indication from the crack opening displacement record that any abrupt instability occurred between the initiation of crack growth and final failure of the panel.

References 1 and 11 have concluded that for conditions in which the flaw penetrated the rear surface prior to fracture, the fracture stress can be estimated by considering the initial crack length and appropriate through-crack toughness. A number of the surface flaw specimen tests (which will be discussed later) were terminated when the crack had propagated through the rear surface. Additionally, some specimens experienced breakthrough but the loading was continued until fracture had occurred. A summary of the fracture data from the surface flaw specimens having crack depths equal to the gage thickness is presented in Figures 20 through 23. The data is presented in plots of gross section failure stress versus initial crack length. The initial crack length presented in these figures represents the maximum lateral crack dimension present at the initiation of fracture loading. All of the data from the base metal specimens fall within the scatter band established for the center crack panels. The agreement between the weld metal results (penetrated surface flaws versus center crack) was not as good as for the base metal. The greatest discrepancy is among the 3.18 mm (0.125 inch) thick specimen results. All of the center crack specimens were 305 mm (12.0 inch) wide, whereas the surface flaw specimen widths were 125 mm (5.0 inch), 229 mm (9.0 inch) and 356 mm (14.0 inch) for the 3.18 mm (0.125 inch), 6.35 mm (0.250 inch) and 9.53 mm (0.375 inch) thick specimens, respectively. The reduction in failure load from the center crack results to the surface flaw results for the 3.18 mm (0.125 inch) thick specimens is related to the increase in net section stress as a result of the narrower specimen width. Although the net and gross section stresses in the center crack panels are very similar for crack lengths of 12.7 to 25.4 mm (0.50 to 1.00 inch), the net section stress in the thinnest surface flaw specimen is 10 to 20% greater than the gross section stress. For specimens in which fracture occurs at elastic stress levels, discrepancy of this magnitude between gross and net section stresses are insignificant. However, the weld metal specimens were failing at gross area stress levels well in excess of yield. In this region the higher net section stress of the penetrated surface flawed specimens would be expected to cause a reduction in their gross area failure stress compared to the gross area failure stresses of the wider center cracked panels. The results for these tests do indeed confirm that the initial surface flaw crack length and the appropriate through-crack toughness can be used to estimate the failure stress of penetrated surface flaws if the panels are of sufficient size to preclude net section stress effects.

5.3 Surface Flaw Growth on Loading Tests

This portion of the experimental program was directed at determination of the growth-on-loading behavior of surface flaws in 2219-T87 aluminum, both parent and weld metal. The various gage thicknesses, test temperature, material condition and flaw shape combinations investigated are presented in Table 13. The primary emphasis has been placed on the low aspect ratio (a/2c) flaws because previous investigations (References 11 and 13) have shown these to be the most critical in terms of the extent of crack growth that can be encountered during loading. The failure mode for most of the conditions tested was leak-before-break. The limited number of conditions for which the failure mode was anticipated to be fractured was confined to the thicker base metal specimens having the lowest aspect ratio flaws. Conceivably, proof-testing a vessel for which the failure mode is leakage rather than fracture could grow a pre-existing flaw sufficient to cause failure by leakage on the first operational cycle. This problem has been recognized for a long time and the subject program was designed to develop data so that a better definition of the severity of the problem could be formulated.

In order for the data to be directly applicable to the failure (either leakage or fracture), stresses of the specimens had to be representative of proof test stresses. Therefore, the initial flaw sizes were selected so that the failure stresses would be 45, 50 and 59 ksi for the R.T., -320^{o}F and -423^{o}F base metal specimens and 22.5, 25.0 and 29.5 ksi for the R.T., -320^{o}F and -423^{o}F weld metal specimens. The base metal failure stress levels represent 90% of the material's minimum yield strength at the corresponding temperature and are typical of proof test stress levels. The weld metal failure stress levels were selected to be one-half the base metal value because weld lands twice the nominal base metal thickness are common in 2219-T87 aluminum pressure vessels. A review of available data was made and the flaw sizes were established before testing was initiated. The failure stresses were generally within 10 percent of the targeted values.

It was the purpose of this portion of the program to determine the growth-on-loading behavior of surface flaws from initiation to imminent failure. Since there will always be specimen-to-specimen variation in failure load even for nominally identical specimens, determining the proximity of failure from the average failure load of several specimens does not provide an accurate assessment of the imminency of failure for a given specimen. The crack opening displacement instrumentation was used extensively for determining the maximum stress to which a specimen could be subjected to without failing. The manner in which this was accomplished is illustrated in Figure 24. The first specimen (3BN21-2) was loaded directly to failure and its crack opening displacement was used as a guideline in determining when to terminate the loading of specimen 2BN21-2. The crack opening displacement record of the failed specimen is typical of those normally encountered, having a linear initial portion and a rounded section which reflects the crack extension and the localized plasticity associated with the surface flaw. It is obvious from Figure 24 that failure was imminent for specimen 2BN21-2 when unloading took place, even though its peak load was somewhat less than that of the previous specimen. All of the crack opening displacement records have been compiled and are presented in Volume II of this report.

All of the growth-on-loading specimens were loaded at a rate such that the maximum load was obtained in approximately one minute; unloading was accomplished at a rate such that zero-load was obtained in less than 15 seconds. Subsequent to the growth-on-loading (or proof load) cycle, the specimens were either subjected to cyclic loading or low stress fatigue marking. The results of the cyclic tests will be presented and discussed in a later section of this report. Using this load sequencing procedure, it was possible to determine the flaw sizes directly from the fracture faces of the specimens.

The results of the growth-on-loading tests have been summarized and are presented in Figures 25 through 36 and Tables 14 through 43. The data is presented in the figures in terms of gross area applied stress versus flaw depth. The flaw depths, both initial and final, are plotted at the maximum stress level the specimen was subjected to. The open symbols denote initial conditions and the closed symbols denote the final condition. When only one open data point is presented, it means that the specimen did not experience any distinguishable crack growth during the loading cycle. The crack depth has been chosen to characterize the results because failure by leakage is a consequence of crack growth in the depth-wise direction and crack depth is a first order parameter in the stress intensity formula. Data from both the growth-on-loading and failure specimens are presented in these figures. Two things are immediately obvious from the figures. First, there is a significant degree of specimen-to-specimen variability in stable crack growth. Second, the crack growth-on-loading is a uniform process which is related to the proximity of failure at maximum load. There was no indication throughout the data that an instability condition exists by which a surface flaw "pops" through the rear surface and then arrests. All the data indicates that the transformation from a surface flaw to a through-crack is a smooth stable growth process. The lack of an instability during the penetration process is certainly not surprising when the center crack results are considered. Here the crack growth was a stable process related to the proximity of failure. A limited amount of work has been conducted at Boeing aimed at determining if the growth-on-loading behavior of surface flaws is sensitive to loading rate. The results of these tests (which were also conducted on 2219-T87 aluminum specimens) indicated that crack growth during loading is a stable process insensitive to loading rate. This conclusion is based on a limited number of tests conducted at two different loading rates, roughly 350 MN/m^2/minute (50 ksi/minute) and 14 MN/m^2/minute (2 ksi/minute). Within these limits, however, the loading rate did not have any distinguishable effect on the crack growth associated with loading.

The other most distinguishable feature of the data presented in Figures 25 through 36 is the variability in results. During the course of the program particular attention was paid to the flaw preparation and testing procedures in the hope that data scatter could be minimized. All specimens of a particular flaw size were precracked under identical conditions because it was believed that variations in precrack could have a significant effect on the results. Delamination at the crack tip, which is often encountered in surface flaw specimen tests of the subject alloy, would be expected to have a significant effect on the growth-on-loading behavior. However, examination of the fracture faces of the specimens with the aid of a 30-power microscope revealed delamination in only three specimens. The results from these specimens are presented in Figure 27 and have been denoted as having delaminated. The extent of crack depth growth experienced by these specimens is indeed less than would be anticipated from the results of the other tests. Since neither the testing procedure nor delamination (except as noted) are responsible for the data scatter, what other parameters could affect the results? The location of the crack tip with relation to grain boundaries, micro-delaminations not visible to a 30-power microscope, localized variation in micro-structure -- all could have influenced the test results. It is not possible, however, to exercise any control over these parameters; therefore, the degree of variability among the results must be accepted as being inherent to this type of testing.

The results of the growth-on-loading tests have been summarized and are presented in Figures 37 through 41. In these figures the data is presented in terms of K_{Ii}/K_{cr} versus percent increase in crack depth. K_{Ii}/K_{cr} were calculated using Equation 7 presented in Section 3.4. The initial flaw size and maximum gross section stress were used to calculated K_{Ii} and the initial flaw size and gross section stress at failure were used to calculate K_{cr}. A K_{cr} was calculated for each particular combination of material condition, gage thickness, flaw shape and test temperature. Where more than one failure point was available, an average value was calculated. Determining K_{cr} in this manner can result in K_{Ii}/K_{cr} values which are not precisely accurate because of the specimen-to-specimen variability in K_{cr}. It is impossible, however, to calculate K_{cr} for each individual specimen and the resultant error of this calculation method will be minor. There are some data points presented at $K_{Ii}/K_{cr} > 1.0$ because of this procedure. The parameters K_{Ii}/K_{cr} and percent increase in flaw depth were selected for summarizing the data because K_{Ii}/K_{cr} expresses the proximity of failure when unloading occurred and the percent increase in crack length is related to the increase in stress intensity. Since stress intensity is proportional to the square root of flaw depth, the percent increase in stress intensity is proportional to the square root of the percent increase in flaw depth if the minor variations in the deep flaw magnification and shape parameter terms are ignored. It is recognized that the basic constraints of the linear elastic fracture mechanics theory are violated by most of the test conditions. For this reason consideration was given to using σ_i / σ_{cr} instead of K_{Ii}/K_{cr}; this was discarded, however, because it ignores variations in flaw depth, flaw length and a/t, all of which would have an influence on the results. The stress intensity concept is useful for characterizing the behavior of flaws, however procedures used to analyze and apply the data must be consistent.

When the results are reviewed in terms of K_{Ii}/K_{cr} versus percent increase in flaw depth (Figures 37 through 41), the parameters exhibiting the greatest influence on the data are the flaw shape and the material condition. All of the a/2c = 0.15 base metal data is presented in Figure 37. Neither the temperature nor the gage thickness had a systematic influence on the results. Since the fracture toughness yield strength ratio is not significantly affected by temperature, the lack of temperature dependance is not surprising. The absolute crack growth is affected by gage thickness; however, the percent increase is not. Therefore, the percent increase in stress intensity would also be insensitive to gage thickness. For the a/2c = 0.15 base metal results, a K_{Ii}/K_{cr} ratio of approximately 0.70 is required for the initiation of crack growth and a value of approximately 0.90 is required if a 10 percent increase in flaw depth is to be obtained. The results of the base metal specimens having a/2c ratios of 0.30 and 0.45 are presented in Figures 38 and 39. The results here are similar to the a/2c = 0.15 results, inasmuch as gage thickness and test temperature did not influence the data and a K_{Ii}/K_{cr} of approximately 0.70 is required to initiate crack growth during loading. For a given K_{Ii}/K_{cr} ratio, there is a significant reduction in the percent increase in flaw depth for the a/2c = 0.45 specimens over the entire range in which growth occurred, and somewhat of a reduction in growth for the a/2c = 0.30 specimens at K_{Ii}/K_{cr} ratios in excess of 0.90. The weld metal specimen tests were restricted to a/2c ratios of 0.15 and 0.30. These test results are presented in Figures 40 and 41. Again, neither the test temperature nor the gage thickness influenced the results. Crack growth did initiate at a lower K_{Ii}/K_{cr} ratio (approximately 0.60) for the weld metal and a 10 percent increase in crack depth also occurred at a lower K_{Ii}/K_{cr} (approximately 0.75) for the weld than for the base metal. Although the weld metal specimens generally experienced a greater percent increase in flaw depth for a given K_{Ii}/K_{cr} ration, the maximum increases were similar between the base and weld metal specimens. Increases in flaw depth of 10 percent (which would correspond to approximately a 5 percent increase in stress intensity) only occurred over a limited range of K_{Ii}/K_{cr} for both base and weld metal.

The discussion of the growth-on-loading tests have thus far been restricted to the depth-wise flaw growth. In a limited number of tests (almost exclusively the base metal specimens having a/2c = 0.30 and 0.45), crack growth in the lateral or 2c direction was also experienced. The manner in which the various aspect ratio flaws grew is illustrated in Figure 42. The fracture faces of several specimens exhibiting the crack growth behavior illustrated in Figure 42 are presented in Figures 43 and 44. The lowest aspect ratio flaws tended to grow mainly in the depth-wise direction, whereas the highest aspect ratio flaws did have a tendency to growth also in the lateral direction. In all cases, however, there was no growth experienced on the front face of the specimen. The final 2c length was always considered to be the maximum lateral dimension. A summary of the percent increases in flaw length is presented in Figure 45. Only the results from base metal specimens having a/2c's of 0.30 and 0.45 are presented in the figure because very few of the other specimens tested experienced any lateral crack growth and in all cases the increase was less than 10 percent. Of the a/2c = 0.30 and 0.45 base metal specimens, only one in three experienced any lateral growth. Although the maximum percent increases in crack length were significantly greater than the percent increases in crack depth, lateral growth did not initiate until K_{Ii}/K_{cr} was in excess of 0.90. Although lateral crack growth was severe when it did occur, the frequency of occurrence was low.

The growth-on-loading results have a significant impact on the discussion of the cyclic results, presented in a later section. For convenience, therefore, a summary of the most important points pertaining to the growth-on-loading behavior is presented below. The observations presented were derived from tests of 2219-T87 aluminum base and weld metal specimens at temperatures ranging from 295°K (72°F) to 78°K (-320°F) for thicknesses from 3.18 to 9.53 mm (0.125 to 0.375 inch).

a) Low aspect ratio flaws (a/2c = 0.15) experience more growth in the depthwise direction than higher aspect ratio flaws (a/2c = 0.30 and 0.45). However, crack growth in the length direction is more prevalent in the rounder flaws, but only at K_{Ii}/K_{cr} ratios in excess of 0.90.

b) Stable crack growth initiates at a lower K_{Ii}/K_{cr} ratio and is more severe in weld metal specimens than in base metal specimens. The ratios of K_{Ii}/K_{cr} required to initiate stable crack growth are approximately 0.70 for base metal and 0.60 for weld metal.

c) Significant stable crack growth under increasing load can occur prior to failure. However, significant variability in results can be anticipated even when carefully controlled laboratory procedures are employed.

d) Initial flaw shapes and material condition (base or weld metal) have a significant influence on the extent of growth occurring during the loading cycle.

e) Neither test temperature nor specimen thickness exhibit any influence on the crack growth behavior when the data is viewed in terms of K_{Ii}/K_{cr} versus percent increase in flaw depth.

As previously noted, the results were empirically derived and attempts to extrapolate them to other alloy systems or beyond the range of the conditions tested should be avoided.

5.4 Fracture Toughness Tests

During the growth-on-loading portion of the program, a limited amount of static fracture data was developed. The K_{IE} values calculated from surface flaw specimens which fractured at stress levels less than 90% of their yield and did not break through prior to fracture are presented in Table 44. The K_{IE} values obtained from these tests are typical for the alloy. The stress intensity formula presented in Equation 2 was used in the calculation of the K_{IE} values.

5.5 Single Cycle Penetration Criteria Tests

Recently, the use of resistance curves to characterize the onset of instability has become increasingly popular. In order to determine if the crack growth resistance techniques could be useful in the evaluation of the surface flaw data, the relationship between load and flaw size must be known. The data from the room temperature base metal specimens, 3.18 and 6.35 mm (0.125 and 0.250 inch) thick, was used to establish the relationship between stress and flaw size (see Figures 46 and 47). From Figures 46 and 47 the stress intensity/flaw depth relationship (resistance curves) was calculated, assuming the flaw shape (a/2c) remained constant. They are presented in Figures 48 and 49. Additional driving curves (i.e., stress intensity/flaw depth curves calculated assuming a constant stress and flaw shape) are also presented in these figures. Neither the tangency point nor the stress intensity at which crack growth initiated were constant for the 3.18 mm (0.125 inch) data. Similar calculations were made for some of the other combinations of test conditions where the failure mode was leakage. Consistent (constant) tangency points were not obtained for any of the cases.

For the thicker room temperature base metal specimens, 6.35 mm (0.250 inch), the driving and resistance curves were tangent at similar stress intensity values for the two lower flaw aspect ratios. This would be expected since the failure mode of these two was fracture rather than leakage. The tangency point for the a/2c = 0.45 curves was significantly less than the previous two. The a/2c = 0.45 is approaching the condition where the failure mode is leakage rather than fracture.

Reference 9 suggested that an estimate of the transition in failure mode from fracture to breakthrough could be made by considering the following criteria:

$$\text{Breakthrough if } t - a < 0.10 \ (K_{IE}/\sigma_{ys})^2 \qquad (6)$$

$$\text{Fracture if } t - a > 0.10 \ (K_{IE}/\sigma_{ys})^2 \qquad (7)$$

t = material thickness

a = flaw depth

σ_{ys} = yield strength

K_{IE} = fracture toughness

Using the above equations and the K_{IE} and σ_{ys} values previously presented, the remaining ligaments (t - a) which separate breakthrough from fracture are 1.91 mm (0.075 inch), 1.52 mm (0.060 inch) and 1.35 mm (0.053 inch) for the R.T., $78^{o}K$ ($-320^{o}F$) and $20^{o}K$ ($-423^{o}F$), respectively. The validity of this criteria, as applied to the data generated in the subject program, is checked in Figure 50. Here the remaining ligament flaw shape combinations are presented in terms of their predicted and actual failure mode. Generally, equations 6 and 7 accurately predicted the failure mode. The major exception to this was the 3.18 mm (0.125 in) liquid hydrogen test results. The remaining ligaments for these specimens were approximately one-half the maximum for which breakthrough should occur. Breakthrough, however, did not occur even though the specimens failed at elastic stress levels. For the few other cases where breakthrough was predicted and fracture occurred, the remaining ligament was 70 percent or greater of the maximum allowed by the criteria.

The breakthrough criteria represented by equations 6 and 7 provides no flaw shape parameters. Flaw shape, however, has a very significant influence on the stress intensity which can be generated in a specimen of a given thickness. Flaw shape also has a significant effect on the extent of stable growth that can be encountered prior to failure. From Figures 37, 38 and 39 it is apparent that the maximum percent increases in flaw depth which can be expected prior to fracture, for base metal specimens, are 25, 20 and 8 for flaw shapes (a/2c) of 0.15, 0.30 and 0.45, respectively.

An alternate method for establishing a ligament penetration criteria can be developed from the growth on loading data presented in Figures 37, 38 and 39. Figures 37 through 39 have defined the maximum flaw growth that can be anticipated prior to fracture. Penetration occurs when the remaining ligament is less than the stable growth that can occur prior to fracture. Therefore, knowing the maximum stable growth which can occur prior to fracture it is possible to determine the failure mode for a given failure stress-thickness-flaw shape combination. The procedures for doing this is outlined below.

1) The following parameters are known or selected

   a) Failure Stress - σ

   b) Flaw Shape - a/2c

   c) Material Thickness - t

2) Determine Q from Figure 6

3) Knowing a/2c determine the maximum percent increase in flaw depth from Figures 37 through 39 (i.e., $\Delta a/a_i$ = 25% for a/2c = 0.15; $\Delta a/a_i$ = 20% for a/2c = 0.30 etc.)

4) Let the initial flaw depth a_i plus the maximum stable growth prior to fracture Δa equal some thickness t_o.

i.e.,
$$a_i + \Delta a = t_o \qquad (8)$$

$$a_i\,(1 + \Delta a/a_i) = t_o \qquad (9)$$

$$a_i/t_o = \frac{1}{1 + \Delta a/a_i} \qquad (10)$$

5) Know a_i/t_o and a/2c determine M_K from Figure 7.

6) From Equation 2, calculate a_i

$$a_i = \left[\frac{K_{IE}\sqrt{Q}}{1.1\sigma M_K\sqrt{\pi}}\right]^2$$

Where K_{IE} is the fracture toughness determined from tests of surface flawed specimens.

$$t_o = a_i(1 + \Delta a/a_i) \quad (9)$$

7) Fracture will occur when

$$t_o < t \quad (11)$$

Penetration will occur when

$$t_o > t \quad (12)$$

The thickness (t_o) calculated is the minimum gage which will yield a failure by fracture for the selected stress and flaw shape. For thicknesses less than those calculated by Equation 9 the failure mode will be leakage because the initial flaw depth plus the stable crack growth during loading will exceed the wall thickness. If, however, the thickness is greater than that calculated by Equation 9 the extent of stable growth occurring during loading will not be sufficient to allow the flaw to penetrate the thickness and failure by fracture will occur. The above calculation procedure permits the calculation of the failure mode for a selected failure stress and flaw shape, therefore, it could be extremely useful in determining the proof stress level which would assure failure by leakage, if a failure did occur, during proof testing.

The above procedure has been used to calculate the remaining ligaments which separate the failure modes for the selected stress levels used in the growth-on-loading tests. The calculated transition ligaments are compared to the test results in Figure 51. The failure mode of every specimen was accurately predicted using the method outlined above (equations 8 through 12). A comparison of the predicted transition ligaments using the procedures described in Equations 8 through 12 (Method II) and Reference 9 criteria, Equations 6 and 7 (Method I) is presented in Figure 52. Flaw shape (a/2c) does not influence the Method I calculation; it does however influence the calculated transition ligament size calculated using the Method II procedure. There is not a very large variation in the sizes of the remaining ligaments calculated using Method II over the range of a/2c's considered. Although the rounder flaws experienced a lower percent increase in flaw depth, their initial size was larger, thereby causing the absolute growth to be comparable.It must be remembered that these calculations are being made for a selected failure stress. The two calculation procedures did yield similar remaining ligaments, however, the Method I values are consistently greater than the Method II values. This is partially a consequence of Method I being derived from data which generally had a lower failure stress than that used in the Method II calculation. There was a wide variety of failure stresses among the data used in deriving Method I, however, among the 2219-T87 aluminum specimens tested at 78°K (-320°F) the average failure stress was approximately 310 MN/m^2 (45 ksi) which is 10 percent lower than the failure stress used for the Method II calculation. The K_{IE} values obtained from the two programs were the same for the 78°K (-320°F) aluminum tests. The Method II procedure is quite sensitive to failure stress since a_i is proportional to σ^2; therefore, the calculated remaining ligaments will be proportional to the failure stress squared. The Reference 9 study also included tests of 7075-T651 aluminum and 6Al-4V STA titanium at room temperature. The results from these tests were also used in determining the breakthrough criteria. Again, among these tests there also was a wide variety in failure stress. Using the average failure stress for each alloy, the remaining ligaments are calculated using both procedures and presented in Figure 53. The predictions from the two procedures are very similar for these two alloys. Since the Method II procedure worked successfully on the 7075-T651 aluminum and 6Al-4V STA titanium data, the growth-on-loading characteristics of these alloys must be similar to the 2219-T87 aluminum behavior.

Both of the procedures yielded acceptable prediction of failure mode for the data considered. For the Method II procedure to be valid for other alloy systems, their growth-on-loading behavior must be similar to that of 2219-T87 aluminum. The range of K_{IE}/σ_{ys} values for the alloys considered is approximately 0.5 to 1.0. Application of these procedures to alloy systems having a K_{IE}/σ_{ys} value significantly different than the above is not advised. The growth-on-loading behavior of alloys having a significantly lower K_{IE}/σ_{ys} value could differ substantially, rendering both methods of failure mode transition to be erroneous.

5.6 Surface Flaw Specimen Cyclic Tests

A total of 107 cyclic tests were conducted during the course of the subject program. All of the specimens were subjected to a simulated proof cycle prior to the cyclic test. Of the 107 specimens, 91 were subjected to a proof cycle such that failure was imminent when the proof stress was obtained. The crack opening displacement recording was used as a guideline in determining the imminency of failure (see Section 5.3). As would be expected, there were several failures during the proof load cycle. Nevertheless, 91 specimens out of better than 100 did successfully survive the proof load cycle. If there had not been any failures during the proof loading, it would have been suspected that the estimates of the failure loads were too conservative. The results of the cyclic tests are presented in the tables. Additionally, they have been summarized and are presented in Figures 54 through 57.

In the figures the cyclic data have been presented in terms of K_{Ii}/K_{cr} versus cycles to failure. Failure means either fracture or breakthrough. For the vast majority of the results the failure mode was breakthrough. Since either occurrance would constitute a failure of a pressure vessel, no attempt has been made to distinguish between the failure modes on the figures. The K_{cr} values were calculated for each combination of temperature/gage/flaw shape and material conditions the same as in Section 5.3. The K_{Ii} values were calculated using the initial (preproof) flaw size and the cyclic stress. The cyclic loading was applied using either a .017 Hz (1 cpm) trapezoidal profile or a sinusoidal profile at 1 or 0.05 Hz (60 or 3 cpm). The 0.017 Hz (1 cpm) data have been distinguished from the rest on the figures. Generally, all of the tests were continued to failure except for the 0.017 Hz (1 cpm) tests, which were terminated at 100 cycles.

The cycles to failure curves from Reference 14 are presented on the figures. These curves are best fit, not lower bound, curves for specimens in which the failure mode was fracture. The results presented in Reference 14 were for straight cyclic tests; none of the specimens were subjected to a prior proof cycle. All of the results from this program compare well with the cycles to failure curve generated in the reference study. The reference study did not present any cycles to failure curves for the weld metal tests, so the base metal curves have been drawn on Figures 55 and 57 so that a comparison can be made between base and weld metal results.

For the cryogenic tests all of the data is fairly evenly dispersed about the reference curves. The room temperature results, however, tend to be to the right of the reference curve. The reference curves were generated from tests in which the failure mode was fracture; whereas, the failure mode for the majority of the data presented is breakthrough. Even for the cases where failure was by fracture, the agreement between proof loaded and non-proof loaded data could be effected by the stable crack growth associated with the proof overload. The previous sections have shown that significant crack growth can occur during the proof cycle. It has also been established (15,18) that the overload of these tests (1.33 or less) is not sufficient to exert a significant influence on the cyclic growth rate. Although the retardation of a slight overload would be small, or non-existent, the difference in the stable crack growth between the overload cycle and the first cycle of the cyclic test would also be small. Since the crack growth associated with the first cycle of a cyclic test cannot be distinguished on the fracture surface, there has been a tendency to assume that the cyclic crack growth progresses at a uniform rate influenced only by the stress intensity. This assumption is not valid and has probably led to the observation that thin specimens have a higher crack growth rate than thick specimens. Consider Figure 58 (Figure 67 in Reference 11), which shows an increase in crack growth with a decrease in thickness. If the data are replotted, and all specimens which received less than 300 cycles are eliminated the resultant plot is presented in Figure 59. There is no apparent effect of thickness on crack growth rate in Figure 59. Thin specimens generally receive less cycles;

therefore, the stable growth associated with the first cycle exhibits a greater influence on the growth rate than it would in thick specimens. Thus, it is possible to influence crack growth rates by selecting the test duration. Therefore, the crack growth rates generated from specimens subjected to a limited number of cycles should not be applied to structures which will see a large number of cycles and conversely growth rates from long-term tests should not be applied to structures which will experience a limited number of loadings. The latter could result in a nonconservative answer; whereas, the former could result in an overly conservative answer.

The results from three specimens have not been included in Figures 54 and 56. These three specimens (3BR11-1, 4BR14-2 and 4BN11-1) all failed on the first loading cycle after proof cycle. The failure mode in each of these specimens was leakage rather than fracture. Two of the specimens, 4BR14-2, and 4BN11-1 were cycled at 0.017 Hz (1 cpm) and breakthrough was noted during the 15 second hold time at the peak cyclic load. Specimen 4BR14-2 was 3.18 mm (0.125 in) thick, tested at room temperature, and had an initial a/2c of 0.45. The proof stress was 293.0 MN/m^2 (42.5 ksi) and the cyclic stress was 263.4 MN/m^2 (38.2 ksi). Specimen 4BN11-1 was also 3.18 mm (0.125 in) thick, tested at 78°K (-320°F) and had an initial a/2c of 0.15; the proof stress was 324.1 MN/m^2 (47.0 ksi) and the cyclic stress was 258.6 MN/m^2 (37.5 ksi). Both of these specimens were subjected to the trapezoidal cyclic loading profile. The leakage rate of the helium was slight, but detectable, on the first cycle. Because there was a hold time at peak load for the cyclic test and there wasn't any during the proof cycle, the possibility does exist that breakthrough occurred during the proof cycle and was not detected. There was, however, no indication on the pressure traces that this had occurred. Specimen 3BR11-1, a 3.18 mm (0.125 in) thick specimen having an initial a/2c of 0.15, was subjected to a room temperature proof cycle to 275.8 MN/m^2 (40.0 ksi). The cyclic test was to be at 1 Hz (60 cpm) with a peak stress of 220.6 MN/m^2 (32 ksi). All of the test machines are equipped with a shutdown system which is activated by an increase in pressure in the rear cup. When the cyclic loading was initiated the shutdown switch was actuated at 129.6 MN/m^2 (18.8 ksi). Since the machine was programmed to run at 1 Hz (60 cpm) and the shutdown load was roughly half the programmed load, the shutdown was activated approximately 1/4 second after the test had been initiated. The unloading time from the proof overload level to 129.6 MN/m^2 (18.8 ksi) was at least two seconds. Although it is possible, it is extremely unlikely that breakthrough occurred undetected on the proof overload cycle.

The purpose of the cyclic test program was to establish the residual cyclic life of flaws subjected to proof load condition causing growth-on-loading damage sufficient to produce an incipient penetration condition at the maximum proof load. In about 3 percent of these tests a leakage failure developed on the first loading cycle. Duplicating the three tests in which failure occurred on the first cycle would probably require another 100 specimens. The condition by which the proof cycle flaw growth could be maximized, without developing a through crack, was known for all of the cyclic tests. The application of these conditions resulted in a first cycle failure only 3 percent of the time. The occurrence of a first cycle failure by leakage will be rare, even under carefully controlled laboratory conditions.

None of the test variables exhibited a significant impact on the cycles required to cause failure for a given K_{Ii}/K_{cr} ratio. The application of the proof test and cyclic loadings at different temperatures was not investigated; therefore, its effect cannot be evaluated. The data does show that the careful selection of a proof and operating stress can be used to ensure, with a high degree of confidence, that minimum required cyclic life can be obtained. The test program was designed to be applicable to spacecraft type pressure vessels. These vessels are generally subjected to a limited number of cycles. Attempts should not be made to extrapolate any of the data beyond the scope of the program or beyond the conditions tested.

5.7 Post Proof Test Inspection

It has been established in the previous sections that significant crack growth can be encountered during proof loading, and under very specialized conditions failure, by leakage, can occur on the first loading cycle subsequent to the proof test. The probability of a first cycle failure is remote. Under carefully controlled conditions it was only possible to accomplish this in 3 out of 100 tests. In these tests, the original flaw size was known and the proof stress was selected such that it would cause maximum damage to the specimen. A first cycle failure, after proof testing, can only be a result of a very deep flaw having grown almost to breakthrough during the proof cycle. References 9, 10, 16 and 19 have all shown that under these conditions there will be a visible dimple located behind the flaw. Therefore, it is proposed that subsequent to a proof test, but prior to placing the vessel in service, a careful surface inspection of the entire vessel be made. This surface inspection should locate any flaw which has grown sufficiently to cause failure on the first loading cycle. Additionally, the crack opening displacement records presented in Volume II clearly indicate that the proof test will induce a residual opening on a pre-existing flaw. The residual opening will be related to the flaw size, the larger flaws having the greatest opening. This residual opening would greatly enhance the probability of detecting the flaw using conventional inspection techniques. The combination of an intelligent proof test and post proof inspection should allow for a high degree of confidence in the safe operation of the vessel. Additionally, the proof test will eliminate any possibility of a first service cycle catastrophic failure.

6.0 CONCLUSIONS

The following conclusions were derived from an experimental program conducted on both center-crack and surface flaw specimens of 2219-T87 aluminum base metal and weld metal. Three thicknesses of material 3.18, 6.35 and 9.53 mm (0.125, 0.250 and 0.375 inch) were tested at each of three different temperatures; 295°K and 20°K (72°F, -320°F and -423°F). All of the tests were conducted using uniaxial specimens. The following conclusions should not be extrapolated to other conditions without additional experimental verification.

1) Significant stable crack growth under increasing load can occur prior to failure. However, significant variability in results can be anticipated even when carefully controlled laboratory procedures are employed.

2. Initial flaw shapes and material conditions have a significant influence on the extent of growth occurring during the loading cycle.

3. Neither test temperature nor specimen thickness exhibit any influence on the crack growth behavior when the data is viewed in terms of K_{Ii}/K_{cr} versus percent increase in flaw depth.

4. Stable crack growth initiates at a lower K_{Ii}/K_{cr} ratio and is more severe in weld metal specimens than in base metal specimens. The ratios of K_{Ii}/K_{cr} required to initiate stable crack growth are approximately 0.70 for base metal and 0.60 for weld metal.

5. Low aspect ratio flaws (a/2c = 0.15) experience more growth in the depthwise direction than higher aspect ratio flaws (a/2c = 0.30 and 0.45). However, crack growth in the length direction is more prevalent in the rounder flaws, but only at K_{Ii}/K_{cr} ratios in excess of 0.90.

6. Proof testing assures that any failure on the first service life cycle will be leakage and not catastrophic.

7. Minimum service lives can be assured, with a high degree of confidence, if an intelligently designed proof test is used in conjunction with a post proof inspection.

REFERENCES

1. J. N. Masters, W. P. Haese and R. W. Finger, "Investigation of Deep Flaws in Thin Walled Tanks," NASA CR-72606, December 1969.

2. F. W. Smith, "The Elastic Analysis of the Part-Circular Surface Flaw Problem by the alternating Method," The Surface Crack: Physical Problems and Computational Solutions, edited by J. L. Swedlow, ASME, November 1972.

3. R. C. Shah and A. S. Kobayashi, "On the Surface Flaw Problem," The Surface Crack: Physical Problems and Computational Solutions, edited by J. L. Swedlow, ASME, November 1972.

4. J. R. Rice and N. Levy, "The Part-Through Surface Crack in an Elastic Plate," Journal of Applied Mechanics, Vol. 39, Trans. of ASME, Vol. 94, March 1972.

5. P. H. Francis, D. L. Davidson and R. G. Forman, "An Experimental Investigation into the Mechanics of Deep Semielliptical Surface Cracks in Mode I Loading," Engineering Fracture Mechanics, Vol. 4 No. 4, December 1972.

6. A. S. Kobayashi and W. L. Moss, "Stress Intensity Magnification Factors to Surface-Flawed Tension Plate and Notched Round Tension Bar," Fracture Proc., 2nd International Conference on Fracture (Brighton), Chapman and Krell, London, 1969.

7. G. R. Irwin, "Crack Extension Force for a Part-Through Crack in a Plate," Journal of Applied Mechanics, Vol. 29, Trans. ASME, Vol. 84, Series E, December 1962.

8. C. F. Tiffany, "Fracture Control of Metallic Pressure Vessels," NASA SP 8040, 1970.

9. J. N. Masters, W. D. Bixler, and R. W. Finger, "Fracture Characteristics of Structural Aerospace Alloys Containing Deep Surface Flaws," NASA CR-134587, December 1973.

10. J. E. Collipriest, Jr., "An Experimentatist's View of the Surface Flaw Problem," The Surface Crack: Physical Problems and Computational Solutions, edited by J. L. Swedlow, ASME, November 1972.

11. J. N. Masters, W. L. Engstrom and W. D. Bixler, "Study of Deep Flaws in Weldments of Aluminum and Titanium," NASA CR-134649, April 1974.

12. W. F. Brown and J. E. Srawley, "Fracture Toughness Testing Methods," p. 10, ASTM STP 410, 1966.

13. W. D. Bixler, "Fracture Control Method for Composite Tanks with Load Sharing Liners," NASA CR-134758, July 1975.

14. W. L. Engstrom, "Determination of Design Allowable Properties - Fracture of 2219-T87 Aluminum Alloy," NASA CR-115388, March 1972.

15. L. R. Hall, R. W. Finger and W. F. Spurr, "Corrosion Fatigue Crack Growth Data for Aircraft Structural Materials," Air Force Materials Laboratory Report AFML-TR-73-204, September 1973.

16. T. D. Gray, "Fatigue Crack Retardation Following a Single Overload," Air Force Flight Dynamics Laboratory Tech. Memorandum AFFDL-TM-73-137-FBR, October 1973.

17. P. H. Francis, D. L. Davidson, H. C. Burghard, "Experimental Study of Plastic Yielding at the Tip of Surface Flaw Cracks," NASA CR-114934, May 1971.

18. L. R. Hall, R. C. Shah and W. L. Engstrom "Fracture and Fatigue Crack Growth Behavior of Surface Flaws and Flaws Originating at Fastener Holes," Air Force Flight Dynamics Laboratory Report AFFDL-TM-74-47, September 1973.

19. P. H. Francis and D. L. Davidson, "Experimental Characterization of Yield Induced by Surface Flaws", The Surface Crack: Physical Problems and Computational Solutions, edited by J. L. Swedlow, ASME November, 1972.

Page Intentionally Left Blank

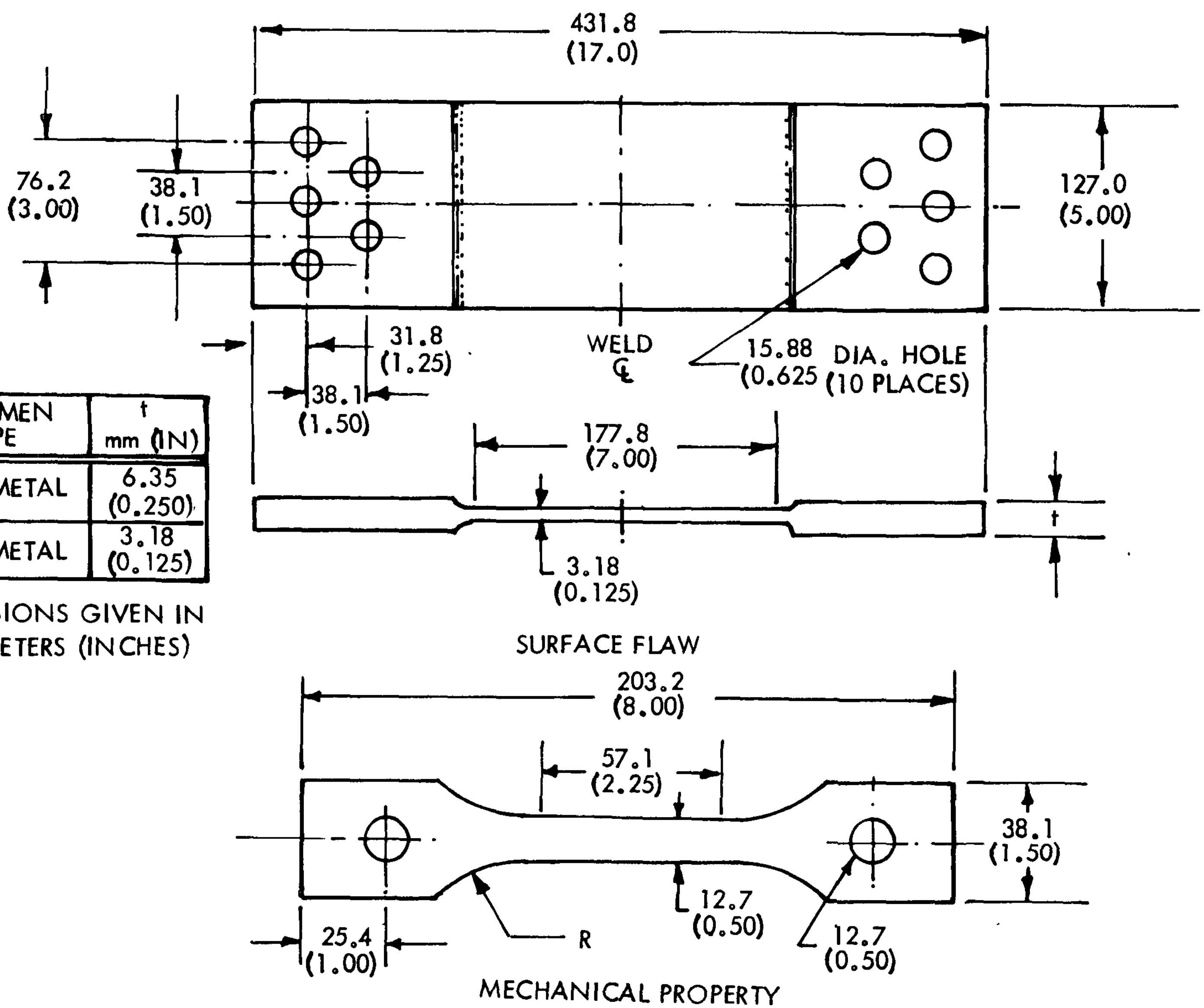

SPECIMEN TYPE	t mm (IN)
BASE METAL	6.35 (0.250)
WELD METAL	3.18 (0.125)

DIMENSIONS GIVEN IN MILLIMETERS (INCHES)

FIGURE 1 : BASE AND WELD METAL SPECIMENS

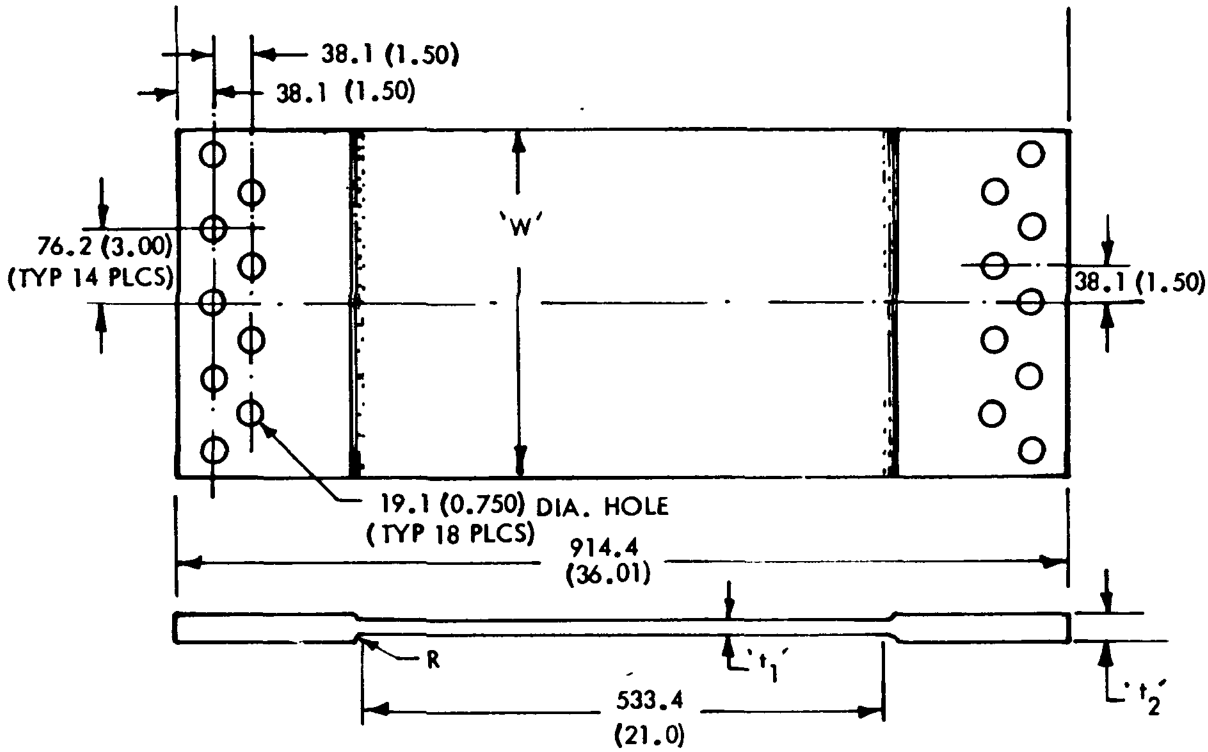

DIMENSIONS GIVEN IN MILLIMETERS (INCHES)

SPECIMEN TYPE	'W'	't1'	't2'
CENTER CRACK (BASE METAL)	304.8 (12.0)	3.18 (0.125)	6.35 (0.250)
		9.53 (0.375)	12.70 (0.500)
CENTER CRACK (WELD METAL)		3.18 (0.125)	3.18 (0.125)
		6.35 (0.250)	6.35 (0.250)
		9.53 375)	9.53 (0.375)
SURFACE FLAWED (BASE METAL)	355.6 (14.0)	9.53 (0.375)	12.70 (0.500)
SURFACE FLAWED (WELD METAL)		9.53 (0.375)	12.70 (0.500)

FIGURE 2: 2219-T87 ALUMINUM SURFACE FLAWED SPECIMEN

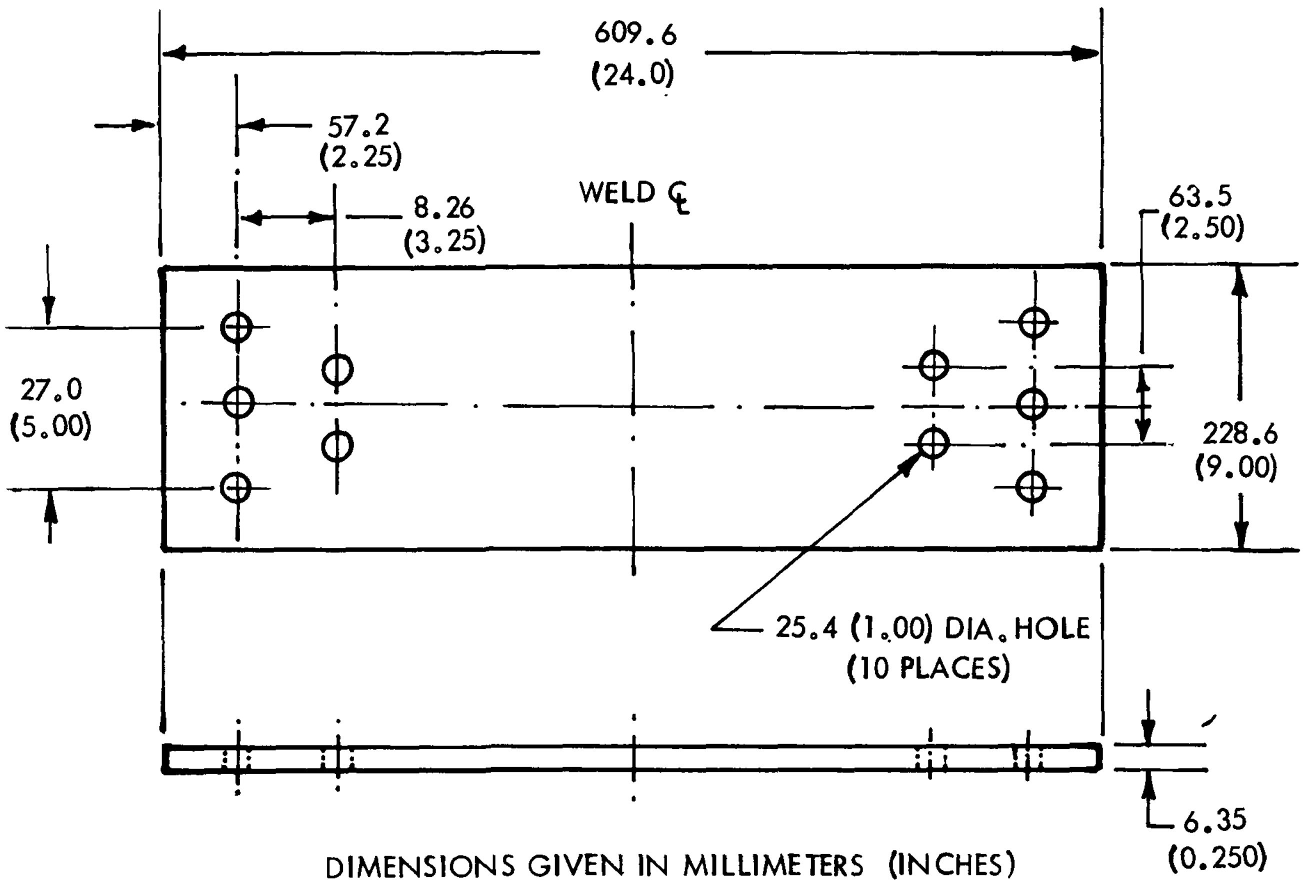

FIGURE 3: ALUMINUM WELD METAL SURFACE FLAWED SPECIMENS

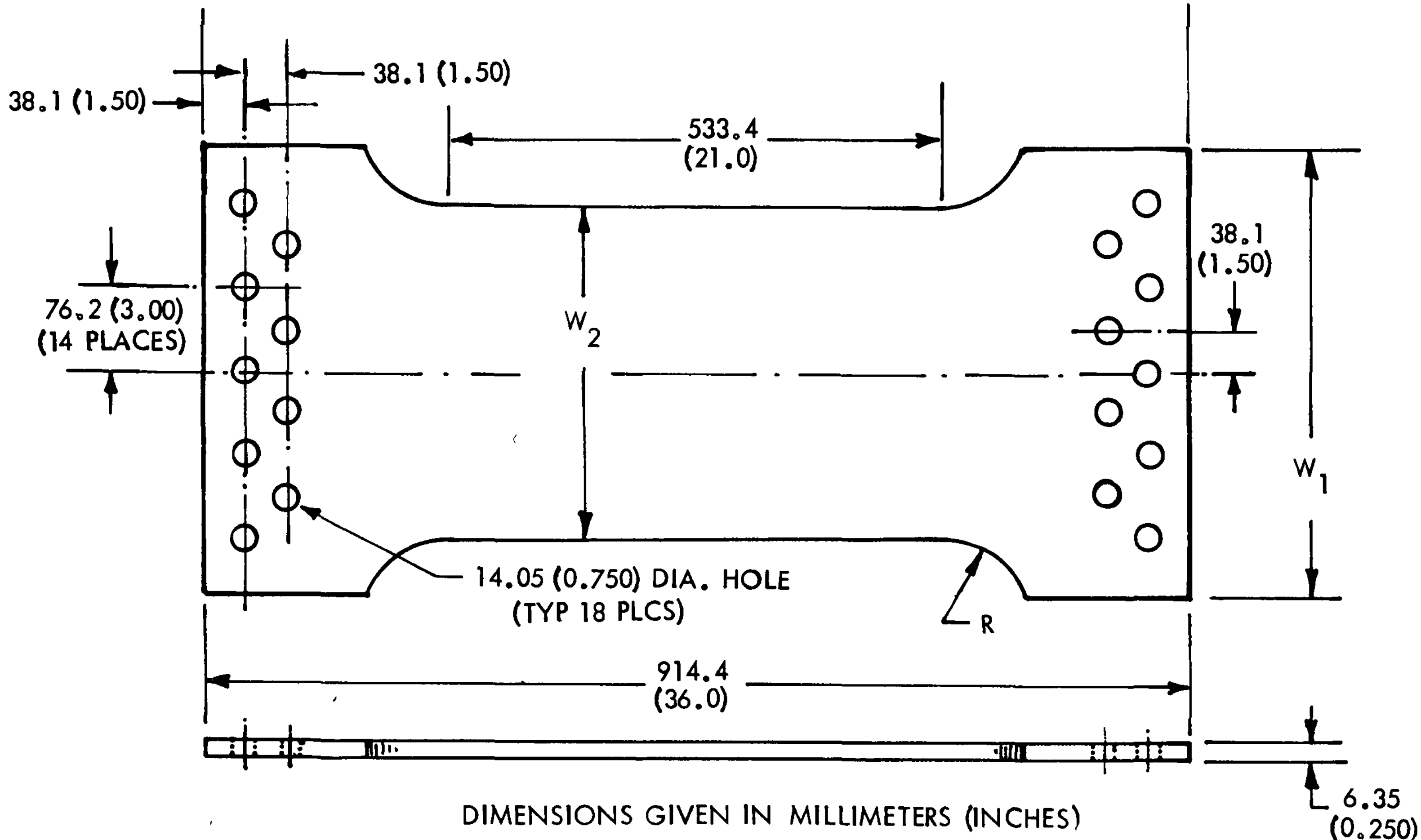

DIMENSIONS GIVEN IN MILLIMETERS (INCHES)

SPECIMEN TYPE	W_1	W_2
CENTER CRACK	406.4 (16.0)	304.8 (12.0)
SURFACE FLAW	355.6 (14.0)	228.6 (9.00)

FIGURE 4: 2219-T87 ALUMINUM SURFACE FLAW SPECIMENS

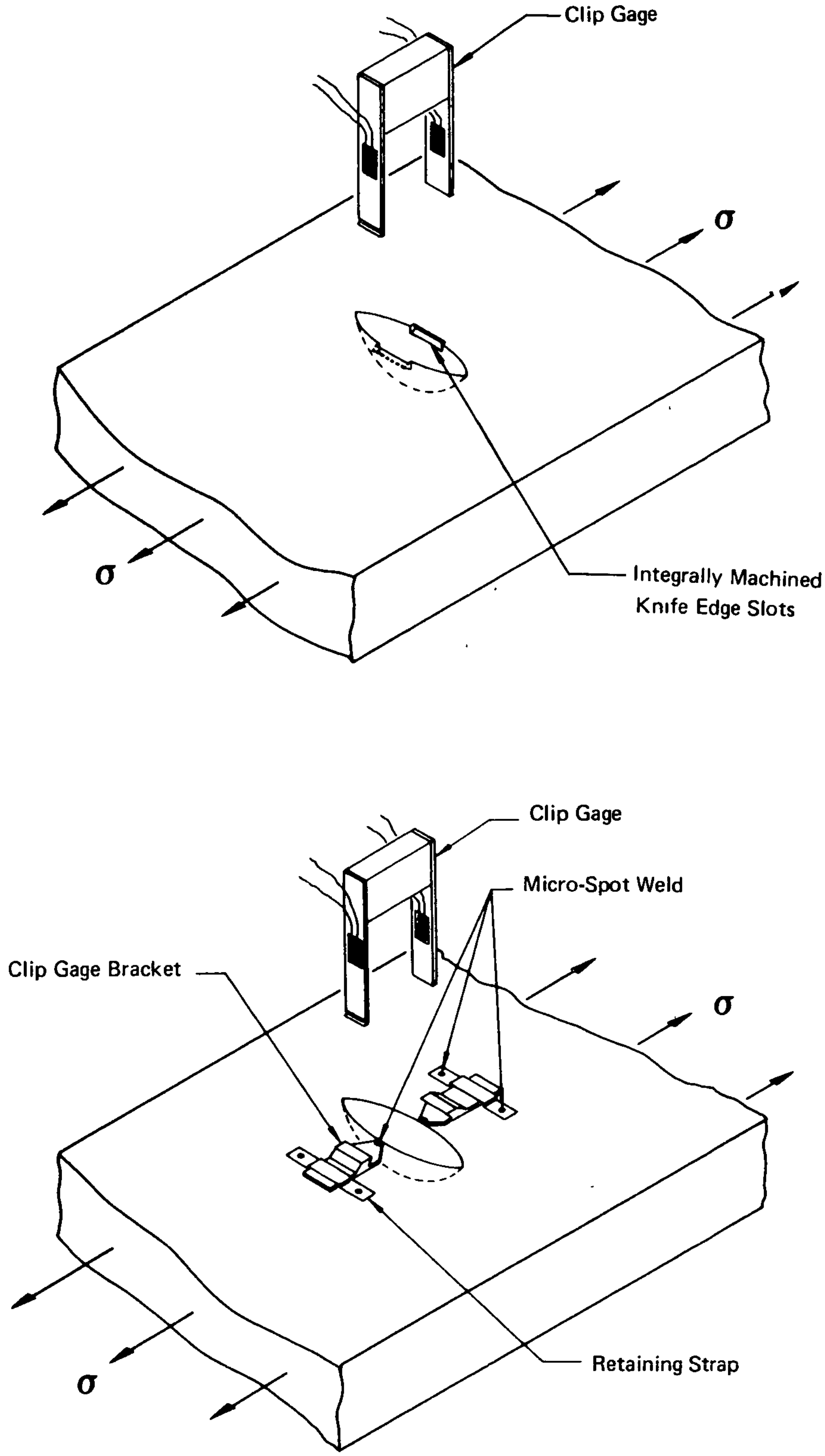

FIGURE 5: FLAW OPENING MEASUREMENT OF SURFACE FLAW SPECIMENS

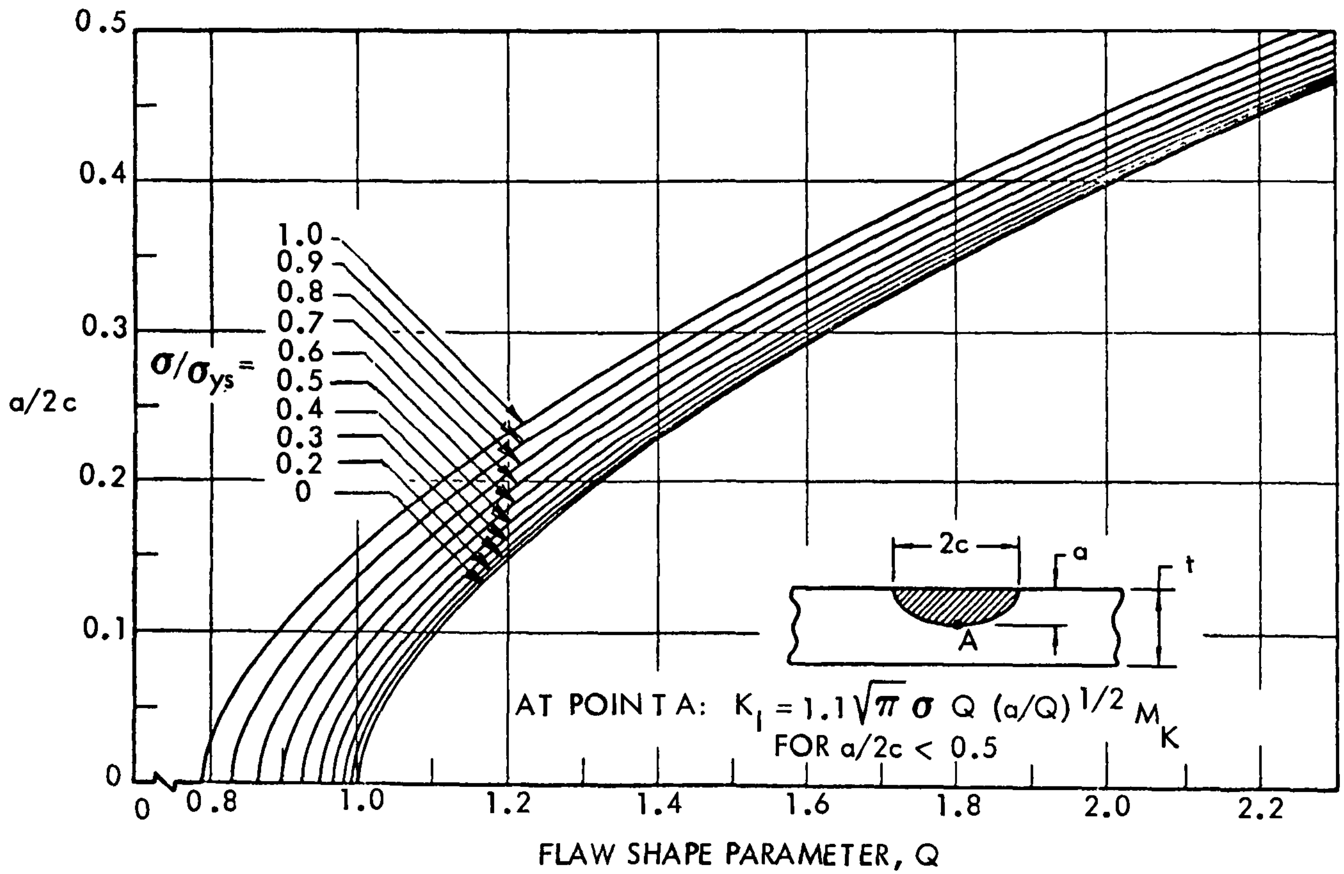

FIGURE 6: SHAPE PARAMETER CURVES FOR SURFACE AND INTERNAL FLAWS

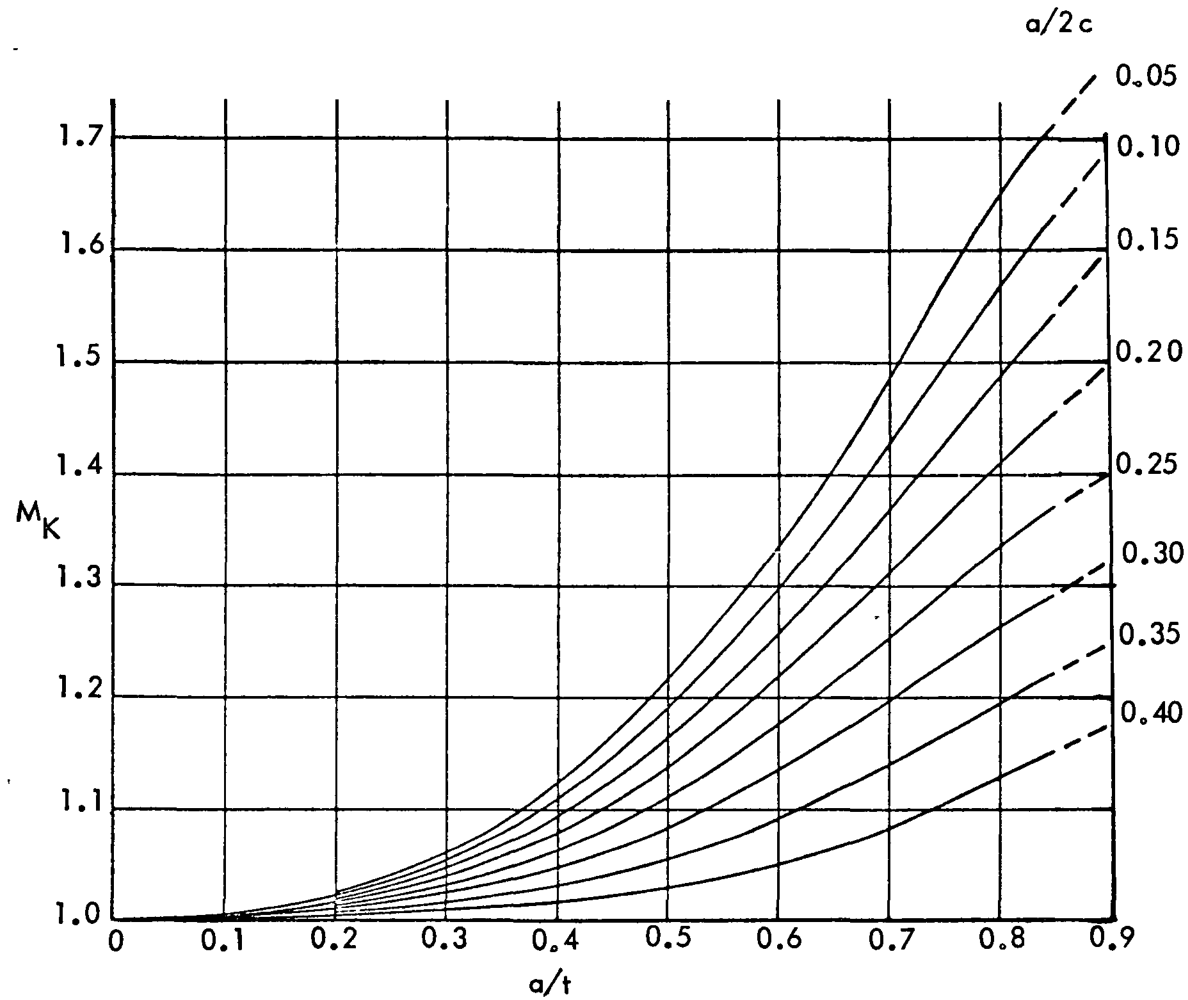

FIGURE 7: DEEP FLAW MAGNIFICATION CURVES (REF. 1)

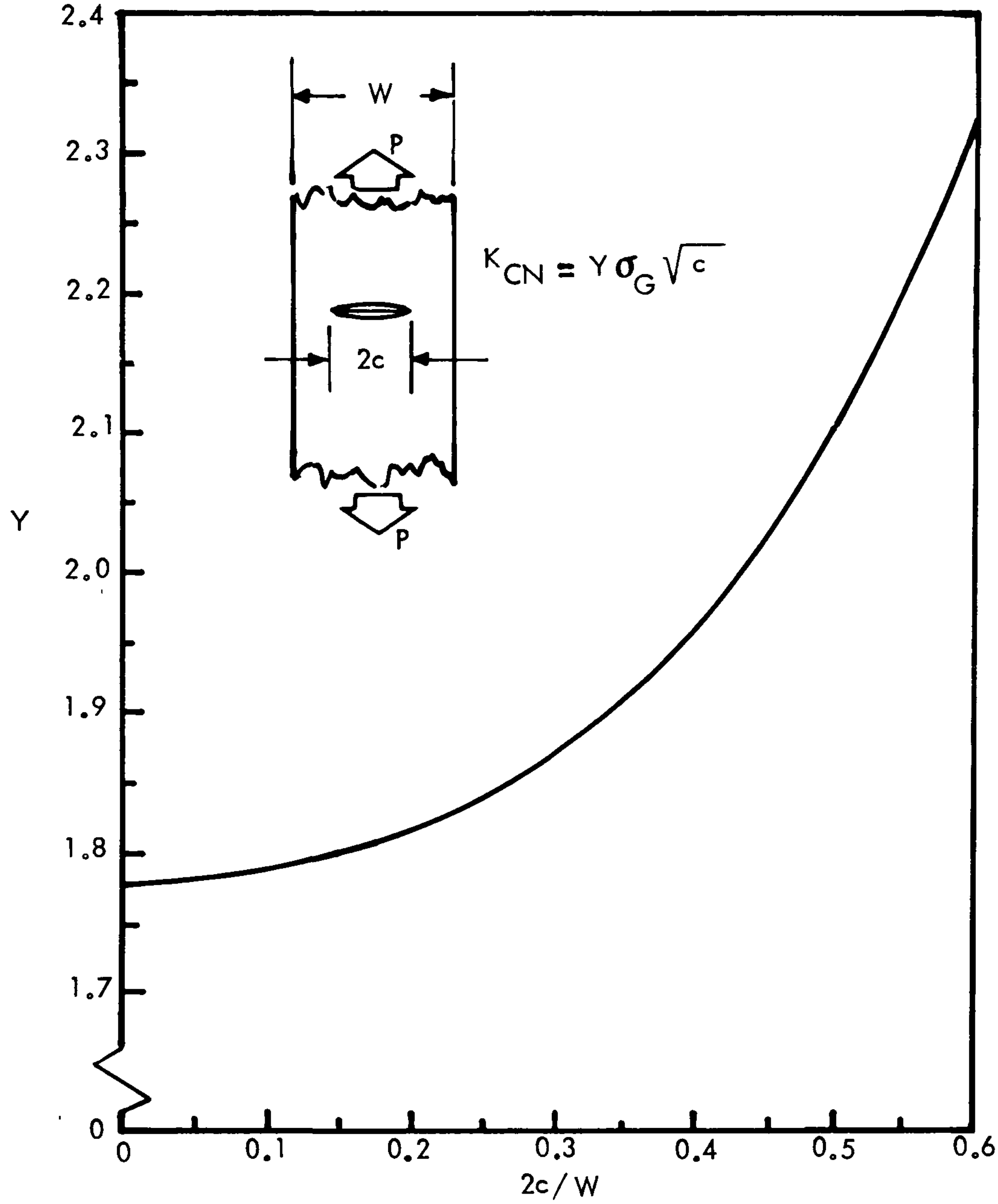

FIGURE 8: RELATIONSHIP FOR CALCULATING K_{CN} FROM CENTER CRACK SPECIMENS

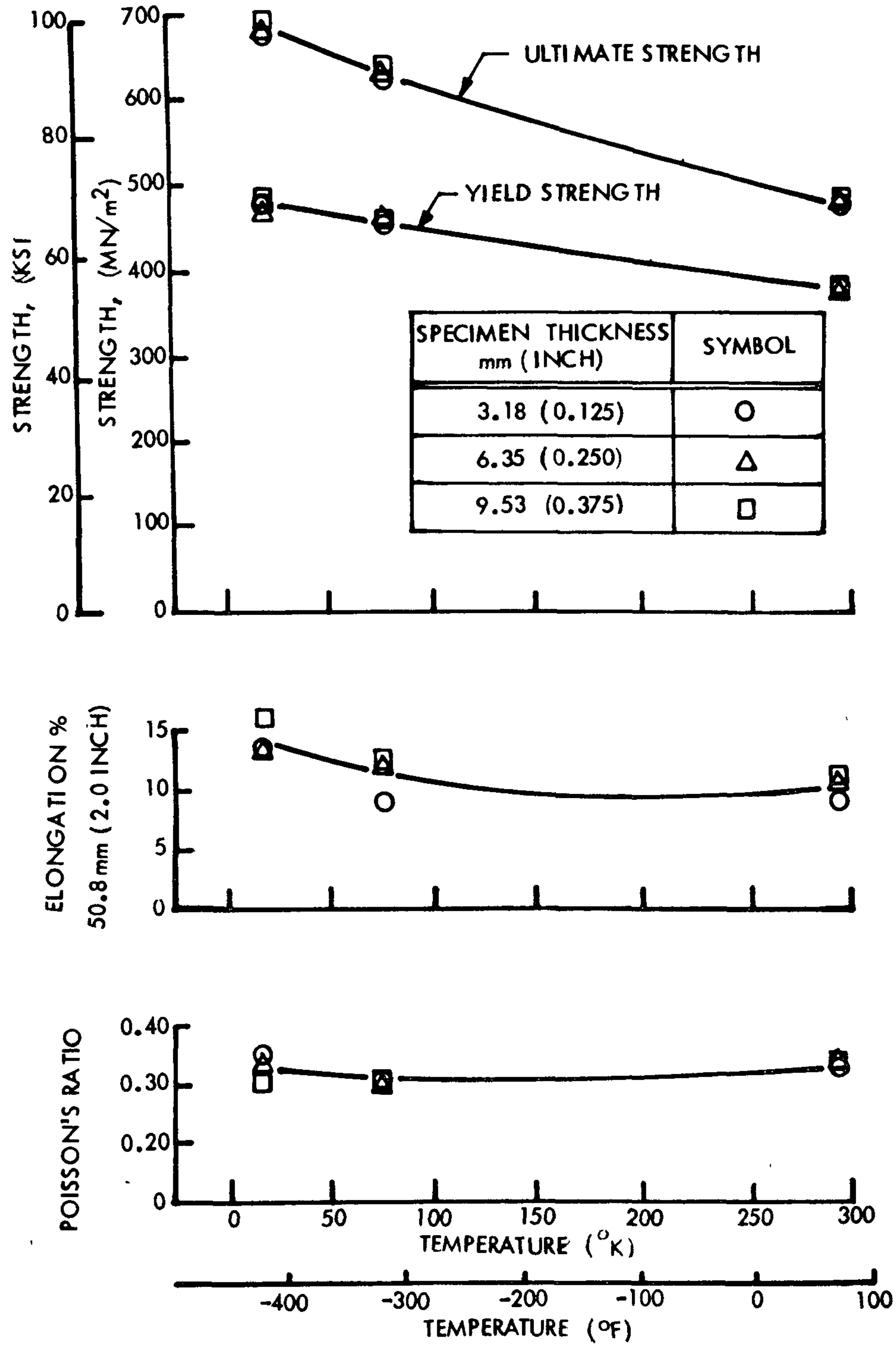

FIGURE 9: TENSILE PROPERTIES OF 2219-T87 ALUMINUM BASE METAL TRANSVERSE GRAIN

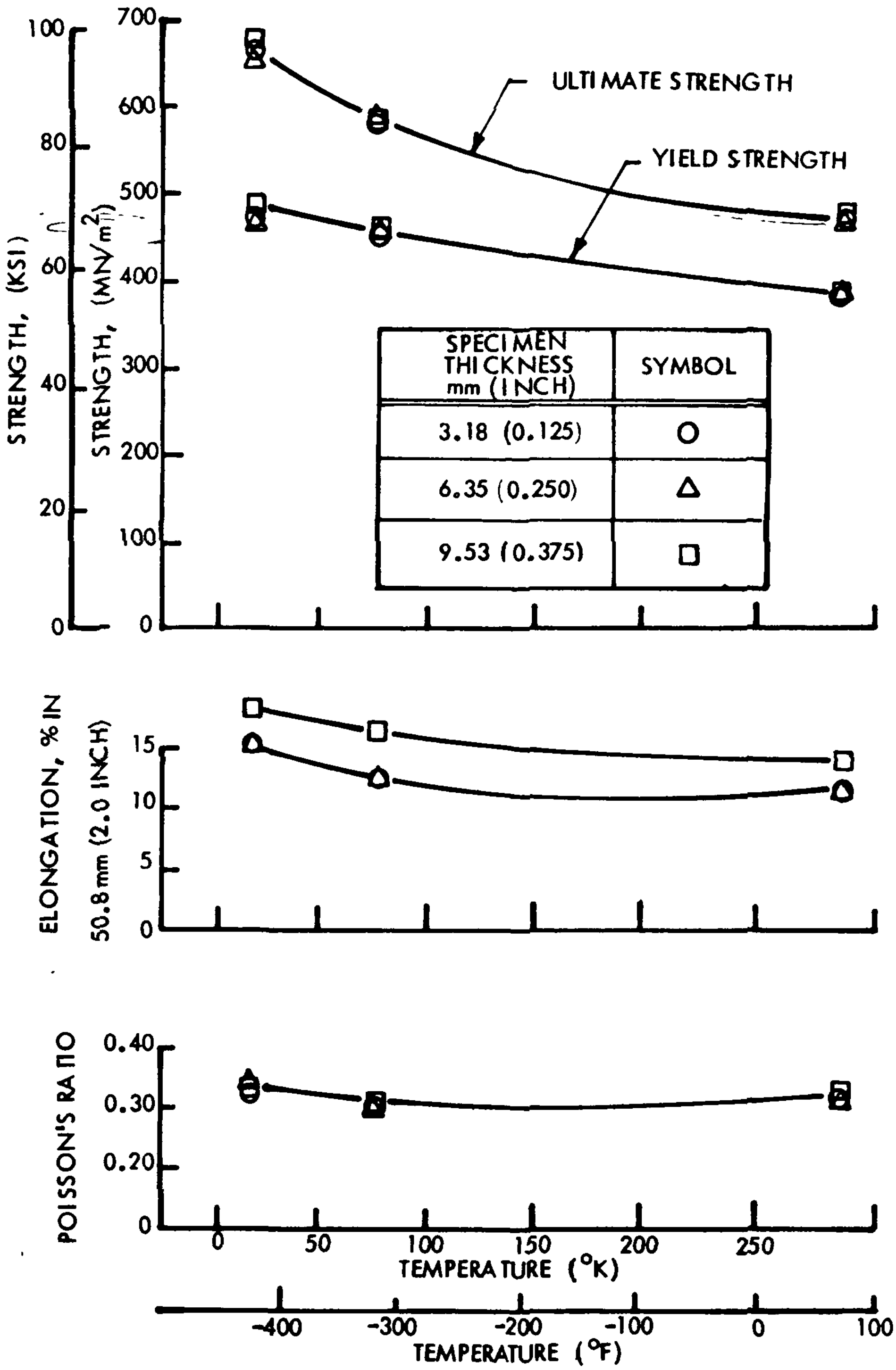

FIGURE 10: TENSILE PROPERTIES OF 2219-T87 ALUMINUM BASE METAL LONGITUDINAL GRAIN

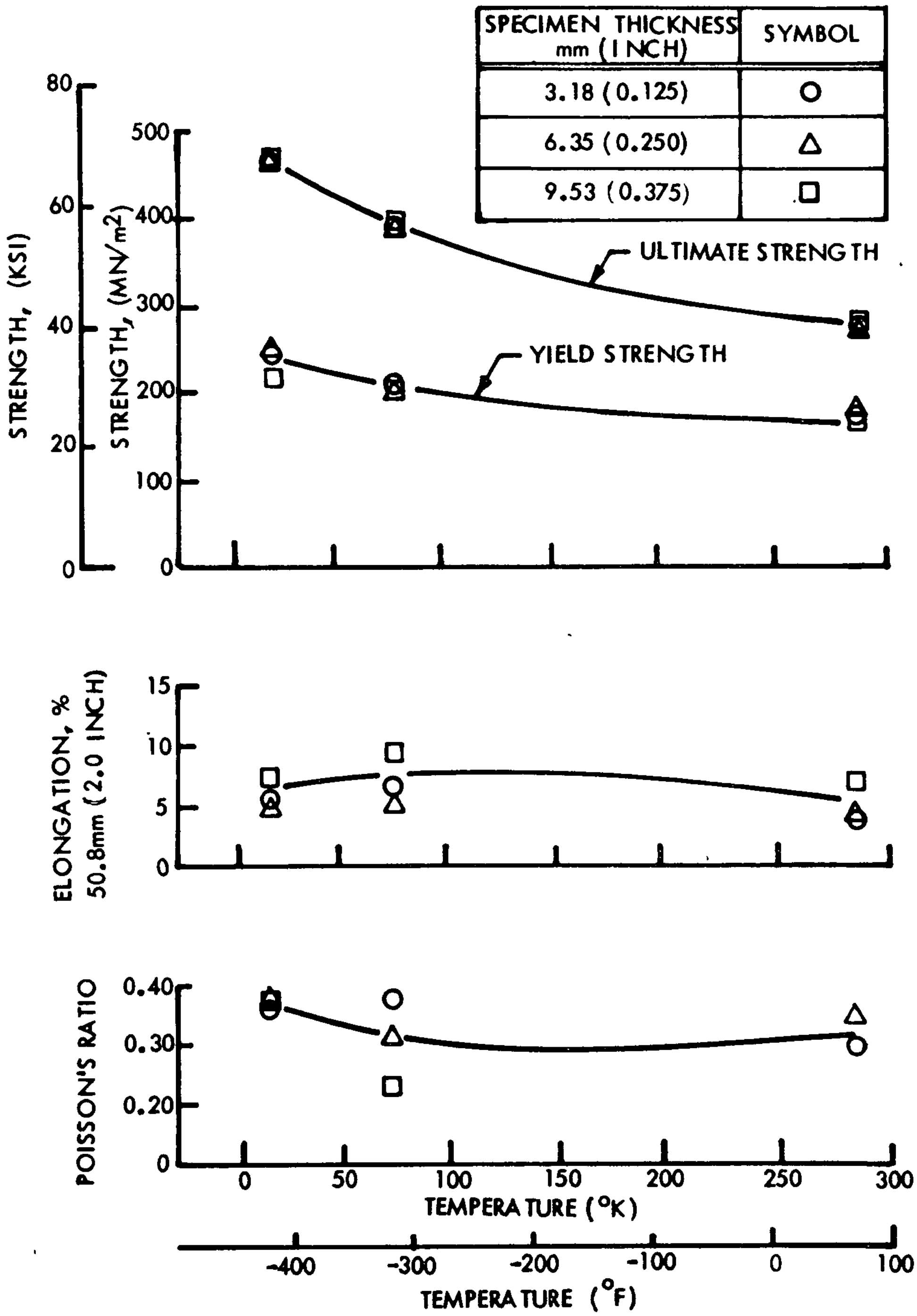

FIGURE 11: TENSILE PROPERTIES OF 2219 ALUMINUM AS-WELDED WELDMENTS

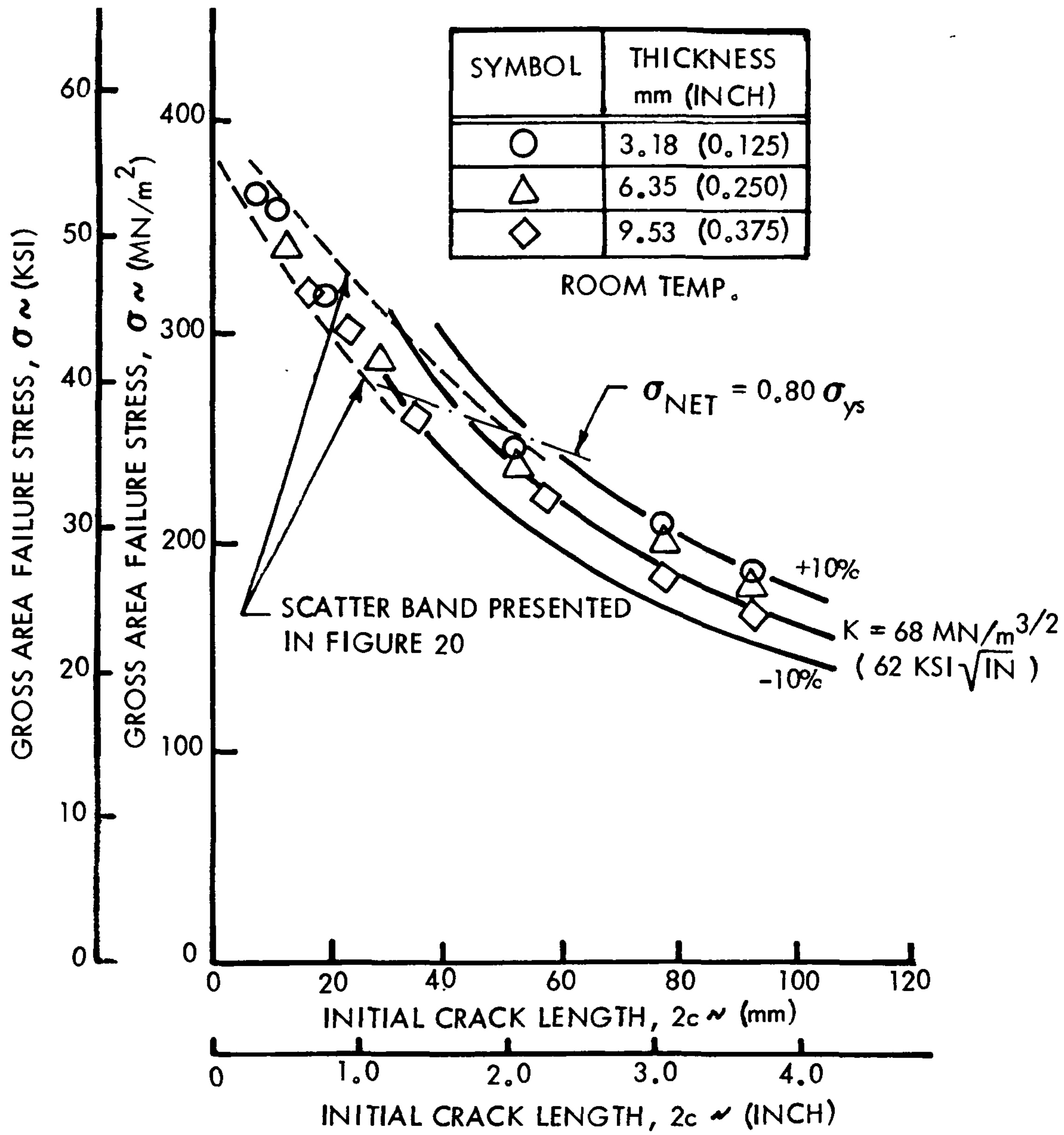

FIGURE 12: GROSS AREA FAILURE STRESS VERSUS INITIAL CRACK LENGTH FOR 2219-T87 ALUMINUM BASE METAL CENTER CRACK PANELS AT ROOM TEMPERATURE

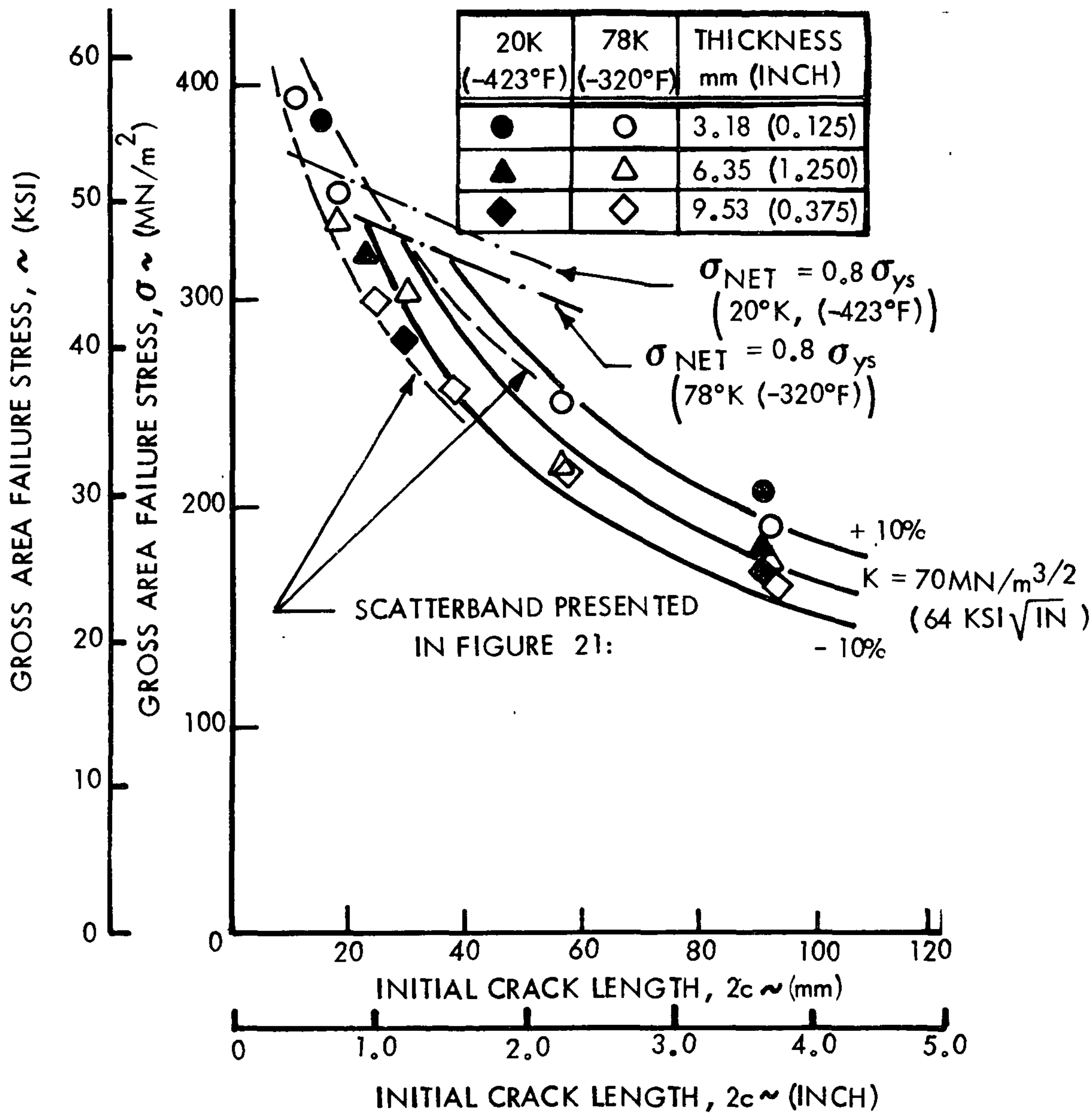

FIGURE 13: GROSS AREA FAILURE STRESS VERSUS INITIAL CRACK LENGTH FOR 2219-T87 ALUMINUM BASE METAL CENTER CRACK PANELS AT CRYOGENIC TEMPERATURE

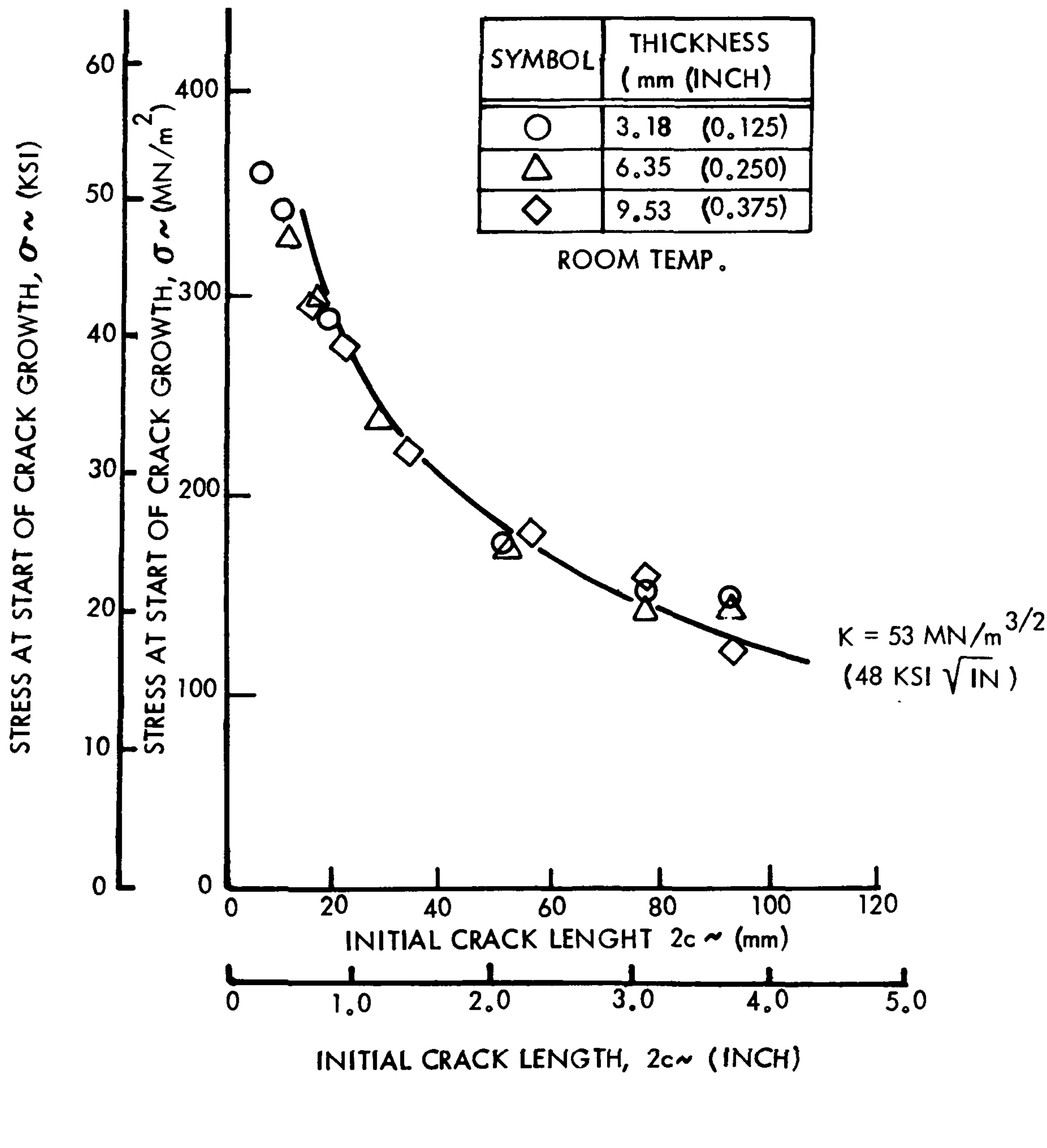

FIGURE 14: GROSS AREA STRESS AT START OF CRACK EXTENSION VERSUS INITIAL CRACK LENGTH FOR 2219-T87 ALUMINUM BASE METAL CENTER CRACK PANELS AT ROOM TEMPERATURE

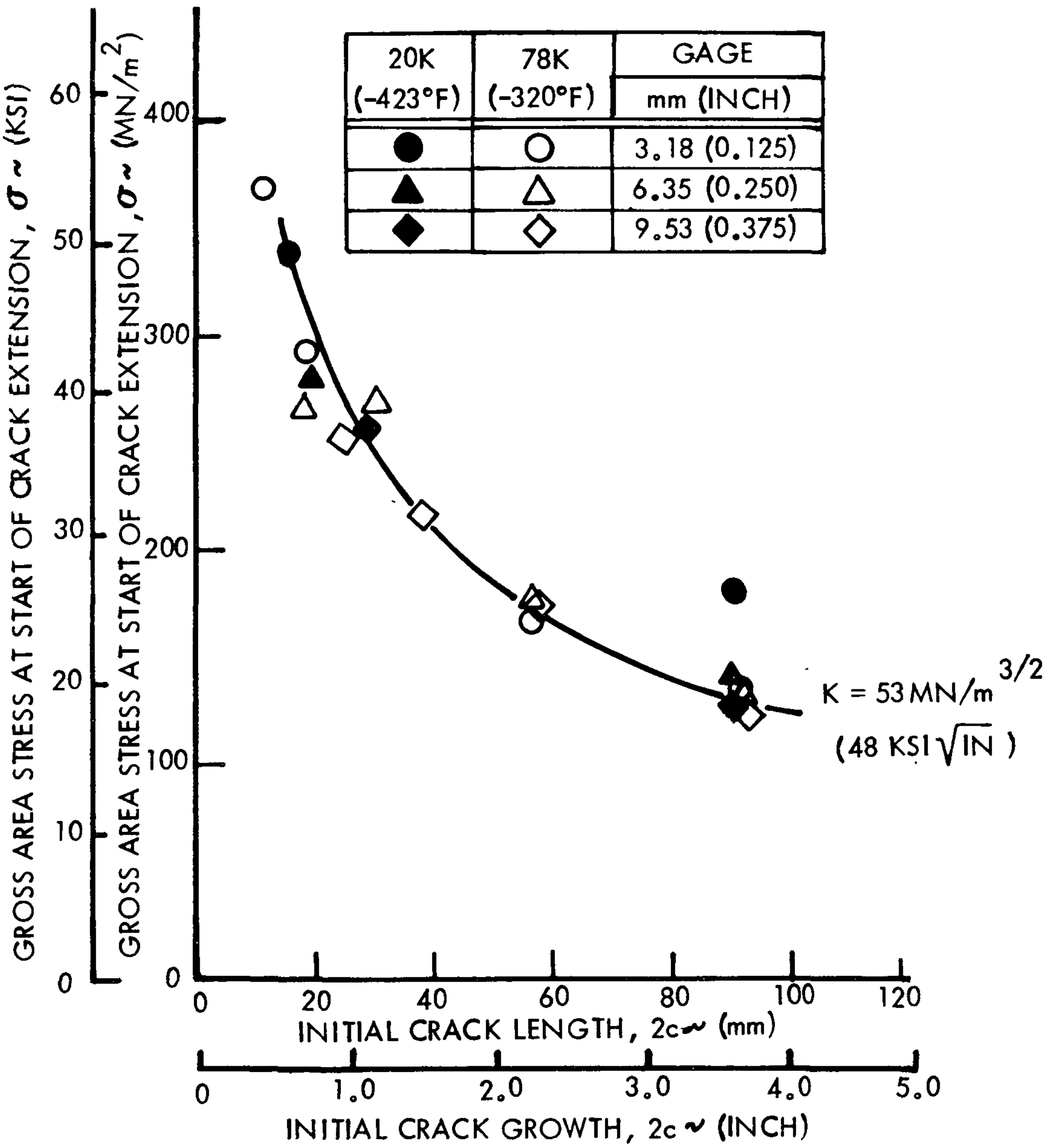

FIGURE 15: GROSS AREA STRESS AT START OF CRACK EXTENSION VERSUS INITIAL CRACK LENGTH FOR 2219-T87 ALUMINUM BASE METAL CENTER CRACK PANELS AT CRYOGENIC TEMPERATURES.

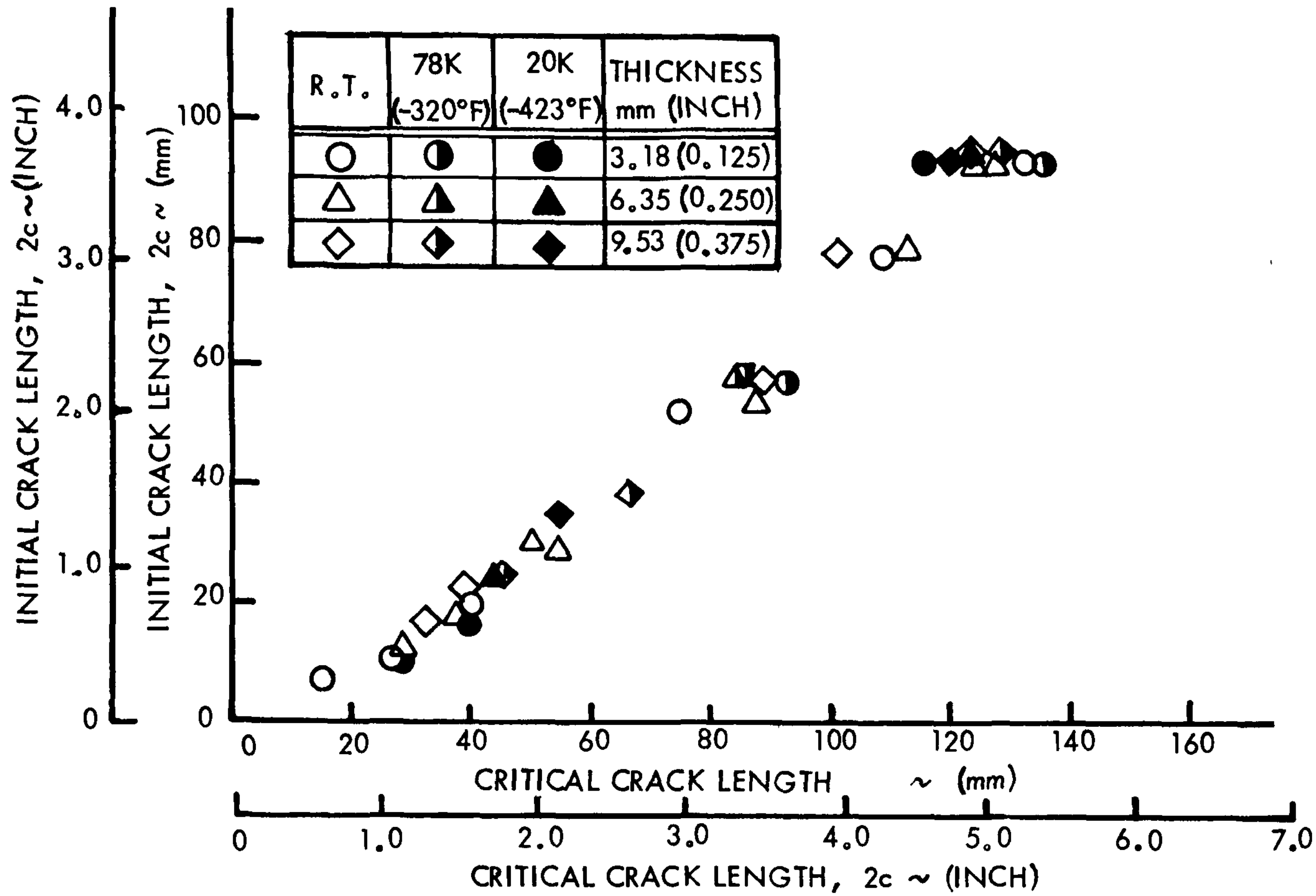

FIGURE 16: INITIAL CRACK LENGTH VERSUS CRITICAL CRACK LENGTH FOR 2219-T87 ALUMINUM BASE METAL CRACK PANELS.

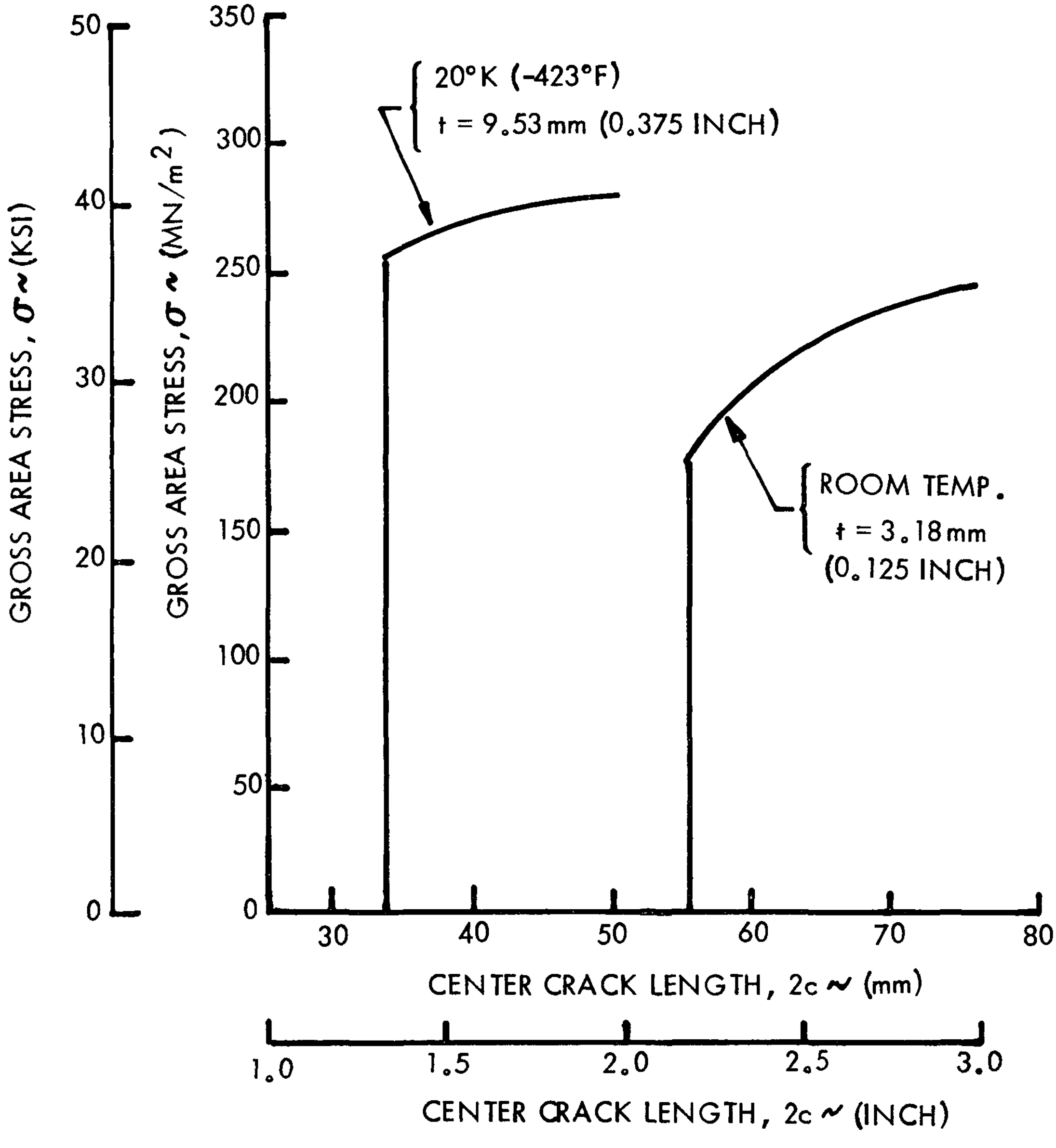

FIGURE 17: APPLIED STRESS VERSUS CRACK LENGTH FOR 2219-T87 ALUMINUM BASE METAL CENTER CRACK PANELS

ROOM TEMP.

SYMBOL	THICKNESS mm (INCH)
○	3.18 (0.125)
△	6.35 (0.250)
◇	9.53 (0.375)

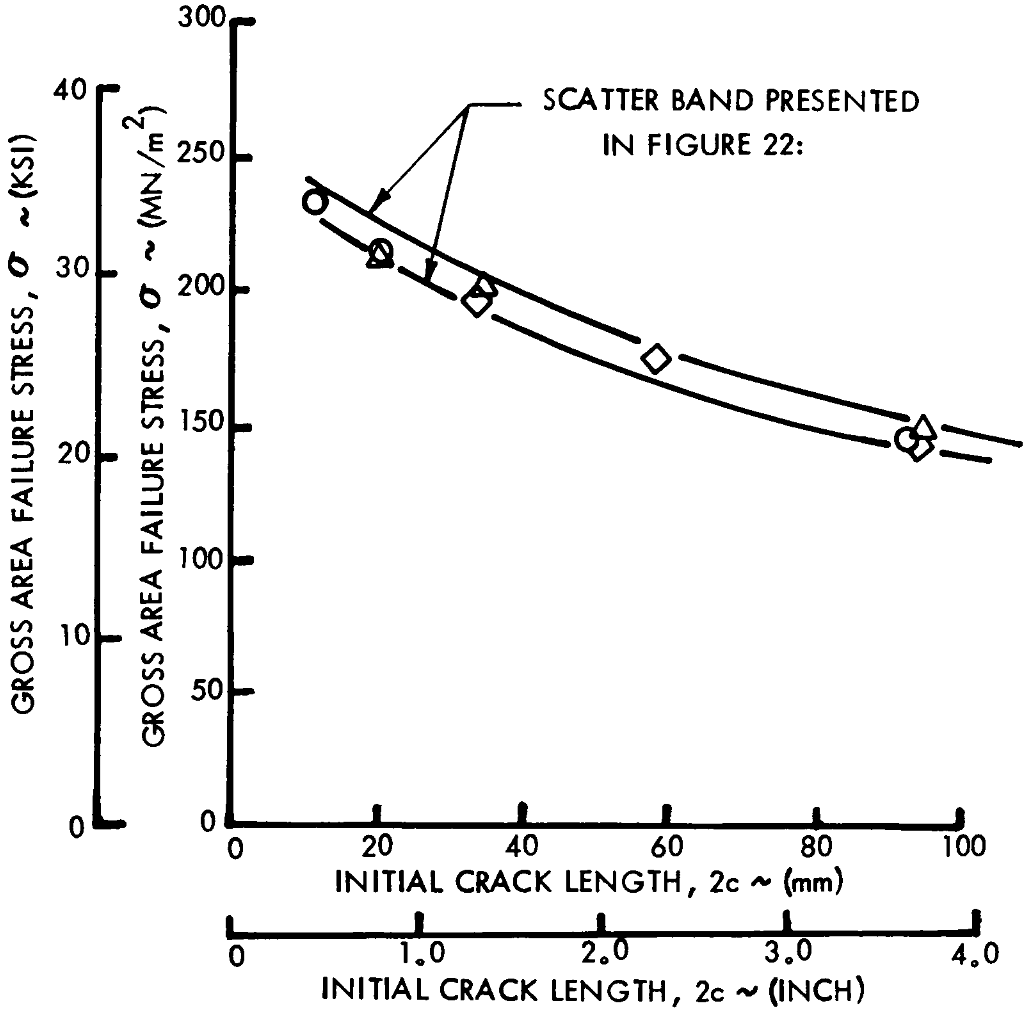

FIGURE 18: GROSS AREA FAILURE STRESS VERSUS INITIAL CRACK LENGTH FOR 2219 ALUMINUM WELD METAL CENTER CRACK PANEL AT ROOM TEMPERATURE

78K (-320°F)	20K (-423°F)	THICKNESS mm (INCH
○	●	3.18 (0.125)
△	▲	6.35 (0.250)
◇	◆	9.53 (0.375)

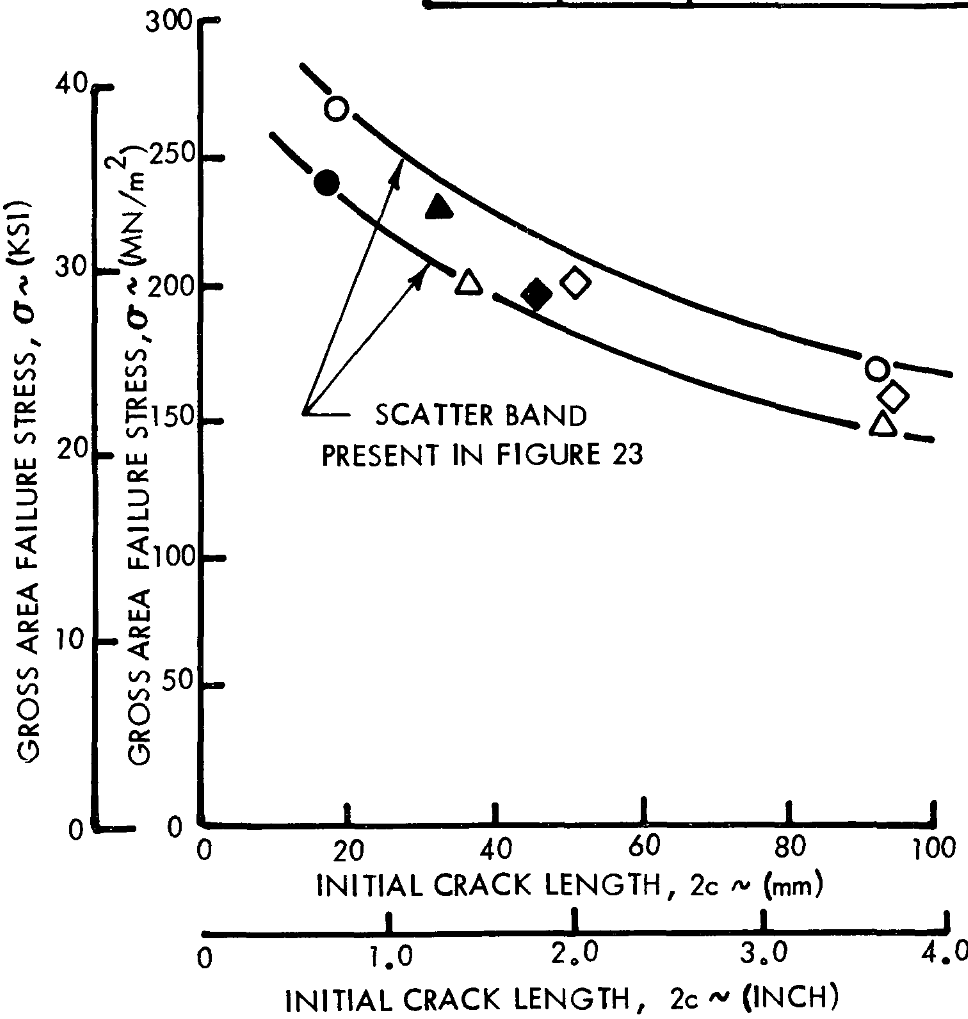

FIGURE 19: GROSS AREA FAILURE STRESS VERSUS INITIAL CRACK LENGTH FOR 2219 ALUMINUM WELD METAL CENTER CRACK PANELS AT CRYOGENIC TEMPERATURES

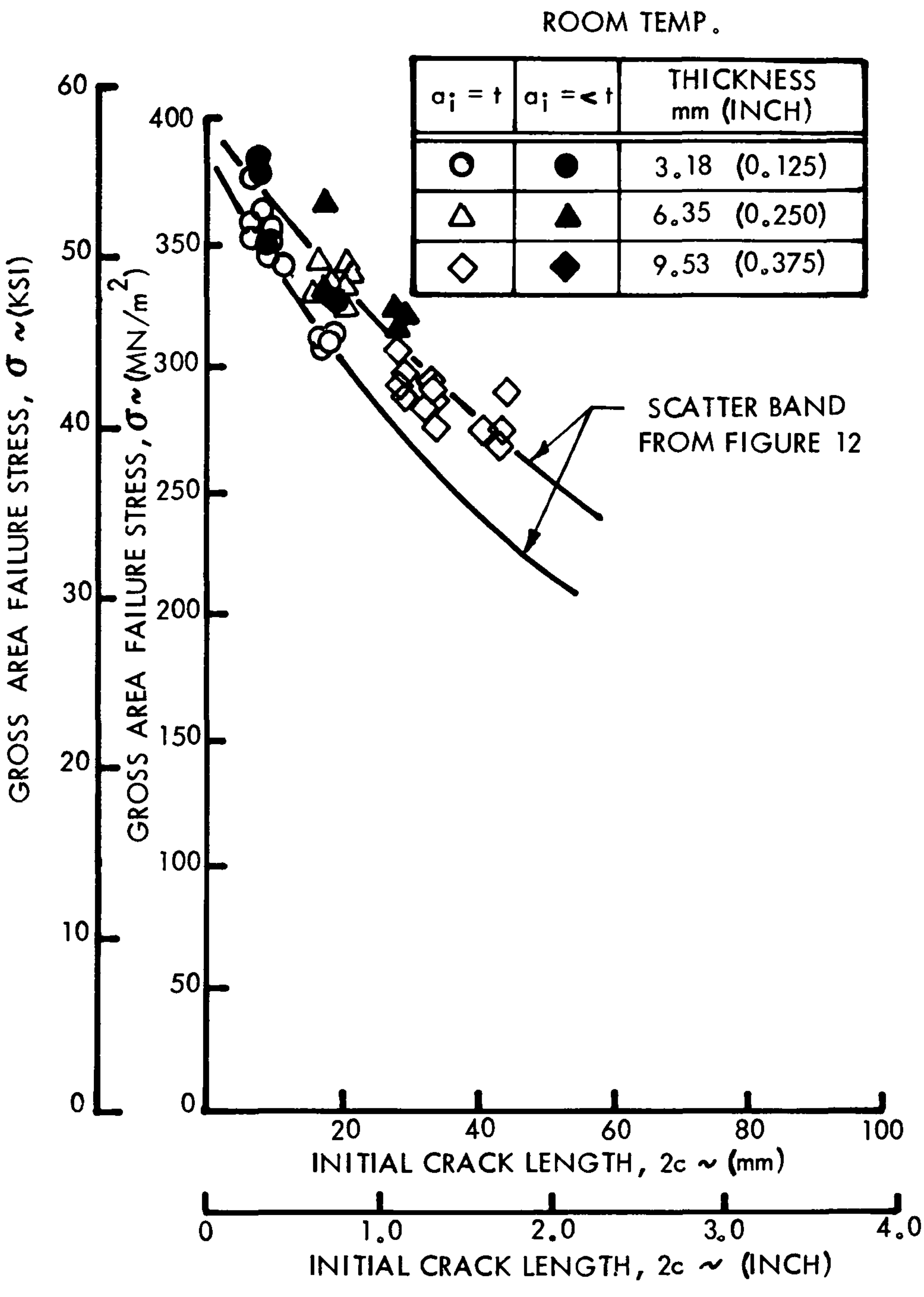

FIGURE 20: GROSS AREA FAILURE STRESS VERSUS SURFACE FLAWED CRACK LENGTH FOR 2219-T87 ALUMINUM BASE METAL SURFACE FLAWED SPECIMENS AT ROOM TEMPERATURE.

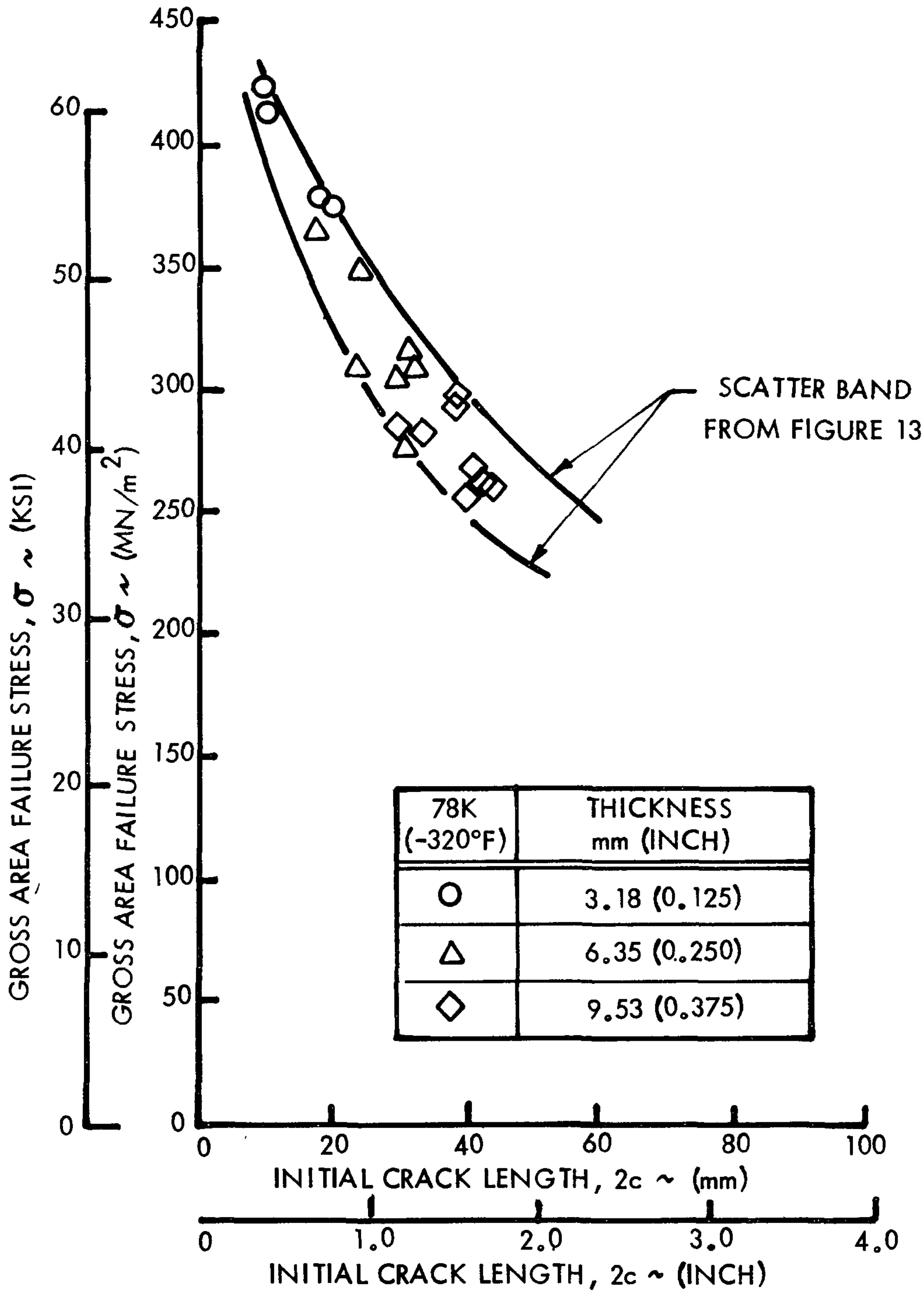

FIGURE 21: GROSS AREA FAILURE STRESS VERSUS SURFACE FLAW CRACK LENGTH FOR PENETRATED (a = t) 2219-T87 ALUMINUM BASE METAL SURFACE FLAWED SPECIMENS AT LIQUID NITROGEN TEMPERATURE

ROOM TEMP.

SYMBOL	THICKNESS mm (INCH)
○	3.18 (0.125)
△	6.35 (0.250)
◇	9.53 (0.375)

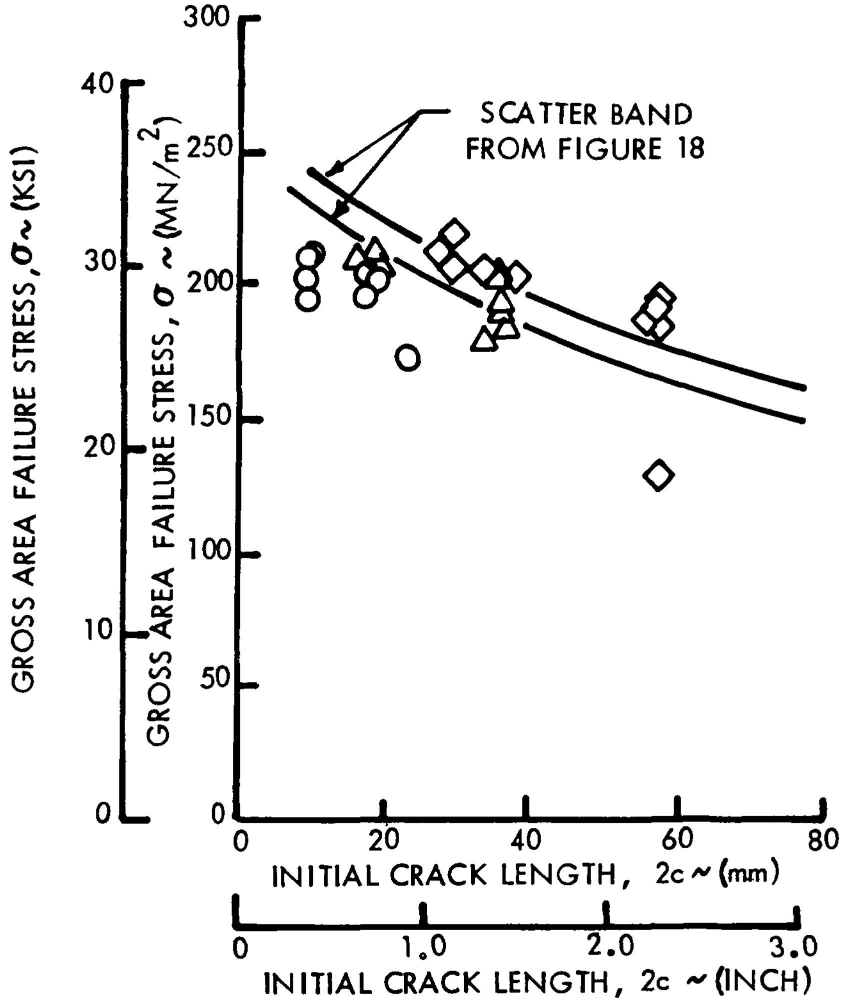

FIGURE 22: GROSS AREA FAILURE STRESS VERSUS INITIAL CRACK LENGTH FOR 2219 ALUMIUM ALUMINUM WELD METAL CENTER CRACK PANELS AT ROOM TEMPERATURE

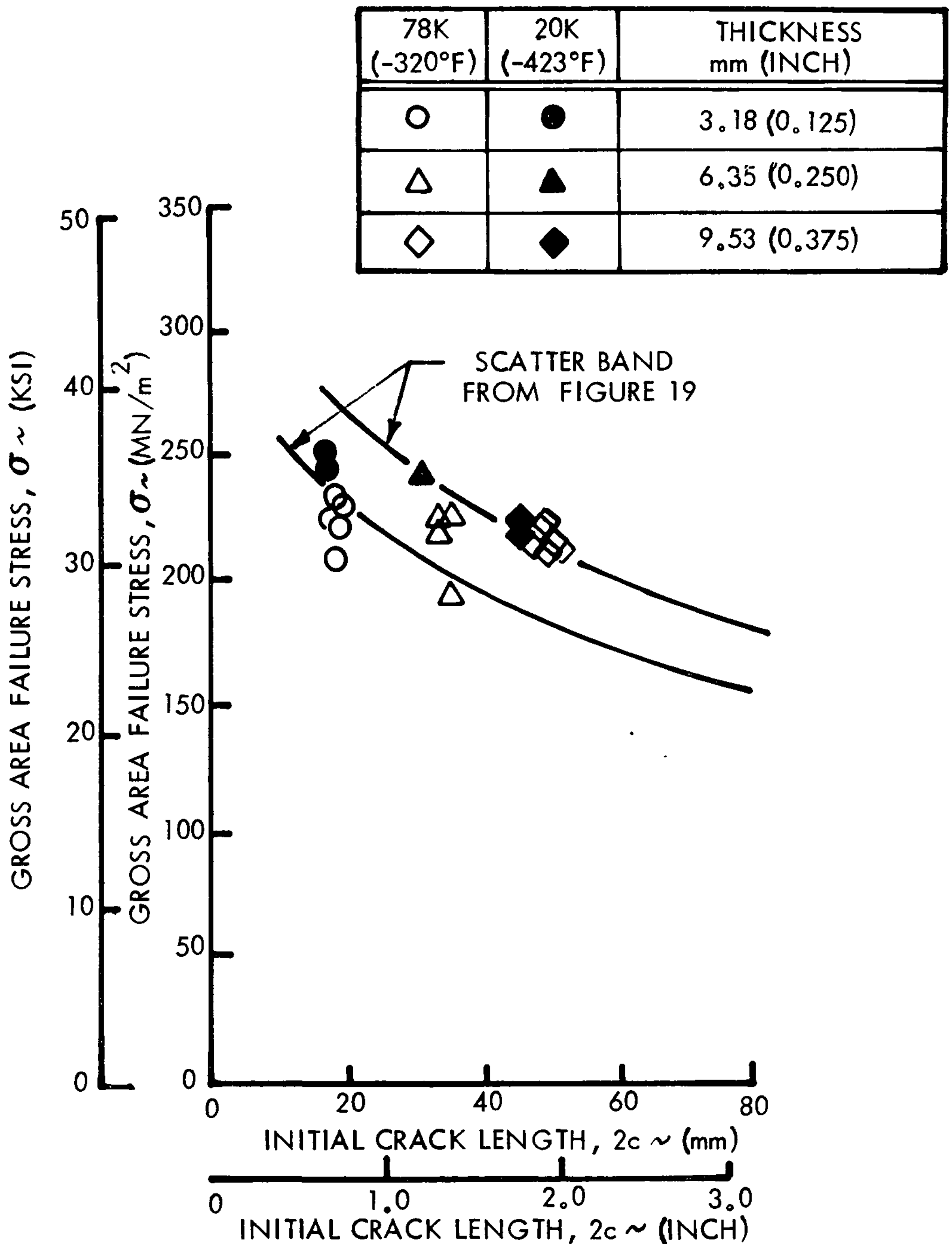

FIGURE 23: GROSS AREA FRACTURE STRESS VERSUS INITIAL CRACK LENGTH FOR 2219 ALUMINUM WELD METAL CENTER CRACK PANELS AT CRYOGENIC TEMPERATURE.

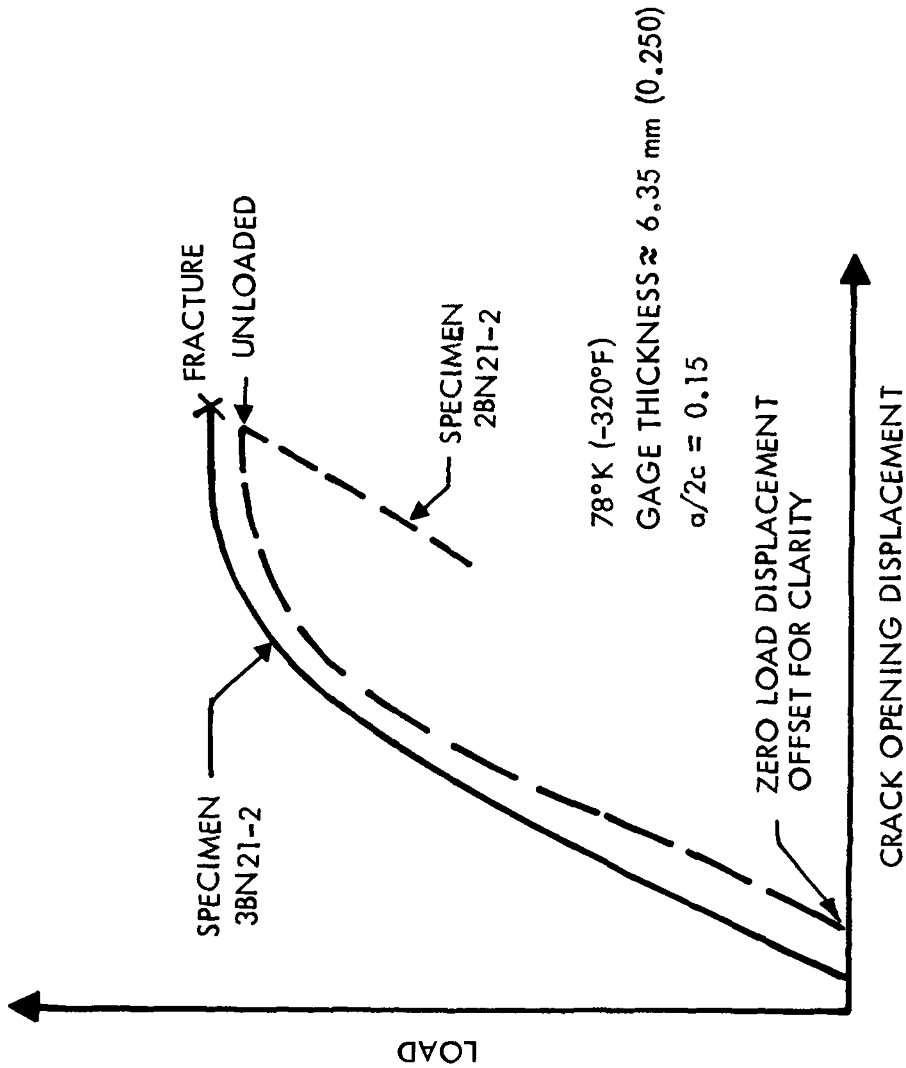

FIGURE 24: LOAD VERSUS CRACK OPENING DISPLACEMENT

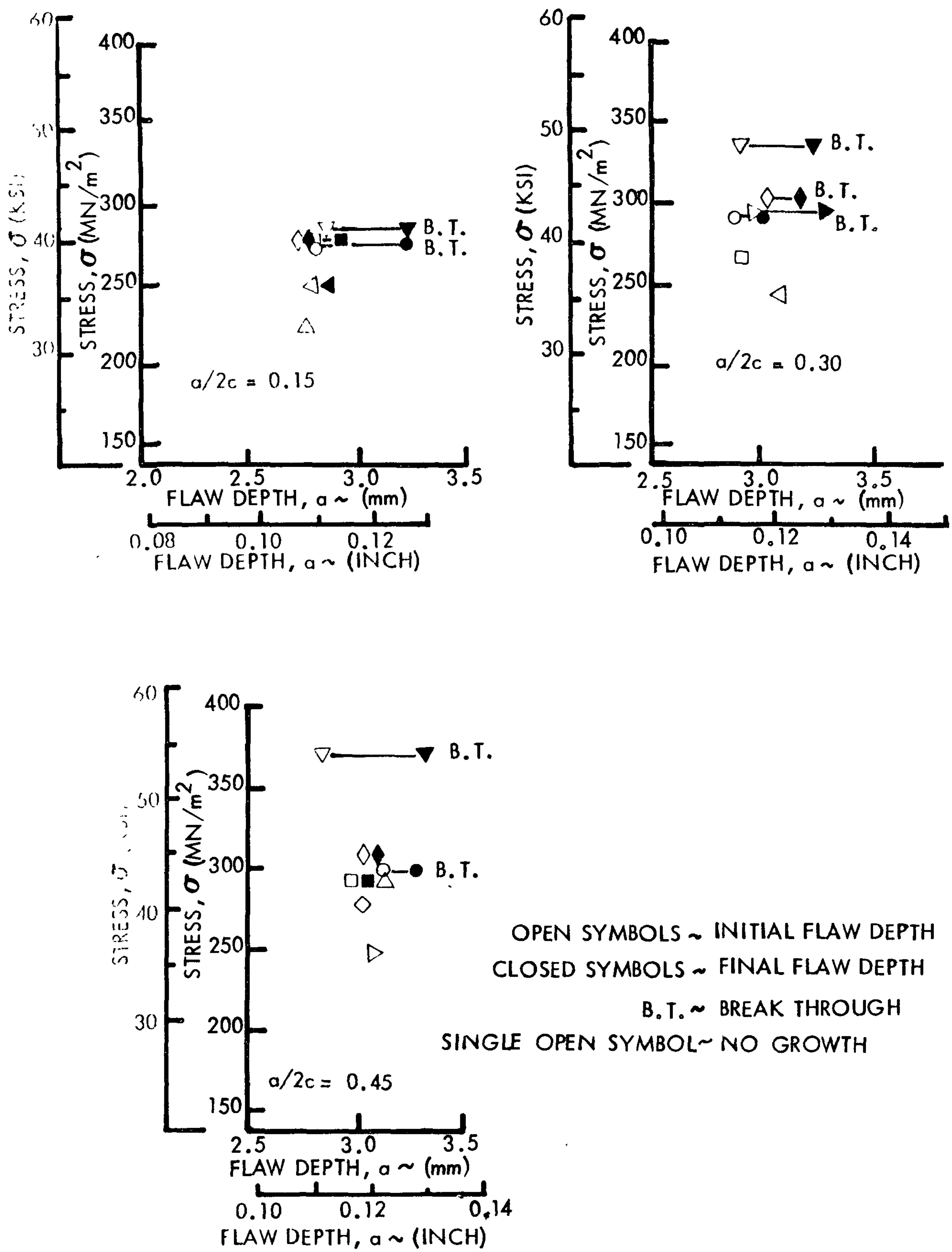

FIGURE 25: GROWTH-ON-LOADING TEST RESULTS FOR 3.18mm (0.125 INCH) THICK 2219-T87 ALUMINUM BASE METAL AT ROOM TEMPERATURE

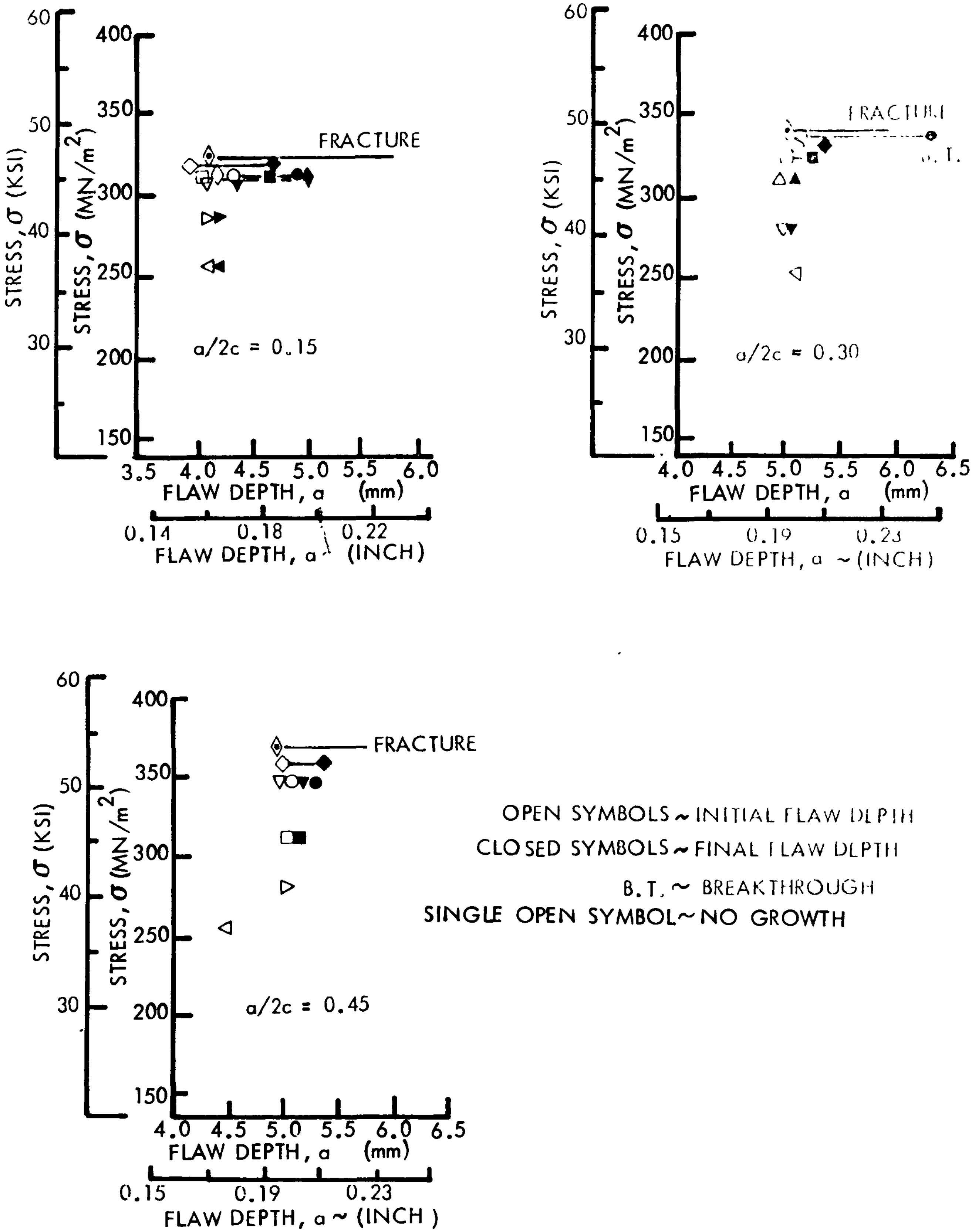

FIGURE 26: GROWTH-ON-LOADING TEST RESULTS FOR 6.35 mm (0.250 INCH) THICK 2219-T87 ALUMINUM BASE METAL AT ROOM TEMPERATURE

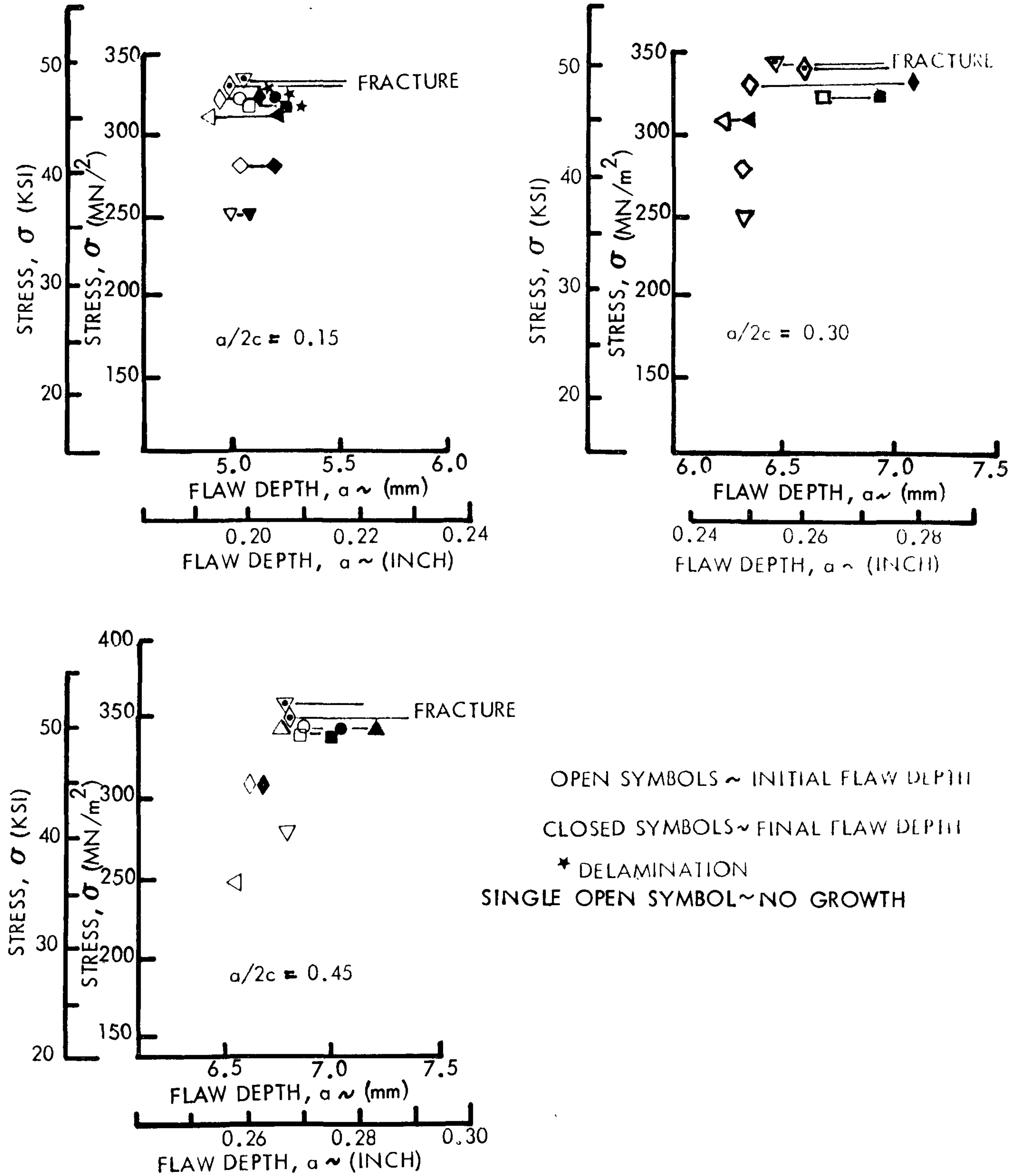

FIGURE 27: GROWTH-ON-LOADING TEST RESULTS FOR 9.53 mm (0.375 INCH) THICK 2219-T87 ALUMINUM BASE METAL AT ROOM TEMPERATURE

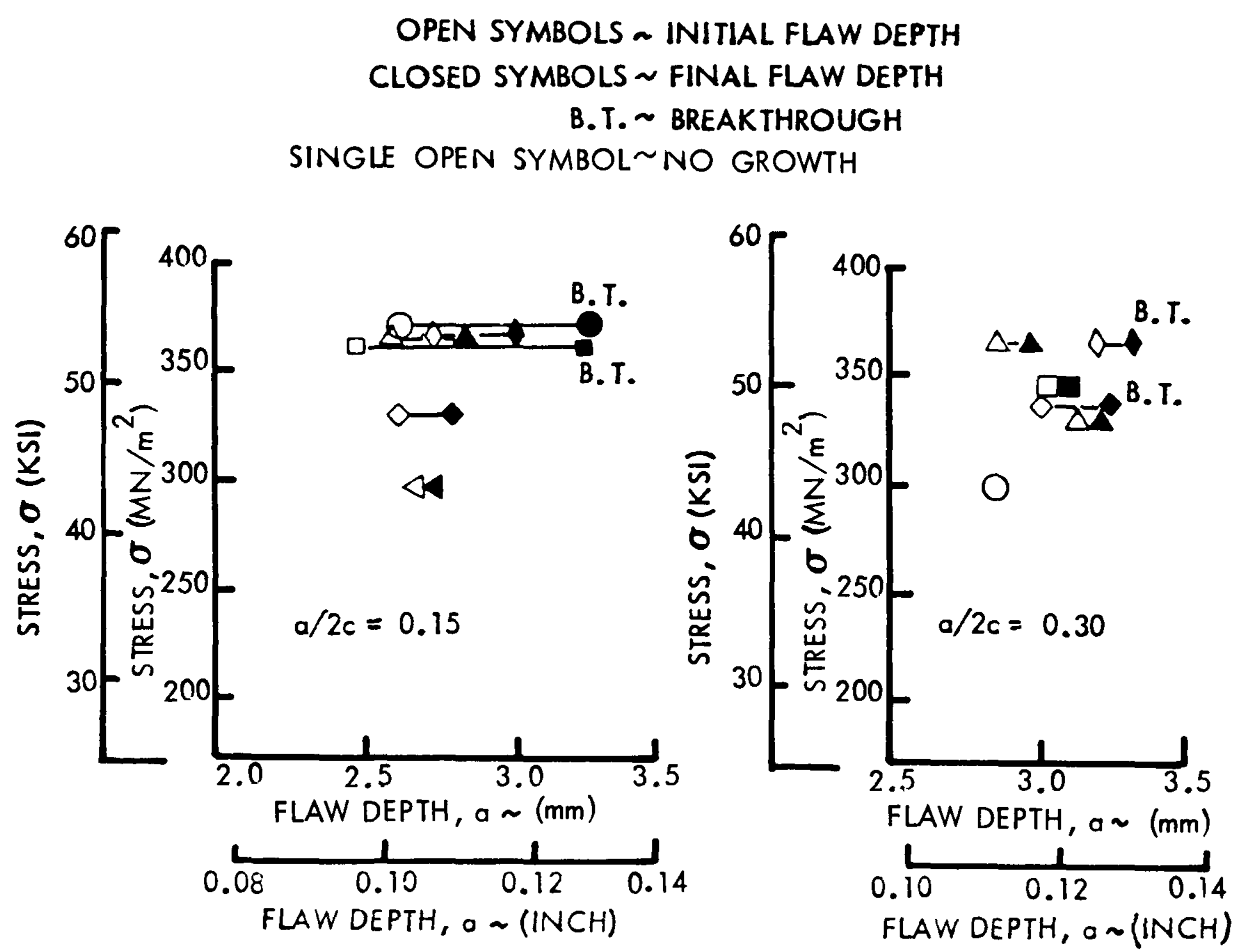

FIGURE 28: GROWTH-ON-LOADING TEST RESULTS FOR 3.18 mm (0.125 INCH) THICK 2219-T87 ALUMINUM BASE METAL AT 78°K (-320°F)

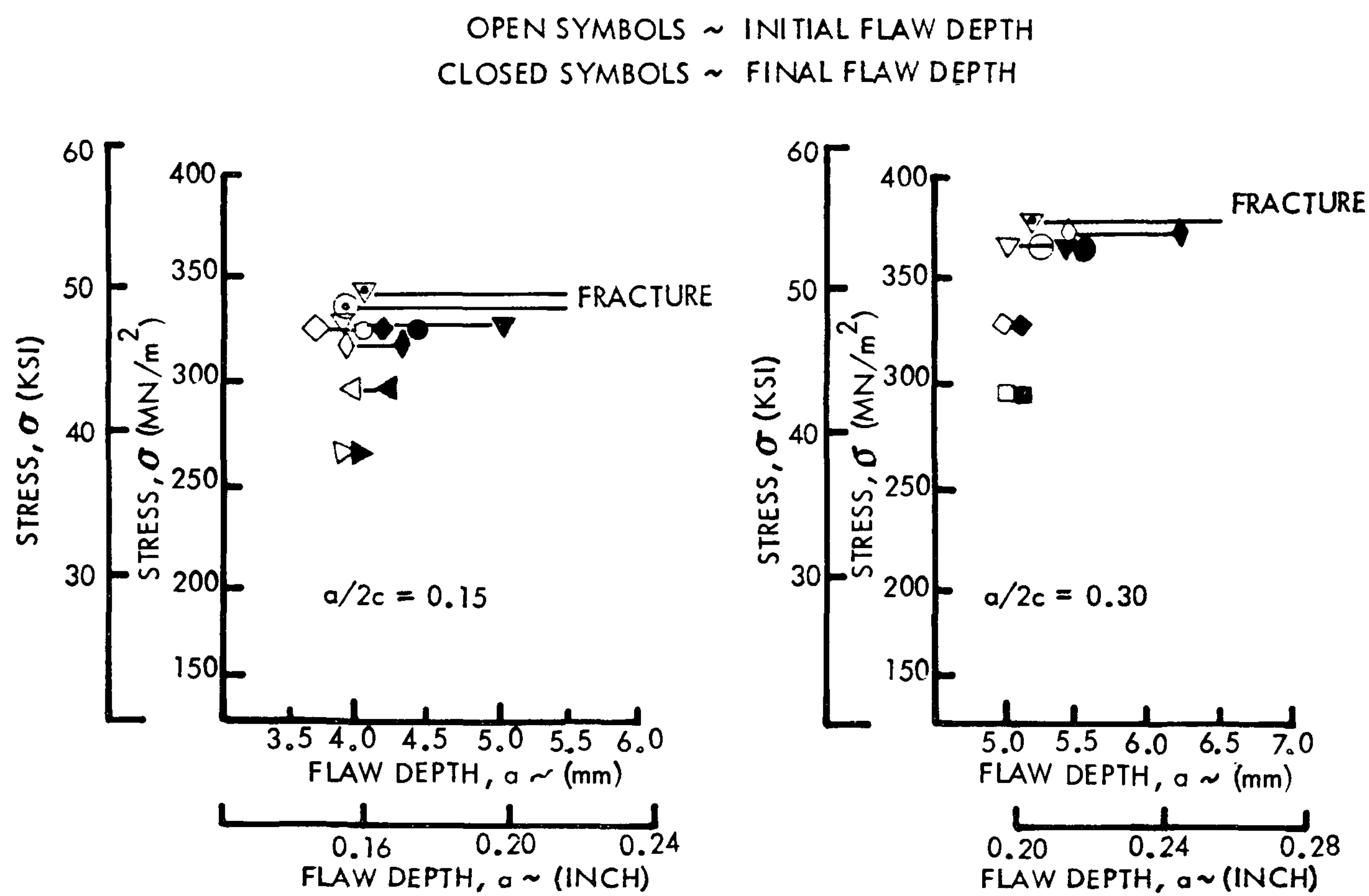

FIGURE 29: GROWTH-ON-LOADING TEST RESULTS FOR 6.35 mm (0.250 INCH) THICK 2219-T87 ALUMINUM BASE METAL AT 78°K (-320°F)

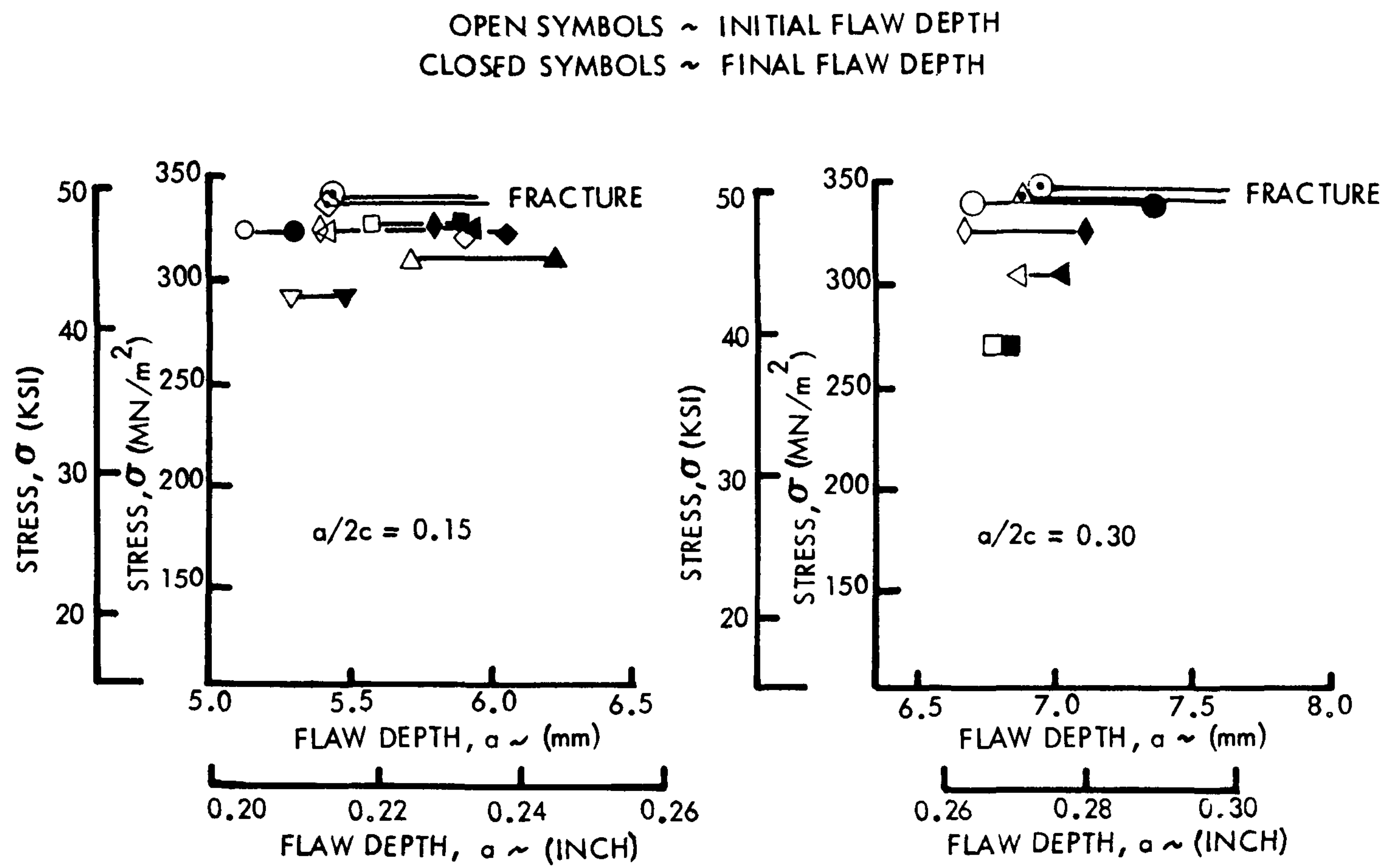

FIGURE 30: GROWTH-ON-LOADING TEST RESULTS FOR 6.35mm (0.375 INCH) THICK 2219-T87 ALUMINUM BASE METAL AT 78°K (-320°F)

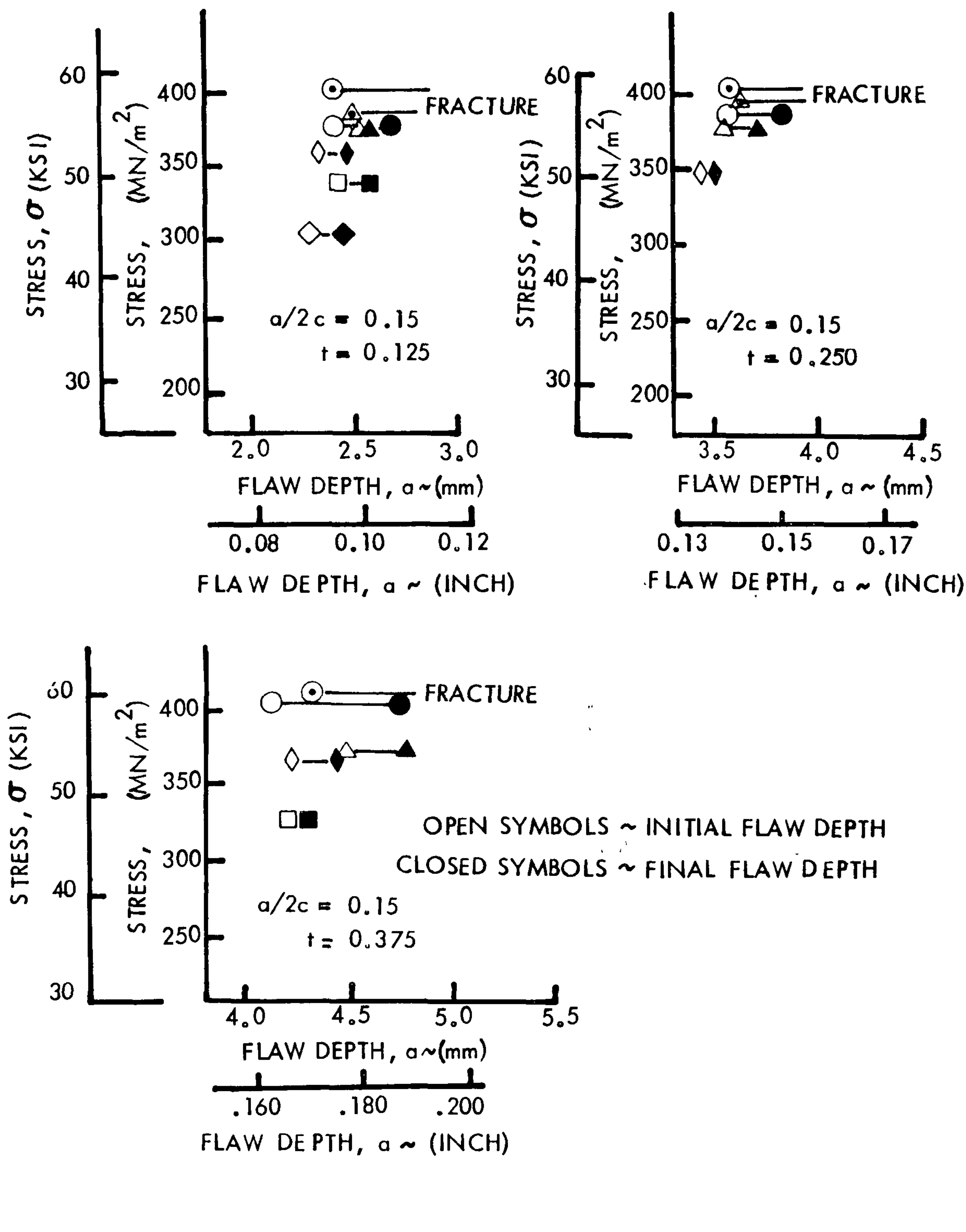

FIGURE 31: GROWTH-ON-LOADING TEST RESULTS FOR 2219-T87 ALUMINUM BASE METAL AT 20°K (-423°F)

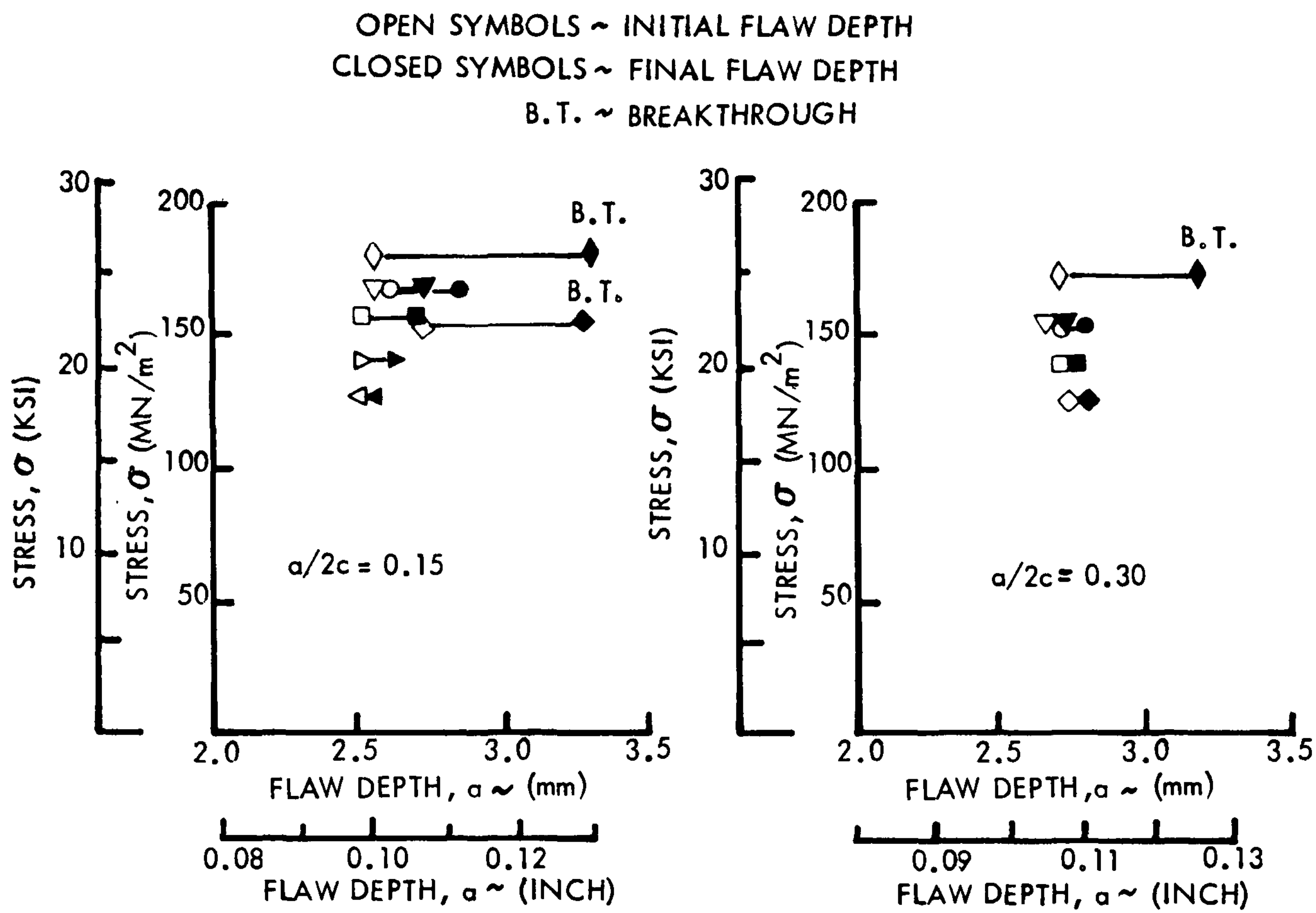

FIGURE 32: GROWTH-ON-LOADING TEST RESULTS FOR 3.18 mm (0.125 INCH) THICK 2219 ALUMINUM WELDMENTS AT ROOM TEMPERATURE

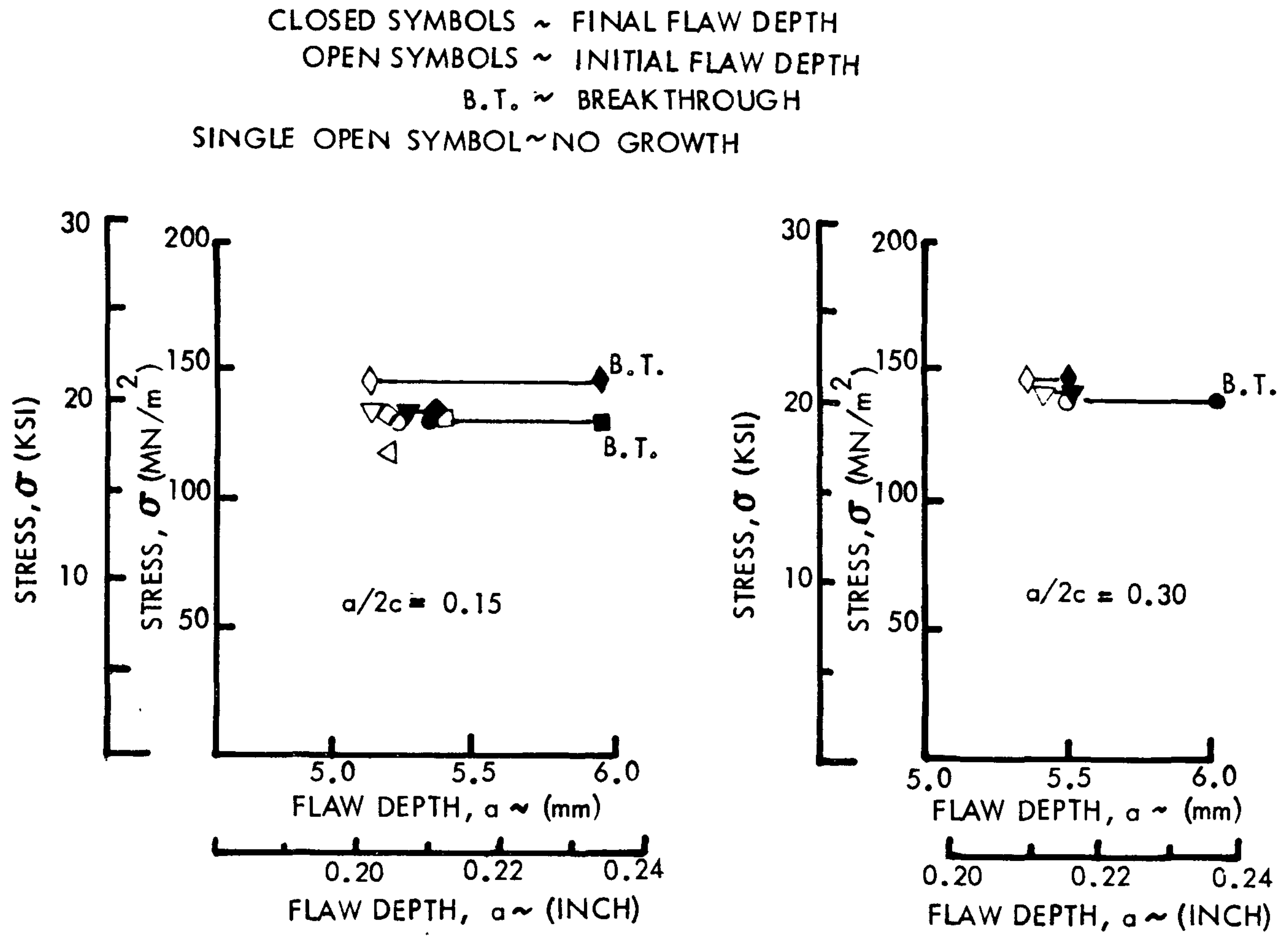

FIGURE 33: GROWTH-ON-LOADING TEST RESULTS FOR 6.35 mm (0.250 INCH) THICK 2219 ALUMINUM WELDMENTS AT ROOM TEMPERATURE

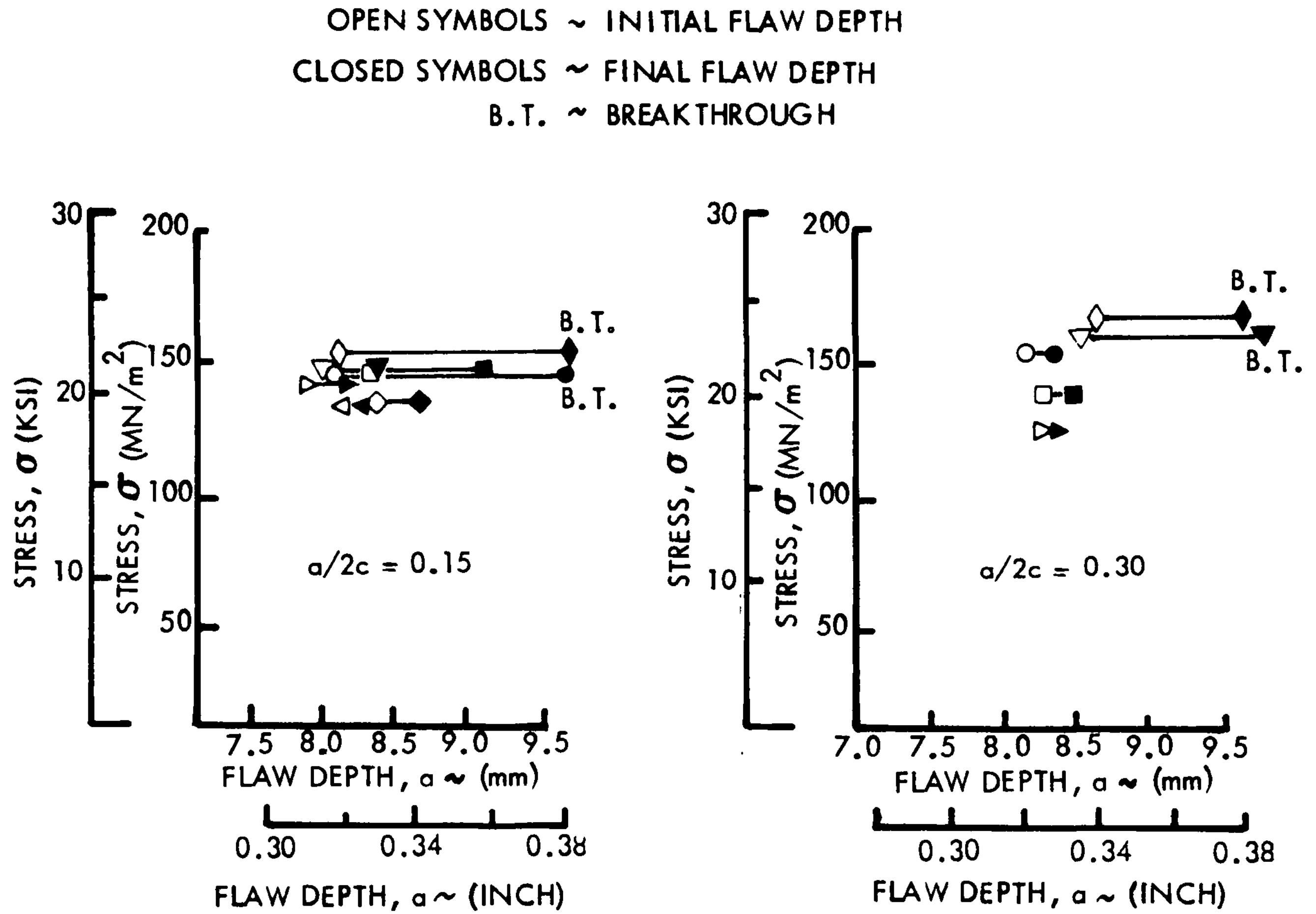

FIGURE 34: GROWTH-ON-LOADING TEST RESULTS FOR 9.53 mm (0.375 INCH) THICK 2219 ALUMINUM WELDMENTS AT ROOM TEMPERATURE

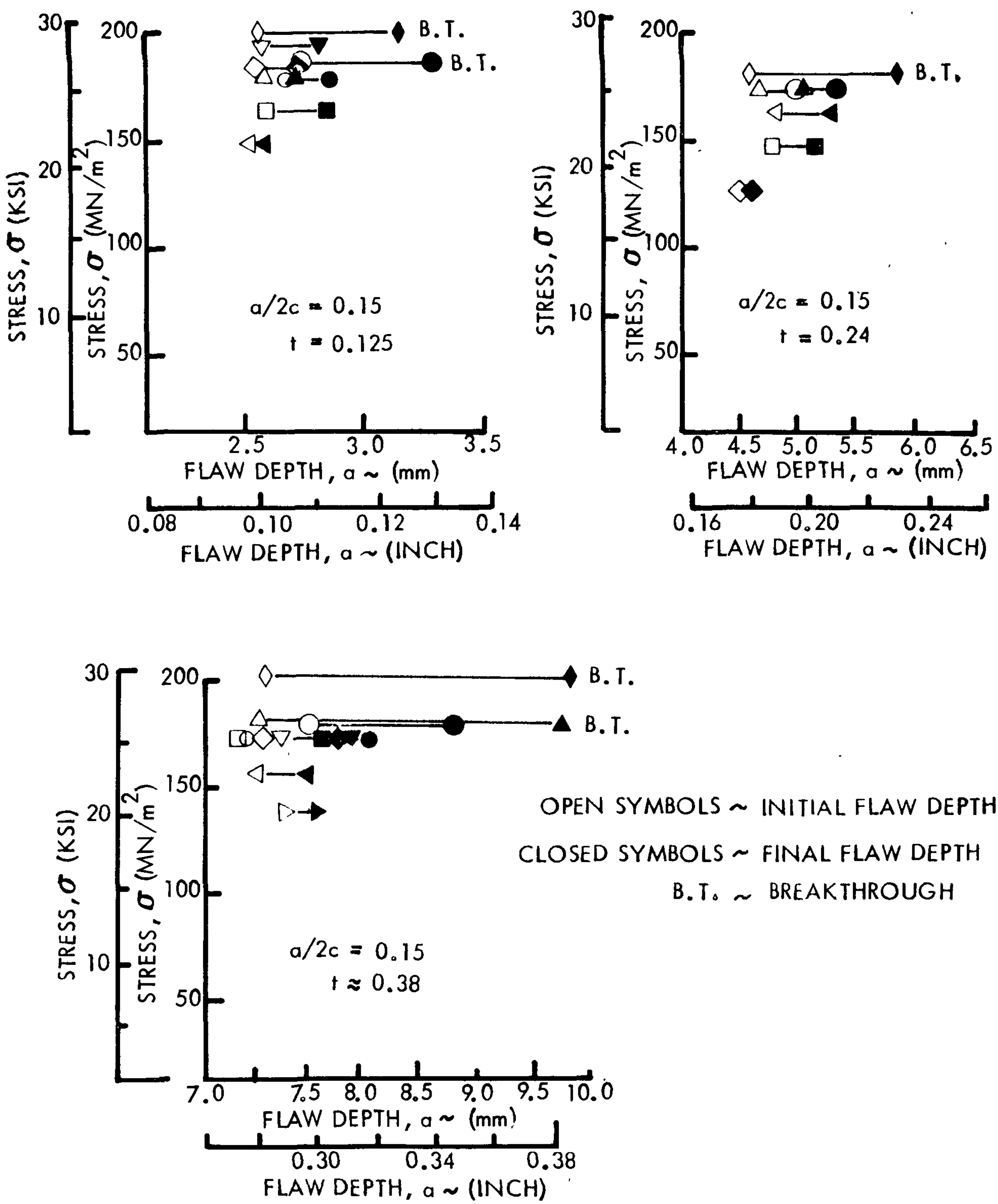

FIGURE 35: GROWTH-ON-LOADING TEST RESULTS FOR 2219 ALUMINUM WELDMENTS AT 78°K (-320°F)

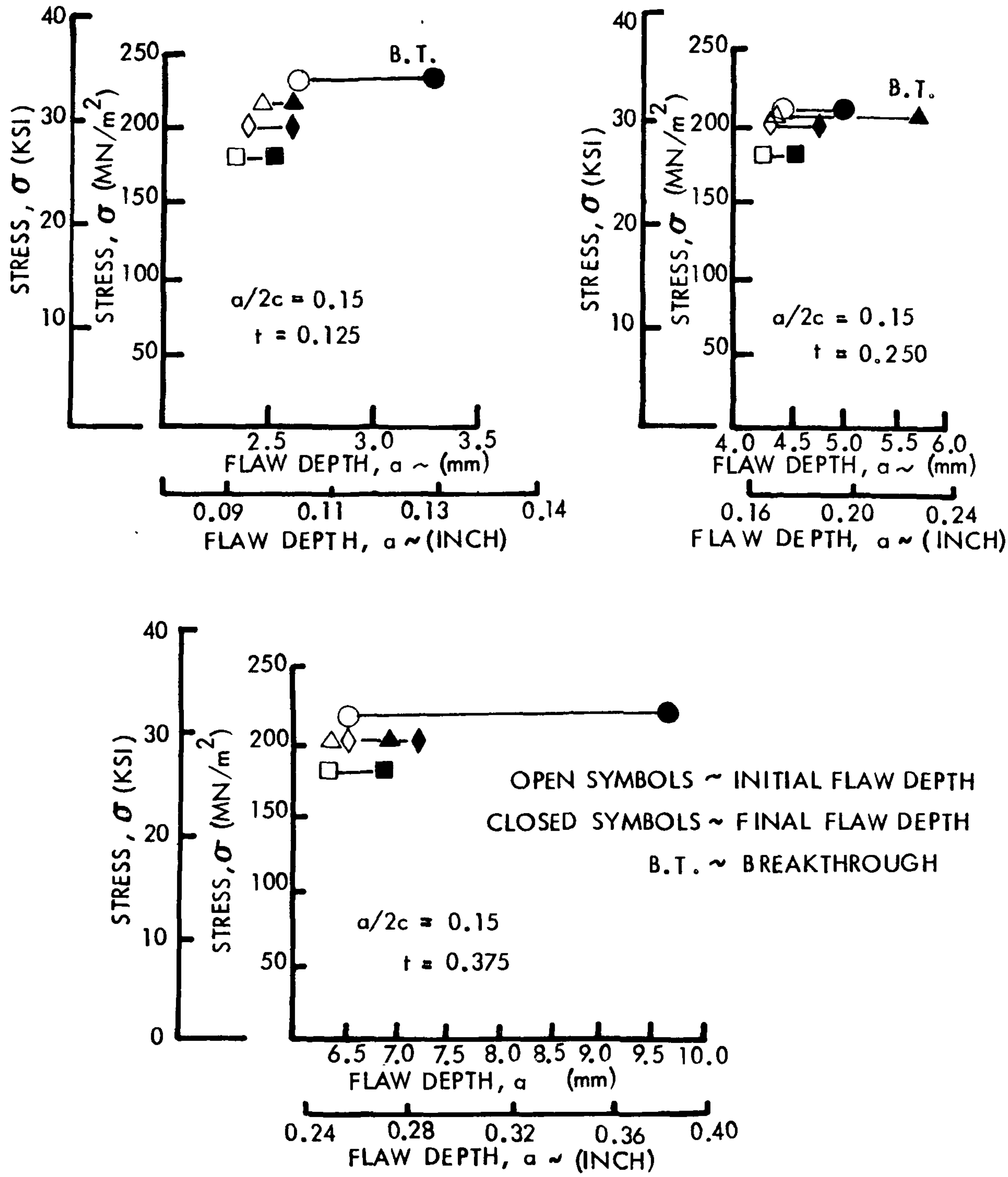

FIGURE 36: GROWTH-ON-LOADING TEST RESULTS FOR 2219 ALUMINUM WELDMENTS AT 20°K (-423°F)

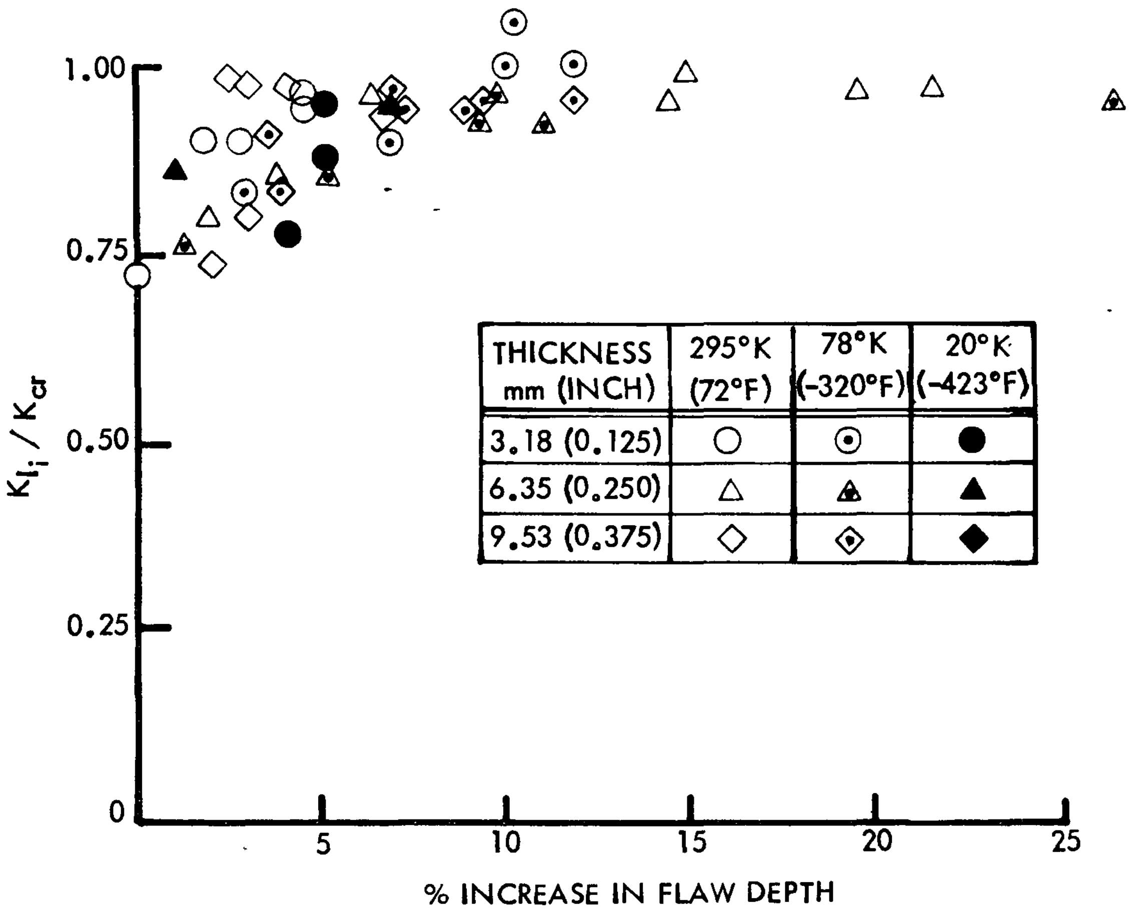

FIGURE 37: 2219-T87 ALUMINUM BASE METAL GROWTH-ON-LOADING TEST RESULTS ($a/2c \approx 0.15$)

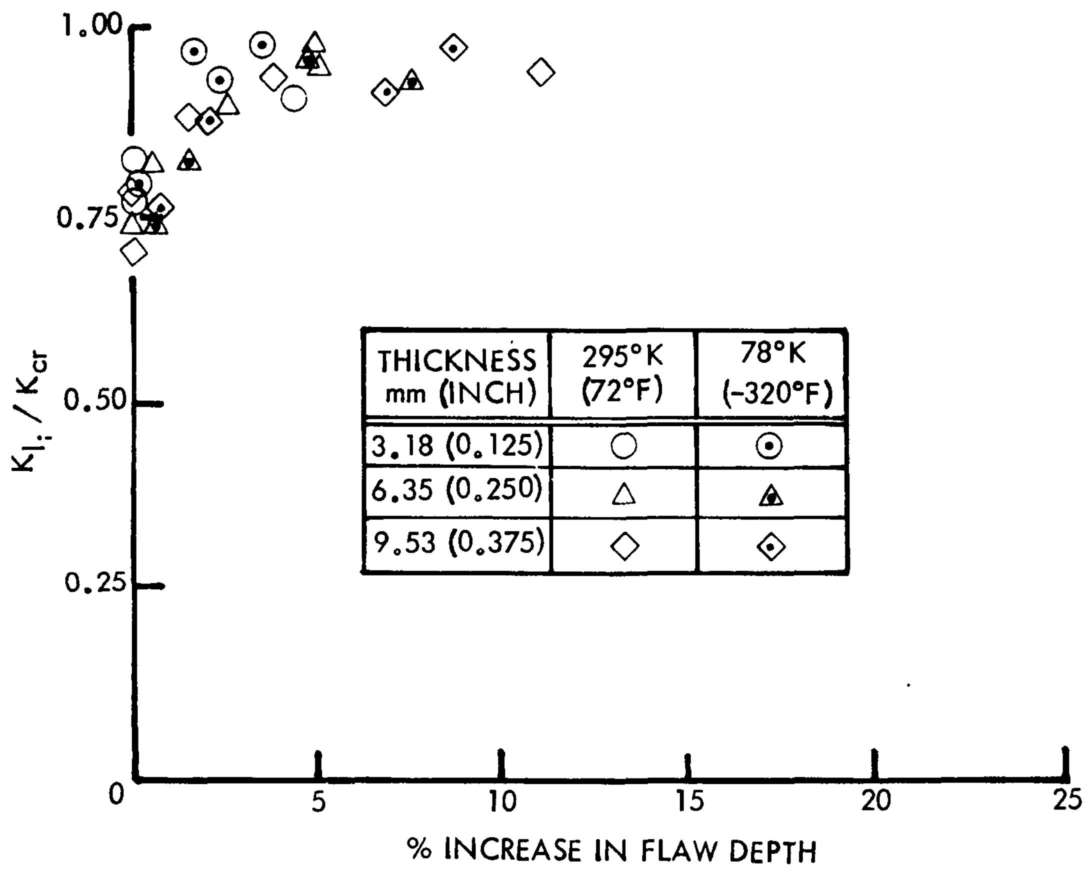

FIGURE 38: 2219-T87 ALUMINUM BASE METAL GROWTH-ON-LOADING TEST RESULTS ($a/2c \approx 0.30$)

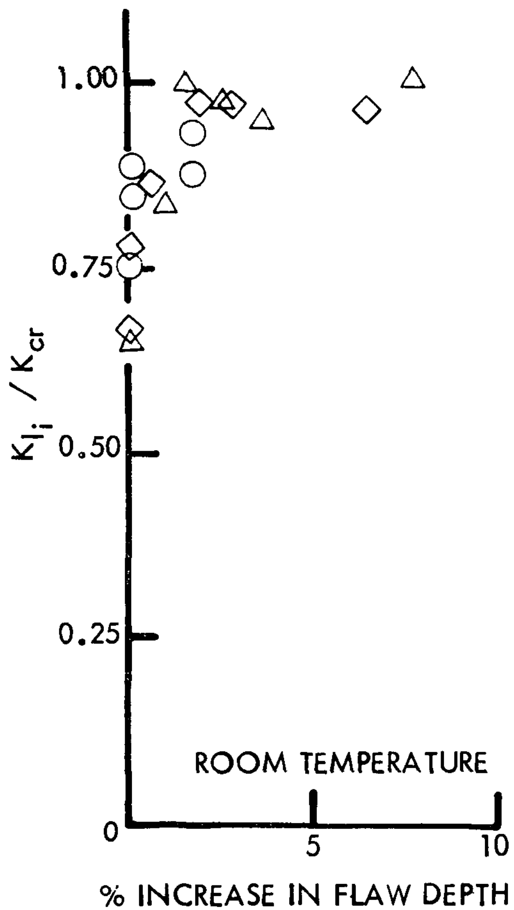

FIGURE 39: 2219-T87 ALUMINUM BASE METAL GROWTH-ON-LOADING TEST RESULTS ($a/2c \approx 0.45$)

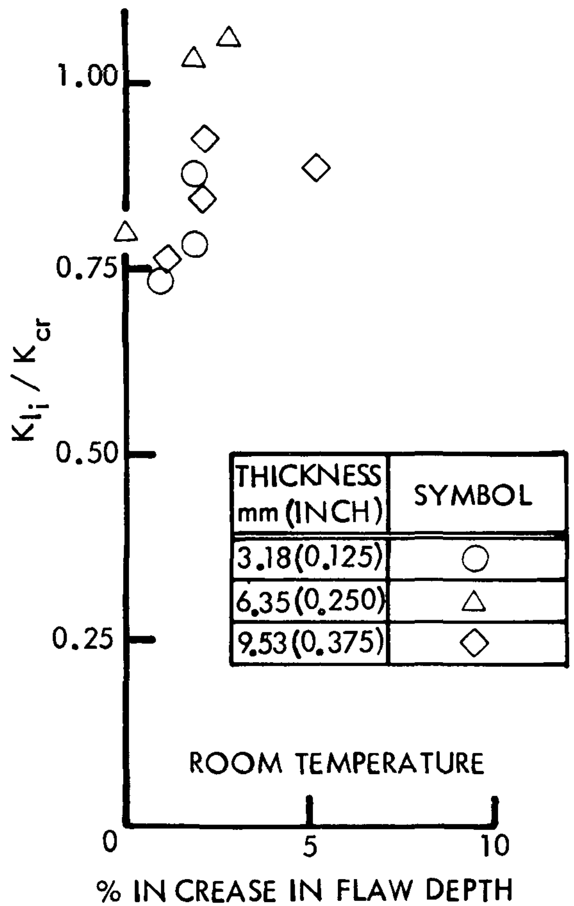

FIGURE 40: 2219 ALUMINUM WELDMENTS GROWTH-ON-LOADING TEST RESULTS ($a/2c \approx 0.30$)

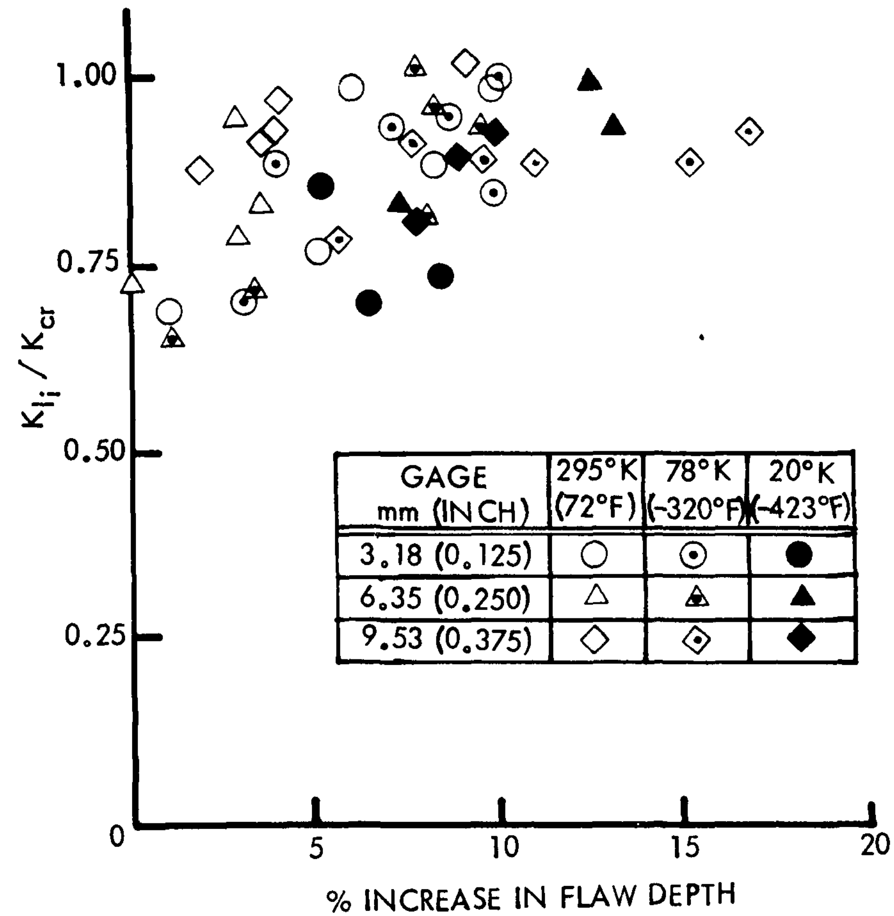

FIGURE 41: 2219 ALUMINUM WELDMENTS GROWTH-ON-LOADING TEST RESULTS (a/2c ≈ 0.15)

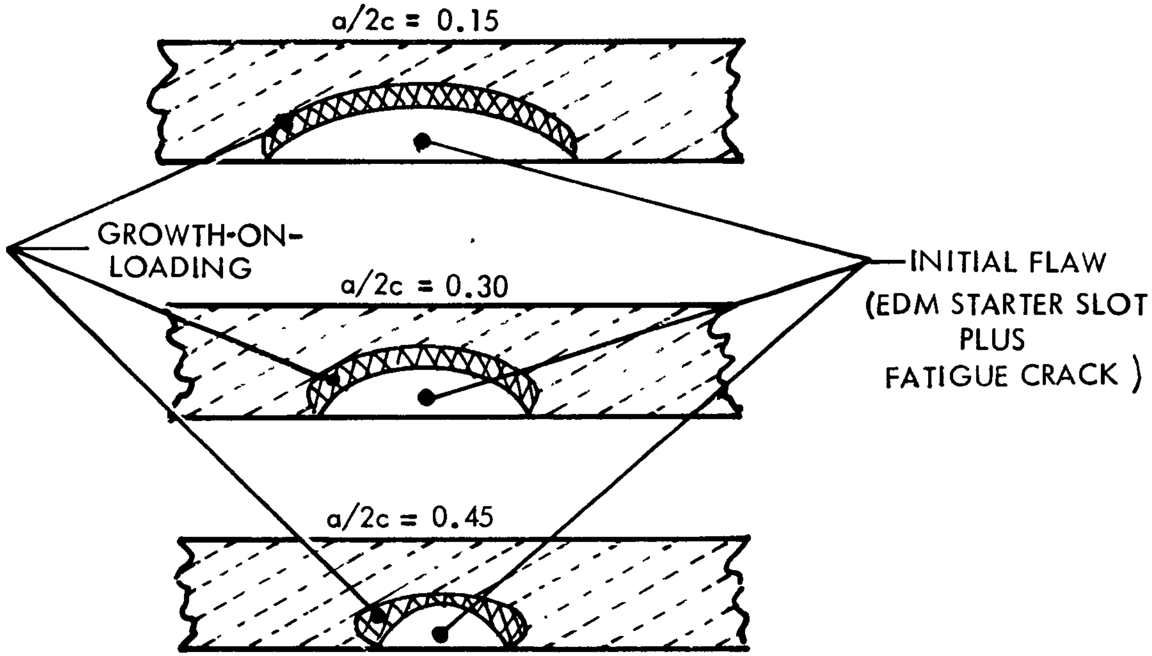

FIGURE 42: ILLUSTRATION OF GROWTH-ON-LOADING FOR VARIOUS FLAW SHAPES

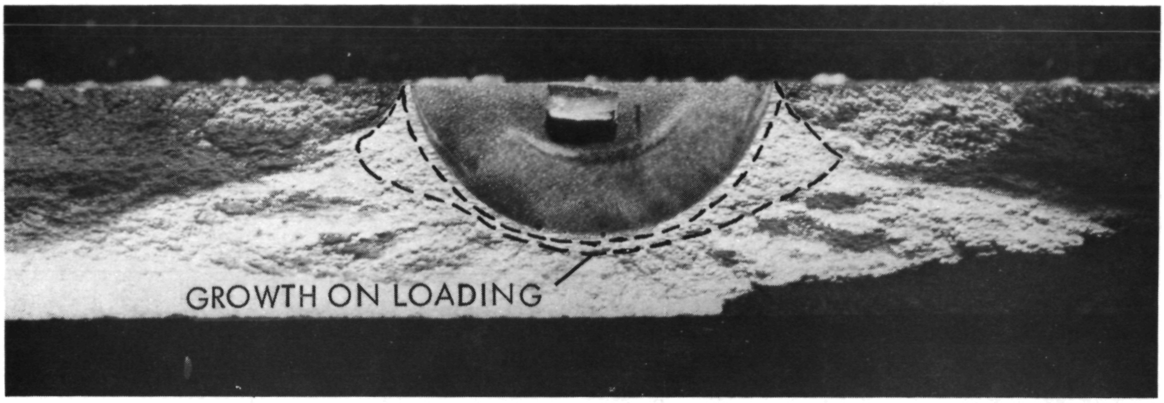

(a) 2BR34-4

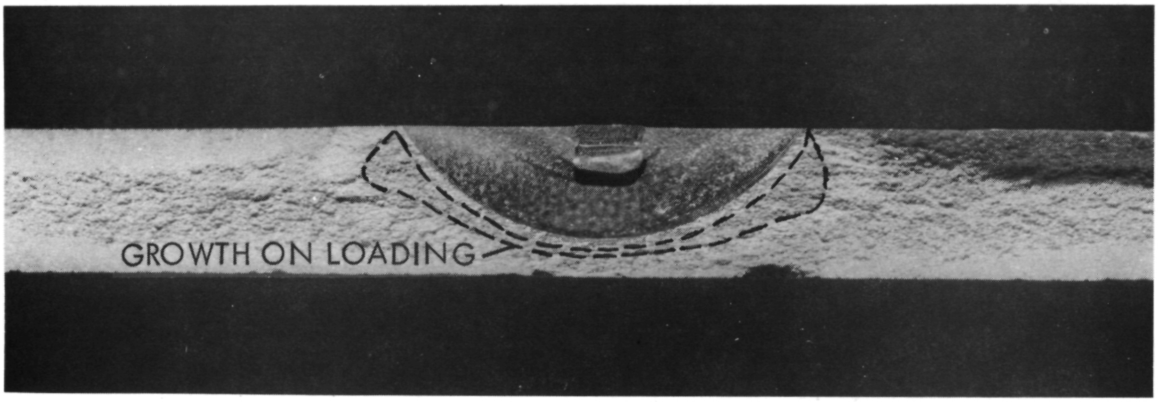

(b) 2BN23-4

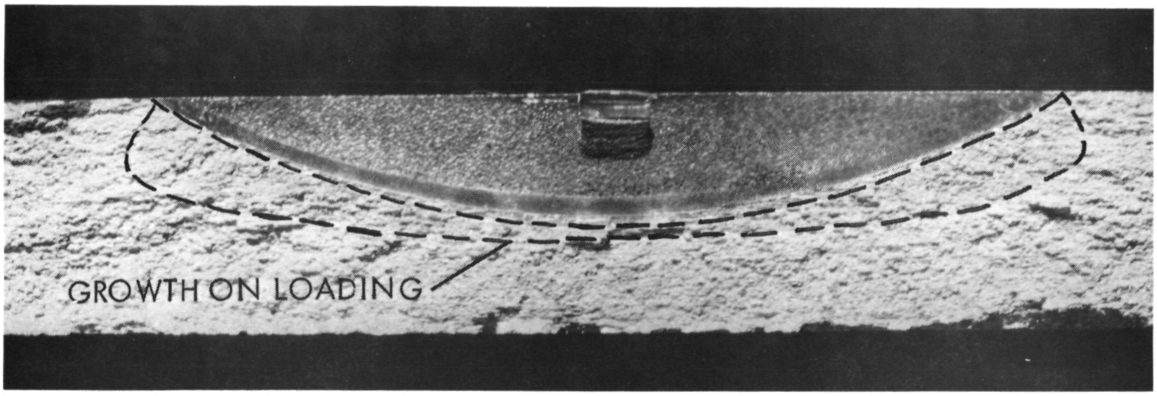

(c) 3BN31-2

Figure 43: FRACTURE SURFACES OF SPECIMENS 2BR34-4, 2BN23-4 AND 3BN31-2

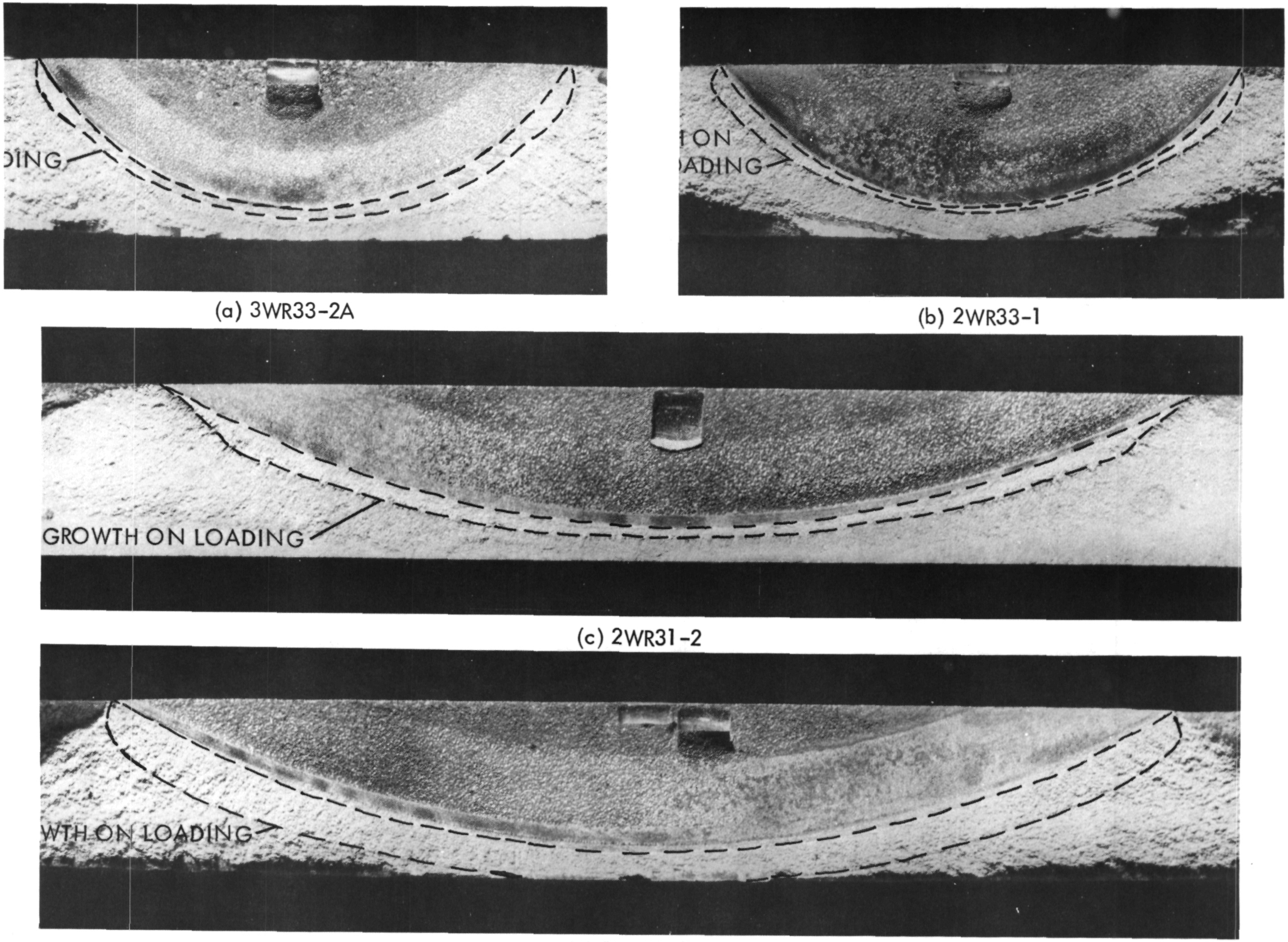

(a) 3WR33-2A

(b) 2WR33-1

(c) 2WR31-2

(d) 2WR31-1

Figure 44: FRACTURE SURFACES OF SPECIMENS 3WR33-2A, 2WR33-1, 2WR31-2 AND 2WR31-1

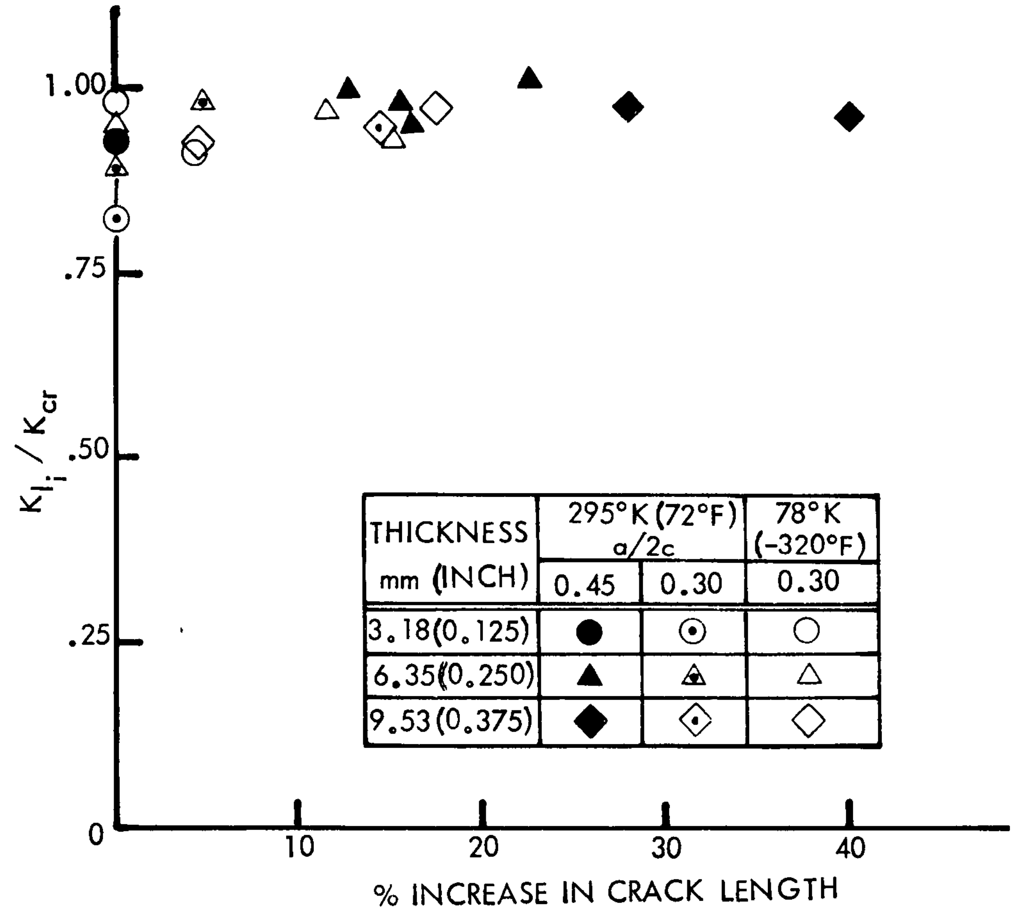

FIGURE 45: 2219-T87 ALUMINUM BASE METAL LENGTHWISE GROWTH-ON-LOADING TEST RESULTS

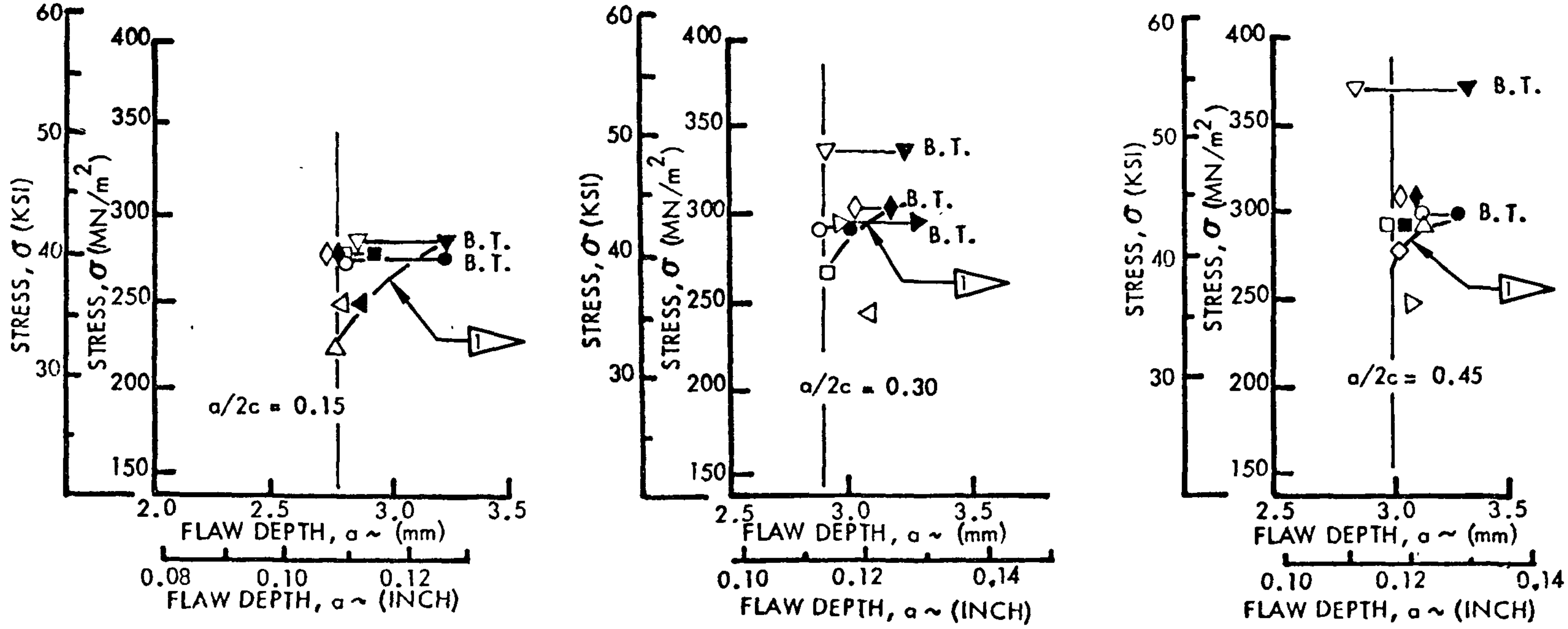

1 ASSUMED FLAW DEPTH-STRESS RELATIONSHIP FOR RESISTANCE CURVE CALCULATION

FIGURE 46: 2219-T87 ALUMINUM SURFACE FLAW DATA
ROOM TEMPERATURE (3.18 mm (0.125 INCH))

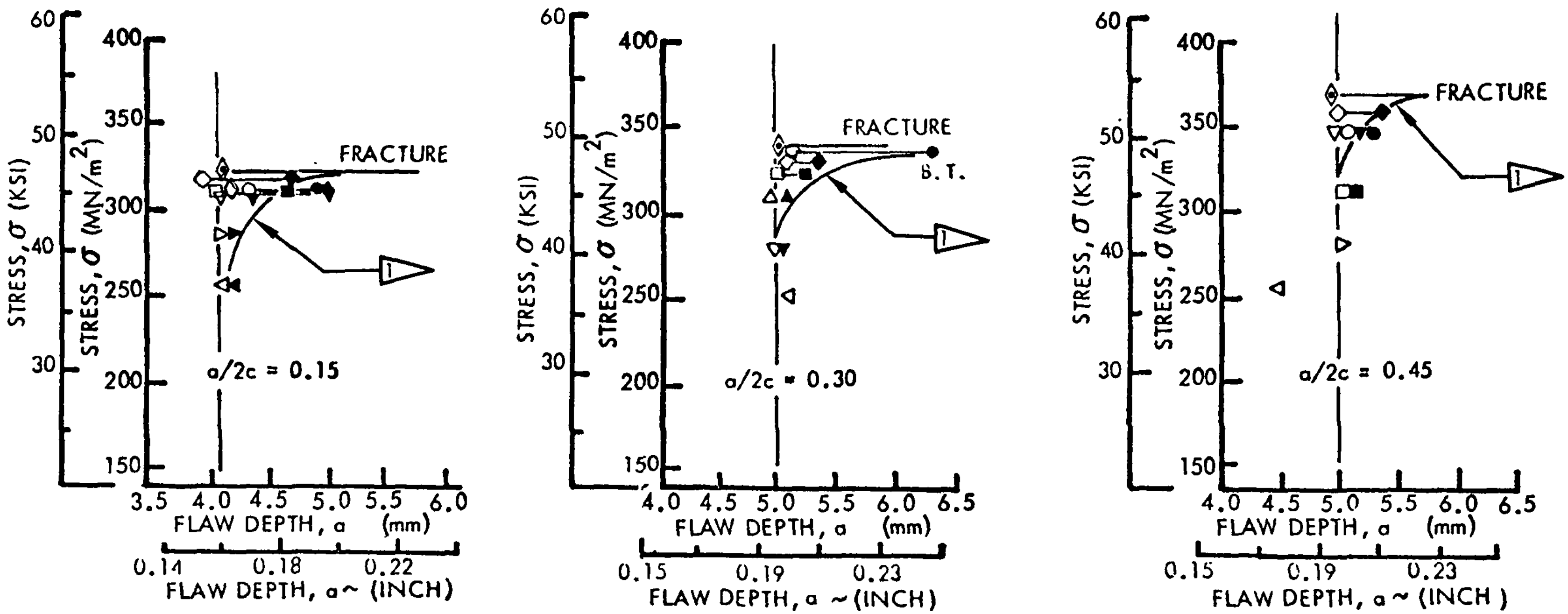

[1] ASSUMED FLAW DEPTH-STRESS RELATIONSHIP FOR RESISTANCE CURVE CALCULATION

FIGURE 47: 2219-T87 ALUMINUM SURFACE FLAW DATA.
ROOM TEMPERATURE (6.35 mm (0.250 INCH))

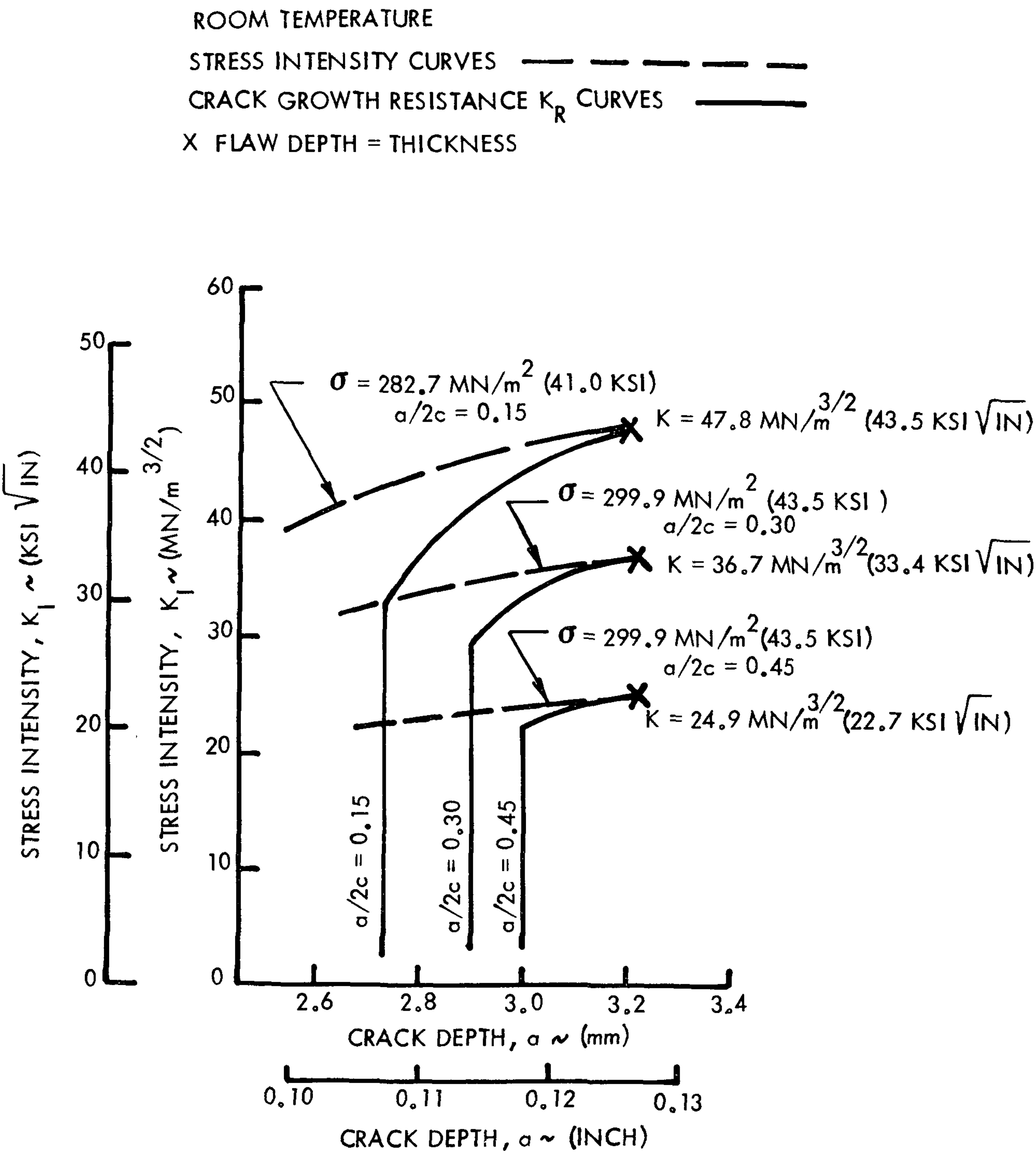

FIGURE 48: STRESS INTENSITY VERSUS FLAW DEPTH FOR 3.18mm (0.125 INCH) THICK 2219-T87 ALUMINUM BASE METAL SURFACE FLAW SPECIMENS

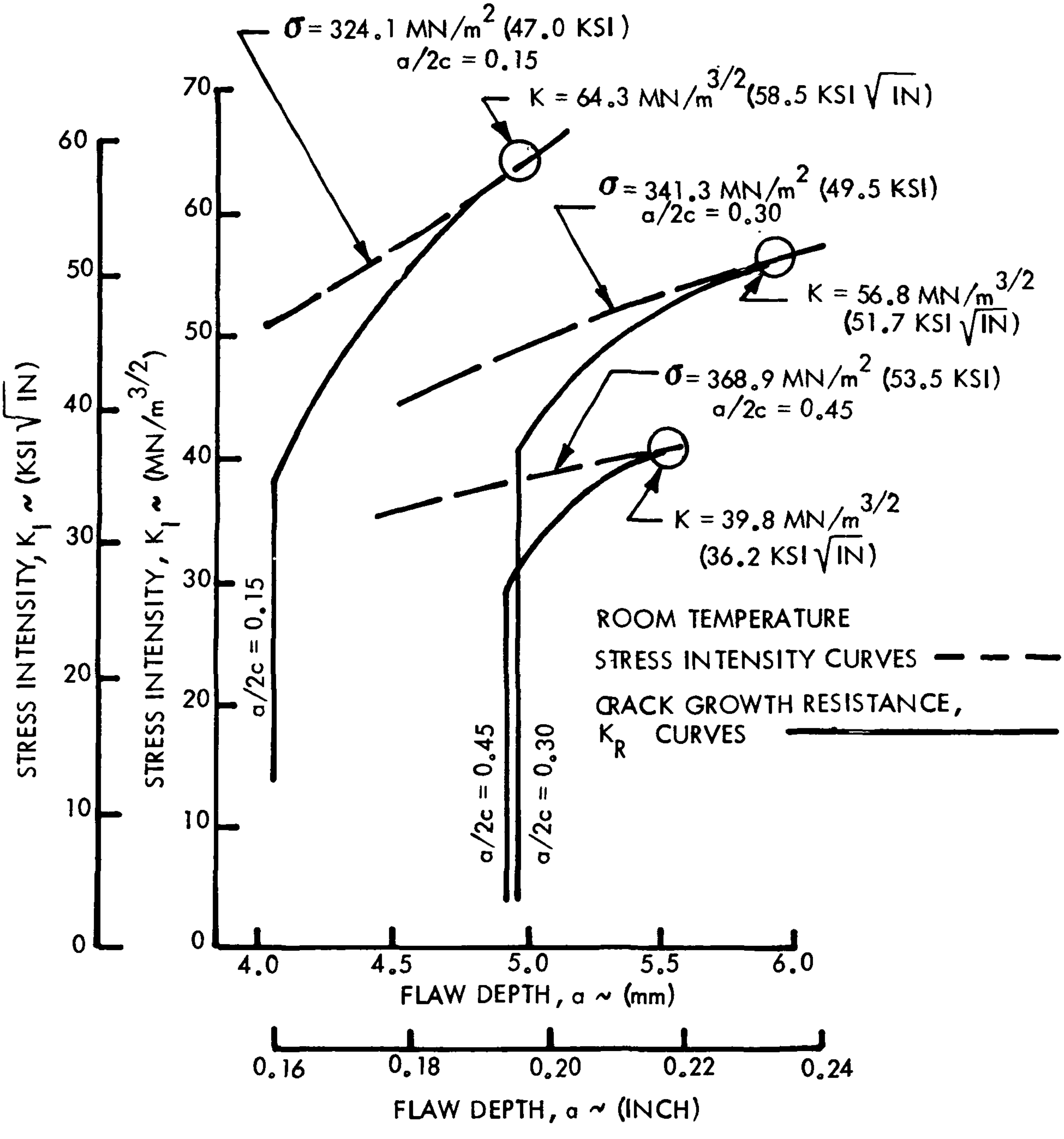

FIGURE 49: STRESS INTENSITY VERSUS FLAW DEPTH FOR 6.35 mm (0.250 INCH) THICK 2219-T87 ALUMINUM BASE METAL SURFACE FLAW SPECIMENS

FRACTURE			SPECIMEN THICKNESS mm (INCH)	BREAKTHROUGH	
20°K (-423°F)	78°K (-320°F)	295°K (72°F)		295°K (72°F)	78°K (-320°F)
●	◑	○	3.18 (0.125)	□	◧
▲	◭	△	6.35 (0.250)	▽	
◆	◈	◇	9.53 (0.375)		

* BREAKTHROUGH PREDICTION ERRONEOUS

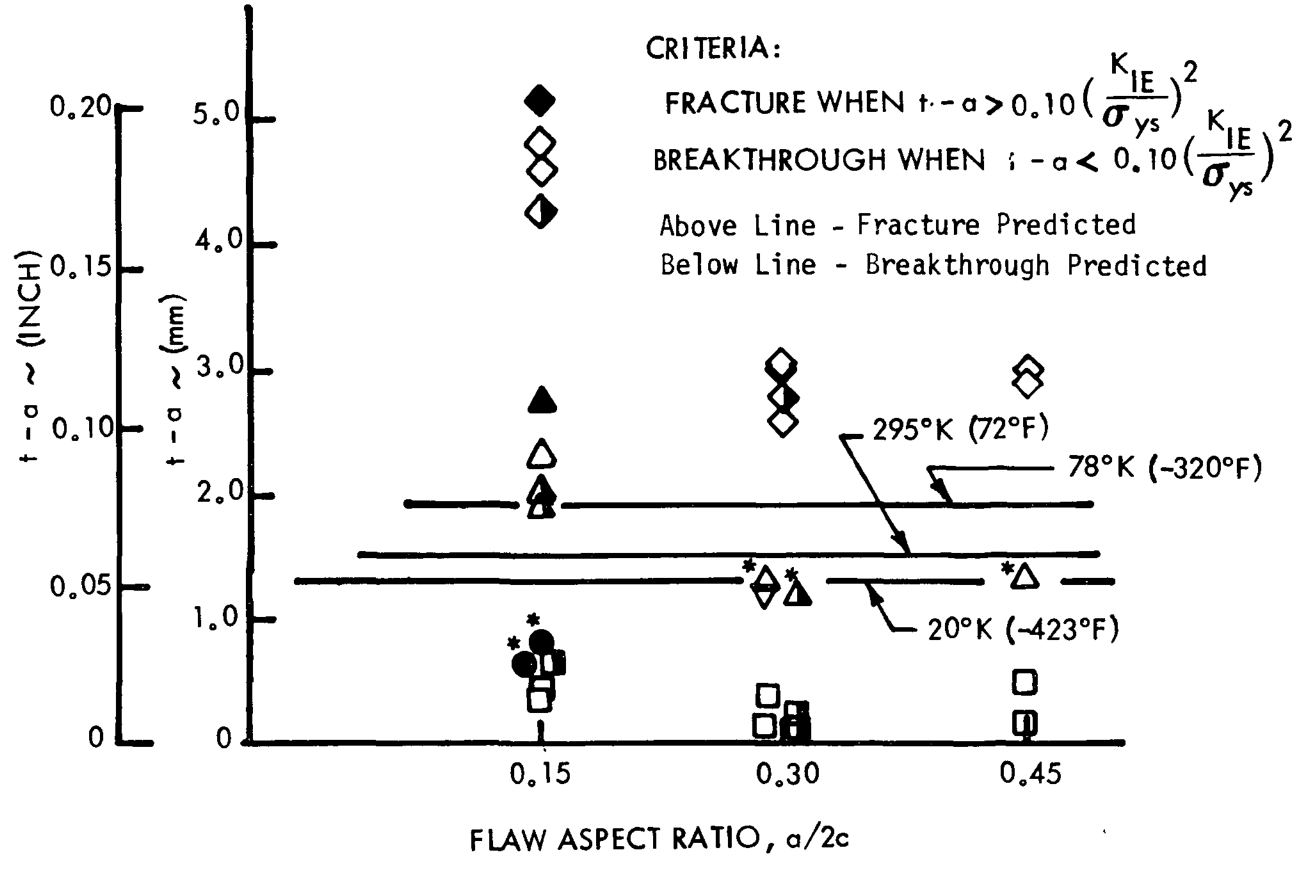

FIGURE 50: COMPARISON OF PREDICTED AND ACTUAL FAILURE MODE (Method I)

FRACTURE			SPECIMEN THICKNESS mm (INCH)	BREAKTHROUGH	
20°K (-423°F)	78°K (-320°F)	295°K (72°F)		295°K (72°F)	78°K (-320°F)
●	◐	○	3.18 (0.125)	□	◧
▲	◭	△	6.35 (0.250)	▽	
◆	◈	◇	9.53 (0.375)		

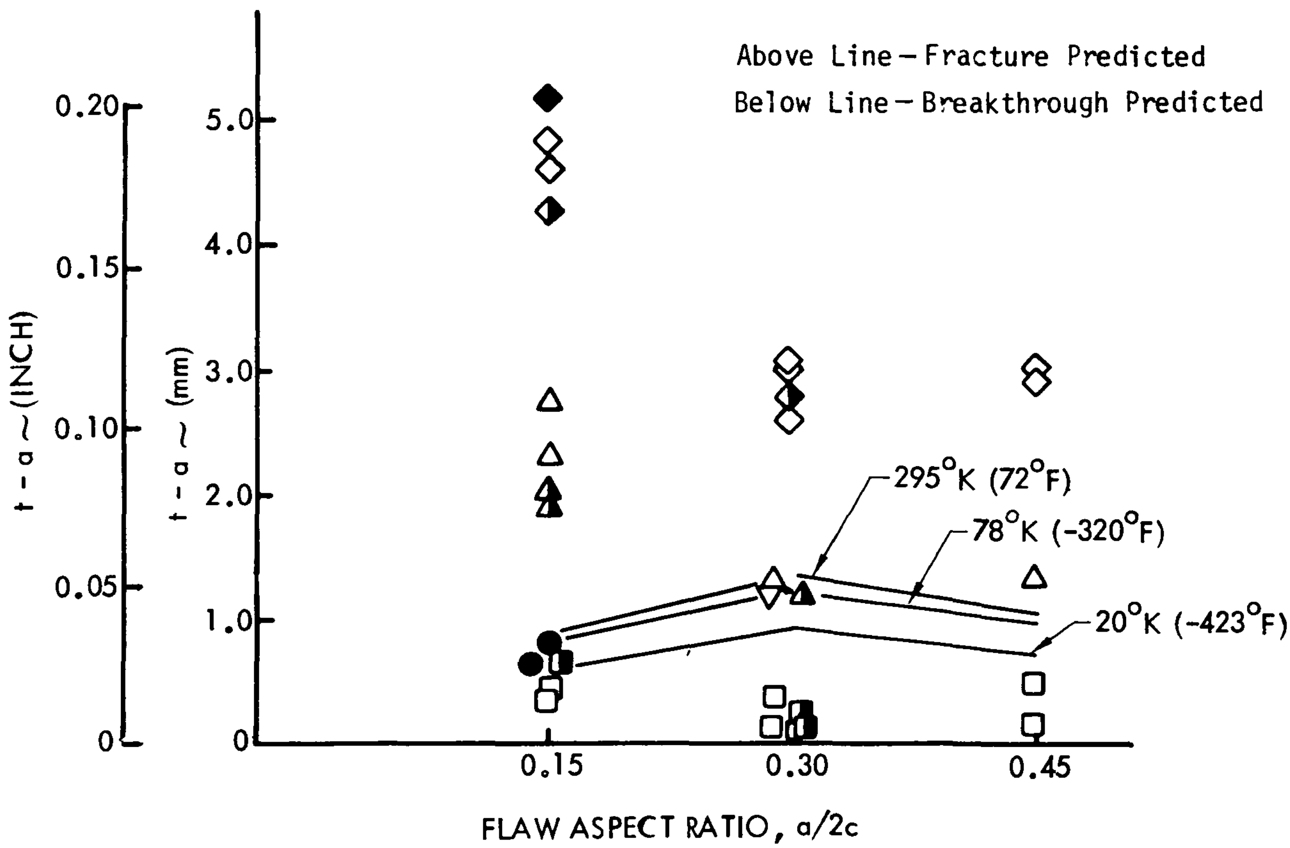

Figure 51: COMPARISON OF PREDICTED AND ACTUAL FAILURE MODE (Method II)

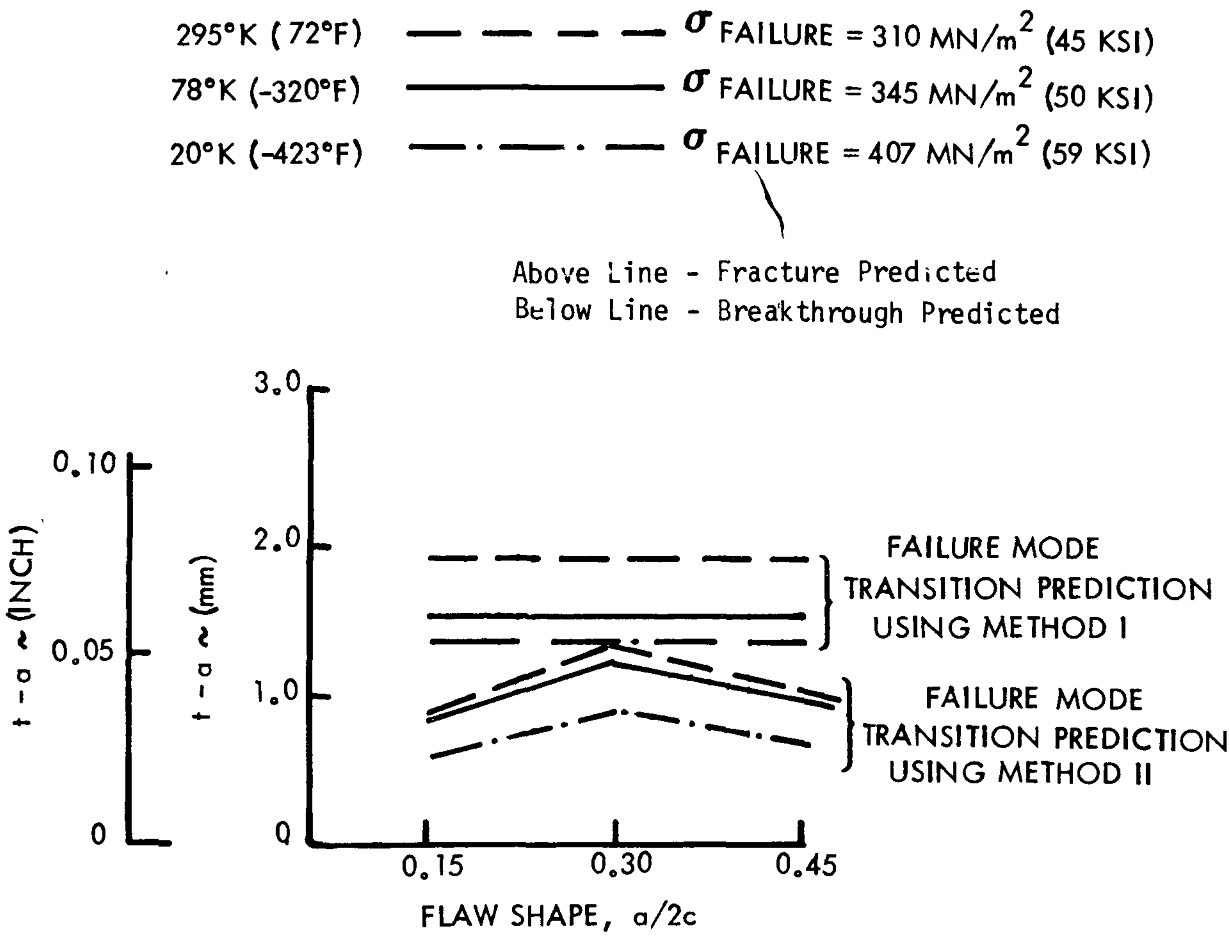

FIGURE 52: COMPARISON OF FAILURE MODE TRANSITION REMAINING LIGAMENT (t - a) PREDICTIONS FOR 2219-T87 ALUMINUM BASE METAL

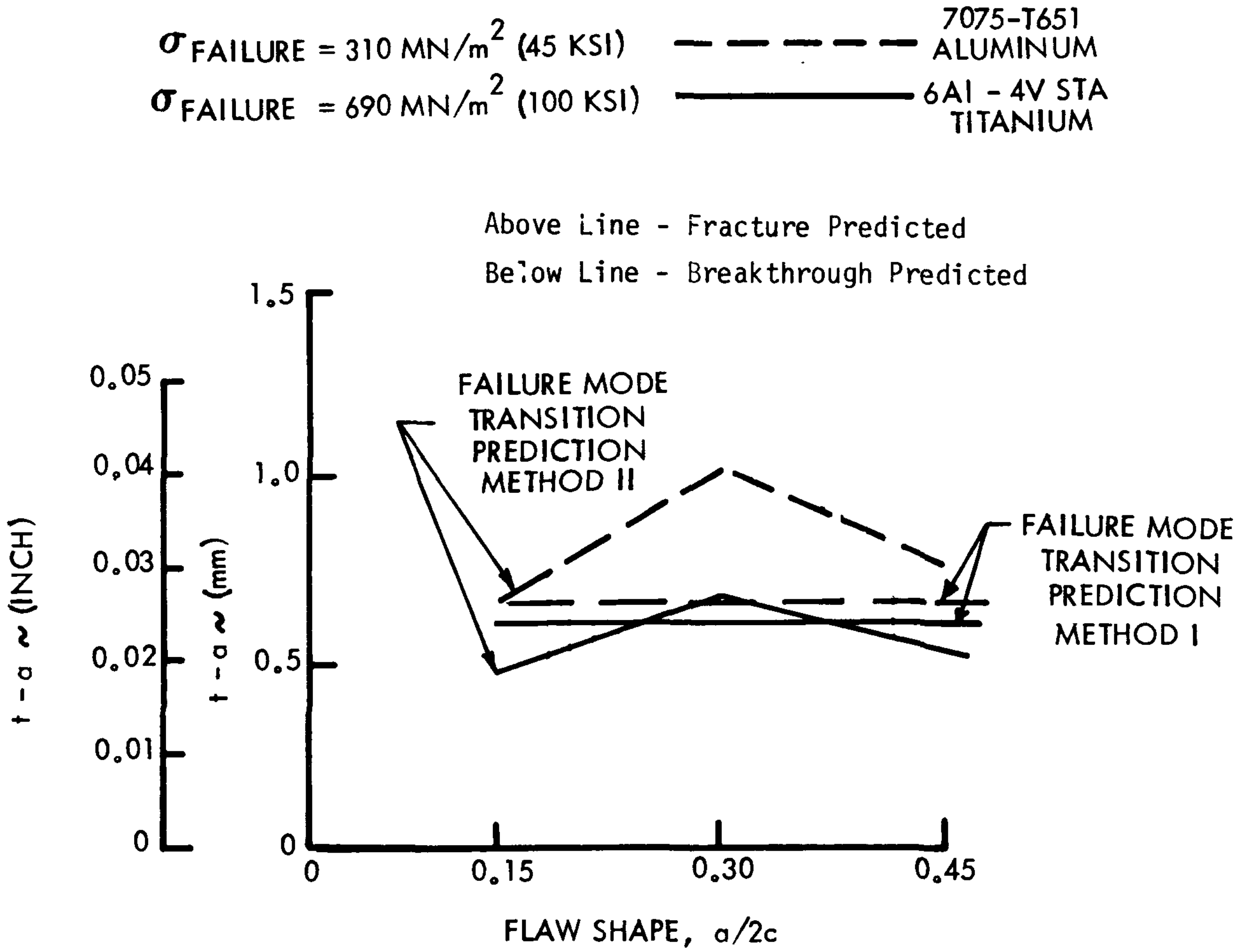

FIGURE 53: COMPARISON OF FAILURE MODE TRANSITION REMAINING LIGAMENT (t - a) PREDICTIONS FOR 7075-T651 ALUMINUM AND 6 Al - 4V STA TITANIUM ALLOY (ROOM TEMPERATURE)

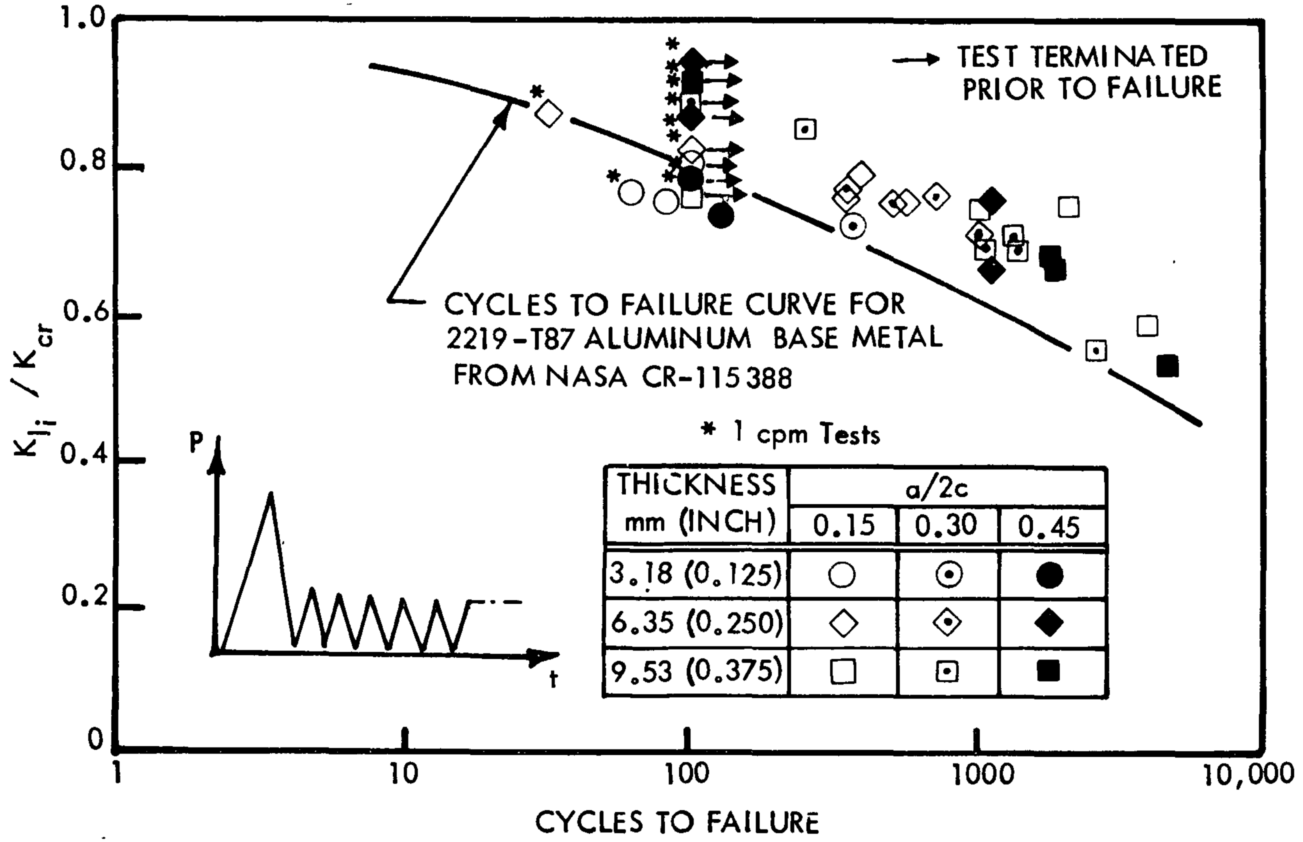

FIGURE 54: K_{I_i} / K_{cr} VERSUS CYCLES TO FAILURE FOR PROOF LOADED 2219-T87 ALUMINUM BASE METAL AT ROOM TEMPERATURE

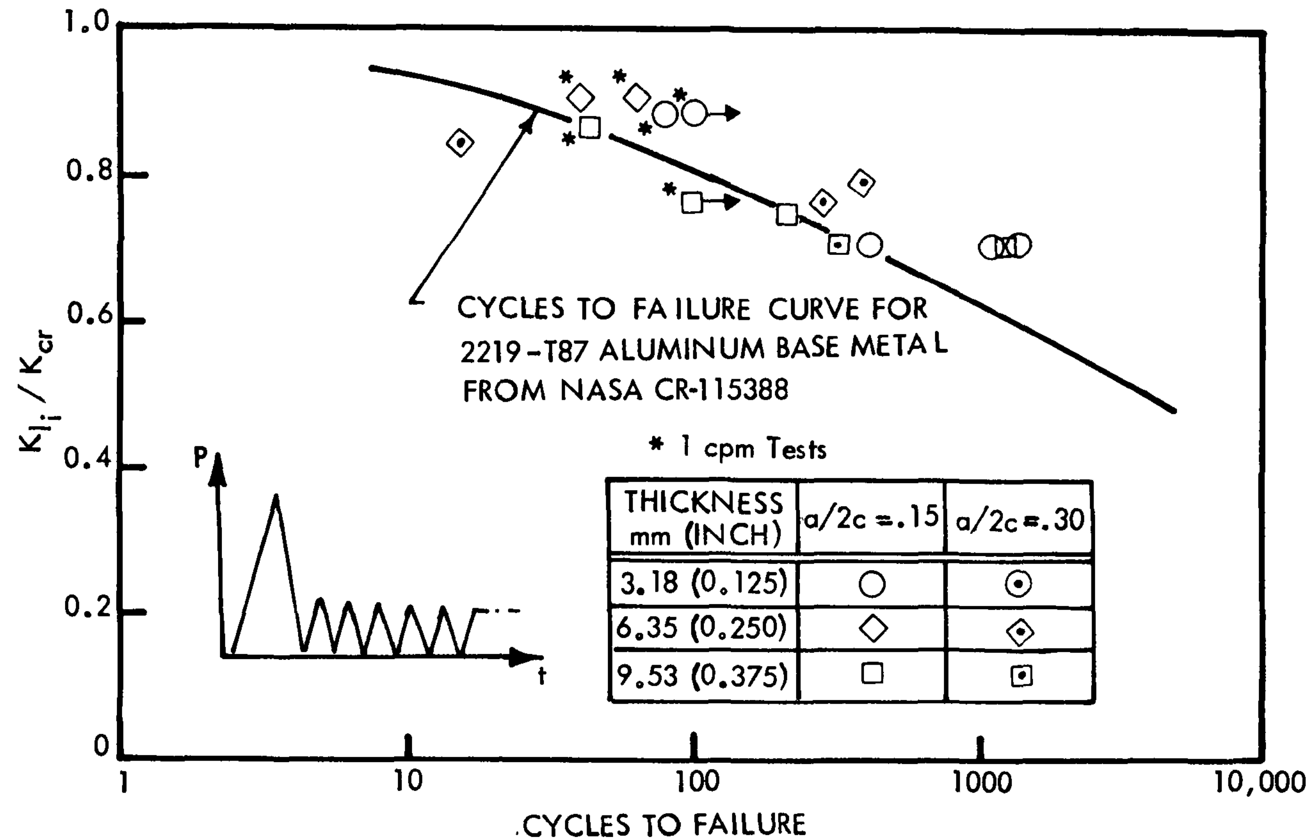

FIGURE 55: K_{I_i} / K_{cr} VERSUS CYCLES TO FAILURE FOR PROOF LOADED 2219 ALUMINUM WELDMENTS AT ROOM TEMPERATURE

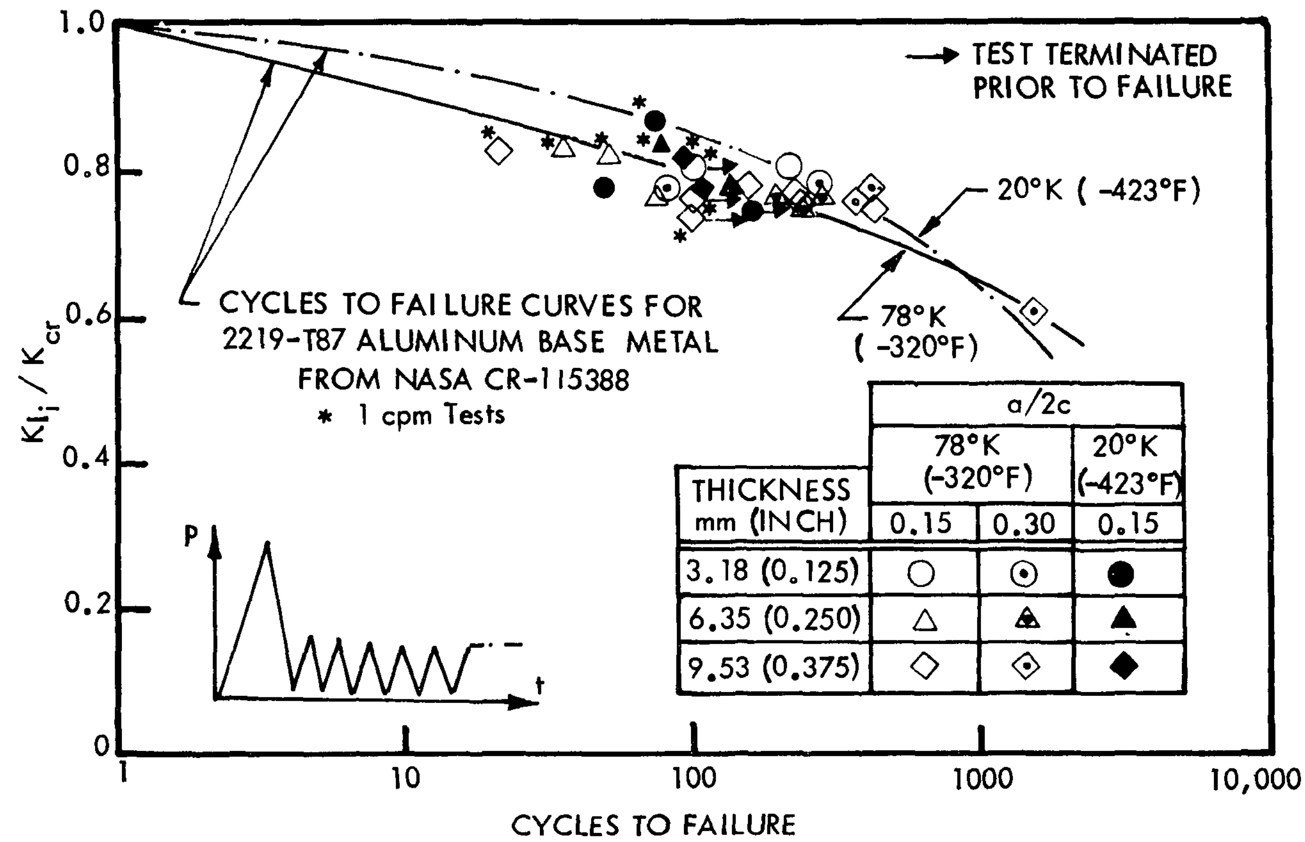

FIGURE 56: K_{I_i} / K_{cr} VERSUS CYCLES TO FAILURE FOR PROOF LOADED 2219-T87 ALUMINUM BASE METAL AT 78°K (-320°F) AND 20°K (-423°F)

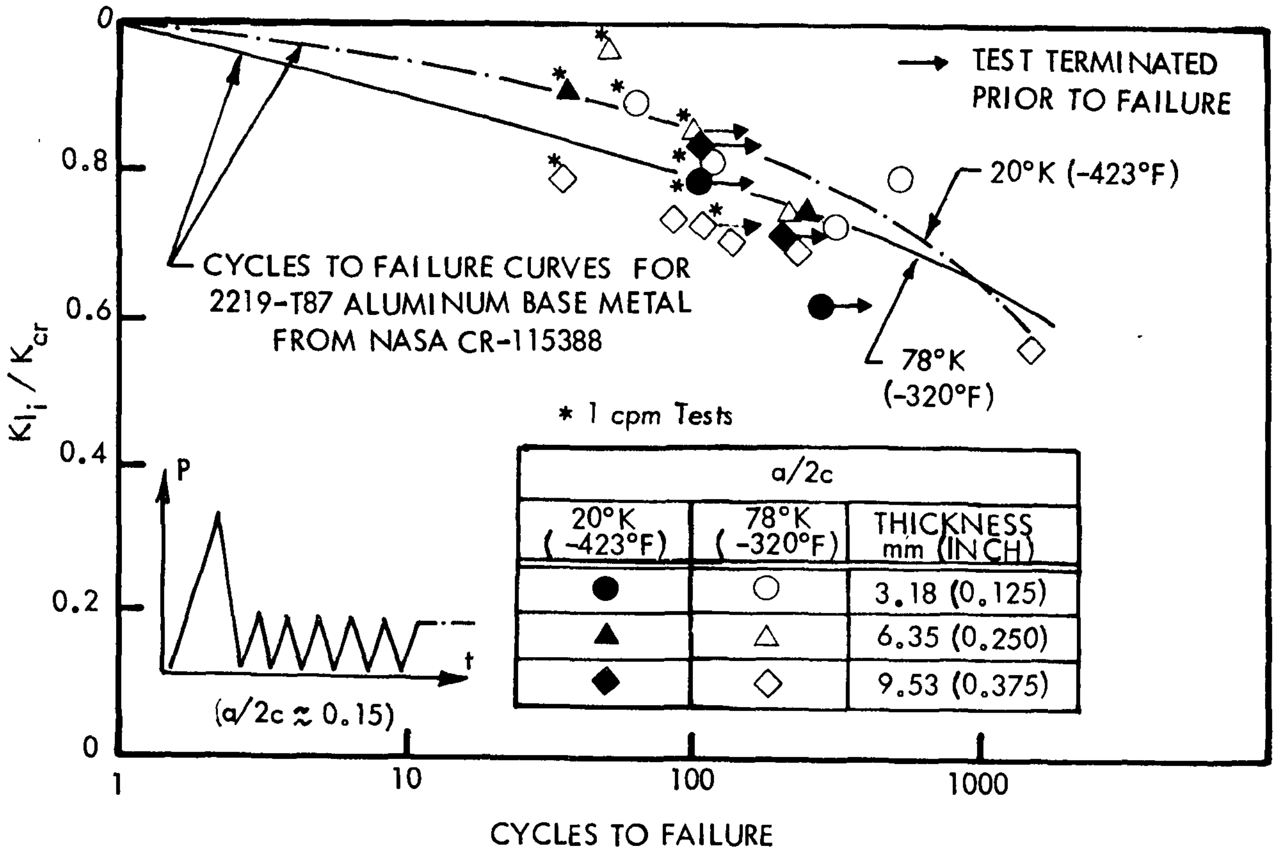

FIGURE 57: K_{I_i} / K_{cr} VERSUS CYCLES TO FAILURE FOR PROOF LOADED 2219 ALUMINUM WELDMENTS AT 78°K (-320°F) AND 20°K (-423°F)

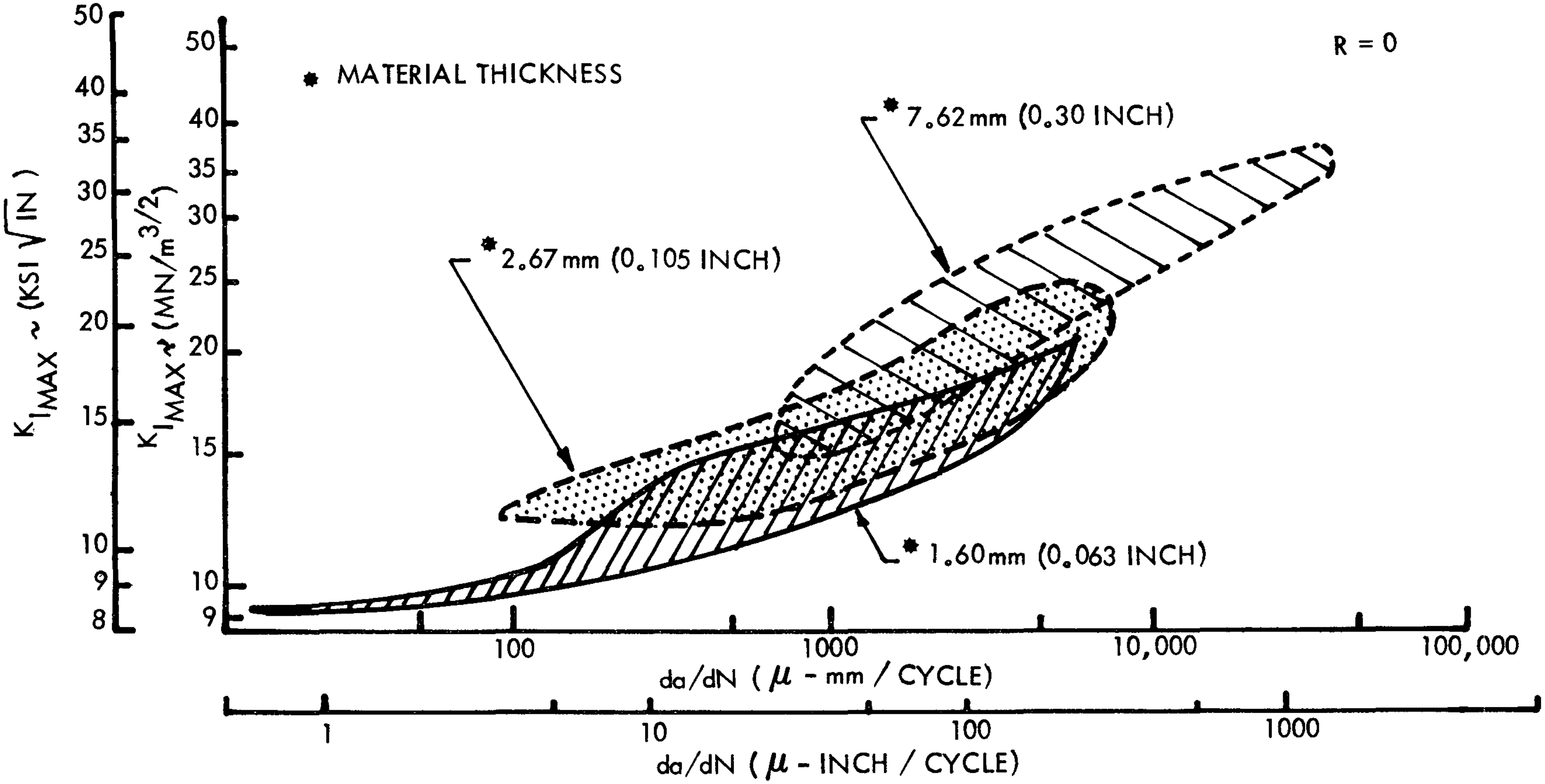

FIGURE 58: da/dN VS. $K_{I_{MAX}}$ SHOWING COMPARISON OF CYCLIC CRACK RATES FOR "AS-WELDED" 2219 ALUMINUM IN ROOM TEMPERATURE AIR (Figure 67 of Reference 10)

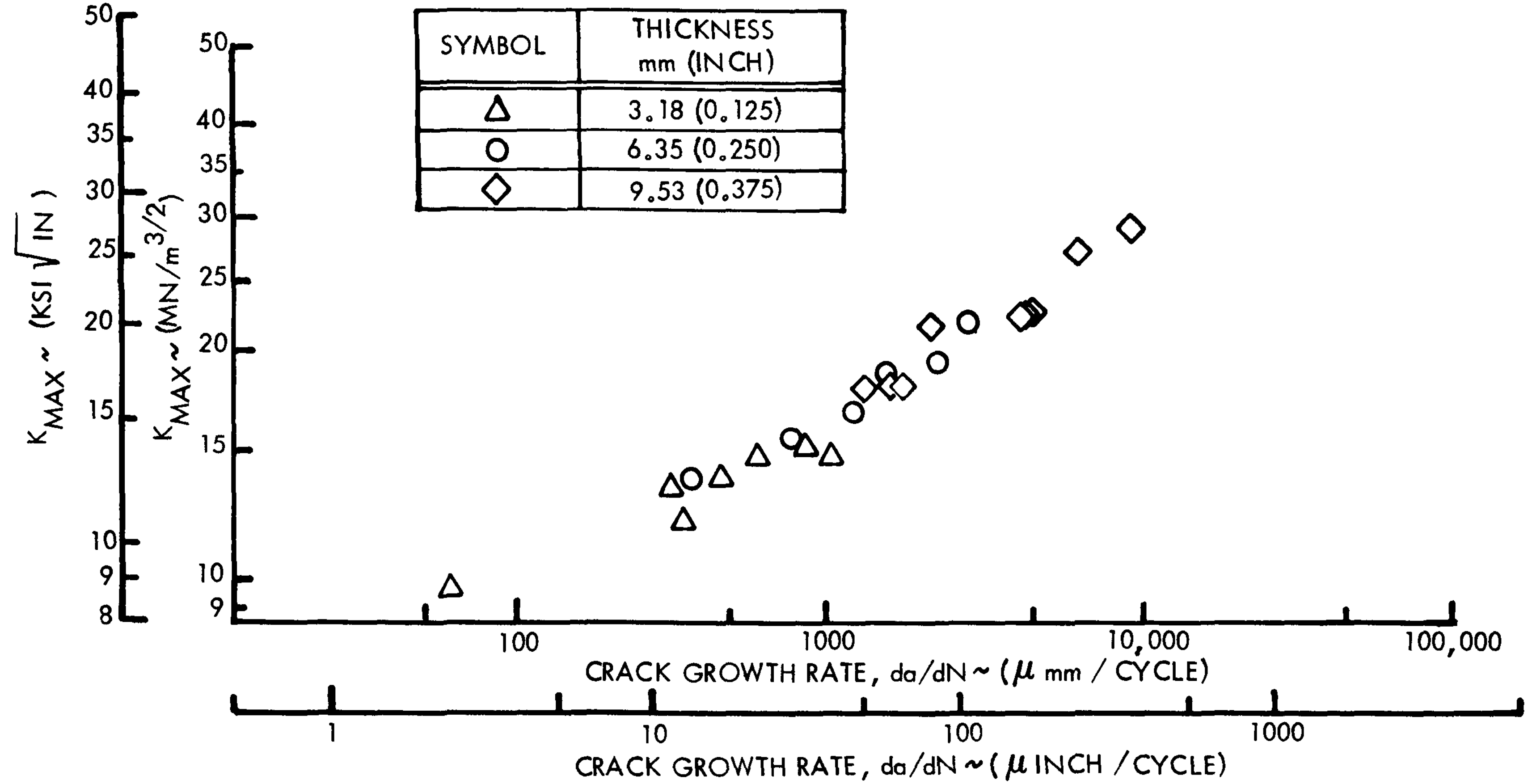

FIGURE 59: da/dN VERSUS $K_{I_{MAX}}$ FOR "AS-WELDED" 2219 ALUMINUM AT ROOM TEMPERATURE

TABLE 1: CHEMICAL COMPOSITIONS OF MATERIALS

ELEMENT (% BY WEIGHT)	2219 ALUMINUM PLATE		2319 ALUMINUM WELD WIRE	
	MIN.	MAX.	MIN.	MAX.
COPPER	5.80	6.80	5.80	6.80
SILICON	-	0.20	-	0.20
MANGANESE	0.20	0.40	0.20	0.40
MAGNESIUM	-	0.20	-	0.02
IRON	-	0.30	-	0.30
CHROMIUM	-	-	-	-
ZINC	-	0.10	-	0.10
VANADIUM	0.05	0.15	0.05	0.15
ZIRCONIUM	0.10	0.25	0.10	0.25
CARBON	-	-	-	-
NITROGEN (ppm)	-	-	-	-
OXYGEN (ppm)	-	-	-	-
HYDROGEN (ppm)	-	-	-	-
TITANIUM	0.02	0.10	0.10	0.20
ALUMINUM	REMAINDER		REMAINDER	
OTHER	-	-	-	0.15

TABLE 2: ROOM TEMPERATURE MECHANICAL PROPERTIES OF 2219-T87 ALUMINUM

MATERIAL CONDITION	SPECIMEN NUMBER	NOMINAL GAGE THICKNESS mm (INCH)	TEST ATMOSPHERE	GRAIN DIRECTION L= LONGITUDINAL T = TRANSVERSE	ULTIMATE STRENGTH MN/m^2 (KSI)	YIELD STRENGTH MN/m^2 (KSI)	ELONGATION % IN 50.8 mm (% IN 2.0 INCH)	REDUCTION IN AREA %	MODULUS OF ELASTICITY $E \times 10^3$ MN/m^2 ($E \times 10^3$ KSI)	POISSON'S RATIO
BASE METAL	1T-1	3.18 (0.125)	AIR @ 295°K (72°F)	T	470.2 (68.2)	377.8 (54.8)	8	22	72.4 (10.5)	0.321
	1T-2				471.6 (68.4)	374.4 (54.3)	10	24	73.8 (10.7)	0.326
	1L-1			L	467.5 (67.8)	378.5 (54.9)	12	40	71.7 (10.4)	0.318
	1L-2				462.0 (67.0)	375.1 (54.4)	11	31	72.4 (10.5)	0.310
	2T-1	6.35 (0.250)		T	473.0 (68.6)	378.5 (54.9)	10	23	69.6 (10.1)	0.320
	2T-2				470.9 (68.3)	376.5 (54.6)	11	25	69.6 (10.1)	0.321
	2L-1			L	464.2 (67.4)	377.8 (54.8)	12	30	73.1 (10.6)	0.316
	2L-2				463.3 (67.2)	379.9 (55.1)	11	31	71.0 (10.3)	0.310
	3T-1	9.53 (0.375)		T	478.5 (69.4)	383.4 (55.6)	11	21	75.8 (11.0)	0.340
	3T-2				479.2 (69.5)	375.8 (54.5)	11	22	77.2 (11.2)	0.340
	3L-1			L	476.4 (69.1)	381.3 (55.3)	14	32	76.5 (11.1)	0.320
	3L-2				476.4 (69.1)	386.8 (56.1)	14	31	73.8 (10.7)	0.335
WELD METAL	W1-1	3.18 (0.125)			273.0 (39.6)	167.6 (24.3)	4	21	71.7 (10.4)	0.298
	W1-2				275.1 (39.9)	166.2 (24.1)	4	24	66.2 (9.6)	—
	W2-1	6.35 (0.250)			268.9 (39.0)	173.1 (25.1)	4	22	—	—
	W2-2				269.6 (39.1)	172.4 (25.0)	5	20	81.4 (11.8)	0.350
	W3-1	9.53 (0.375)			285.5 (41.4)	158.6 (23.0)	7	32	83.4 (12.1)	0.356
	W3-2				286.1 (41.5)	159.3 (23.1)	7	31	65.5 (9.5)	0.238

TABLE 3: LIQUID NITROGEN TEMPERATURE MECHANICAL PROPERTIES OF 2219-T87 ALUMINUM

MATERIAL CONDITION	SPECIMEN NUMBER	NOMINAL GAGE THICKNESS mm (INCH)	TEST ATMOSPHERE	GRAIN DIRECTION L = LONGITUDINAL T = TRANSVERSE	ULTIMATE STRENGTH MN/m^2 (KSI)	YIELD STRENGTH MN/m^2 (KSI)	ELONGATION % IN 50.8 mm (% IN 2.0 INCH)	REDUCTION IN AREA %	MODULUS OF ELASTICITY $E \times 10^3$ MN/m^2 ($E \times 10^3$ KSI)	POISSON'S RATIO
BASE METAL	1T-3	3.18 (0.125)	LN_2 @ 78°K (-320°F)	T	584.7 (84.8)	443.3 (64.3)	8	22	81.4 (11.8)	0.317
	1T-4				588.1 (85.3)	453.7 (65.8)	10	24	84.8 (12.3)	0.309
	1L-3			L	575.0 (83.4)	450.2 (65.3)	13	31	80.7 (11.7)	0.312
	1L-4				575.0 (83.4)	448.9 (65.1)	12	29	76.5 (11.1)	0.316
	2T-3	6.35 (0.250)		T	590.9 (85.7)	453.0 (65.7)	11	16	79.3 (11.5)	0.311
	2T-4				587.5 (85.2)	455.1 (66.0)	12	18	75.8 (11.0)	0.289
	2L-3			L	573.7 (83.2)	451.6 (65.5)	12	25	80.7 (11.7)	0.310
	2L-4				580.6 (84.2)	457.1 (66.3)	13	27	80.0 (11.6)	0.308
	3T-3	9.53 (0.375)		T	592.3 (85.9)	454.4 (65.9)	13	20	80.0 (11.6)	0.310
	3T-4				591.6 (85.8)	455.1 (66.0)	12	19	80.7 (11.7)	0.310
	3L-3			L	584.7 (84.8)	462.0 (67.0)	16	31	81.4 (11.8)	0.304
	3L-4				584.7 (84.8)	461.3 (66.9)	17	31	78.6 (11.4)	0.307
WELD METAL	W1-3	3.18 (0.125)			388.2 (56.3)	213.8 (31.0)	7	29	91.7 (13.2)	0.387
	W1-4				389.6 (56.5)	208.2 (30.2)	6	29	89.6 (13.0)	0.367
	W2-3	6.35 (0.250)			387.5 (56.2)	202.0 (29.3)	—	24	74.5 (10.8)	0.295
	W2-4				388.9 (56.4)	188.9 (27.4)	5	21	90.3 (13.1)	0.327
	W3-3	9.53 (0.375)			393.0 (57.0)	196.5 (28.5)	9	18	62.7 (9.5)	0.222
	W3-4				398.5 (57.8)	198.6 (28.8)	10	22	82.7 (12.0)	0.241

TABLE 4: LIQUID HYDROGEN TEMPERATURE MECHANICAL PROPERTIES OF 2219-T87 ALUMINUM

MATERIAL CONDITION	SPECIMEN NUMBER	NOMINAL GAGE THICKNESS mm (INCH)	TEST ATMOSPHERE	GRAIN DIRECTION L= LONGITUDINAL T = TRANSVERSE	ULTIMATE STRENGTH MN/m^2 (KSI)	YIELD STRENGTH MN/m^2 (KSI)	ELONGATION % IN 50.8 mm (% IN 2.0 INCH)	REDUCTION IN AREA %	MODULUS OF ELASTICITY E x 10^3 MN/m^2 (E x 10^3 KSI)	POISSON'S RATIO
BASE METAL	1T-5	3.18 (0.125)	L H_2 @ 20°K (-423°F)	T	675.0 (97.9)	483.3 (70.1)	15	16	77.2 (11.2)	0.342
	1T-6				672.3 (97.5)	470.2 (68.2)	12	16	77.2 (11.2)	0.352
	1L-5			L	657.1 (95.3)	475.1 (68.9)	15	24	76.5 (11.1)	0.362
	1L-6				661.2 (95.9)	470.2 (68.2)	16	23	78.6 (11.4)	0.296
	2T-5	6.35 (0.250)		T	674.3 (97.8)	460.6 (66.8)	13	16	75.2 (10.9)	0.328
	2T-6				675.0 (97.9)	470.2 (68.2)	14	17	77.2 (11.2)	0.339
	2L-5			L	654.3 (94.9)	469.5 (68.1)	15	24	77.9 (11.3)	0.351
	2L-6				643.3 (93.3)	461.3 (66.9)	15	22	73.8 (10.7)	0.326
	3T-5	9.53 (0.375)		T	690.9 (100.2)	475.1 (68.9)	16	17	75.8 (11.0)	0.309
	3T-6				688.8 (99.9)	485.4 (70.4)	16	17	77.9 (11.3)	0.301
	3L-5			L	674.3 (97.8)	480.6 (69.7)	18	23	75.2 (10.9)	0.323
	3L-6				679.2 (98.5)	487.5 (70.7)	19	25	74.5 (10.8)	0.337
WELD METAL	W1-5	3.18 (0.125)			475.1 (68.9)	241.3 (35.0)	6	15	75.2 (10.9)	0.369
	W1-6				468.9 (68.0)	245.5 (35.6)	5	12	82.1 (11.9)	0.403
	W2-5	6.35 (0.250)			478.5 (69.4)	250.3 (36.3)	5	13	82.7 (12.0)	0.330
	W2-6				448.2 (65.0)	241.3 (35.0)	4	9	83.4 (12.1)	0.507
	W3-5	9.53 (0.375)			468.8 (70.6)	220.0 (31.9)	8	13	75.8 (11.0)	0.370
	W3-6				457.8 (66.4)	212.4 (30.8)	7	11	78.6 (11.4)	0.380

TABLE 5: ROOM TEMPERATURE 2219-T87 ALUMINUM BASE METAL CENTER CRACK DATA (t=3.18mm (0.125in.))

SPECIMEN NUMBER	GAGE THICKNESS, t mm (INCH)	GAGE WIDTH, W mm (INCH)	TEST TEMPERATURE °K (°F)	INITIAL FLAW LENGTH, 2c mm (INCH)	STRESS AT START OF CRACK GROWTH, σ_s MN/m^2 (KSI)	MAXIMUM GROSS SECTION STRESS, σ_G MN/m^2 (KSI)	MAXIMUM NET SECTION STRESS, σ_N MN/m^2 (KSI)	CRITICAL CRACK LENGTH, 2c mm (INCH)	K_{cn} $MN/m^{3/2}$ ($KSI\sqrt{IN}$)
BCR11-1	3.20 (0.126)	304.8 (12.0)	R.T.	19.30 (0.76)	287.5 (41.9)	316.5 (45.9)	364.1 (52.8)	39.62 (1.56)	55.4 (50.4)
BCR11-2	3.15 (0.124)	304.8 (12.0)	R.T.	51.31 (2.02)	175.1 (25.4)	245.5 (35.6)	326.8 (47.4)	75.69 (2.98)	71.2 (64.8)
BCR13-1	3.28 (0.129)	304.8 (12.0)	R.T.	10.41 (0.41)	343.4 (49.8)	357.2 (51.8)	391.6 (56.8)	26.67 (1.05)	45.1 (41.0)
BCR13-2	3.12 (0.123)	304.8 (12.0)	R.T.	76.96 (3.03)	151.7 (22.0)	208.2 (30.2)	324.7 (47.1)	109.47 (4.31)	75.1 (68.3)
BCR14-1	3.23 (0.127)	304.8 (12.0)	R.T.	7.11 (0.28)	362.0 (52.5)	365.4 (53.0)	384.7 (55.8)	15.24 (0.60)	38.6 (35.1)
BCR14-2	3.23 (0.129)	304.8 (12.0)	R.T.	92.46 (3.64)	151.0 (21.9)	185.5 (26.9)	329.6 (47.8)	133.1 (5.24)	74.6 (67.9)

TABLE 6: ROOM TEMPERATURE 2219-T87 ALUMINUM BASE METAL CENTER CRACK DATA (t=6.35mm (0.250in.))

SPECIMEN NUMBER	GAGE THICKNESS, t mm (INCH)	GAGE WIDTH, W mm (INCH)	TEST TEMPERATURE °K (°F)	INITIAL FLAW LENGTH, 2c mm (INCH)	STRESS AT START OF CRACK GROWTH, σ_s MN/m² (KSI)	MAXIMUM GROSS SECTION STRESS, σ_G MN/m² (KSI)	MAXIMUM NET SECTION STRESS, σ_N MN/m² (KSI)	CRITICAL CRACK LENGTH, 2c mm (INCH)	K_{cn} MN/m$^{3/2}$ (KSI$\sqrt{IN}$)
BCR21-1	6.27 (0.247)	304.8 (12.0)	R.T.	28.19 (1.11)	236.5 (34.3)	285.5 (41.4)	344.8 (50.0)	52.58 (2.07)	60.7 (55.2)
BCR21-2	6.34 (0.250)	304.8 (12.0)	R.T.	52.07 (2.05)	171.7 (24.9)	234.4 (34.0)	330.3 (47.9)	88.65 (3.49)	68.5 (62.3)
BCR23-1	6.32 (0.249)	304.8 (12.0)	R.T.	17.27 (0.68)	298.6 (43.3)	315.8 (45.8)	359.9 (52.2)	37.59 (1.48)	52.2 (47.5)
BCR23-2	6.27 (0.247)	304.8 (12.0)	R.T.	77.47 (3.05)	142.0 (20.6)	198.6 (28.8)	317.2 (46.0)	114.05 (4.49)	71.9 (65.4)
BCR24-1	6.30 (0.248)	304.8 (12.0)	R.T.	12.19 (0.48)	326.8 (47.4)	338.5 (49.1)	373.7 (54.2)	284.5 (1.12)	46.8 (42.6)
BCR24-2	6.30 (0.248)	304.8 (12.0)	R.T.	92.46 (3.64)	146.2 (21.2)	178.6 (25.9)	309.6 (44.9)	12.90 (5.08)	71.8 (65.3)

TABLE 7: ROOM TEMPERATURE 2219-T87 ALUMINUM BASE METAL CENTER CRACK DATA (t=9.53mm (0.375in.))

SPECIMEN NUMBER	GAGE THICKNESS, t mm (INCH)	GAGE WIDTH, W mm (INCH)	TEST TEMPERATURE °K (°F)	INITIAL FLAW LENGTH, 2c mm (INCH)	STRESS AT START OF CRACK GROWTH, σ_s MN/m^2 (KSI)	MAXIMUM GROSS SECTION STRESS, σ_G MN/m^2 (KSI)	MAXIMUM NET SECTION STRESS, σ_N MN/m^2 (KSI)	CRITICAL CRACK LENGTH, 2c mm (INCH)	K_{cn} MN/m$^{3/2}$ (KSI$\sqrt{IN}$)
BCR31-1	9.63 (0.379)	304.8 (12.0)	R.T.	34.54 (1.36)	221.3 (32.1)	259.3 (37.6)	313.0 (45.4)	54.86 (2.16)	61.0 (55.5)
BCR31-2	9.68 (0.381)	304.8 (12.0)	R.T.	56.39 (2.22)	181.3 (26.3)	220.0 (31.9)	310.3 (45.0)	88.90 (3.50)	66.9 (60.9)
BCR33-1	9.68 (0.381)	304.8 (12.0)	R.T.	22.61 (0.89)	275.1 (39.9)	301.3 (43.7)	345.4 (50.1)	38.86 (1.53)	52.2 (47.5)
BCR33-2	9.65 (0.380)	304.8 (12.0)	R.T.	77.22 (3.04)	159.3 (23.1)	182.0 (26.4)	273.0 (39.6)	101.6 (4.00)	65.8 (59.9)
BCR34-1	9.65 (0.380)	304.8 (12.0)	R.T.	16.51 (0.65)	295.1 (42.8)	319.2 (46.3)	357.9 (51.9)	32.77 (1.29)	46.8 (42.6)
BCR34-2	255.1 (0.370)	304.8) (12.0)	R.T.	92.71 (3.65)	123.4 (17.9)	164.8 (23.9)	279.2 (40.5)	125.2 (4.93)	66.4 (60.4)

TABLE 8: 78K (-320°F) 2219-T87 ALUMINUM BASE METAL CENTER CRACK DATA

SPECIMEN NUMBER	GAGE THICKNESS, t mm (INCH)	GAGE WIDTH, W mm (INCH)	TEST TEMPERATURE °K (°F)	INITIAL FLAW LENGTH, 2c mm (INCH)	STRESS AT START OF CRACK GROWTH, σ_s MN/m^2 (KSI)	MAXIMUM GROSS SECTION STRESS, σ_G MN/m^2 (KSI)	MAXIMUM NET SECTION STRESS, σ_N MN/m^2 (KSI)	CRITICAL CRACK LENGTH, 2c mm (INCH)	K_{cn} $MN/m^{3/2}$ ($KSI\sqrt{IN}$)
BCN11-1	3.30 (0.130)	304.8 (12.0)	78 (-320)	18.03 (0.71)	293.7 (42.6)	348.7 (50.5)	398.5 (57.8)	38.35 (1.51)	58.9 (53.6)
BCN11-2	3.18 (0.125)	304.8 (12.0)	78 (-320)	56.39 (2.22)	167.5 (24.3)	248.9 (36.1)	357.9 (51.9)	92.96 (3.66)	75.7 (68.9)
BCN13-1	3.18 (0.125)	304.8 (12.0)	78 (-320)	10.41 (0.41)	369.6 (53.6)	394.4 (57.6)	432.3 (62.7)	26.67 (1.05)	49.8 (45.3)
BCN13-2	2.97 (0.117)	304.8 (12.0)	78 (-320)	91.95 (3.62)	136.5 (19.8)	191.7 (27.8)	347.5 (50.4)	13.67 (5.38)	76.8 (69.9)
BCN21-1	6.32 (0.249)	304.8 (12.0)	78 (-320)	29.72 (1.17)	271.0 (39.3)	300.6 (43.6)	359.9 (52.2)	50.04 (1.97)	65.6 (59.7)
BCN21-2	6.30 (0.248)	304.8 (12.0)	78 (-320)	56.6 (2.23)	177.2 (25.7)	217.9 (31.6)	303.4 (44.0)	85.1 (3.35)	66.4 (60.4)
BCN23-1	6.30 (0.248)	304.8 (12.0)	78 (-320)	18.03 (0.71)	266.8 (38.7)	334.4 (48.5)	382.7 (55.5)	38.35 (1.51)	56.5 (51.4)
BCN23-2	6.32 (0.249)	304.8 (12.0)	78 (-320)	91.9 (3.62)	135.1 (19.6)	173.8 (25.2)	293.7 (42.6)	124.5 (4.90)	69.7 (63.4)
BCN31-1	9.73 (0.383)	304.8 (12.0)	78 (-320)	37.85 (1.49)	216.5 (31.4)	257.9 (37.2)	327.5 (47.5)	66.29 (2.61)	63.2 (57.5)
BCN31-2	9.68 (0.381)	304.8 (12.0)	78 (-320)	57.40 (2.26)	176.5 (25.6)	215.8 (31.3)	300.6 (43.6)	85.85 (3.38)	66.2 (60.2)
BCN33-1	9.63 (0.379)	304.8 (12.0)	78 (-320)	24.38 (0.96)	252.4 (36.6)	297.9 (43.2)	348.9 (50.6)	44.70 (1.76)	58.6 (53.3)
BCN33-2	9.65 (0.380)	304.8 (12.0)	78 (-320)	92.96 (3.66)	124.8 (18.1)	163.4 (23.7)	284.1 (41.2)	129.5 (5.10)	65.5 (59.6)

TABLE 9: LIQUID HYDROGEN TEMPERATURE 2219-T87 ALUMINUM BASE METAL CENTER CRACK DATA

SPECIMEN NUMBER	GAGE THICKNESS, t mm (INCH)	GAGE WIDTH, W mm (INCH)	TEST TEMPERATURE °K (°F)	INITIAL FLAW LENGTH, 2c mm (INCH)	STRESS AT START OF CRACK GROWTH, σ_s MN/m^2 (KSI)	MAXIMUM GROSS SECTION STRESS, σ_G MN/m^2 (KSI)	MAXIMUM NET SECTION STRESS, σ_N MN/m^2 (KSI)	CRITICAL CRACK LENGTH, 2c mm (INCH)	K_{cn} $MN/m^{3/2}$ ($KSI\sqrt{IN}$)
BCH11-1	3.30 (0.130)	304.8 (12.0)	20 (-423)	15.75 (0.62)	338.5 (49.1)	388.2 (56.3)	444.7 (64.5)	40.13 (1.58)	61.3 (55.8)
BCH11-2	3.30 (0.130)	304.8 (12.0)	20 (-423)	91.69 (3.61)	180.6 (26.2)	210.3 (30.5)	341.3 (49.5)	116.1 (4.57)	84.2 (76.6)
BCH21-1	6.30 (0.248)	304.8 (12.0)	20 (-423)	23.88 (0.94)	279.2 (40.5)	322.7 (46.8)	377.2 (54.7)	44.20 (1.74)	62.8 (57.1)
BCH21-2	6.35 (0.250)	304.8 (12.0)	20 (-423)	92.46 (3.64)	136.5 (19.8)	180.0 (26.1)	304.8 (44.2)	125.0 (4.92)	72.8 (66.2)
BCH31-1	9.73 (0.383)	304.8 (12.0)	20 (-423)	29.72 (1.17)	254.4 (36.9)	279.9 (40.6)	335.1 (48.6)	50.04 (1.97)	61.1 (55.6)
BCH31-2	9.65 (0.380)	304.8 (12.0)	20 (-423)	92.71 (3.65)	128.2 (18.6)	170.3 (24.7)	282.7 (41.0)	121.2 (4.77)	68.9 (62.7)

TABLE 10: ROOM TEMPERATURE 2219 ALUMINUM WELD METAL CENTER CRACK DATA

SPECIMEN NUMBER	GAGE THICKNESS, t mm (INCH)	GAGE WIDTH, W mm (INCH)	TEST TEMPERATURE °K (°F)	INITIAL FLAW LENGTH, 2c mm (INCH)	MAXIMUM GROSS SECTION STRESS, σ_G MN/m^2 (KSI)	K_{cn} MN/m$^{3/2}$ (KSI$\sqrt{IN}$)
WCN11-1	3.20 (0.126)	304.8 (12.0)	RT	20.32 (0.80)	213.8 (31.0)	54.2 (49.3)
WCR11-2	3.18 (0.125)	304.8 (12.0)	RT	91.95 (3.62)	144.1 (20.9)	57.8 (52.6)
WCR13-1	3.18 (0.125)	304.8 (12.0)	RT	10.92 (0.43)	232.4 (33.7)	42.5 (38.6)
WCN21-1	6.02 (0.237)	304.8 (12.0)	RT	34.29 (1.35)	199.3 (28.9)	46.7 (42.5)
WCR21-2	5.99 (0.236)	304.8 (12.0)	RT	92.96 (3.66)	146.2 (21.2)	59.0 (53.6)
WCR23-1	5.79 (0.228)	304.8 (12.0)	RT	20.32 (0.80)	214.4 (31.1)	54.3 (49.4)
WCR31-1	9.65 (0.380)	304.8 (12.0)	RT	58.17 (2.29)	173.1 (25.1)	53.5 (48.6)
WCR31-2	9.63 (0.379)	304.8 (12.0)	RT	93.98 (3.70)	142.0 (20.6)	57.6 (52.4)
WCR33-1	9.65 (0.380)	304.8 (12.0)	RT	32.00 (1.26)	195.8 (28.4)	44.4 (40.4)

TABLE 11: LIQUID NITROGEN TEMPERATURE 2219 ALUMINUM WELD METAL CENTER CRACK DATA

SPECIMEN NUMBER	GAGE THICKNESS, t mm (INCH)	GAGE WIDTH, W mm (INCH)	TEST TEMPERATURE °K (°F)	INITIAL FLAW LENGTH, 2c mm (INCH)	MAXIMUM GROSS SECTION STRESS, σ_G MN/m^2 (KSI)	K_{cn} $MN/m^{3/2}$ (KSI $\sqrt{IN}$)
WCR11-1	3.25 (0.128)	304.8 (12.0)	78K (-320°F)	18.54 (0.73)	266.8 (38.7)	45.5 (41.5)
WCN11-2	3.28 (0.129)	304.8 (12.0)	"	91.95 (3.62)	169.6 24.6)	68.1 (61.9)
WCR21-1	5.94 (0.234)	304.8 (12.0)	"	36.83 (1.45)	200.6 (29.1)	48.7 (44.3
WCN21-2	6.02 (0.237)	304.8 (12.0)	"	9.32 (3.67)	148.2 (21.5)	59.8 (54.4)
WCN31-1	9.63 (0.379)	304.8 (12.0)	"	50.80 (2.00)	202.0 (29.3)	58.0 (52.7)
WCN31-2	9.55 (0.376)	304.8 (12.0)	"	94.23 (3.71)	159.3 (23.1)	64.8 (58.9)

TABLE 12: LIQUID HYDROGEN TEMPERATURE 2219 ALUMINUM WELD METAL CENTER CRACK DATA

SPECIMEN NUMBER	GAGE THICKNESS, t mm (INCH)	GAGE WIDTH, W mm (INCH)	TEST TEMPERATURE °K (°F)	INITIAL FLAW LENGTH, 2c mm (INCH)	MAXIMUM GROSS SECTION STRESS, σ_G MN/m^2 (KSI)	K_{cn} $MN/m^{3/2}$ (KSI $\sqrt{IN}$)
WCH11-1	3.33 (0.131)	304.8 (12.0)	20K (-423°F)	16.76 (0.66)	239.9 (34.8)	39.0 (35.5)
WCH21-1	5.94 (0.234)	304.8 (12.0)	"	32.51 (1.28)	228.9 (33.2)	52.2 (47.5)
WCH31-1	9.53 (0.375)	304.8 (12.0)	"	45.97 (1.81)	197.2 (28.6)	53.9 (49.0)

TABLE 13: 2219-T87 ALUMINUM TEST PROGRAM

MATERIAL CONDITION	TEST TEMPERATURE	a/2c		
		0.15	0.30	0.45
BASE METAL	R.T.	X	X	X
	-320°F	X	X	
	-423°F	X		
WELD METAL	R.T.	X	X	
	-320°F	X		
	-423°F	X		

IDENTICAL TEST PROGRAMS WERE CONDUCTED FOR EACH OF THREE THICKNESSES 0.125, 0.250 AND 0.375 INCH.

X ~ DENOTES CONDITIONS UNDER WHICH BOTH GROWTH -ON-LOADING AND POST PROOF CYCLIC TESTS WERE CONDUCTED

TABLE 14: ROOM TEMPERATURE 2219-T87 ALUMINUM BASE METAL TEST RESULTS
($a/2c = 0.15$ and $t = 3.18$ mm (0.125 inch))

SPECIMEN NUMBER	GAGE THICKNESS, t mm (INCH)	GAGE WIDTH, W mm (INCH)	TEST TEMPERATURE °K (°F)	TEST TYPE	STRESS, σ MN/m^2 (KSI)	INITIAL FLAW DEPTH, a_i mm (INCH)	INITIAL FLAW LENGTH, $2c_i$ mm (INCH)	INITIAL STRESS INTENSITY, K_{I_i} $MN/m^{3/2}$ (KSI$\sqrt{IN}$)	$(a/2c)_i$	$(a/t)_i$	FINAL FLAW DEPTH, a_f mm (INCH)	FINAL FLAW LENGTH, $2c_f$ mm (INCH)	FINAL STRESS INTENSITY, K_{I_f} $MN/m^{3/2}$ (KSI$\sqrt{IN}$)	$(a/2C)_f$	$(a/t)_f$	REMARKS
2BR11-1	3.22 (0.127)	127.0 (5.00)	295 (72)	LUL	282.7 (41.0)	2.84 (0.112)	18.80 (0.740)	44.3 (40.3)	0.151	0.882	a = t	18.80 (0.740)	45.4 (41.3)	0.172	1.00	
			"	FRACTURE	308.9 (44.8)	a = t	18.80 (0.740)	50.1 (45.6)	0.172	1.00						
2BR11-2	3.28 (0.129)	127.0 (5.00)	"	LUL	275.8 (40.0)	2.79 (0.110)	18.80 (0.740)	42.4 (38.6)	0.149	0.853	2.92 (0.115)	18.80 (0.740)	43.4 (39.5)	0.155	0.891	
			"	CYCLIC	220.6 (32.0)	2.92 (0.115)	18.80 (0.740)	34.1 (31.1)	0.155	0.891	a = t	18.80 (0.740)	34.8 (31.7)	0.174	1.00	60 cpm, 81 cycles to B.T.
			"	FRACTURE	313.0 (45.4)	a = t	18.80 (0.740)	51.0 (46.4)	0.174	1.00						
2BR11-3	3.25 (0.128)	127.0 (5.00)	"	LUL	248.2 (36.0)	2.79 (0.110)	18.80 (0.740)	37.9 (34.5)	0.149	0.859	2.84 (0.112)	18.80 (0.740)	38.2 (34.8)	0.151	0.875	
			"	LUL	270.3 (39.2)	2.90 (0.114)	18.80 (0.740)	42.4 (38.6)	0.154	0.891	a = t	18.80 (0.740)	43.3 (39.4)	0.173	1.00	
			"	FRACTURE	311.7 (45.2)	a = t	18.80 (0.740)	50.7 (46.1)	0.173	1.00						
2BR11-4	3.28 (0.129)	127.0 (5.00)	"	LUL	220.6 (32.0)	2.74 (0.108)	18.80 (0.740)	32.8 (29.9)	0.146	0.837	2.74 (0.108)	18.80 (0.740)	32.9 (29.9)	0.146	0.837	
			"	LUL	248.2 (36.0)	2.79 (0.110)	18.80 (0.740)	37.8 (34.4)	0.149	0.853	2.82 (0.111)	18.80 (0.740)	38.0 (34.6)	0.150	0.860	
			"	CYCLIC	198.6 (28.8)	2.82 (0.111)	18.80 (0.740)	29.9 (27.2)	0.150	0.860	a = t	19.05 (0.750)	31.3 (28.5)	0.172	1.00	60 cpm, 312 cycles to B.T.
			"	FRACTURE	313.7 (45.5)	a = t	19.05 (0.750)	51.4 (46.7)	0.172	1.00						
3BR11-1	3.12 (0.123)	127.0 (5.00)	"	LUL	275.8 (40.0)	2.82 (0.111)	18.80 (0.740)	43.4 (39.5)	0.150	0.902		18.80 (0.740)				
			"	CYCLIC	129.6 (18.8)		18.80 (0.740)				a = t	18.80 (0.740)	19.9 (18.1)	0.166	1.00	60 cpm, 1 cycle to B.T.
			"	FRACTURE	325.4 (47.2)	a = t	18.80 (0.740)	52.9 (48.1)	0.166	1.00						
4BR11-1	3.25 (0.128)	127.0 (5.00)	"	LUL	275.8 (40.0)	2.79 (0.110)	19.05 (0.750)	42.7 (38.9)	0.147	0.859	2.92 (0.115)	19.05 (0.750)	43.7 (39.8)	0.153	0.898	
			"	CYCLIC	220.6 (32.0)	2.92 (0.115)	19.05 (0.750)	34.4 (31.3)	0.153	0.898	a = t	19.05 (0.750)	34.9 (31.8)	0.171	1.00	1cpm, 66 cycles to B.T.
			"	FRACTURE	326.1 (47.3)	a = t	19.05 (0.750)	53.6 (48.8)	0.171	1.00						

TABLE 14: (Continued)

SPECIMEN NUMBER	GAGE THICKNESS, t mm (INCH)	GAGE WIDTH, W mm (INCH)	TEST TEMPERATURE °K (°F)	TEST TYPE	STRESS, σ MN/m² (KSI)	INITIAL FLAW DEPTH, a_i mm (INCH)	INITIAL FLAW LENGTH, $2c_i$ mm (INCH)	INITIAL STRESS INTENSITY, K_{I_i} MN/m^3/2 (KSI√IN)	$(a/2c)_i$	$(a/t)_i$	FINAL FLAW DEPTH, a_f mm (INCH)	FINAL FLAW LENGTH, $2c_f$ mm (INCH)	FINAL STRESS INTENSITY, K_{I_f} MN/m^3/2 (KSI√IN)	$(a/2C)_f$	$(a/t)_f$	REMARKS
4BR11-2	3.23 (0.127)	127.0 (5.00)	295 (72)	FRACTURE	325.4 (47.2)	2.79 (0.110)	19.05 (0.750)	51.7 (47.0)	0.147	0.866						B.T. at 273.0 MN/m² (39.6 KSI)
3BN11-1A	3.28 (0.129)	127.0 (5.00)	"	LUL	275.8 (40.0)	2.72 (0.107)	17.91 (0.705)	40.8 (37.1)	0.152	0.829	2.79 (0.110)	17.91 (0.705)	41.8 (38.0)	0.156	0.853	
			"	CYCLE	248.2 (36.0)	2.79 (0.110)	17.91 (0.705)	37.1 (33.8)	0.156	0.853	3.00 (0.118)	17.91 (0.705)	38.4 (34.9)	0.167	0.915	1 cpm, 100 cycles total
			"	FRACTURE	332.2 (48.2)	3.00 (0.118)	17.91 (0.705)	53.1 (48.3)	0.167	0.915						B.T. at 303.4 MN/m² (44.0 KSI)

TABLE 15: ROOM TEMPERATURE 2219-T87 ALUMINUM BASE METAL TEST RESULTS ($a/2c = 0.30$ and $t = 3.18$ mm (0.125 inch))

SPECIMEN NUMBER	GAGE THICKNESS, t mm (INCH)	GAGE WIDTH, W mm (INCH)	TEST TEMPERATURE °K (°F)	TEST TYPE	STRESS, σ MN/m^2 (KSI)	INITIAL FLAW DEPTH, a_i mm (INCH)	INITIAL FLAW LENGTH, $2c_i$ mm (INCH)	INITIAL STRESS INTENSITY, K_{I_i} $MN/m^{3/2}$ ($KSI\sqrt{IN}$)	$(a/2c)_i$	$(a/t)_i$	FINAL FLAW DEPTH, a_f mm (INCH)	FINAL FLAW LENGTH, $2c_f$ mm (INCH)	FINAL STRESS INTENSITY, K_{I_f} $MN/m^{3/2}$ ($KSI\sqrt{IN}$)	$(a/2C)_f$	$(a/t)_f$	REMARKS
2BR13-1	3.18 (0.125)	127.0 (5.00)	295 (72)	LUL	300.6 (43.6)	3.02 (0.119)	9.78 (0.385)	33.8 (30.8)	0.309	0.952	a = t	9.78 (0.385)	33.6 (30.6)	0.325	1.00	
			"	FRACTURE	345.4 (50.1)	a = t	9.78 (0.385)	39.1 (35.6)	0.325	1.00						
2BR13-2	3.25 (0.128)	127.0 (5.00)	"	LUL	289.6 (42.0)	2.87 (0.113)	9.65 (0.380)	32.4 (29.5)	0.311	0.883	3.00 (0.118)	9.65 (0.380)	32.4 (29.5)	0.311	0.922	
			"	CYCLIC	231.7 (33.6)	3.00 (0.118)	9.65 (0.380)	25.5 (23.2)	0.311	0.922	a = t	10.16 (0.400)	26.0 (23.7)	0.320	1.00	60 cpm, 370 cycles to B.T.
			"	FRACTURE	348.2 (50.5)	a = t	10.16 (0.400)	40.4 (36.8)	0.320	1.00						
2BR13-3	3.25 (0.128)	127.0 (5.00)	"	LUL	333.7 (48.4)	2.90 (0.114)	9.78 (0.385)	38.2 (34.8)	0.296	0.891	a = t	9.78 (0.385)	37.5 (34.1)	0.332	1.00	
			"	FRACTURE	348.9 (50.6)	a = t	9.78 (0.385)	39.5 (35.9)	0.332	1.00						
3BR13-1	3.28 (0.129)	127.0 (5.00)	"	LUL	264.8 (38.4)	2.90 (0.114)	9.53 (0.375)	29.1 (26.5)	0.304	0.884	2.90 (0.114)	9.53 (0.375)	29.1 (26.5)	0.304	0.884	
			"	FRACTURE	347.5 (50.4)	2.92 (0.115)	9.53 (0.375)	39.2 (35.7)	0.307	0.891						B.T. at 335.1 MN/m^2 (48.6 KSI)
2BR13-4	3.23 (0.127)	127.0 (5.00)	"	LUL	240.6 (34.9)	3.07 (0.121)	9.80 (0.386)	26.7 (24.3)	0.313	0.953	3.07 (0.121)	9.80 (0.386)	26.7 (24.3)	0.313	0.953	
			"	LUL	270.3 (39.2)	3.10 (0.122)	9.80 (0.386)	30.1 (27.4)	0.316	0.961	3.10 (0.122)	9.80 (0.386)	30.1 (27.4)	0.316	0.961	
			"	CYCLIC	216.5 (31.4)	3.10 (0.122)	9.80 (0.386)	23.7 (21.6)	0.316	0.961	a = t	9.91 (0.390)	23.8 (21.7)	0.326	1.00	60 cpm, 106 cycles to B.T.
			"	FRACTURE	351.6 (51.0)	a = t	9.91 (0.390)	40.2 (36.6)	0.326	1.00						
3BR13-2	3.28 (0.129)	127.0 (5.00)	"	LUL	292.3 (42.4)	2.97 (0.117)	9.91 (0.390)	33.2 (30.2)	0.300	0.907	a = t	9.91 (0.390)	32.8 (29.8)	0.331	1.00	
			"	FRACTURE	354.4 (51.4)	a = t	9.91 (0.390)	40.4 (36.8)	0.331	1.00						

TABLE 16: ROOM TEMPERATURE 2219-T87 ALUMINUM BASE METAL TEST RESULTS
(a/2c = 0.45 and t = 3.18 mm (0.125 inch))

SPECIMEN NUMBER	GAGE THICKNESS, t mm (INCH)	GAGE WIDTH, W mm (INCH)	TEST TEMPERATURE °K (°F)	TEST TYPE	STRESS, σ MN/m² (KSI)	INITIAL FLAW DEPTH, a_i mm (INCH)	INITIAL FLAW LENGTH, $2c_i$ mm (INCH)	INITIAL STRESS INTENSITY, K_{I_i} MN/m^{3/2} (KSI√IN)	$(a/2c)_i$	$(a/t)_i$	FINAL FLAW DEPTH, a_f mm (INCH)	FINAL FLAW LENGTH, $2c_f$ mm (INCH)	FINAL STRESS INTENSITY, K_{I_f} MN/m^{3/2} (KSI√IN)	$(a/2C)_f$	$(a/t)_f$	REMARKS
2BR14-1	3.25 (0.128)	127.0 (5.00)	295 (72)	LUL	310.3 (45.0)	3.02 (0.119)	6.86 (0.270)	26.6 (24.2)	0.441	0.930	3.07 (0.121)	6.86 (0.270)	26.4 (24.0)	0.448	0.945	
			"	CYCLIC	248.2 (36.0)	3.07 (0.121)	6.86 (0.270)	20.8 (18.9)	0.448	0.945	a = t	7.11 (0.280)	21.0 (19.1)	0.457	1.00	60 CPM, 125 Cycles to B.T.
			"	FRACTURE	357.9 (51.9)	a = t	7.11 (0.280)	31.0 (28.2)	0.457	1.00						
2BR14-2	3.25 (0.128)	127.0 (5.00)	"	LUL	279.2 (40.5)	3.00 (0.118)	7.01 (0.276)	24.3 (22.1)	0.428	0.922	3.05 (0.118)	7.01 (0.276)	24.3 (22.1)	0.428	0.922	
			"	FRACTURE	349.6 (50.7)	a = t	7.11 (0.280)	30.2 (27.5)	0.457	1.00						
2BR14-3	3.30 (0.130)	127.0 (5.00)	"	LUL	248.2 (36.0)	3.05 (0.120)	7.11 (0.280)	21.7 (19.7)	0.429	0.923	3.10 (0.120)	7.11 (0.280)	21.7 (19.7)	0.429	0.923	
			"	FRACTURE	351.6 (51.0)	a = t	7.11 (0.280)	30.2 (27.5)	0.464	1.00						
3BR14-1	3.25 (0.128)	127.0 (5.00)	"	LUL	299.9 (43.5)	3.10 (0.122)	7.01 (0.276)	25.8 (23.5)	0.442	0.953	a = t	7.06 (0.278)	25.5 (23.2)	0.460	1.00	
			"	FRACTURE	359.2 (52.1)	a = t	7.06 (0.278)	30.9 (28.1)	0.460	1.00						
3BR14-2	3.23 (0.127)	127.0 (5.00)	"	FRACTURE	356.5 (51.7)	a = t	6.73 (0.265)	29.3 (26.7)	0.479	1.00						
2BR14-4	3.25 (0.128)	127.0 (5.00)	"	FRACTURE	362.7 (52.6)	a = t	6.86 (0.270)	30.3 (27.6)	0.474	1.00						
4BR14-1	3.25 (0.128)	127.0 (5.00)	"	LUL	293.0 (42.5)	2.97 (0.117)	6.78 (0.267)	24.9 (22.7)	0.438	0.914	3.02 (0.119)	6.78 (0.267	24.7 (22.5)	0.446	0.930	
			"	CYCLIC	263.4 (38.2)	3.02 (0.119)	6.78 (0.267)	22.1 (20.1)	0.446	0.930	3.10 (0.122)	6.86 (0.270)	22.1 (20.1)	0.452	0.953	1 CPM, 100 Cycles Total
			"	FRACTURE	382.7 (55.5)	3.10 (0.122)	6.86 (0.270)	33.0 (30.0)	0.452	0.953						B.T. at 359.9 MN/m² (52.2 ksi)
4BR14-2	3.18 (0.125)	127.0 (5.00)	"	LUL	293.0 (42.5)	3.10 (0.122)	6.93 (0.273)	24.9 (22.7)	0.447	0.976	3.10 (0.122)	6.93 (0.273)	24.9 (22.7)	0.447	0.976	
			"	CYCLIC	263.4 (38.2)	3.10 (0.122)	6.93 (0.273)	22.3 (20.3)	0.447	0.976	a = t	6.93 (0.273)	22.1 (20.1)	0.458	1.00	1 CPM, 1 cycle to B.T. 3 Total
			"	FRACTURE	376.5 (54.6)	a = t	6.93 (0.273)	32.3 (29.4)	0.458	1.00						
3BR14-1A	3.28 (0.129)	127.0 (5.00)	"	FRACTURE	374.4 (54.3)	2.82 (0.111)	6.71 (0.264)	32.2 (29.3)	0.420	0.860				.		B.T. at 373.0 MN/m² (54.1 ksi)

TABLE 17: ROOM TEMPERATURE 2219-T87 ALUMINUM BASE METAL TEST RESULTS ($a/2c$ = 0.15 and t = 6.35mm (0.250 inch))

SPECIMEN NUMBER	GAGE THICKNESS, t mm (INCH)	GAGE WIDTH, W mm (INCH)	TEST TEMPERATURE °K (°F)	TEST TYPE	STRESS, σ MN/m^2 (KSI)	INITIAL FLAW DEPTH, a_i mm (INCH)	INITIAL FLAW LENGTH, $2c_i$ mm (INCH)	INITIAL STRESS INTENSITY, K_{I_i} $MN/m^{3/2}$ (KSI$\sqrt{IN}$)	$(a/2c)_i$	$(a/t)_i$	FINAL FLAW DEPTH, a_f mm (INCH)	FINAL FLAW LENGTH, $2c_f$ mm (INCH)	FINAL STRESS INTENSITY, K_{I_f} $MN/m^{3/2}$ (KSI$\sqrt{IN}$)	$(a/2C)_f$	$(a/t)_f$	REMARKS
2BR21-1	6.35 (0.250)	228.9 (9.01)	295 (72)	LUL	308.2 (44.7)	4.06 (0.160)	27.18 (1.070)	48.5 (44.1)	0.150	0.640	4.65 (0.183)	27.18 (1.070)	53.6 (48.8)	0.171	0.732	
			"	CYCLIC	248.2 (36.0)	4.65 (0.183)	27.18 (1.070)	42.3 (38.5)	0.171	0.732	a = t	30.48 (1.200)	50.8 (46.2)	0.208	1.00	60 cpm, 343 cycles to B.T.
			"	FRACTURE	288.2 (41.8)	a = t	30.48 (1.200)	59.8 (54.4)	0.208	1.00						
2BR21-2	6.35 (0.250)	228.9 (9.01)	"	LUL	278.6 (40.4)	4.06 (0.160)	27.31 (1.075)	43.4 (39.5)	0.149	0.640	4.22 (0.166)	27.31 (1.075)	44.6 (40.6)	0.154	0.664	
			"	FRACTURE	314.4 (45.6)	4.29 (0.169)	27.31 (1.075)	51.8 (47.1)	0.157	0.676						
2BR21-3	6.32 (0.249)	228.9 (9.01)	"	LUL	251.7 (36.5)	4.11 (0.162)	27.18 (1.070)	39.2 (35.7)	0.151	0.651	4.19 (0.165)	27.18 (1.070)	39.8 (36.2)	0.154	0.663	
			"	LUL	279.2 (40.5)	4.24 (0.167)	27.18 (1.070)	44.9 (40.9)	0.156	0.671	4.34 (0.171)	27.18 (1.070)	45.8 (41.7)	0.160	0.687	
			"	FRACTURE	319.9 (46.4)	4.39 (0.173)	27.18 (1.070)	53.7 (48.9)	0.162	0.695						
3BR21-1	6.35 (0.250)	228.9 (9.01)	"	FRACTURE	322.0 (46.7)	4.06 (0.160)	26.67 (1.050)	50.8 (46.2)	0.152	0.640						
2BR21-4	6.30 (0.248)	228.9 (9.01)	"	LUL	310.3 (45.0)	4.27 (0.168)	27.69 (1.090)	51.2 (46.6)	0.154	0.677	4.90 (0.193)	27.69 (1.090)	56.8 (51.7)	0.177	0.778	
			"	CYCLIC	248.2 (36.0)	4.90 (0.193)	27.69 (1.090)	44.5 (40.5)	0.177	0.778	a = t	30.73 (1.210)	51.0 (46.4)	0.204	1.00	60 cpm, 382 cycles to B.T.
			"	FRACTURE	287.5 (41.7)	a = t	30.73 (1.210)	59.8 (54.4)	0.204	1.00						
4BR21-1	6.32 (0.249)	228.9 (9.01)	"	LUL	310.3 (45.0)	4.11 (0.162)	27.18 (1.070)	49.5 (45.0)	0.151	0.651	5.00 (0.197)	29.46 (1.160)	58.9 (53.6)	0.170	0.791	
			"	CYCLIC	297.2 (40.5)	5.00 (0.197)	29.46 (1.160)	52.4 (47.7)	0.170	0.791	a = t	30.48 (1.200)	57.7 (52.5)	0.206	1.00	1cpm, 31 cycles to B.T.
			"	FRACTURE	293.7 (42.6)	a = t	30.48 (1.200)	61.0 (55.5)	0.206	1.00						
4BR21-2	6.40 (0.252)	228.9 (9.01)	"	LUL	310.3 (45.0)	40.64 (0.160)	27.94 (1.100)	49.0 (44.6)	0.145	0.635	4.32 (0.170)	[illegible] (1.100)	51.3 (46.7)	0.155	0.675	1 cpm, 100 cycles total
			"	CYCLIC	264.1 (38.3)	4.32 (0.170)	27.94 (1.100)	43.0 (39.1)	0.155	0.675	4.83 (0.190)	27.94 (1.100)	46.7 (42.5)	0.173	0.754	
			"	FRACTURE	319.2 (46.3)	4.83 (0.190)	27.94 (1.100)	57.7 (52.5)	0.173	0.754						

TABLE 17: (Continued)

SPECIMEN NUMBER	GAGE THICKNESS, t mm (INCH)	GAGE WIDTH, W mm (INCH)	TEST TEMPERATURE °K (°F)	TEST TYPE	STRESS, σ MN/m² (KSI)	INITIAL FLAW DEPTH, a_i mm (INCH)	INITIAL FLAW LENGTH, $2c_i$ mm (INCH)	INITIAL STRESS INTENSITY, K_{I_i} MN/m$^{3/2}$ (KSI$\sqrt{IN}$)	$(a/2c)_i$	$(a/t)_i$	FINAL FLAW DEPTH, a_f mm (INCH)	FINAL FLAW LENGTH, $2c_f$ mm (INCH)	FINAL STRESS INTENSITY, K_{I_f} MN/m$^{3/2}$ (KSI$\sqrt{IN}$)	$(a/2C)_f$	$(a/t)_f$	REMARKS
3BR21-2	6.27 (0.247)	228.9 (9.01)	295 (72)	LUL	317.2 (46.0)	3.91 (0.154)	27.18 (1.07)	49.0 (44.6)	0.144	0.623	4.67 (0.184)	27.18 (1.07)	56.0 (51.0)	0.172	0.745	
				CYCLIC	248.2 (36.0)	4.67 (0.184)	27.18 (1.07)	42.8 (38.9)	0.172	0.745	a = t	29.46 (1.16)	50.0 (45.5)	0.213	1.00	60 cpm, 562 cycles to B.T.
				FRACTURE	296.5 (43.0)	a = t	29.46 (1.16)	60.6 (55.1)	0.213	1.00						

TABLE 18: ROOM TEMPERATURE 2219-T87 ALUMINUM BASE METAL TEST RESULTS
((a/2c = 0.30 and t = 6.35 mm (0.250 inch))

SPECIMEN NUMBER	GAGE THICKNESS, t mm (INCH)	GAGE WIDTH, W mm (INCH)	TEST TEMPERATURE °K (°F)	TEST TYPE	STRESS, σ MN/m² (KSI)	INITIAL FLAW DEPTH, a_i mm (INCH)	INITIAL FLAW LENGTH, $2c_i$ mm (INCH)	INITIAL STRESS INTENSITY, K_{I_i} MN/m$^{3/2}$ (KSI$\sqrt{IN}$)	$(a/2c)_i$	$(a/t)_i$	FINAL FLAW DEPTH, a_f mm (INCH)	FINAL FLAW LENGTH, $2c_f$ mm (INCH)	FINAL STRESS INTENSITY, K_{I_f} MN/m$^{3/2}$ (KSI$\sqrt{IN}$)	$(a/2C)_f$	$(a/t)_f$	REMARKS
2BR23-1	6.32 (0.249)	228.6 (9.00)	295 (72)	LUL	310.3 (45.0)	4.93 (0.194)	16.00 (0.630)	42.6 (38.8)	0.308	0.779	5.05 (0.199)	16.00 (0.630)	42.9 (39.0)	0.316	0.799	
			"	CYCLIC	248.2 (36.0)	5.05 (0.199)	16.00 (0.630)	33.7 (30.7)	0.316	0.799	a = t	21.34 (0.840)	41.0 (37.3)	0.296	1.00	60 cpm, 1030 cycles to B.T.
			"	FRACTURE	337.9 (49.0)	a = t	21.34 (0.840)	57.4 (52.2)	0.296	1.00						
2BR23-2	6.30 (0.248)	228.9 (9.01)	"	LUL	279.2 (40.5)	4.98 (0.196)	16.51 (0.650)	39.0 (35.5)	0.302	0.790	5.00 (0.197)	16.51 (0.650)	39.1 (35.6)	0.303	0.794	
			"	FRACTURE	364.7 (52.9)	5.08 (0.200)	16.51 (0.650)	52.6 (47.9)	0.308	0.806						B.T. at 328.2 MN/m² (47.6 KSI)
2BR23-3	6.35 (0.250)	228.9 (9.01)	"	LUL	251.7 (36.5)	5.08 (0.200)	16.76 (0.660)	35.4 (32.2)	0.303	0.800	5.08 (0.200)	16.76 (0.660)	35.4 (32.2)	0.303	0.800	
			"	LUL	279.2 (40.5)	5.16 (0.203)	16.76 (0.660)	39.7 (36.1)	0.308	0.812	5.18 (0.204)	16.89 (0.665)	39.9 (36.3)	0.307	0.816	
			"	FRACTURE	330.3 (47.9)	5.26 (0.207)	17.02 (0.670)	48.4 (44.0)	0.309	0.828						
3BR23-1	6.32 (0.249)	228.9 (9.01)	"	LUL	337.9 (49.0)	5.08 (0.200)	16.76 (0.660)	48.7 (44.3)	0.303	0.803	a = t	20.32 (0.800)	55.5 (50.5)	0.311	1.00	
			"	FRACTURE	332.3 (48.2)	a = t	20.32 (0.800)	54.5 (49.6)	0.311	1.00						
2BR23-4	6.35 (0.250)	228.6 (9.00)	"	LUL	324.1 (47.0)	4.98 (0.196)	16.26 (0.640)	45.3 (41.2)	0.306	0.784	5.23 (0.206)	16.26 (0.640)	45.8 (41.7)	0.322	0.824	
				CYCLIC	259.3 (37.6)	5.23 (0.206)	16.26 (0.640)	36.0 (32.8)	0.322	0.824	a = t	20.32 (0.800)	41.7 (37.9)	0.313	100	60 cpm, 492 cycles to B.T.
				FRACTURE	322.7 (46.8)	a = t	20.32 (0.800)	52.8 (48.0)	0.313	1.00						
3BR23-2	6.27 (0.247)	228.9 (9.01)	"	LUL	331.0 (48.0)	5.08 (0.200)	16.00 (0.630)	46.3 (42.1)	0.317	0.810	5.33 (0.210)	16.76 (0.660)	48.5 (44.1)	0.318	0.850	
			"	CYCLIC	259.3 (37.6)	5.33 (0.210)	16.76 (0.660)	37.1 (33.8)	0.318	0.850	a = t	20.57 (0.810)	42.0 (33.2)	0.305	1.00	60 cpm, 716 cycles to B.T.
			"	FRACTURE	326.1 (47.3)	a = t	20.57 (0.810)	53.9 (49.0)	0.305	1.00						
3BR23-3	6.30 (0.248)	228.9 (9.01)	"	FRACTURE	341.3 (49.5)	4.98 (0.196)	16.51 (0.650)	46.8 (42.6)	0.311	0.790						

TABLE 19: ROOM TEMPERATURE 2219-T87 ALUMINUM BASE METAL TEST RESULTS
(a/2c = 0.45 and t = 6.35 mm (0.250 inch))

SPECIMEN NUMBER	GAGE THICKNESS, t mm (INCH)	GAGE WIDTH, W mm (INCH)	TEST TEMPERATURE °K (°F)	TEST TYPE	STRESS, σ MN/m² (KSI)	INITIAL FLAW DEPTH, a_i mm (INCH)	INITIAL FLAW LENGTH, $2c_i$ mm (INCH)	INITIAL STRESS INTENSITY, K_{I_i} MN/m^3/2 (KSI√IN)	$(a/2c)_i$	$(a/t)_i$	FINAL FLAW DEPTH, a_f mm (INCH)	FINAL FLAW LENGTH, $2c_f$ mm (INCH)	FINAL STRESS INTENSITY, K_{I_f} MN/m^3/2 (KSI√IN)	$(a/2C)_f$	$(a/t)_f$	REMARKS
2BR24-1	6.30 (0.248)	228.6 (9.00)	295 (72)	LUL	310.3 (45.0)	5.08 (0.200)	10.67 (0.420)	30.9 (28.1)	0.476	0.806	5.13 (0.202)	10.67 (0.420)	30.8 (28.0)	0.481	0.815	
			"	CYCLIC	248.2 (36.0)	5.13 (0.202)	10.67 (0.420)	24.4 (22.2)	0.481	0.815	a = t	15.49 (0.610)	32.5 (29.6)	0.470	1.00	60 cpm, 1063 cycles to B.T.
			"	FRACTURE	328.2 (47.6)	a = t	15.49 (0.610)	43.9 (39.9)	0.407	1.00						
2BR24-2	6.32 (0.249)	229.1 (9.02)	"	LUL	279.2 (40.5)	5.00 (0.197)	11.18 (0.440)	28.8 (26.2)	0.448	0.791	5.00 (0.197)	11.18 (0.440)	28.8 (26.2)	0.448	0.791	
			"	FRACTURE	348.2 (50.5)	5.08 (0.200)	11.30 (0.445)	36.7 (33.4)	0.449	0.803						
2BR24-3	6.35 (0.250)	228.9 (9.01)	"	LUL	251.7 (36.5)	4.47 (0.176)	11.18 (0.440)	25.6 (23.3)	0.400	0.704	4.47 (0.176)	11.18 (0.440)	25.6 (23.3)	0.400	0.704	
			"	LUL	279.2 (40.5)	4.52 (0.178)	11.30 (0.445)	28.9 (26.3)	0.402	0.712	4.52 (0.178)	11.30 (0.445)	28.9 (26.3)	0.402	0.712	
			"	FRACTURE	348.9 (50.6)	4.60 (0.181)	11.43 (0.450)	37.0 (33.7)	0.402	0.724						
3BR24-1	6.35 (0.250)	228.9 (9.01)	"	FRACTURE	364.7 (52.9)	4.93 (0.194)	10.92 (0.430)	37.6 (34.2)	0.451	0.776						
2BR24-4	6.30 (0.248)	228.6 (9.00)	"	LUL	344.8 (50.0)	4.98 (0.196)	10.92 (0.430)	35.4 (32.2)	0.456	0.790	5.16 (0.203)	12.70 (0.500)	40.1 (36.5)	0.406	0.819	
			"	CYCLIC	275.8 (40.0)	5.16 (0.203)	12.70 (0.500)	31.5 (28.7)	0.406	0.819	a = t	19.05 (0.750)	42.6 (38.8)	0.331	1.00	60 cpm, 1088 cycles to B.T.
			"	FRACTURE	334.4 (48.5)	a = t	19.05 (0.750)	52.5 (47.8)	0.331	1.00						
4BR24-1	6.32 (0.249)	228.9 (9.01)	"	LUL	344.8 (50.0)	5.08 (0.200)	11.43 (0.450)	36.7 (33.4)	0.444	0.803	5.21 (0.205)	13.21 (0.520)	41.4 (37.7)	0.394	0.823	
			"	CYCLIC	310.3 (45.0)	5.21 (0.205)	13.21 (0.520)	37.0 (33.7)	0.394	0.823	5.54 (0.218)	14.48 (0.570)	40.2 (36.6)	0.382	0.876	1 cpm, 100 cycles total
			"	FRACTURE	347.5 (50.5)	5.54 (0.218)	14.48 (0.570)	45.5 (41.4)	0.382	0.876						
4BR24-2	6.32 (0.249)	228.9 (9.01)	"	LUL	344.8 (50.0)	4.98 (0.196)	11.94 (0.470)	38.0 (34.6)	0.417	0.787	5.05 (0.199)	13.46 (0.530)	42.1 (38.3)	0.375	0.799	
			"	CYCLIC	327.5 (47.5)	5.05 (0.199)	13.46 (0.530)	39.8 (36.2)	0.375	0.799	5.72 (0.225)	15.75 (0.620)	45.7 (41.6)	0.363	0.904	1 cpm, 100 cycles total
			"	FRACTURE	351.0 (50.9)	5.72 (0.225)	15.75 (0.620)	49.3 (44.9)	0.363	0.904						

TABLE 19: Continued)

SPECIMEN NUMBER	GAGE THICKNESS, t mm (INCH)	GAGE WIDTH, W mm (INCH)	TEST TEMPERATURE °K (°F)	TEST TYPE	STRESS, σ MN/m^2 (KSI)	INITIAL FLAW DEPTH, a_i mm (INCH)	INITIAL FLAW LENGTH, $2c_i$ mm (INCH)	INITIAL STRESS INTENSITY, K_{I_i} $MN/m^{3/2}$ ($KSI\sqrt{IN}$)	$(a/2c)_i$	$(a/t)_i$	FINAL FLAW DEPTH, a_f mm (INCH)	FINAL FLAW LENGTH, $2c_f$ mm (INCH)	FINAL STRESS INTENSITY, K_{I_f} $MN/m^{3/2}$ ($KSI\sqrt{IN}$)	$(a/2C)_f$	$(a/t)_f$	REMARKS
3BR24-2	6.27 (0.247)	228.9 (9.01)	295 (72)	LUL	358.5 (52.0)	4.98 (0.196)	11.18 (0.440)	37.7 (34.3)	0.445	0.794	5.36 (0.211)	13.72 (0.540)	45.1 (41.0)	0.391	0.854	
			"	CYCLIC	275.8 (40.0)	5.36 (0.211)	13.72 (0.540)	34.0 (30.9)	0.391	0.854	a = t	16.51 (0.650)	38.4 (34.9)	0.380	1.00	60 cpm, 345 cycles to B.T.
			"	FRACTURE	342.0 (49.6)	a = t	16.51 (0.650)	48.4 (44.0)	0.380	1.00						

TABLE 20: ROOM TEMPERATURE 2219-T87 ALUMINUM BASE METAL TEST RESULTS
($a/2c = 0.15$ and $t = 9.53$ mm (0.375 inch))

SPECIMEN NUMBER	GAGE THICKNESS, t mm (INCH)	GAGE WIDTH, W mm (INCH)	TEST TEMPERATURE °K (°F)	TEST TYPE	STRESS, σ MN/m² (KSI)	INITIAL FLAW DEPTH, a_i mm (INCH)	INITIAL FLAW LENGTH, $2c_i$ mm (INCH)	INITIAL STRESS INTENSITY, K_{I_i} MN/m$^{3/2}$ (KSI$\sqrt{IN}$)	$(a/2c)_i$	$(a/t)_i$	FINAL FLAW DEPTH, a_f mm (INCH)	FINAL FLAW LENGTH, $2c_f$ mm (INCH)	FINAL STRESS INTENSITY, K_{I_f} MN/m$^{3/2}$ (KSI$\sqrt{IN}$)	$(a/2C)_f$	$(a/t)_f$	REMARKS
2BR31-1	9.63 (0.379)	355.6 (14.0)	295 (72)	LUL	310.3 (45.0)	4.88 (0.192)	33.78 (1.33)	49.5 (44.1)	0.144	0.507	5.21 (0.205)	33.78 (1.33)	50.8 (46.2)	0.154	0.541	
			"	CYCLIC	248.2 (36.0)	5.21 (0.205)	33.78 (1.33)	39.7 (36.1)	0.154	0.507	a = t	44.45 (1.75)	61.3 (55.8)	0.217	1.00	60 CPM, 1773 Cycles to B.T.
			"	FRACTURE	290.3 (42.1)	a = t	44.45 (1.75)	72.8 (66.2)	0.217	1.00						
2BR31-2	9.65 (0.380)	355.6 (14.0)	"	LUL	279.2 (40.5)	5.03 (0.198)	33.78 (1.33)	44.0 (40.0)	0.149	0.521	5.18 (0.204)	33.78 (1.33)	44.9 (40.9)	0.153	0.537	
			"	CYCLIC	248.2 (36.0)	5.18 (0.204)	33.78 (1.33)	39.5 (35.9)	0.153	0.537	a = t	43.18 (1.70)	60.4 (55.0)	0.224	1.00	60 CPM, 1029 Cycles to B.T.
			"	FRACTURE	268.2 (38.9)	a = t	43.18 (1.70)	65.7 (59.8)	0.224	1.00						
2BR31-3	9.65 (0.380)	355.6 (14.0)	"	LUL	248.2 (36.0)	4.98 (0.196)	33.53 (1.32)	38.4 (34.9)	0.148	0.516	5.08 (0.200)	33.53 (1.32)	38.9 (35.4)	0.152	0.526	
			"	CYCLIC	198.6 (28.8)	5.08 (0.200)	33.53 (1.32)	30.7 (27.9)	0.152	0.526	a = t	40.64 (1.60)	46.3 (42.1)	0.238	1.00	60 CPM, 3842 Cycles to B.T.
			"	FRACTURE	275.1 (39.9)	a = t	40.64 (1.60)	65.4 (59.5)	0.238	1.00						
3BR31-1	9.63 (0.379)	355.6 (14.0)	"	FRACTURE	333.0 (48.3)	5.03 (0.198)	33.27 (1.31)	53.5 (48.7)	0.151	0.522						
2BR31-4	9.65 (0.380)	355.6 (14.0)	"	LUL	320.6 (46.5)	4.93 (0.194)	33.27 (1.31)	50.4 (45.9)	0.148	0.511	5.13 (0.202)	33.27 (1.31)	51.9 (47.2)	0.154	0.532	Slight Delamination
			"	CYCLIC	248.2 (36.0)	5.13 (0.202)	33.27 (1.31)	39.0 (35.5)	0.154	0.532	a = t	43.18 (1.70)	60.4 (55.0)	0.224	1.00	60 CPM, 2021 Cycles to B.T.
			"	FRACTURE	274.4 (39.8)	a = t	43.18 (1.70)	67.4 (61.3)	0.224	1.00						
4BR31-1	9.75 (0.384)	355.6 (14.0)	"	FRACTURE	328.9 (47.7)	4.98 (0.196)	33.20 (1.30)	52.1 (47.4)	0.150	0.510						
3BR31-2	9.55 (0.376)	355.6 (14.0)	"	LUL	320.6 (46.5)	5.03 (0.198)	33.27 (1.31)	51.5 (46.8)	0.151	0.527	5.16 (0.203)	33.27 (1.31)	52.3 (47.6)	0.155	0.540	Some Delamination
			"	CYCLIC	248.2 (36.0)	5.16 (0.203)	33.27 (1.31)	39.3 (35.8)	0.155	0.540	5.41 (0.213)	33.27 (1.31)	40.7 (37.0)	0.163	0.566	1 CPM, 100 Cycles Total
			"	FRACTURE	340.6 (49.4)	5.41 (0.213)	33.27 (1.31)	57.9 (52.7)	0.163	0.566						

TABLE 20: (Continued)

SPECIMEN NUMBER	GAGE THICKNESS, t mm (INCH)	GAGE WIDTH, W mm (INCH)	TEST TEMPERATURE °K (°F)	TEST TYPE	STRESS, σ MN/m^2 (KSI)	INITIAL FLAW DEPTH, a_i mm (INCH)	INITIAL FLAW LENGTH, $2c_i$ mm (INCH)	INITIAL STRESS INTENSITY, K_{I_i} MN/m$^{3/2}$ (KSI $\sqrt{IN}$)	$(a/2c)_i$	$(a/t)_i$	FINAL FLAW DEPTH, a_f mm (INCH)	FINAL FLAW LENGTH, $2c_f$ mm (INCH)	FINAL STRESS INTENSITY, K_{I_f} MN/m$^{3/2}$ (KSI $\sqrt{IN}$)	$(a/2C)_f$	$(a/t)_f$	REMARKS
4BR31-2	9.53 (0.375)	355.6 (14.0)	295 (72)	LUL	317.2 (46.0)	5.08 (0.200)	34.04 (1.34)	51.4 (46.8)	0.149	0.533	5.23 (0.206)	34.04 (1.34)	52.5 (47.8)	0.154	0.549	Some Delamination
			"	CYCLIC	285.5 (41.4)	5.23 (0.206)	34.04 (1.34)	46.7 (42.5)	0.154	0.549	(0.225)	34.04 1.34)	49.5 (45.0)	0.168	0.600	1 CPM, 100 Cycles Total
			"	FRACTURE	331.0 (48.0)	5.71 (0.225)	34.04 (1.34)	58.5 (53.2)	0.168	0.600						

TABLE 21: ROOM TEMPERATURE 2219-T87 ALUMINUM 22 BASE METAL TEST RESULTS
($a/2c = 0.30$ and $t = 9.53$ mm (0.375 inch))

SPECIMEN NUMBER	GAGE THICKNESS, t mm (INCH)	GAGE WIDTH, W mm (INCH)	TEST TEMPERATURE °K (°F)	TEST TYPE	STRESS, σ MN/m² (KSI)	INITIAL FLAW DEPTH, a_i mm (INCH)	INITIAL FLAW LENGTH, $2c_i$ mm (INCH)	INITIAL STRESS INTENSITY, K_{I_i} MN/m^3/2 (KSI √IN)	$(a/2c)_i$	$(a/t)_i$	FINAL FLAW DEPTH, a_f mm (INCH)	FINAL FLAW LENGTH, $2c_f$ mm (INCH)	FINAL STRESS INTENSITY, K_{I_f} MN/m^3/2 (KSI √IN)	$(a/2C)_f$	$(a/t)_f$	REMARKS
2BR33-1	9.60 (0.378)	355.6 (14.0)	295 (72)	LUL	310.3 (45.0)	6.25 (0.246)	21.34 (0.84)	46.3 (42.1)	0.293	0.651	6.35 (0.250)	21.34 (0.840)	46.5 (42.3)	0.298	0.661	
			"	CYCLIC	248.2 (36.0)	6.35 (0.250)	21.34 (0.84)	36.6 (33.3)	0.298	0.661	a = t	34.04 (1.34)	52.4 (47.7)	0.282	1.00	60 CPM, 1244 Cycles to B.T.
			"	FRACTURE	276.5 (40.1)	a = t	34.04 (1.34)	58.8 (53.5)	0.282	1.00						
2BR33-2	9.65 (0.380)	355.6 (14.0)	"	LUL	279.2 (40.5)	6.32 (0.249)	20.83 (0.820)	40.8 (37.1)	0.304	0.655	6.32 (0.249)	20.83 (0.820)	40.8 (37.1)	0.304	0.655	
			"	CYCLIC	248.2 (36.0)	6.32 (0.249)	20.83 (0.820)	35.9 (32.7)	0.304	0.655	a = t	33.53 (1.32)	(47.1)	0.288	1.00	60 CPM, 1029 Cycles to B.T.
			"	FRACTURE	286.8 (41.6)	a = t	33.53 (1.32)	60.4 (55.0)	0.288	1.00						
2BR33-3	9.53 (0.375)	355.6 (14.0)	"	LUL	248.2 (36.0)	6.32 (0.249)	21.34 (0.84)	36.6 (33.3)	0.296	0.664	6.32 (0.249)	21.34 (0.84)	36.6 (33.3)	0.296	0.664	
			"	CYCLIC	198.6 (28.8)	6.32 (0.249)	21.34 (0.84)	29.0 (26.4)	0.296	0.664	a = t	32.26 (1.27)	40.0 (36.4)	0.295	1.00	60 CPM, 2530 Cycles to B.T.
			"	FRACTURE	284.1 (41.2)	a = t	32.26 (1.27)	58.4 (53.1)	0.295	1.00						
3BR33-1	9.68 (0.381)	355.6 (14.0)	"	FRACTURE	342.0 (49.6)	6.63 (0.261)	21.34 (0.840)	52.1 (47.4)	0.311	0.685						
2BR33-4	9.70 (0.382)	355.6 (14.0)	"	LUL	331.0 (48.0)	6.40 (0.252)	21.08 (0.83)	49.5 (45.0)	0.304	0.660	7.11 (0.280)	24.13 (0.95)	55.3 (50.3)	0.295	0.733	
			"	CYCLIC	248.2 (36.0)	7.11 (0.280)	24.13 (0.95)	40.4 (36.8)	0.295	0.733						60 CPM, 1290 Cycles to B.T. 1313 Cycles to Frac.
3BR33-2	9.50 (0.374)	355.6 (14.0)	"	FRACTURE	345.4 (50.1)	6.48 (0.255)	21.08 (0.830)	52.4 (47.7)	0.307	0.682						
3BR33-3	9.65 (0.380)	355.6 (14.0)	"	LUL	324.1 (47.0)	6.71 (0.264)	21.08 (0.830)	48.9 (44.5)	0.318	0.695	6.96 (0.274)	21.08 (0.830)	49.1 (44.7)	0.330	0.721	
			"	CYCLIC	291.7 (42.3)	6.96 (0.274)	21.08 (0.830)	43.9 (39.9)	0.330	0.721	a = t	33.02 (1.30)	60.9 (55.4)	0.292	.00	60 CPM, 255 Cycles to B.T.
			"	FRACTURE	294.4 (42.7)	a = t	33.02 (1.30)	61.5 (56.0)	0.292	1.00						

TABLE 22: ROOM TEMPERATURE 2219-T87 ALUMINUM BASE METAL TEST RESULTS
($a/2c = 0.45$ and $t = 9.53$ mm (0.375 inch))

SPECIMEN NUMBER	GAGE THICKNESS, t mm (INCH)	GAGE WIDTH, W mm (INCH)	TEST TEMPERATURE °K (°F)	TEST TYPE	STRESS, σ MN/m^2 (KSI)	INITIAL FLAW DEPTH, a_i mm (INCH)	INITIAL FLAW LENGTH, $2c_i$ mm (INCH)	INITIAL STRESS INTENSITY, K_{I_i} $MN/m^{3/2}$ (KSI$\sqrt{IN}$)	$(a/2c)_i$	$(a/t)_i$	FINAL FLAW DEPTH, a_f mm (INCH)	FINAL FLAW LENGTH, $2c_f$ mm (INCH)	FINAL STRESS INTENSITY, K_{I_f} $MN/m^{3/2}$ (KSI$\sqrt{IN}$)	$(a/2C)_f$	$(a/t)_f$	REMARKS
2BR34-1	9.53 (0.375)	355.6 (14.0)	295 (72)	LUL	310.3 (45.0)	6.63 (0.261)	15.24 (0.60)	36.7 (33.4)	0.435	0.696	6.65 (0.262)	15.24 (0.60)	36.7 (33.4)	0.437	0.699	
			"	CYCLIC	248.2 (36.0)	6.65 (0.262)	15.24 (0.60)	29.0 (26.4)	0.437	0.699	a = t	27.94 (1.10)	45.9 (41.8)	0.341	1.00	60 CPM, 1776 Cycles to B.T.
			"	FRACTURE	306.8 (44.5)	a = t	27.94 (1.10)	57.6 (52.4)	0.341	1.00						
2BR34-2	9.68 (0.381)	355.6 (14.0)	"	LUL	279.2 (40.5)	6.78 (0.267)	15.49 (0.610)	33.1 (30.1)	0.438	0.701	6.78 (0.267)	15.49 (0.610)	33.1 (30.1)	0.438	0.701	
			"	CYCLIC	248.2 (36.0)	6.78 (0.267)	[illegible]	29.2 (26.6)	0.438	0.701	a = t	28.45 (1.12)	46.4 (42.2)	0.340	1.00	60 CPM, 1377 Cycles to B.T.
			"	FRACTURE	290.0 (42.0)	a = t	28.45 (1.12)	54.7 (49.7)	0.340	1.00						
2BR34-3	9.53 (0.375)	355.6 (14.0)	"	LUL	248.2 (36.0)	6.55 (0.258)	14.86 (0.585)	28.5 (25.9)	0.441	0.688	6.55 (0.258)	14.86 (0.585)	28.5 (25.9)	0.441	0.688	
			"	CYCLIC	198.6 (28.8)	6.55 (0.258)	14.86 (0.585)	22.6 (20.[illegible])	0.441	0.688	a = t	28.70 (1.13)	37.0 (33.7)	0.332	1.00	60 CPM, 4469 Cycles to B.T.
			"	FRACTURE	293.0 (42.5)	a = t	28.70 (1.13)	55.8 (50.8)	0.332	1.00						
3BR34-1	9.68 (0.381)	355.6 (14.0)	"	FRACTURE	360.6 (52.3)	6.78 (0.267)	15.06 (0.593)	42.8 (38.9)	0.450	0.701						
2BR34-4	9.63 (0.379)	355.6 (14.0)	"	LUL	344.8 (50.0)	6.78 (0.267)	15.24 (0.60)	41.0 (37.3)	0.445	0.704	7.21 (0.284)	21.34 (0.84)	53.4 (48.6)	0.338	0.749	
			"	CYCLIC	248.2 (36.0)	7.21 (0.284)	21.34 (0.84)	37.5 (34.1)	0.338	0.749	a = t	33.53 (1.32)	51.8 (47.1)	0.287	1.00	60 CPM, 1327 Cycles to B.T.
			"	FRACTURE	291.0 (42.2)	a = t	33.53 (1.32)	61.4 (55.9)	0.287	1.00						
4BR34-1	9.65 (0.380)	355.6 (14.0)	"	LUL	344.8 (50.0)	6.86 (0.270)	15.49 (0.610)	41.4 (37.7)	0.443	0.711	7.04 (0.277)	19.81 (0.780)	50.3 (45.8)	0.355	0.729	
			"	CYCLIC	310.3 (45.0)	7.04 (0.277)	19.81 (0.780)	44.8 (40.8)	0.355	0.729	8.13 (0.320)	22.86 (0.900)	51.0 (46.4)	0.356	0.842	1 CPM, 100 Cycles Total
			"	FRACTURE	343.4 (49.8)	8.13 (0.320)	22.86 (0.900)	57.0 (51.8)	0.356	0.842						

TABLE 22: (Continued)

SPECIMEN NUMBER	GAGE THICKNESS, t mm (INCH)	GAGE WIDTH, W mm (INCH)	TEST TEMPERATURE °K (°F)	TEST TYPE	STRESS, σ MN/m² (KSI)	INITIAL FLAW DEPTH, a_i mm (INCH)	INITIAL FLAW LENGTH, $2c_i$ mm (INCH)	INITIAL STRESS INTENSITY, K_{I_i} MN/m^3/2 (KSI$\sqrt{IN}$)	$(a/2c)_i$	$(a/t)_i$	FINAL FLAW DEPTH, a_f mm (INCH)	FINAL FLAW LENGTH, $2c_f$ mm (INCH)	FINAL STRESS INTENSITY, K_{I_f} MN/m^3/2 (KSI$\sqrt{IN}$)	$(a/2C)_f$	$(a/t)_f$	REMARKS
4BR34-2	9.65 (0.379)	355.6 (14.0)	295 (72)	LUL	342.7 (49.7)	6.86 (0.270)	15.49 (0.610)	41.2 (37.5)	0.443	0.712	6.99 (0.275)	19.81 (0.780)	50.0 (45.5)	0.353	0.726	
			"	CYCLIC	325.4 (47.2)	6.99 (0.275)	19.81 (0.780)	47.3 (43.0)	0.353	0.726	8.26 (0.325)	23.37 (0.920)	54.8 (49.9)	0.353	0.858	1 CPM, 100 Cycles Total
			"	FRACTURE	343.4 (49.8)	8.26 (0.325)	23.37 (0.920)	58.1 (52.9)	0.353	0.858						
3BR34-2	9.75 (0.384)	355.6 (14.0)	"	FRACTURE	349.6 (50.7)	6.78 (0.267)	15.57 (0.613)	42.2 (38.4)	0.436	0.695						

TABLE 23: LIQUID NITROGEN TEMPERATURE 2219-T87 ALUMINUM BASE METAL TEST RESULTS ($a/2c = 0.15$ and $t = 3.18$ mm (0.125 inch))

SPECIMEN NUMBER	GAGE THICKNESS, t mm (INCH)	GAGE WIDTH, W mm (INCH)	TEST TEMPERATURE °K (°F)	TEST TYPE	STRESS, σ MN/m² (KSI)	INITIAL FLAW DEPTH, a_i mm (INCH)	INITIAL FLAW LENGTH, $2c_i$ mm (INCH)	INITIAL STRESS INTENSITY, K_{I_i} MN/m$^{3/2}$ (KSI$\sqrt{IN}$)	$(a/2c)_i$	$(a/t)_i$	FINAL FLAW DEPTH, a_f mm (INCH)	FINAL FLAW LENGTH, $2c_f$ mm (INCH)	FINAL STRESS INTENSITY, K_{I_f} MN/m$^{3/2}$ (KSI$\sqrt{IN}$)	$(a/2C)_f$	$(a/t)_f$	REMARKS
2BN11-1	3.24 (0.128)	127.0 (5.00)	78 (-320)	LUL	365.4 (53.0)	2.57 (0.101)	17.15 (0.675)	51.7 (47.0)	0.150	0.789	2.87 (0.113)	17.15 (0.675)	55.9 (50.9)	0.167	0.883	
			"	CYCLIC	292.3 (42.4)	2.87 (0.113)	17.15 (0.675)	44.0 (40.0)	0.167	0.883	a = t	17.15 (0.675)	44.6 (40.6)	0.190	1.00	60 CPM, 218 Cycles to B.T.
			295 (72)	FRACTURE	307.5 (44.6)	a = t	17.15 (0.675)	47.1 (42.9)	0.190	1.00						
2BN11-2	3.28 (0.129)	127.0 (5.00)	78 (-320)	LUL	328.9 (47.7)	2.59 (0.102)	17.15 (0.675)	46.0 (41.9)	0.151	0.791	2.77 (0.109)	17.15 (0.675)	48.7 (44.3)	0.161	0.845	
			295 (72)	FRACTURE	312.3 (45.3)	2.84 (0.112)	17.15 (0.675)	46.7 (42.5)	0.166	0.868						B.T. at 275.8 MN/m² (40.0 ksi)
2BN11-3	3.20 (0.126)	127.0 (5.00)	78 (-320)	LUL	295.8 (42.9)	2.64 (0.104)	17.02 (0.670)	42.3 (38.5)	0.155	0.825	2.72 (0.107)	17.02 (0.670)	43.3 (39.4)	0.160	0.849	
			"	LUL	328.9 (47.7)	2.74 (0.108)	17.02 (0.670)	48.8 (44.4)	0.161	0.857	2.87 (0.113)	17.02 (0.670)	50.0 (45.5)	0.169	0.897	
			"	CYCLIC	262.0 (38.0)	2.87 (0.113)	17.02 (0.670)	39.1 (35.6)	0.169	0.897	a = t	17.02 (0.670)	39.6 (36.0)	0.188	1.00	60 CPM, 30 Cycles to B.T. 64 Total
			295 (72)	FRACTURE	311.0 (45.1)	a = t	17.02 (0.670)	47.5 (43.2)	0.188	1.00						
3BN11-1	3.24 (0.128)	127.0 (5.00)	78 (-320)	LUL	368.9 (53.5)	2.59 (0.102)	17.27 (0.680)	52.8 (48.0)	0.150	0.797	a = t	17.27 (0.680)	57.8 (52.6)	0.188	1.00	
			"	FRACTURE	378.5 (54.9)	a = t	17.27 (0.680)	59.5 (54.1)	0.188	1.00						
3BN11-2	3.23 (0.127)	127.0 (5.00)	"	FRACTURE	374.4 (54.3)	2.44 (0.096)	17.78 (0.700)	51.7 (47.0)	0.137	0.756						B.T. at 360.6 MN/m² (52.3 ksi)
4BN11-1	3.25 (0.128)	127.0 (5.00)	"	LUL	365.4 (53.0)	2.57 (0.101)	17.15 (0.675)	51.7 (47.0)	0.150	0.789	2.82 (0.111)	17.15 (0.675)	55.5 (50.5)	0.164	0.867	
			"	CYCLIC	292.3 (42.4)	2.82 (0.111)	17.15 (0.675)	43.4 (39.5)	0.164	0.867	3.02 (0.119)	17.15 (0.675)	44.4 (40.4)	0.176	0.903	1 CPM, 100 Cycles Total
			"	FRACTURE	387.5 (56.2)	3.02 (0.119)	17.15 (0.675)	60.6 (55.1)	0.176	0.930						B.T. at 341.3 MN/m² (49.5 ksi)
4BN11-2	3.28 (0.129)	127.0 (5.00)	"	LUL	365.4 (53.0)	2.72 (0.107)	17.27 (0.680)	54.1 (49.2)	0.157	0.829	3.00 (0.118)	17.27 (0.680)	56.8 (51.7)	0.174	0.915	
			"	CYCLIC	328.9 (47.7)	3.00 (0.118)	17.27 (0.680)	50.6 (46.0)	0.174	0.915	a = t	19.30 (0.760)	53.3 (48.5)	0.170	1.00	1 CPM, 1 Cycle to B.T. 29 Total
			"	FRACTURE	375.1 (54.4)	a = t	19.30 (0.760)	61.8 (56.2)	0.170	1.00						

TABLE 24: LIQUID NITROGEN TEMPERATURE 2219-T87 ALUMINUM BASE METAL TEST RESULTS ($a/2c = 0.30$ and $t = 3.18$ mm (0.125 inch))

SPECIMEN NUMBER	GAGE THICKNESS, t mm (INCH)	GAGE WIDTH, W mm (INCH)	TEST TEMPERATURE °K (°F)	TEST TYPE	STRESS, σ MN/m^2 (KSI)	INITIAL FLAW DEPTH, a_i mm (INCH)	INITIAL FLAW LENGTH, $2c_i$ mm (INCH)	INITIAL STRESS INTENSITY, K_{Ii} $MN/m^{3/2}$ (KSI$\sqrt{IN}$)	$(a/2c)_i$	$(a/t)_i$	FINAL FLAW DEPTH, a_f mm (INCH)	FINAL FLAW LENGTH, $2c_f$ mm (INCH)	FINAL STRESS INTENSITY, K_{If} $MN/m^{3/2}$ (KSI$\sqrt{IN}$)	$(a/2C)_f$	$(a/t)_f$	REMARKS
2BN13-1	3.30 (0.130)	127.0 (5.00)	78 (-320)	LUL	365.4 (53.0)	3.18 (0.125)	9.78 (0.385)	40.9 (37.2)	0.325	0.962	a = t	9.78 (0.385)	40.7 (37.0)	0.338	1.00	
			"	CYCLIC	292.3 (42.4)	a = t	9.78 (0.385)	32.0 (29.1)	0.338	1.00	a = t	11.43 (0.450)	35.5 (32.3)	0.289	1.00	60 CPM, 314 Cycles Total
			295 (72)	FRACTURE	339.9 (49.3)	a = t	11.43 (0.450)	41.8 (38.0)	0.289	1.00						
2BN13-2	3.25 (0.128)	127.0 (5.00)	78 (-320)	LUL	328.9 (47.7)	3.12 (0.123)	9.91 (0.390)	36.9 (33.6)	0.315	0.961	3.20 (0.126)	9.91 (0.390)	36.8 (33.5)	0.323	0.984	
			295 (72)	FRACTURE	342.7 (49.7)	a = t	9.91 (0.390)	38.4 (34.9)	0.328	1.00						
2BN13-3	3.23 (0.127)	127.0 (5.00)	78 (-320)	LUL	295.8 (42.9)	2.84 (0.112)	9.40 (0.370	32.2 (29.3)	0.303	0.882	2.84 (0.112)	9.40 (0.370)	32.2 (29.3)	0.303	0.882	
			"	LUL	328.9 (47.7)	2.87 (0.113)	9.40 (0.370)	36.0 (32.8)	0.305	0.890	2.90 (0.114)	9.40 (0.370)	36.0 (32.8)	0.308	0.898	
			"	CYCLIC	262.0 (38.0)	2.90 (0.114)	9.40 (0.370)	28.4 (25.8)	0.308	0.898	a = t	10.16 (0.400)	29.3 (26.7)	0.317	1.00	60 CPM, 300 Cycles to B.T. 720 Total
			295 (72)	FRACTURE	344.1 (49.9)	a = t	10.16 (0.400)	39.2 (35.7)	0.317	1.00						
2BN13-4	3.25 (0.128)	127.0 (5.00)	78 (-320)	LUL	365.4 (53.0)	2.84 (0.112)	9.53 (0.375)	40.6 (36.9)	0.299	0.862	2.95 (0.116)	9.53 (0.375)	40.7 (37.0)	0.309	0.892	
			"	CYCLIC	292.3 (42.4)	2.95 (0.116)	9.53 (0.375)	32.0 (29.1)	0.309	0.892	a = t	10.03 (0.395)	32.6 (29.7)	0.324	1.00	60 CPM, 276 Cycles to B.T.
			"	FRACTURE	413.0 (59.9)	a = t	10.03 (0.395)	47.5 (43.2)	0.324	1.00						
3BN13-1	3.23 (0.127)	127.0 (5.00)	"	LUL	344.8 (50.0)	3.02 (0.119)	9.65 (0.380)	38.4 (34.9)	0.313	0.937	3.07 (0.121)	9.65 (0.380)	38.4 (34.9)	0.318	0.953	
			"	CYCLIC	275.8 (40.0)	3.07 (0.121)	9.65 (0.380)	30.2 (27.5)	0.318	0.953	a = t	9.65 (0.380)	30.0 (27.3)	0.3[illegible]	1.00	60 CPM, 80 Cycles to B.T.
			"	FRACTURE	422.7 (61.3)	a = t	9.65 (0.380)	47.5 (43.2)	0.334	1.00						
3BN13-2	3.23 (0.127)	127.0 (5.00)	"	FRACTURE	427.5 (62.0)	3.00 (0.118)	10.03 (0.395)	50.0 (45.5)	0.299	0.929						B.T. at 335.8 MN/m^2 (48.7 ksi)

TABLE 25: LIQUID NITROGEN TEMPERATURE 2219-T87 ALUMINUM BASE METAL TEST RESULTS
($a/2c = 0.15$ and $t = 6.35$ mm (0.250 inch))

SPECIMEN NUMBER	GAGE THICKNESS, t mm (INCH)	GAGE WIDTH, W mm (INCH)	TEST TEMPERATURE °K (°F)	TEST TYPE	STRESS, σ MN/m^2 (KSI)	INITIAL FLAW DEPTH, a_i mm (INCH)	INITIAL FLAW LENGTH, $2c_i$ mm (INCH)	INITIAL STRESS INTENSITY, K_{I_i} $MN/m^{3/2}$ (KSI$\sqrt{IN}$)	$(a/2c)_i$	$(a/t)_i$	FINAL FLAW DEPTH, a_f mm (INCH)	FINAL FLAW LENGTH, $2c_f$ mm (INCH)	FINAL STRESS INTENSITY, K_{I_f} $MN/m^{3/2}$ (KSI$\sqrt{IN}$)	$(a/2C)_f$	$(a/t)_f$	REMARKS
2BN21-1	6.30 (0.248)	228.6 (9.00)	78 (-320)	LUL	326.1 (47.3)	4.32 (0.170)	28.70 (1.13)	54.1 (49.2)	0.150	0.685	5.46 (0.215)	30.48 (1.20)	65.8 (59.9)	0.179	0.867	
			"	CYCLIC	262.0 (38.0)	5.46 (0.215)	30.48 (1.20)	52.0 (47.3)	0.179	0.867	a = t	30.48 (1.20)	53.2 (48.4)	0.207	1.00	60 CPM, 76 Cycles to B.T.
			"	FRACTURE	275.1 (39.9)	a = t	30.48 (1.20)	55.9 (50.9)	0.207	1.00						
2BN21-2	6.38 (0.251)	228.6 (9.00)	"	LUL	294.4 (42.7)	4.42 (0.174)	29.21 (1.15)	49.1 (44.7)	0.151	0.693	4.65 (0.183)	29.21 (1.15)	51.2 (46.6)	0.159	0.729	
			"	FRACTURE	327.5 (47.5)	4.67 (0.184)	29.21 (1.15)	57.7 (52.5)	0.159	0.729						
3BN21-1	6.35 (0.250)	228.9 (9.01)	"	FRACTURE	335.1 (48.6)	4.37 (0.172)	28.70 (1.13)	55.9 (50.9)	0.152	0.688						
2BN21-3	6.35 (0.250)	228.9 (9.01)	"	LUL	264.8 (38.4)	4.37 (0.172)	28.96 (1.14)	43.4 (39.5)	0.151	0.688	4.42 (0.174)	28.96 (1.14)	43.9 (39.9)	0.153	0.696	
			"	LUL	294.4 (42.7)	4.47 (0.176)	28.96 (1.14)	49.6 (45.1)	0.154	0.704	4.60 (0.181)	28.96 (1.14)	50.7 (46.1)	0.159	0.724	
			"	FRACTURE	322.0 (46.7)	4.62 (0.182)	28.96 (1.14)	56.2 (51.1)	0.160	0.728						
2BN21-4	6.30 (0.248)	228.6 (9.00)	"	LUL	317.2 (46.0)	4.37 (0.172)	28.70 (1.13)	52.9 (48.1)	0.152	0.694	4.78 (0.188)	28.70 (1.13)	56.7 (51.6)	0.166	0.758	
			"	CYCLIC	262.0 (38.0)	4.78 (0.188)	28.70 (1.13)	46.3 (42.1)	0.166	0.758	a = t	29.21 (1.15)	52.1 (47.4)	0.216	1.00	60 CPM, 292 Cycles to B.T.
			"	FRACTURE	303.4 (44.0)	a = t	29.21 (1.15)	60.9 (55.4)	0.216	1.00						
4BN21-1	6.30 (0.248)	228.9 (9.01)	"	LUL	324.1 (47.0)	4.17 (0.164)	28.96 (1.14)	52.3 (47.6)	0.144	0.661	4.62 (0.182)	28.96 (1.14)	56.3 (51.7)	0.160	0.734	
			"	CYCLIC	291.7 (42.3)	4.62 (0.182)	28.96 (1.14)	50.7 (46.1)	0.160	0.734	a = t	30.73 (1.21)	59.8 (54.4)	0.205	1.00	1 CPM, 35 Cycles to B.T.
			"	FRACTURE	314.4 (45.6)	a = t	30.73 (1.21)	64.8 (59.0)	0.205	1.00						
4BN21-2	6.30 (0.248)	228.9 (9.01)	"	LUL	324.1 (47.0)	4.47 (0.176)	28.70 (1.13)	55.2 (50.2)	0.156	0.710	4.90 (0.193)	28.70 (1.13)	59.2 (53.9)	0.171	0.778	
			"	CYCLIC	275.8 (40.0)	4.90 (0.193)	28.70 (1.13)	49.8 (45.3)	0.171	0.778	a = t	32.00 (1.26)	57.4 (52.2)	0.197	1.00	1 CPM, 51 Cycles to B.T.
			"	FRACTURE	309.6 (44.9)	a = t	32.00 (1.26)	65.0 (59.1)	0.197	1.00						
3BN21-2	6.35 (0.250)	22.89 (9.01)	78 (-320)	FRACTURE	342.0 (49.6)	4.47 (0.176)	28.70 (1.13)	58.2 (53.0)	0.156	0.704						

TABLE 26: LIQUID NITROGEN TEMPERATURE 2219-T87 ALUMINUM BASE METAL TEST RESULTS ($a/2c = 0.30$ and $t = 6.35$ mm (0.250 inch))

SPECIMEN NUMBER	GAGE THICKNESS, t mm (INCH)	GAGE WIDTH, W mm (INCH)	TEST TEMPERATURE °K (°F)	TEST TYPE	STRESS, σ MN/m^2 (KSI)	INITIAL FLAW DEPTH, a_i mm (INCH)	INITIAL FLAW LENGTH, $2c_i$ mm (INCH)	INITIAL STRESS INTENSITY, K_{I_i} $MN/m^{3/2}$ (KSI$\sqrt{IN}$)	$(a/2c)_i$	$(a/t)_i$	FINAL FLAW DEPTH, a_f mm (INCH)	FINAL FLAW LENGTH, $2c_f$ mm (INCH)	FINAL STRESS INTENSITY, K_{I_f} $MN/m^{3/2}$ (KSI$\sqrt{IN}$)	$(a/2C)_f$	$(a/t)_f$	REMARKS
2BN23-1	6.32 (0.249)	228.6 (9.00)	78 (-320)	LUL	365.4 (53.0)	5.03 (0.198)	16.76 (0.660)	52.0 (47.3)	0.300	0.792	5.41 (0.213)	19.30 (0.760)	58.4 (53.1)	0.280	0.760	
			"	CYCLIC	292.3 (42.4)	5.41 (0.213)	19.30 (0.760)	45.8 (41.7)	0.280	0.760	a = t	22.86 (0.900)	70.9 (64.5)	0.277	1.00	60 CPM, 250 Cycles to B.T.
			"	FRACTURE	309.6 (44.9)	a = t	22.86 (0.900)	75.6 (68.7)	0.277	1.00						
2BN23-2	6.35 (0.250)	228.6 (9.00)	"	LUL	328.9 (47.7)	5.00 (0.197)	16.76 (0.660)	46.3 (42.1)	0.298	0.788	5.08 (0.200)	16.76 (0.660)	46.5 (42.3)	0.303	0.800	
			295 (72)	FRACTURE	334.4 (48.5)	5.13 (0.202)	16.89 (0.665)	48.5 (44.1)	0.304	0.808						
3BN23-1	6.35 (0.250)	228.9 (9.01)	78 (-320)	FRACTURE	377.2 (54.7)	5.16 (0.203)	17.02 (0.670)	54.6 (49.7)	0.303	0.812						
2BN23-3	6.32 (0.249)	228.9 (9.01)	"	LUL	295.8 (42.9)	5.03 (0.198)	16.76 (0.660)	41.4 (37.7)	0.300	0.795	5.05 (0.199)	16.76 (0.660)	41.5 (37.8)	0.302	0.799	
			"	LUL	328.9 (47.7)	5.08 (0.200)	16.76 (0.660)	46.5 (42.3)	0.303	0.803	5.11 (0.201)	16.76 (0.660)	46.6 (42.4)	0.305	0.807	
			"	FRACTURE	382.0 (55.4)	5.13 (0.202)	16.76 (0.660)	55.0 (50.0)	0.306	0.811						
2BN23-4	6.35 (0.250)	228.9 (9.01)	78 (-320)	LUL	365.4 (53.0)	5.26 (0.207)	17.02 (0.670)	53.1 (48.3)	0.309	0.828	5.51 (0.217)	19.81 (0.780)	59.5 (54.1)	0.278	0.868	
			"	CYCLIC	292.3 (42.4)	5.51 (0.217)	19.81 (0.780)	46.7 (42.5)	0.278	0.868	a = t	23.37 (0.920)	51.5 (46.8)	0.272	1.00	60 CPM, 193 Cycles to B.T.
			"	FRACTURE	348.2 (50.5)	a = t	23.37 (0.920)	33.7 (30.6)	0.272	1.00						
3BN23-2	6.25 (0.246)	228.9 (9.01)	"	LUL	371.6 (53.9)	5.41 (0.213)	17.02 (0.670)	54.6 (49.7)	0.318	0.866	a = t	17.02 (0.670)	53.6 (48.7)	0.367	1.00	
			"	FRACTURE	363.4 (52.7)	a = t	17.02 (0.670)	52.2 (47.5)	0.367	1.00						

TABLE 27: LIQUID NITROGEN TEMPERATURE 2219-T87 ALUMINUM BASE METAL TEST RESULTS ($a/2c = 0.15$ and $t = 9.53$ mm (0.375 inch))

SPECIMEN NUMBER	GAGE THICKNESS, t mm (INCH)	GAGE WIDTH, W mm (INCH)	TEST TEMPERATURE °K (°F)	TEST TYPE	STRESS, σ MN/m² (KSI)	INITIAL FLAW DEPTH, a_i mm (INCH)	INITIAL FLAW LENGTH, $2c_i$ mm (INCH)	INITIAL STRESS INTENSITY, K_{I_i} MN/m$^{3/2}$ (KSI$\sqrt{IN}$)	$(a/2c)_i$	$(a/t)_i$	FINAL FLAW DEPTH, a_f mm (INCH)	FINAL FLAW LENGTH, $2c_f$ mm (INCH)	FINAL STRESS INTENSITY, K_{I_f} MN/m$^{3/2}$ (KSI$\sqrt{IN}$)	$(a/2C)_f$	$(a/t)_f$	REMARKS
2BN31-1	9.58 (0.377)	355.6 (14.0)	78 (-320)	FRACTURE	335.8 (48.7)	5.33 (0.210)	36.07 (1.42)	56.2 (51.1)	0.148	0.557						
2BN31-2	9.65 (0.380)	355.6 (14.0)	"	LUL	324.1 (47.0)	5.33 (0.210)	35.81 (1.41)	53.7 (48.9)	0.149	0.553	5.97 (0.235)	35.81 (1.41)	58.1 (52.9)	0.167	0.618	
			"	CYCLIC	259.3 (37.6)	5.97 (0.235)	35.81 (1.41)	45.7 (41.6)	0.167	0.618	a = t	39.37 (1.55)	59.6 (54.2)	0.245	1.00	60 CPM, 250 Cycles to B.T.
			"	FRACTURE	255.8 (37.1)	a = t	39.37 (1.55)	58.7 (53.4)	0.245	1.00						
2BN31-3	9.70 (0.382)	355.6 (14.0)	"	LUL	291.7 (42.3)	5.18 (0.204)	36.07 (1.42)	46.9 (42.7)	0.144	0.534	5.38 (0.212)	36.07 (1.42)	48.1 (43.8)	0.149	0.555	
			"	CYCLIC	259.3 (37.6)	5.38 (0.212)	36.07 (1.42)	42.5 (38.7)	0.149	0.555	a = t	40.64 (1.60)	60.6 (55.1)	0.239	1.00	60 CPM, 422 Cycles to B.T.
			"	FRACTURE	268.9 (39.0)	a = t	40.64 (1.60)	63.0 (57.3)	0.239	1.00						
3BN31-1	9.60 (0.378)	355.6 (14.0)	"	FRACTURE	339.2 (49.2)	5.33 (0.210)	35.56 (1.40)	56.5 (51.4)	0.150	0.556						
2BN31-4	9.65 (0.380)	355.6 (14.0)	"	LUL	310.3 (45.0)	5.64 (0.222)	36.07 (1.42)	53.3 (48.5)	0.156	0.584	6.15 (0.242)	36.07 (1.42)	56.7 (51.6)	0.170	0.637	
			"	CYCLIC	259.3 (37.6)	6.15 (0.242)	36.07 (1.42)	46.7 (42.5)	0.170	0.637	a = t	43.18 (1.70)	62.6 (57.0)	0.224	1.00	60 CPM, 156 Cycles to B.T.
			"	FRACTURE	260.6 (37.8)	a = t	43.18 (1.70)	63.0 (57.3)	0.224	1.00						
4BN31-1	9.65 (0.380)	355.6 (14.0)	"	LUL	324.1 (47.0)	5.33 (0.210)	35.56 (1.40)	53.6 (48.8)	0.150	0.553	5.84 (0.230)	35.56 (1.40)	57.0 (51.9)	0.164	0.605	
			"	CYCLIC	291.7 (42.3)	5.84 (0.230)	35.56 (1.40)	50.9 (46.3)	0.164	0.605	6.86 (0.270)	35.56 (1.40)	56.7 (51.6)	0.193	0.711	1 CPM, 20 Cycles Total
			"	FRACTURE	275.8 (40.0)	6.86 (0.270)	35.56 (1.40)	53.4 (48.6)	0.193	0.711						Specimen Fractured on 21st Cycle
4BN31-3	9.45 (0.372)	355.6 (14.0)	"	LUL	324.1 (47.0)	5.03 (0.198)	33.53 (1.32)	51.2 (46.6)	0.150	0.532	5.21 (0.205)	33.53 (1.32)	52.5 (47.8)	0.155	0.551	Slight Delamination
			"	CYCLIC	259.3 (37.6)	5.21 (0.205)	33.53 (1.32)	41.2 (37.5)	0.155	0.551	5.64 (0.222)	33.53 (1.32)	43.5 (39.6)	0.168	0.597	1 CPM, 100 Cycles Total
			"	FRACTURE	338.5 (49.1)	5.64 (0.222)	33.53 (1.32)	58.0 (52.8)	0.168	0.597						

TABLE 27: (Continued)

SPECIMEN NUMBER	GAGE THICKNESS, t mm (INCH)	GAGE WIDTH, W mm (INCH)	TEST TEMPERATURE °K (°F)	TEST TYPE	STRESS, σ MN/m² (KSI)	INITIAL FLAW DEPTH, a_i mm (INCH)	INITIAL FLAW LENGTH, $2c_i$ mm (INCH)	INITIAL STRESS INTENSITY, K_{I_i} $MN/m^{3/2}$ ($KSI\sqrt{IN}$)	$(a/2c)_i$	$(a/t)_i$	FINAL FLAW DEPTH, a_f mm (INCH)	FINAL FLAW LENGTH, $2c_f$ mm (INCH)	FINAL STRESS INTENSITY, K_{I_f} $MN/m^{3/2}$ ($KSI\sqrt{IN}$)	$(a/2C)_f$	$(a/t)_f$	REMARKS
4BN31-2	9.70 (0.382)	355.6 (14.0)	78 (-320)	LUL	324.1 (47.0)	5.33 (0.210)	35.31 (1.39)	53.4 (48.6)	0.151	0.550	5.72 (0.225)	35.31 (1.39)	55.9 (50.9)	0.162	0.589	
			"	CYCLIC	259.3 (37.6)	5.72 (0.225)	35.31 (1.39)	44.1 (40.1)	0.162	0.589	5.97 (0.235)	35.31 (1.39)	45.4 (41.3)	0.169	0.615	1 CPM, 100 Cycles Total
			"	FRACTURE	333.7 (48.4)	5.97 (0.235)	35.31 (1.39)	59.6 (54.2)	0.169	0.615						
3BN31-2	9.63 (0.379)	355.6 (14.0)	"	LUL	326.1 (47.3)	5.49 (0.216)	36.07 (1.42)	55.3 (50.3)	0.152	0.570	5.87 (0.231)	36.07 (1.42)	57.9 (52.7)	0.163	0.609	
			"	CYCLIC	259.3 (37.6)	5.87 (0.216)	36.07 (1.42)	45.3 (41.2)	0.163	0.609	a = t	41.91 (1.65)	61.6 (56.1)	0.230	1.00	60 CPM, 221 Cycles to B.T.
			"	FRACTURE	262.0 (38.0)	a = t	41.91 (1.65)	62.3 (56.7)	0.230	1.00						

TABLE 28: LIQUID NITROGEN TEMPERATURE 2219-T87 ALUMINUM BASE METAL TEST RESULTS ($a/2c = 0.30$ and $t = 9.53$ mm (0.375 inch))

SPECIMEN NUMBER	GAGE THICKNESS, t mm (INCH)	GAGE WIDTH, W mm (INCH)	TEST TEMPERATURE °K (°F)	TEST TYPE	STRESS, σ MN/m^2 (KSI)	INITIAL FLAW DEPTH, a_i mm (INCH)	INITIAL FLAW LENGTH, $2c_i$ mm (INCH)	INITIAL STRESS INTENSITY, K_{I_i} $MN/m^{3/2}$ (KSI$\sqrt{IN}$)	$(a/2c)_i$	$(a/t)_i$	FINAL FLAW DEPTH, a_f mm (INCH)	FINAL FLAW LENGTH, $2c_f$ mm (INCH)	FINAL STRESS INTENSITY, K_{I_f} $MN/m^{3/2}$ (KSI$\sqrt{IN}$)	$(a/2C)_f$	$(a/t)_f$	REMARKS
2BN33-1	9.55 (0.376)	355.6 (14.0)	78 (-320)	LUL	339.9 (49.3)	6.71 (0.264)	22.48 (0.885)	53.0 (48.2)	0.298	0.702	7.34 (0.289	26.42 (1.04)	60.3 (54.8)	0.278	0.769	
			"	CYCLIC	271.7 (39.4)	7.34 (0.289)	26.42 (1.04)	47.4 (43.1)	0.278	0.769	a = t	33.02 (1.30)	55.9 (50.9)	0.289	1.00	60 CPM, 280 Cycles to B.T.
			"	FRACTURE	283.4 (41.1)	a = t	33.02 (1.30)	58.5 (53.2)	0.289	1.00						
2BN33-2	9.50 (0.374)	355.6 (14.0)	"	LUL	306.1 (44.4)	6.86 (0.270)	22.61 (0.890)	47.9 (43.6)	0.303	0.722	7.01 (0.276)	22.61 (0.890)	48.1 (43.8)	0.310	0.738	
			"	CYCLIC	271.7 (39.4)	7.01 (0.276)	22.61 (0.890)	42.5 (38.7)	0.310	0.738	a = t	33.02 (1.30)	55.9 (50.9)	0.288	1.00	60 CPM, 406 Cycles to B.T.
			"	FRACTURE	297.9 (43.2)	a = t	33.02 (1.300)	61.7 (56.1)	0.288	1.00						
2BN33-3	9.58 (0.377)	355.6 (14.0)	"	LUL	271.7 (39.4)	6.78 (0.267)	22.61 (0.890)	42.0 (38.2)	0.300	0.708	6.83 (0.269)	22.61 (0.890)	42.1 (38.3)	0.302	0.714	
			"	CYCLIC	217.2 (31.5)	6.83 (0.269)	22.61 (0.890)	33.3 (30.3)	0.302	0.714	a = t	33.02 (1.30)	44.3 (40.3)	0.290	1.00	60 CPM, 1545 Cycles to B.T.
			"	FRACTURE	293.7 (42.6)	a = t	33.02 (1.30)	60.7 (55.2)	0.290	1.00						
3BN33-1	9.63 (0.379)	355.6 (14.0)	"	FRACTURE	342.7 (49.7)	6.86 (0.270)	22.73 (0.895)	54.1 (49.2)	0.302	0.716						
2BN33-4	9.73 (0.383)	355.6 (14.0)	"	LUL	327.5 (47.5)	6.65 (0.262)	22.35 (0.880)	50.3 (45.8)	0.298	0.684	7.11 (0.280)	23.37 (0.920)	52.6 (47.9)	0.304	0.731	
			"	CYCLIC	271.7 (39.4)	7.11 (0.280)	23.37 (0.920)	43.2 (39.3)	0.304	0.731	a = t	29.72 (1.17)	52.0 (47.3)	0.327	1.00	60 CPM, 376 Cycles to B.T.
			"	FRACTURE	284.1 (41.2)	a = t	29.72 (1.17)	54.4 (49.5)	0.327	1.00						
3BN33-2	9.55 (0.376)	355.6 (14.0)	"	FRACTURE	348.2 (50.5)	6.93 (0.273)	22.73 (0.895)	55.3 (50.3)	0.305	0.726						

TABLE 29: LIQUID HYDROGEN TEMPERATURE 2219-T87 ALUMINUM BASE METAL TEST RESULTS (t = 3.18 mm (0.125 inch))

SPECIMEN NUMBER	GAGE THICKNESS, t mm (INCH)	GAGE WIDTH, W mm (INCH)	TEST TEMPERATURE °K (°F)	TEST TYPE	STRESS, σ MN/m² (KSI)	INITIAL FLAW DEPTH, a_i mm (INCH)	INITIAL FLAW LENGTH, $2c_i$ mm (INCH)	INITIAL STRESS INTENSITY, K_{I_i} MN/m³/² (KSI√IN)	$(a/2c)_i$	$(a/t)_i$	FINAL FLAW DEPTH, a_f mm (INCH)	FINAL FLAW LENGTH, $2c_f$ mm (INCH)	FINAL STRESS INTENSITY, K_{I_f} MN/m³/² (KSI√IN)	$(a/2C)_f$	$(a/t)_f$	REMARKS
2BH11-1	3.25 (0.128)	127.0 (5.00)	20 (-423)	FRACTURE	403.4 (58.5)	2.39 (0.094)	16.00 (0.630)	53.0 (48.2)	0.149	0.734						
2BH11-2	3.25 (0.128)	127.0 (5.00)	"	LUL	379.2 (55.0)	2.41 (0.095)	15.75 (0.620)	49.6 (45.1)	0.153	0.742	2.54 (0.100)	15.75 (0.620)	51.7 (47.0)	0.161	0.781	
			"	CYCLIC	303.4 (44.0)	2.54 (0.100)	15.75 (0.620)	40.4 (36.8)	0.161	0.781	2.77 (0.109)	15.75 (0.620)	43.2 (39.3)	0.176	0.852	3 CPM, 161 Cycles Total
			295 (72)	FRACTURE	333.7 (48.4)	2.77 (0.109)	15.75 (0.620)	49.2 (44.8)	0.176	0.852						
2BH11-3	3.33 (0.131)	127.0 (5.00)	20 (-423)	LUL	341.3 (49.5)	2.41 (0.095)	15.49 (0.610)	43.3 (39.4)	0.156	0.725	2.54 (0.100)	15.49 (0.610)	45.1 (41.0)	0.164	0.763	
			295 (72)	FRACTURE	333.0 (48.3)	2.57 (0.101)	15.49 (0.610)	45.4 (41.3)	0.166	0.771						
3BH11-1	3.23 (0.127)	127.0 (5.00)	20 (-423)	LUL	306.8 (44.5)	2.29 (0.090)	15.49 (0.610)	37.6 (34.2)	0.148	0.709	2.39 (0.094)	15.49 (0.610)	38.9 (35.4)	0.154	0.740	
2BH11-4	3.10 (0.122)	127.0 (5.00)	"	FRACTURE	386.8 (56.1)	2.46 (0.097)	16.51 (0.650)	54.0 (49.1)	0.149	0.795						
3BH11-2	3.10 (0.122)	(5.00)	"	LUL	359.9 (52.2)	2.31 (0.091)	15.24 (0.600)	46.0 (41.9)	0.152	0.746	2.44 (0.096)	15.24 (0.600)	48.1 (43.8)	0.160	0.787	
			"	CYCLIC	324.1 (47.0)	2.44 (0.096)	15.24 (0.600)	42.9 (39.0)	0.160	0.787						3 CPM, 48 Cycles to Fracture
4BH11-1	3.25 (0.128)	127.0 (5.00)	20 (-423)	LUL	378.5 (54.9)	2.51 (0.099)	15.75 (0.620)	51.2 (46.6)	0.160	0.773	2.64 (0.104)	15.75 (0.620)	53.2 (48.4)	0.168	0.813	
			"	CYCLIC	341.3 (49.5)	2.64 (0.104)	15.75 (0.620)	47.4 (43.1)	0.168	0.813	a = t	15.75 (0.620)		0.206	1.00	1 CPM, 72 Cycles to B.T.

TABLE 30: LIQUID HYDROGEN TEMPERATURE 2219-T87 ALUMINUM BASE METAL TEST RESULTS (t = 6.35 mm (0.250 inch))

SPECIMEN NUMBER	GAGE THICKNESS, t mm (INCH)	GAGE WIDTH, W mm (INCH)	TEST TEMPERATURE °K (°F)	TEST TYPE	STRESS, σ MN/m² (KSI)	INITIAL FLAW DEPTH, a_i mm (INCH)	INITIAL FLAW LENGTH, $2c_i$ mm (INCH)	INITIAL STRESS INTENSITY, K_{I_i} MN/m$^{3/2}$ (KSI$\sqrt{IN}$)	$(a/2c)_i$	$(a/t)_i$	FINAL FLAW DEPTH, a_f mm (INCH)	FINAL FLAW LENGTH, $2c_f$ mm (INCH)	FINAL STRESS INTENSITY, K_{I_f} MN/m$^{3/2}$ (KSI$\sqrt{IN}$)	$(a/2C)_f$	$(a/t)_f$	REMARKS
2BH21-1	6.32 (0.249)	228.9 (9.01)	20 (-423)	FRACTURE	404.7 (58.7)	3.58 (0.141)	22.86 (0.900)	56.0 (51.0)	0.157	0.566						
2BH21-2	6.32 (0.249)	228.9 (9.01)	"	LUL	386.1 (56.0)	3.56 (0.140)	23.11 (0.910)	53.0 (48.2)	0.154	0.562	3.81 (0.150)	23.11 (0.910)	55.5 (50.5)	0.165	0.602	
			"	CYCLIC	308.9 (44.8)	3.81 (0.150)	23.11 (0.910)	43.4 (39.5)	0.165	0.602	5.66 (0.223)	24.89 (0.980)	56.9 (51.8)	0.228	0.896	3 CPM, 130 Cycles Failure Imminent
			295 (72)	FRACTURE	304.1 (44.1)	5.66 (0.223)	24.89 (0.980)	57.1 (52.0)	0.228	0.896						
2BH21-3	6.38 (0.251)	228.9 (9.01)	20 (-423)	LUL	347.5 (50.4)	3.43 (0.135)	22.86 (0.900)	45.7 (41.6)	0.150	0.538	3.51 (0.138)	22.86 (0.900)	46.4 (42.2)	0.153	0.550	
4BH21-1	6.34 (0.250)	228.9 (9.01)	20 (-423)	LUL	379.2 (55.0)	3.53 (0.139)	22.86 (0.900)	51.8 (47.1)	0.150	0.540	3.71 (0.146)	22.86 (0.900)	53.2 (48.4)	0.162	0.584	
			"	CYCLIC	341.3 (49.5)	3.71 (0.146)	22.86 (0.900)	47.4 (43.1)	0.162	0.584	a = t	26.92 (1.06)	65.9 (60.0)	0.236	1.00	1 CPM, 79 Cycles to B.T.
3BH21-1	6.34 (0.250)	228.6 (9.00)	"	FRACTURE	396.5 (57.5)	3.58 (0.141)	23.37 (0.920)	55.0 (50.0)	0.153	0.564						
2BH21-4	6.34 (0.250)	228.6 (9.00)	"	LUL	313.0 (45.4)	3.51 (0.138)	23.11 (0.910)	41.5 (37.8)	0.152	0.552	3.56 (0.140)	23.11 (0.910)	42.0 (38.2)	0.154	0.560	

TABLE 31: LIQUID HYDROGEN TEMPERATURE 2219-T87 ALUMINUM BASE METAL TEST RESULTS (t = 9.53 mm (0.375 inch))

SPECIMEN NUMBER	GAGE THICKNESS, t mm (INCH)	GAGE WIDTH, W mm (INCH)	TEST TEMPERATURE °K (°F)	TEST TYPE	STRESS, σ MN/m² (KSI)	INITIAL FLAW DEPTH, a_i mm (INCH)	INITIAL FLAW LENGTH, $2c_i$ mm (INCH)	INITIAL STRESS INTENSITY, K_{I_i} MN/m$^{3/2}$ (KSI$\sqrt{IN}$)	$(a/2c)_i$	$(a/t)_i$	FINAL FLAW DEPTH, a_f mm (INCH)	FINAL FLAW LENGTH, $2c_f$ mm (INCH)	FINAL STRESS INTENSITY, K_{I_f} MN/m$^{3/2}$ (KSI$\sqrt{IN}$)	$(a/2C)_f$	$(a/t)_f$	REMARKS
2BH31-1	9.68 (0.381)	355.6 (14.0)	20 (-423)	LUL	406.9 (59.0)	4.11 (0.162)	28.19 (1.11)	55.7 (50.7)	0.146	0.425	4.75 (0.187)	28.19 (1.11)	60.2 (54.8)	0.168	0.491	
			"	CYCLIC	325.4 (47.2)	4.75 (0.187)	28.19 (1.11)	47.0 (42.8)	0.168	0.491	6.60 (0.260)	31.75 (1.25)	59.3 (54.0)	0.208	0.682	3 cpm, 107 Cycles Fracture Immenent
			295 (72)	FRACTURE	302.7 (43.9)	6.60 (0.260)	31.75 (1.25)	56.1 (51.0)	0.208	0.682						
2BH31-2	9.53 (0.375)	355.6 (14.0)	20 (-423)	LUL	366.1 (53.1)	4.22 (0.166)	28.19 (1.11)	50.4 (45.8)	0.150	0.443	4.45 (0.175)	28.19 (1.11)	51.9 (47.2)	0.158	0.467	
			295 (72)	FRACTURE	305.4 (44.3)	7.39 (0.291)	28.96 (1.14)	57.7 (52.5)	0.255	0.776						
2BH31-3	9.42 (0.371)	355.6 (14.0)	20 (-423)	LUL	325.4 (47.2)	4.22 (0.166)	28.19 (1.11)	44.3 (40.3)	0.150	0.447	4.29 (0.169)	28.19 (1.11)	44.8 (40.8)	0.152	0.456	
			295 (72)	FRACTURE	305.4 (44.3)	7.01 (0.276)	28.96 (1.14)	56.8 (51.6)	0.242	0.744						
3BH31-1	9.63 (0.379)	355.6 (14.0)	20 (-423)	LUL	373.0 (54.1)	4.47 (0.176)	28.45 (1.12)	53.1 (48.3)	0.157	0.464	4.78 (0.188)	28.45 (1.12)	55.0 (50.0)	0.168	0.496	
			"	CYCLIC	373.0 (48.7)	4.78 (0.188)	28.45 (1.12)	48.9 (44.5)	0.168	0.496						1 CPM, 95 Cycles to Fracture
4BH31-1	9.47 (0.373)	355.6 (14.01)	"	FRACTURE	412.3 (59.8)	4.32 (0.170)	27.94 (1.10	58.4 (53.1)	0.155	0.456						

TABLE 32: ROOM TEMPERATURE 2219 ALUMINUM WELD METAL TEST RESULTS
($a/2c = 0.15$ and $t = 3.18$ mm (0.125 INCH))

SPECIMEN NUMBER	GAGE THICKNESS, t mm (INCH)	GAGE WIDTH, W mm (INCH)	TEST TEMPERATURE °K (°F)	TEST TYPE	STRESS, σ MN/m² (KSI)	INITIAL FLAW DEPTH, a_i mm (INCH)	INITIAL FLAW LENGTH, $2c_i$ mm (INCH)	INITIAL STRESS INTENSITY, K_{I_i} MN/m³ᐟ² (KSI√IN)	$(a/2c)_i$	$(a/t)_i$	FINAL FLAW DEPTH, a_f mm (INCH)	FINAL FLAW LENGTH, $2c_f$ mm (INCH)	FINAL STRESS INTENSITY, K_{I_f} MN/m³ᐟ² (KSI√IN)	$(a/2C)_f$	$(a/t)_f$	REMARKS
2WR11-1	3.25 (0.128)	127.0 (5.00)	295 (72)	LUL	155.1 (22.5)	2.49 (0.098)	17.53 (0.690)	22.0 (20.0)	0.142	0.766	2.69 (0.106)	17.53 (0.690)	23.5 (21.4)	0.154	0.828	
			"	CYCLIC	124.1 (18.0)	2.69 (0.106)	17.53 (0.690)	18.2 (16.6)	0.154	0.828	a = t	17.53 (0.690)	19.3 (17.6)	0.186	1.00	60 cpm, 414 cycles to B.T.
			"	FRACTURE	197.9 (28.7)	a = t	17.53 (0.690)	32.2 (29.3)	0.186	1.00						
2WR11-2	3.33 (0.131)	127.0 (5.00	"	LUL	140.0 (20.3)	2.49 (0.098)	17.27 (0.680)	19.1 (17.4)	0.144	0.748	2.62 (0.103)	17.27 (0.680)	20.0 (18.2)	0.151	0.786	
			"	FRACTURE	196.5 (28.5)	2.67 (0.105)	17.27 (0.680)	29.3 (26.7)	0.154	0.802						B.T. at 172.4 MN/m² (25.0 KSI)
2WR11-3	3.28 (0.129)	127.0 (5.00)	"	LUL	125.5 (18.2)	2.49 (0.098)	17.40 (0.685)	17.1 (15.6)	0.143	0.760	2.51 (0.099)	17.40 (0.685)	17.3 (15.7)	0.145	0.767	
			"	LUL	140.0 (20.3)	2.57 (0.101)	17.40 (0.685)	19.9 (18.1)	0.147	0.783	2.62 (0.103)	17.40 (0.685)	20.2 (18.4)	0.150	0.798	
			"	FRACTURE	194.4 (28.2)	2.67 (0.105)	17.40 (0.685)	29.4 (26.8)	0.153	0.814						B.T. at 162.0 MN/m² (23.5 KSI)
3WR11-1	3.30 (0.130)	127.0 (5.00)	"	LUL	177.2 (25.7)	2.54 (0.100)	17.53 (0.690)	26.0 (23.7)	0.769	0.145	a = t	17.78 (0.700)	28.0 (26.4)	0.186	1.00	
			"	FRACTURE	201.3 (29.2)	a = t	17.78 (0.700)	33.0 (30.0)	0.186	1.00						
3WR11-2	3.25 (0.128)	127.0 (5.00)	"	FRACTURE	201.3 (29.2)	2.69 (0.106)	19.05 (0.750)	31.7 (28.8)	0.141	0.828						B.T. at 152.4 MN/m² (22.1 KSI)
4WR11-1	3.25 (0.128)	127.0 (5.00)	"	LUL	165.5 (24.0)	2.59 (0.102)	17.53 (0.690)	24.6 (22.4)	0.148	0.797	2.84 (0.112)	17.53 (0.690)	26.4 (24.0)	0.162	0.875	
			"	CYCLIC	148.9 (21.6)	2.84 (0.112)	17.53 (0.690)	23.3 (21.2)	0.162	0.875	a = t	17.53 (0.690)	23.7 (21.6)	0.186	1.00	1 cpm, 79 Cycles to B.T.
			"	FRACTURE	201.3 (29.2)	a = t	17.53 (0.690)	32.8 (29.8)	0.186	1.00						
4WR11-2	3.18 (0.125)	127.0 (5.00)	"	LUL	165.5 (24.0)	2.54 (0.100)	17.53 (0.690)	24.6 (22.4)	0.145	0.800	2.69 (0.106)	17.53 (0.690)	25.8 (23.5)	0.154	0.848	
			"	CYCLIC	148.9 (21.6)	2.69 (0.106)	17.53 (0.690)	22.7 (20.7)	0.154	0.848	2.95 (0.116)	17.53 (0.690)	23.6 (21.5)	0.168	0.928	1 cpm, 100 Cycles Total
			"	FRACTURE	200.0 (29.0)	2.95 (0.116)	17.53 (0.690)	32.3 (29.4)	0.168	0.928						

TABLE 33: ROOM TEMPERATURE 2219 ALUMINUM WELD METAL TEST RESULTS
($a/2c$ = 0.30 and t = 3.18 mm (0.125 inch))

SPECIMEN NUMBER	GAGE THICKNESS, t mm (INCH)	GAGE WIDTH, W mm (INCH)	TEST TEMPERATURE °K (°F)	TEST TYPE	STRESS, σ MN/m^2 (KSI)	INITIAL FLAW DEPTH, a_i mm (INCH)	INITIAL FLAW LENGTH, $2c_i$ mm (INCH)	INITIAL STRESS INTENSITY, K_{I_i} $MN/m^{3/2}$ ($KSI\sqrt{IN}$)	$(a/2c)_i$	$(a/t)_i$	FINAL FLAW DEPTH, a_f mm (INCH)	FINAL FLAW LENGTH, $2c_f$ mm (INCH)	FINAL STRESS INTENSITY, K_{I_f} $MN/m^{3/2}$ ($KSI\sqrt{IN}$)	$(a/2C)_f$	$(a/t)_f$	REMARKS
2WR13-1	3.15 (0.124)	126.5 (4.98)	295 (72)	LUL	155.1 (22.5)	2.69 (0.106)	9.14 (0.360)	17.1 (15.6)	0.294	0.855	2.74 (0.108)	9.14 (0.360)	17.1 (15.6)	0.300	0.871	
			"	CYCLIC	124.1 (18.0)	2.74 (0.108)	9.14 (0.360)	13.4 (12.2)	0.300	0.871	a = t	9.91 (0.390)	14.0 (12.7)	0.318	1.00	60 CPM, 1108 Cycles to B.T.
			"	FRACTURE	202.0 (29.3)	a = t	9.91 (0.390)	23.4 (21.3)	0.318	1.00						
2WR13-2	3.25 (0.128)	127.0 (5.00)	"	LUL	140.0 (20.3)	2.72 (0.107)	9.40 (0.370)	15.4 (14.0)	0.289	0.836	2.74 (0.109)	9.40 (0.370)	15.5 (14.1)	0.295	0.852	
			"	FRACTURE	202.0 (29.3)	2.79 (0.110)	9.40 (0.370)	22.4 (20.4)	0.297	0.859						B.T. at 176.5 MN/m^2 (25.6 ksi)
2WR13-3	3.10 (0.122)	127.0 (5.00)	"	LUL	126.2 (18.3)	2.51 (0.099)	9.53 (0.375)	13.8 (12.6)	0.264	0.811	2.59 (0.100)	9.53 (0.375)	14.0 (12.7)	0.267	0.820	
			"	FRACTURE	195.1 (28.3)	a = t	10.03 (0.395)	22.9 (20.8)	0.309	1.00						
3WR13-1	3.20 (0.126)	127.0 (5.00)	"	LUL	172.4 (25.0)	2.72 (0.107)	9.40 (0.370)	19.6 (17.8)	0.289	0.849	a = t	9.91 (0.390)	19.9 (18.1)	0.323	1.00	
			"	FRACTURE	210.3 (30.5)	a = t	9.91 (0.390)	24.3 (22.1)	0.323	1.00						
3WR13-2	3.23 (0.127)	127.0 (5.00)	"	LUL	155.1 (22.5)	2.74 (0.108)	9.27 (0.365)	17.3 (15.7)	0.296	0.850	2.79 (0.110)	9.27 (0.365)	17.3 (15.7)	0.301	0.866	
			"	CYCLIC	124.1 (18.0)	2.79 (0.110)	9.27 (0.365)	13.5 (12.3)	0.301	0.866	a = t	10.03 (0.395)	14.1 (12.8)	0.322	1.00	60 CPM, 1319 Cycles to B.T.
			"	FRACTURE	211.0 (30.6)	a = t	10.03 (0.395)	24.6 (22.4)	0.322	1.00						

TABLE 34: ROOM TEMPERATURE 2219 ALUMINUM WELD METAL TEST RESULTS
($a/2c = 0.15$ and $t = 6.35$ mm (0.250 inch))

SPECIMEN NUMBER	GAGE THICKNESS, t mm (INCH)	GAGE WIDTH, W mm (INCH)	TEST TEMPERATURE °K (°F)	TEST TYPE	STRESS, σ MN/m² (KSI)	INITIAL FLAW DEPTH, a_i mm (INCH)	INITIAL FLAW LENGTH, $2c_i$ mm (INCH)	INITIAL STRESS INTENSITY, K_{I_i} MN/m^3/2 (KSI √IN)	$(a/2c)_i$	$(a/t)_i$	FINAL FLAW DEPTH, a_f mm (INCH)	FINAL FLAW LENGTH, $2c_f$ mm (INCH)	FINAL STRESS INTENSITY, K_{I_f} MN/m^3/2 (KSI √IN)	$(a/2C)_f$	$(a/t)_f$	REMARKS
2WR21-1	5.94 (0.234)	228.6 (9.00)	295 (72)	LUL	145.5 (21.1)	5.11 (0.201)	36.07 (1.42)	31.5 (28.7)	0.142	0.859	a = t	36.07 (1.42	32.9 (29.9)	0.165	1.00	
			"	FRACTURE	184.1 (26.7)	a = t	36.07 (1.42)	42.5 (38.7)	0.165	1.00						
2WR21-2	5.94 (0.234)	228.9 (9.01)	"	LUL	129.6 (18.8)	5.16 (0.203)	36.32 (1.43)	27.9 (25.4)	0.142	0.868	a = t	36.32 (1.43)	28.9 (26.3)	0.164	1.00	
			"	FRACTURE	184.1 (26.7)	a = t	36.32 (1.43)	42.8 (38.9)	0.104	1.00						
2WR21-3	6.12 (0.241)	228.6 (9.00)	"	LUL	131.0 (19.0)	5.18 (0.204)	36.07 (1.42)	27.8 (25.3)	0.144	0.846	5.33 (0.210)	36.07 (1.42)	28.4 (25.8)	0.148	0.871	
			"	CYCLIC	104.8 (15.2)	5.33 (0.210)	36.07 (1.42)	22.2 (20.2)	0.148	0.871	a = t	36.07 (1.42)	23.0 (20.9)	0.170	1.00	60 cpm, 281 cycles to B.T.
			"	FRACTURE	188.9 (27.4)	a = t	36.07 (1.42)	43.9 (39.9)	0.170	1.00						
3WR21-1	5.94 (0.234)	228.6 (9.00)	"	LUL	117.2 (17.0)	5.18 (0.204)	35.81 (1.41)	24.8 (22.6)	0.145	0.872	5.18 (0.204)	35.81 (1.41)	24.8 (22.6)	0.145	0.872	
			"	CYCLIC	105.5 (15.3)	5.18 (0.204)	35.81 (1.41)	22.2 (20.2)	0.145	0.872	a = t	35.81 (1.41)	23.0 (20.9)	0.166	1.00	60 cpm, 397 cycles to B.T.
			"	FRACTURE	193.1 (28.0)	a = t	35.81 (1.41)	44.5 (40.5)	0.166	1.00						
4WR21-2	5.94 (0.234)	228.6 (9.00)	"	LUL	131.0 (19.0)	5.23 (0.206)	35.56 (1.40)	28.2 (25.7)	0.147	0.880	5.38 (0.212)	35.56 (1.40)	28.7 (26.1)	0.151	0.906	
			"	CYCLIC	117.9 (17.1)	5.38 (0.212)	35.56 (1.40)	25.5 (23.2)	0.151	0.906	a = t	35.81 (1.41)	25.9 (23.6)	0.166	1.00	1 cpm, 64 cycles to B.T.
			"	FRACTURE	191.7 (27.8)	a = t	35.81 (1.41)	44.2 (40.2)	0.166	1.00						
4WR21-1	5.87 (0.231)	228.6 (9.00)	"	LUL	131.0 (19.0)	5.13 (0.202)	36.07 (1.42)	28.2 (25.7)	0.142	0.874	5.31 (0.209)	36.07 (1.42)	28.7 (26.1)	0.147	0.905	
			"	CYCLIC	117.9 (17.1)	5.31 (0.209)	36.07 (1.42)	25.5 (23.2)	0.147	0.905	a = t	36.07 (1.42)	25.9 (23.6)	0.163	1.00	1 cpm, 40 cycles to B.T.
			"	FRACTURE	202.7 (29.4)	a = t	36.07 (1.42)	46.8 (42.6)	0.163	1.00						

TABLE 35: ROOM TEMPERATURE 2219 ALUMINUM WELD METAL TEST RESULTS
(a/2c = 0.30 and t = 6.35 mm (0.250 inch))

SPECIMEN NUMBER	GAGE THICKNESS, t mm (INCH)	GAGE WIDTH, W mm (INCH)	TEST TEMPERATURE °K (°F)	TEST TYPE	STRESS, σ MN/m² (KSI)	INITIAL FLAW DEPTH, a_i mm (INCH)	INITIAL FLAW LENGTH, $2c_i$ mm (INCH)	INITIAL STRESS INTENSITY, K_{I_i} MN/m^3/2 (KSI√IN)	$(a/2c)_i$	$(a/t)_i$	FINAL FLAW DEPTH, a_f mm (INCH)	FINAL FLAW LENGTH, $2c_f$ mm (INCH)	FINAL STRESS INTENSITY, K_{I_f} MN/m^3/2 (KSI√IN)	$(a/2C)_f$	$(a/t)_f$	REMARKS
2WR23-1	5.82 (0.229)	228.6 (9.00)	295 (72)	LUL	144.8 (21.0)	5.33 (0.210)	18.42 (0.725)	22.9 (20.8)	0.290	0.917	5.49 (0.216)	18.42 (0.725)	22.8 (20.7)	0.298	0.943	
			"	CYCLIC	115.8 (16.8)	5.49 (0.216)	18.42 (0.725)	17.8 (16.2)	0.298	0.943	a = t	18.42 (0.725)	17.1 (16.1)	0.316	1.00	60 CPM, 15 Cycles to B.T.
			"	FRACTURE	201.3 (29.2)	a = t	18.42 (0.725)	31.9 (29.0)	0.316	1.00						
2WR23-2	5.99 (0.236)	228.6 (9.00)	"	LUL	140.0 (20.3)	5.41 (0.213)	18.42 (0.725)	22.0 (20.0)	0.294	0.903	5.51 (0.217)	18.42 (0.725)	21.9 (19.9)	0.299	0.919	
			"	FRACTURE	209.6 (30.4)	5.54 (0.218)	18.42 (0.725)	33.4 (30.4)	0.301	0.924						B.T. at 166.9 MN/m² (24.2 ksi)
2WR23-3	5.84 (0.230)	228.6 (9.00)	"	LUL	124.1 (18.0)	4.11 (0.162)	16.76 (0.660)	16.9 (15.4)	0.245	0.704	4.11 (0.162)	16.76 (0.660)	16.9 (15.4)	0.245	0.704	
			"	LUL	140.0 (20.3)	4.14 (0.163)	16.76 (0.660)	19.5 (17.7)	0.247	0.709	4.22 (0.166)	16.76 (0.660)	19.6 (17.8)	0.252	0.722	
			"	FRACTURE	209.6 (30.4)	4.24 (0.167)	16.76 (0.660)	30.1 (27.4)	0.253	0.726						B.T. at 193.7 MN/m² (28.1 ksi)
3WR23-1	6.02 (0.237)	228.6 (9.00)	"	FRACTURE	211.0 (30.6)	5.49 (0.216)	18.42 (0.725)	33.8 (30.7)	0.298	0.911						B.T. at 137.9 MN/m² (20.0 ksi)

TABLE 36: ROOM TEMPERATURE 2219 ALUMINUM WELD METAL TEST RESULTS
($a/2c = 0.15$ and $t = 9.53$ mm (0.375 inch))

SPECIMEN NUMBER	GAGE THICKNESS, t mm (INCH)	GAGE WIDTH, W mm (INCH)	TEST TEMPERATURE °K (°F)	TEST TYPE	STRESS, σ MN/m² (KSI)	INITIAL FLAW DEPTH, a_i mm (INCH)	INITIAL FLAW LENGTH, $2c_i$ mm (INCH)	INITIAL STRESS INTENSITY, K_{I_i} MN/m^{3/2} (KSI√IN)	$(a/2c)_i$	$(a/t)_i$	FINAL FLAW DEPTH, a_f mm (INCH)	FINAL FLAW LENGTH, $2c_f$ mm (INCH)	FINAL STRESS INTENSITY, K_{I_f} MN/m^{3/2} (KSI√IN)	$(a/2C)_f$	$(a/t)_f$	REMARKS
2WR31-1	9.73 (0.383)	355.6 (14.0)	295 (72)	LUL	155.1 (22.5)	8.08 (0.318)	55.88 (2.20)	41.7 (37.9)	0.145	0.830	a = t	55.88 (2.20)	44.3 (40.3)	0.174	1.00	
			"	FRACTURE	186.2 (27.0)	a = t	57.66 (2.27)	54.6 (49.7)	0.174	1.00						
2WR31-2	9.70 (0.382)	355.6 (14.0)	"	LUL	148.2 (21.5)	8.00 (0.315)	55.88 (2.20)	39.2 (35.7)	0.143	0.825	8.33 (0.328)	55.88 (2.20)	40.4 (36.8)	0.149	0.859	
			"	CYCLIC	118.6 (17.2)	8.33 (0.328)	55.88 (2.20)	31.4 (28.6)	0.149	0.859	a = t	57.15 (2.25)	33.0 (30.0)	0.170	1.00	60 cpm, 1056 cycles total B.T.<< 1000 cycles
			"	FRACTURE	127.6 (18.5)	a = t	57.15 (2.25)	35.8 (32.6)	0.170	1.00						
2WR31-3	9.63 (0.379)	355.6 (14.0)	"	LUL	133.8 (19.4)	8.13 (0.320)	55.88 (2.20)	35.3 (32.1)	0.145	0.838	8.28 (0.326)	55.88 (2.20)	35.8 (32.6)	0.148	0.853	
			"	FRACTURE	188.9 (27.4)	8.41 (0.331)	55.88 (2.20)	53.1 (48.3)	0.150	0.866						B.T. at 158.6 MN/m² (23.0 KSI)
3WR31-1	9.70 (0.382)	355.6 (14.0)	"	LUL	146.2 (21.2)	8.08 (0.318)	56.39 (2.22)	39.0 (35.5)	0.143	0.832	a = t	56.39 (2.22)	41.5 (37.8)	0.172	1.00	
			"	FRACTURE	191.0 (27.7)	a = t	56.39 (2.22)	55.5 (50.5)	0.172	1.00						
4WR31-1	9.50 (0.374)	355.6 (14.0)	"	LUL	148.2 (21.5)	8.38 (0.330)	56.90 (2.24)	41.2 (37.5)	0.147	0.882	9.14 (0.360)	56.90 (2.24)	42.1 (38.3)	0.161	0.963	
			"	CYCLIC	118.6 (17.2)	9.14 (0.360)	56.90 (2.24)	32.8 (29.8)	0.161	0.963	a = t	56.90 (2.24)	32.9 (29.9)	0.167	1.00	1 cpm, 44 cycles to B.T.
			"	FRACTURE	196.5 (28.5)	a = t	56.90 (2.24)	57.1 (52.0)	0.167	1.00						
4WR31-2	9.58 (0.377)	355.6 (14.0)	"	LUL	142.7 (20.7)	7.87 (0.310)	56.64 (2.23)	37.5 (34.1)	0.139	0.822	8.18 (0.322)	56.64 (2.23)	38.7 (35.2)	0.144	0.854	
			"	CYCLIC	118.6 (17.2)	8.18 (0.322)	56.64 (2.23)	31.4 (28.6)	0.144	0.854	9.09 (0.358)	56.64 (2.23)	32.6 (29.7)	0.161	0.950	1 cpm, 100 cycles total
			"	FRACTURE	194.4 (28.2)	9.09 (0.358)	56.64 (2.23)	56.2 (51.1)	0.161	0.950						
3WR31-2	9.75 (0.384)	355.6 (14.0)	"	LUL	135.8 (19.7)	8.38 (0.330)	56.90 (2.24)	36.9 (33.6)	0.147	0.859	8.69 (0.342)	56.90 (2.24)	37.6 (34.2)	0.153	0.891	
			"	CYCLIC	108.9 (15.8)	8.69 (0.342)	56.90 (2.24)	29.5 (26.8)	0.153	0.891	a = t	56.90 (2.24)	30.1 (27.4)	0.171	1.00	60cpm, 210 cycles to B.T.
			"	FRACTURE	189.6 (27.5)	a = t	56.90 (2.24)	55.3 (50.3)	0.171	1.00						

TABLE 37: ROOM TEMPERATURE 2219 ALUMINUM WELD METAL TEST RESULTS ($a/2c = 0.30$ and $t = 9.53$ mm (0.375 inch))

SPECIMEN NUMBER	GAGE THICKNESS, t mm (INCH)	GAGE WIDTH, W mm (INCH)	TEST TEMPERATURE °K (°F)	TEST TYPE	STRESS, σ MN/m² (KSI)	INITIAL FLAW DEPTH, a_i mm (INCH)	INITIAL FLAW LENGTH, $2c_i$ mm (INCH)	INITIAL STRESS INTENSITY, K_{I_i} MN/m$^{3/2}$ (KSI$\sqrt{IN}$)	$(a/2c)_i$	$(a/t)_i$	FINAL FLAW DEPTH, a_f mm (INCH)	FINAL FLAW LENGTH, $2c_f$ mm (INCH)	FINAL STRESS INTENSITY, K_{I_f} MN/m$^{3/2}$ (KSI$\sqrt{IN}$)	$(a/2C)_f$	$(a/t)_f$	REMARKS
2WR33-1	9.65 (0.380)	355.6 (14.0)	295 (72)	LUL	155.1 (22.5)	8.13 (0.320)	27.94 (1.10)	29.9 (27.2)	0.291	0.842	8.31 (0.327)	29.46 (1.16)	31.1 (28.3)	0.282	0.861	
			"	CYCLIC	124.1 (18.0)	8.31 (0.327)	29.46 (1.16)	24.3 (22.1)	0.282	0.861	a = t	38.10 (1.50)	28.5 (25.7)	0.253	1.00	60 cpm, 1236 cycles to B.T.
			"	FRACTURE	204.1 (29.6)	a = t	38.10 (1.50)	48.5 (44.1)	0.253	1.00						
2WR33-2	9.73 (0.383)	355.6 (14.0)	"	LUL	140.0 (20.3)	8.26 (0.325)	28.96 (1.14)	27.4 (24.9)	0.285	0.849	8.43 (0.332)	28.96 (1.14)	27.4 (24.9)	0.291	0.867	
			"	FRACTURE	218.6 (31.7)	8.59 (0.338)	28.96 (1.14)	43.6 (39.7)	0.296	0.886						B.T. at 175.1 MN/m² (25.4 KSI)
2WR33-3	9.68 (0.381)	355.6 (14.0)	"	LUL	126.2 (18.3)	8.23 (0.324)	29.21 (1.15)	24.6 (22.4)	0.282	0.850	8.33 (0.328)	29.21 (1.15)	24.6 (22.4)	0.285	0.861	
			"	LUL	140.0 (20.3)	8.43 (0.332)	31.75 (1.25)	29.2 (26.6)	0.266	0.871	8.51 (0.335)	31.75 (1.25)	29.2 (26.6)	0.268	0.879	
			"	LUL	168.9 (24.5)	8.56 (0.337)	33.53 (1.32)	37.5 (34.1)	0.267	0.885	a = t	33.53 (1.32)	36.7 (33.4)	0.289	1.00	
			"	FRACTURE	206.2 (29.9)	a = t	33.53 (1.32)	44.8 (40.8)	0.289	1.00						
3WR33-1	9.75 (0.384)	355.6 (14.0)	"	FRACTURE	215.8 (31.3)	8.51 (0.335)	28.45 (1.12)	42.5 (38.7)	0.299	0.872						B.T. at 161.3 MN/m² (23.4 KSI)
3WR33-2	9.65 (0.380)	355.6 (14.0)	"	FRACTURE	211.7 (30.7)	8.59 (0.338)	27.94 (1.10)	41.3 (37.6)	0.307	0.889						B.T. at 168.2 MN/m² (24.4 KSI)
3WR33-2A	9.68 (0.381)	355.6 (14.0)	"	LUL	148.9 (21.6)	8.38 (0.330)	28.19 (1.11)	28.8 (26.2)	0.297	0.866	8.81 (0.347)	28.19 (1.11)	28.8 (26.2)	0.313	0.911	
			"	CYCLIC	119.3 (17.3)	8.81 (0.347)	28.19 (1.11)	22.6 (20.6)	0.313	0.911	a = t	29.72 (1.17)	23.1 (21.0)	0.326	1.00	60 cpm, 319 cycles to B.T.
			"	FRACTURE	206.9 (30.0)	a = t	29.72 (1.17)	41.3 (37.6)	0.326	1.00						

TABLE 38: LIQUID NITROGEN TEMPERATURE 2219 ALUMINUM WELD METAL TEST RESULTS (t = 3.18 mm (0.125 inch))

SPECIMEN NUMBER	GAGE THICKNESS, t mm (INCH)	GAGE WIDTH, W mm (INCH)	TEST TEMPERATURE °K (°F)	TEST TYPE	STRESS, σ MN/m^2 (KSI)	INITIAL FLAW DEPTH, a_i mm (INCH)	INITIAL FLAW LENGTH, $2c_i$ mm (INCH)	INITIAL STRESS INTENSITY, K_{I_i} $MN/m^{3/2}$ (KSI$\sqrt{IN}$)	$(a/2c)_i$	$(a/t)_i$	FINAL FLAW DEPTH, a_f mm (INCH)	FINAL FLAW LENGTH, $2c_f$ mm (INCH)	FINAL STRESS INTENSITY, K_{I_f} $MN/m^{3/2}$ (KSI$\sqrt{IN}$)	$(a/2C)_f$	$(a/t)_f$	REMARKS
2WN11-1	3.25 (0.128)	127.0 (5.00)	78 (-320)	LUL	182.7 (26.5)	2.51 (0.099)	18.03 (0.710)	26.3 (23.9)	0.139	0.773	2.69 (0.106)	18.03 (0.710)	27.8 (25.3)	0.149	0.828	
			"	CYCLIC	146.2 (21.2)	2.69 (0.106)	18.03 (0.710)	21.7 (19.7)	0.149	0.828	a = t	23.11 (0.910)	25.2 (22.9)	0.142	1.00	60cpm, 310 cycles to B.T. 966 total
			295 (72)	FRACTURE	173.1 (25.1)	a = t	23.11 (0.910)	31.3 (28.5)	0.142	1.00						
2WN11-2	3.10 (0.122)	1.27 (5.01)	78 (-320)	LUL	164.8 (23.9)	2.57 (0.101)	18.03 (0.710)	24.5 (22.3)	0.142	0.828	2.82 (0.111)	18.03 (0.710)	25.9 (23.6)	0.156	0.910	
			"	FRACTURE	207.5 (30.1)	2.84 (0.112)	18.03 (0.710)	33.7 (30.7)	0.158	0.918						B.T. @ 162.7 MN/m^2 (23.6 KSI)
2WN11-3	3.30 (0.130)	127.0 (5.00)	"	LUL	148.2 (21.5)	2.49 (0.098)	17.65 (0.695)	20.2 (18.4)	0.141	0.754	2.57 (0.101)	17.65 (0.695)	20.8 (18.9)	0.145	0.777	
			"	LUL	164.8 (23.9)	2.59 (0.102)	17.65 (0.695)	23.5 (21.4)	0.147	0.785	2.72 (0.107)	17.65 (0.695)	24.5 (22.3)	0.154	0.823	
			"	FRACTURE	224.8 (32.6)	2.74 (0.108)	17.65 (0.695)	31.7 (28.8)	0.155	0.831						B.T. @ 204.1 MN/m^2 (29.6 KSI)
3WN11-1	3.15 (0.124)	127.0 (5.00)	"	LUL	200.0 (29.0)	2.51 (0.099)	17.27 (0.680)	29.5 (26.8)	0.146	0.798	a = t	17.27 (0.680)	32.2 (29.3)	0.182	1.00	
			"	FRACTURE	224.8 (32.6)	a = t	17.27 (0.680)	36.3 (33.0)	0.182	1.00						
2WN11-4	3.30 (0.130)	127.0 (5.00)	"	LUL	179.3 (26.0)	2.54 (0.100)	17.83 (0.702)	25.6 (23.3)	0.142	0.769	2.64 (0.104)	17.83 (0.702)	26.4 (24.0)	0.148	0.800	
			"	CYCLIC	161.3 (23.4)	2.64 (0.104)	17.83 (0.702)	23.4 (21.3)	0.148	0.800	a = t	17.83 (0.702)	25.6 (23.3)	0.185	1.00	60cpm, 501 cycles to B.T.
			"	FRACTURE	230.3 (33.4)	a = t	17.83 (0.702)	37.8 (34.4)	0.185	1.00						
3WN11-2	3.15 (0.124)	127.0 (5.00)	"	LUL	177.9 (25.8)	2.62 (0.103)	18.80 (0.740)	27.3 (24.8)	0.139	0.831)	2.84 (0.112)	18.80 (0.740)	28.7 (26.1)	0.151	0.903	
			"	CYCLIC	154.4 (22.4)	2.84 (0.112)	18.80 (0.740)	24.5 (22.3)	0.151	0.903	a = t	18.80 (0.740)	24.8 (22.6)	0.168	1.00	60 cpm, 114 cycles to B.T.
			"	FRACTURE	220.6 (32.0)	a = t	18.80 (0.740)	36.9 (33.6)	0.168	1.00						

TABLE 38: (Continued)

SPECIMEN NUMBER	GAGE THICKNESS, t mm (INCH)	GAGE WIDTH, W mm (INCH)	TEST TEMPERATURE °K (°F)	TEST TYPE	STRESS, σ MN/m² (KSI)	INITIAL FLAW DEPTH, a_i mm (INCH)	INITIAL FLAW LENGTH, $2c_i$ mm (INCH)	INITIAL STRESS INTENSITY, K_{I_i} MN/m^3/2 (KSI √IN)	$(a/2c)_i$	$(a/t)_i$	FINAL FLAW DEPTH, a_f mm (INCH)	FINAL FLAW LENGTH, $2c_f$ mm (INCH)	FINAL STRESS INTENSITY, K_{I_f} MN/m^3/2 (KSI √IN)	$(a/2C)_f$	$(a/t)_f$	REMARKS
4WN11-2	3.20 (0.126)	127.0 (5.00)	78 (-320)	LUL	194.4 (28.2)	2.54 (0.100)	18.03 (0.710)	28.8 (26.2)	0.141	0.794	2.79 (0.110)	18.03 (0.710)	31.0 (28.2)	0.155	0.873	
			"	CYCLIC	175.1 (25.4)	2.79 (0.110)	18.03 (0.710)	27.4 (24.9)	0.155	0.873	a = t	18.03 (0.710)	28.1 (25.6)	0.177	1.00	1 cpm, 62 cycles to B.T.
			"	FRACTURE	230.3 (33.4)	a = t	18.0[illegible]	37.9 (34.5)	0.177	1.00						
;WN11-1	3.28 (0.129)	127.0 (5.00)	"	FRACTURE	232.4 (33.7)	2.72 (0.107)	17.91 (0.705)	35.8 (32.6)	0.152	0.829						B.T. @ 185.5 MN/m² (26.9 KSI)

TABLE 39: LIQUID NITROGEN TEMPERATURE 2219 ALUMINUM WELD METAL TEST RESULTS (t = 6.35 mm (0.250 inch))

SPECIMEN NUMBER	GAGE THICKNESS, t mm (INCH)	GAGE WIDTH, W mm (INCH)	TEST TEMPERATURE °K (°F)	TEST TYPE	STRESS, σ MN/m^2 (KSI)	INITIAL FLAW DEPTH, a_i mm (INCH)	INITIAL FLAW LENGTH, $2c_i$ mm (INCH)	INITIAL STRESS INTENSITY, K_{I_i} $MN/m^{3/2}$ (KSI$\sqrt{IN}$)	$(a/2c)_i$	$(a/t)_i$	FINAL FLAW DEPTH, a_f mm (INCH)	FINAL FLAW LENGTH, $2c_f$ mm (INCH)	FINAL STRESS INTENSITY, K_{I_f} $MN/m^{3/2}$ (KSI$\sqrt{IN}$)	$(a/2C)_f$	$(a/t)_f$	REMARKS
2WN21-1	5.87 (0.231)	228.6 (9.00)	78 (-320)	LUL	180.0 (26.1)	4.57 (0.180)	32.77 (1.29)	34.9 (31.8)	0.140	0.779	a = t	34.29 (1.35)	39.9 (36.3)	0.171	1.00	
			"	FRACTURE	193.7 (28.1)	a = t	34.29 (1.35)	43.5 (39.6)	0.171	1.00						
2WN21-2	5.79 (0.228)	228.6 (9.00)	"	LUL	162.0 (23.5)	4.83 (0.190)	32.77 (1.29)	32.8 (29.8)	0.147	0.833	5.28 (0.208)	33.27 (1.31)	34.6 (31.5)	0.159	0.912	
			"	CYCLIC	129.6 (18.8)	5.28 (0.208)	33.27 (1.31)	27.0 (24.6)	0.159	0.912	a = t	33.53 (1.32)	27.5 (25.0)	0.173	1.00	60 cpm, 201 cycles to B.T.
			295 (72)	FRACTURE	178.6 (25.9)	a = t	33.53 (1.32)	39.1 (35.6)	0.173	1.00						
2WN21-3	5.94 (0.234)	228.6 (9.00)	78 (-320)	LUL	146.2 (21.2)	4.78 (0.188)	32.77 (1.29)	28.5 (25.9)	0.146	0.803	5.16 (0.203)	32.77 (1.29)	30.1 (27.4)	0.157	0.868	
			"	FRACTURE	218.6 (31.7)	5.26 (0.207)	32.77 (1.29)	47.6 (43.3)	0.160	0.885						B.T. at 168.9 MN/m^2 (24.5 KSI)
2WN21-4	5.99 (0.236)	228.6 (9.00)	"	LUL	124.1 (18.0)	4.52 (0.178)	32.77 (1.29)	22.5 (20.5)	0.138	0.754	4.57 (0.180)	32.77 (1.29)	22.7 (20.7)	0.140	0.763	
			"	FRACTURE	224.8 (32.6)	4.62 (0.182)	32.77 (1.29)	44.4 (40.4)	0.141	0.771						B.T. at 203.4 MN/m^2 (29.5 KSI)
4WN21-2	6.02 (0.237)	228.6 (9.00)	"	LUL	172.3 (25.0)	4.67 (0.184)	32.77 (1.29)	33.3 (30.3)	0.143	0.776	5.05 (0.199)	32.77 (1.29)	35.6 (32.4)	0.154	0.840	
			"	CYCLIC	155.1 (22.5)	5.05 (0.199)	32.77 (1.29)	31.5 (28.7)	0.154	0.840	5.82 (0.229)	33.53 (1.32)	33.4 (30.4)	0.173	0.966	1 cpm, 100 cycles total
			"	FRACTURE	222.7 (32.3)	5.82 (0.229)	33.53 (1.32)	49.9 (45.4)	0.173	0.966						B.T. at 170.3 MN/m^2 (24.7 KSI)
4WN21-1	5.97 (0.235)	228.6 (9.00)	"	LUL	172.3 (25.0)	4.98 (0.196)	32.77 (1.29)	35.3 (32.1)	0.152	0.834	5.36 (0.211)	32.77 (1.29)	36.9 (33.6)	0.164	0.898	
			"	CYCLIC	164.1 (23.8)	5.36 (0.211)	32.77 (1.29)	34.9 (31.8)	0.164	0.898	a = t	34.80 (1.37)	36.3 (33.0)	0.172	1.00	1 cpm, 52 cycles to B.T.
			"	FRACTURE	224.8 (32.6)	a = t	34.80 (1.37)	51.3 (46.7)	0.172	1.00						

TABLE 40: LIQUID NITROGEN TEMPERATURE 2219 ALUMINUM WELD METAL TEST RESULTS (t = 9.53 mm (0.375 inch))

SPECIMEN NUMBER	GAGE THICKNESS, t mm (INCH)	GAGE WIDTH, W mm (INCH)	TEST TEMPERATURE °K (°F)	TEST TYPE	STRESS, σ MN/m^2 (KSI)	INITIAL FLAW DEPTH, a_i mm (INCH)	INITIAL FLAW LENGTH, $2c_i$ mm (INCH)	INITIAL STRESS INTENSITY, K_{I_i} $MN/m^{3/2}$ (KSI $\sqrt{IN}$)	$(a/2c)_i$	$(a/t)_i$	FINAL FLAW DEPTH, a_f mm (INCH)	FINAL FLAW LENGTH, $2c_f$ mm (INCH)	FINAL STRESS INTENSITY, K_{I_f} $MN/m^{3/2}$ (KSI $\sqrt{IN}$)	$(a/2C)_f$	$(a/t)_f$	REMARKS
2WN31-1	9.73 (0.383)	355.6 (14.0)	78 (-320)	LUL	180.6 (26.2)	7.11 (0.280)	48.51 (1.91)	41.4 (37.7)	0.147	0.731	a = t	49.02 (1.93)	48.4 (44.0)	0.198	1.00	
			"	FRACTURE	213.7 (31.0)	a = t	49.02 (1.93)	58.4 (53.1)	0.198	1.00				.		
2WN31-2	9.70 (0.382)	355.6 (14.0)	"	LUL	172.4 (25.0)	7.16 (0.282)	48.26 (1.90)	39.5 (35.9)	0.148	0.738	7.85 (0.309)	48.26 (1.90)	42.4 (38.6)	0.163	0.809	
			"	CYCLIC	137.9 (20.0)	7.85 (0.309)	48.26 (1.90)	33.1 (30.1)	0.163	0.809	8.23 (0.324)	48.26 (1.90)	34.4 (31.3)	0.171	0.848	60 CPM, 133 Cycles Total
			"	FRACTURE	222.7 (32.3)	8.23 (0.324)	48.26 (1.90)	58.5 (53.2)	0.171	0.848						
2WN31-3	9.70 (0.382)	355.6 (14.0)	"	LUL	155.1 (22.5)	7.11 (0.280)	47.75 (1.88)	34.7 (31.6)	0.149	0.733	7.52 (0.296)	47.75 (1.88)	36.3 (33.0)	0.157	0.775	
			"	CYCLIC	137.9 (20.0)	7.52 (0.296)	47.75 (1.88)	31.9 (29.0)	0.157	0.775	a = t	50.29 (1.98)	36.3 (33.0)	0.193	1.00	60 CPM, 235 Cycles to B.T.
			"	FRACTURE	213.7 (31.0)	a = t	50.29 (1.98)	59.0 (53.7)	0.193	1.00						
2WN31-4	9.70 (0.382)	355.6 (14.0)	"	LUL	137.9 (20.0)	7.39 (0.291)	48.01 (1.89)	31.5 (28.7)	0.154	0.762	7.65 (0.301)	48.01 (1.89)	32.4 (29.5)	0.159	0.788	
			"	CYCLIC	110.3 (16.0)	7.65 (0.301)	48.01 (1.89)	25.5 (23.2)	0.159	0.788	a = t	48.26 (1.90)	28.0 (25.5)	0.201	1.00	60 CPM, 1494 Cycles to B.T.
			"	FRACTURE	219.3 (31.8)	a = t	48.26 (1.90)	59.3 (54.0)	0.201	1.00						
3WN31-1	9.80 (0.386)	355.6 (14.0)	"	LUL	172.4 (25.0)	7.54 (0.297)	48.26 (1.90)	40.9 (37.2)	0.156	0.769	8.81 (0.347)	48.77 (1.92)	45.5 (41.4)	0.181	0.899	
			"	CYCLIC	137.9 (20.0)	8.81 (0.347)	48.77 (1.92)	35.5 (32.3)	0.181	0.899	a = t	49.02 (1.93)	35.8 (32.6)	0.200	1.00	60 CPM, 80 Cycles to B.T. 95 Total
			"	FRACTURE	214.4 (31.1)	a = t	49.02 (1.93)	58.5 (53.2)	0.200	1.00						
4WN31-2	9.80 (0.386)	355.6 (14.0)	"	LUL	172.4 (25.0)	6.93 (0.273)	49.02 (1.93)	38.4 (34.9)	0.141	0.707	7.70 (0.303)	49.02 (1.93)	41.8 (38.0)	0.157	0.785	
			"	CYCLIC	155.1 (22.5)	7.70 (0.303)	49.02 (1.93)	37.0 (33.7)	0.157	0.785	a = t	49.02 (1.93)	40.8 (37.1)	0.200	1.00	1 CPM, 34 Cycles to B.T.
			"	FRACTURE	213.1 (30.9)	a = t	49.02 (1.93)	58.1 (52.9)	0.200	1.00						
4WN31-1	9.70 (0.382)	355.6 (14.0)	"	LUL	172.4 (25.0)	7.01 (0.276)	48.77 (1.92)	38.9 (35.4)	0.144	0.723	8.08 (0.318)	48.77 (1.92)	43.6 (39.7)	0.166	0.832	

TABLE 40: (Continued)

SPECIMEN NUMBER	GAGE THICKNESS, t mm (INCH)	GAGE WIDTH, W mm (INCH)	TEST TEMPERATURE °K (°F)	TEST TYPE	STRESS, σ MN/m^2 (KSI)	INITIAL FLAW DEPTH, a_i mm (INCH)	INITIAL FLAW LENGTH, $2c_i$ mm (INCH)	INITIAL STRESS INTENSITY, K_{I_i} $MN/m^{3/2}$ (KSI$\sqrt{IN}$)	$(a/2c)_i$	$(a/t)_i$	FINAL FLAW DEPTH, a_f mm (INCH)	FINAL FLAW LENGTH, $2c_f$ mm (INCH)	FINAL STRESS INTENSITY, K_{I_f} $MN/m^{3/2}$ (KSI$\sqrt{IN}$)	$(a/2C)_f$	$(a/t)_f$	REMARKS
3WN31-2	9.63 (0.379)	355.6 (14.0)	78 (-320)	LUL	172.4 (25.0)	7.32 (0.288)	48.51 (1.91)	40.4 (36.8)	0.151	0.760	7.87 (0.310)	48.51 (1.91)	42.9 (39.0)	0.162	0.818	
			"	CYCLIC	137.9 (20.0)	7.87 (0.310)	48.51 (1.91)	33.4 (30.4)	0.162	0.818	8.13 (0.320)	48.51 (1.91)	34.3 (31.2)	0.168	0.844	1 CPM, 100 Cycles Total
			"	FRACTURE	216.5 (31.4)	8.13 (0.320)	48.51 (1.91)	54.7 (49.8)	0.168	0.844						B.T. at 207.5 MN/m^2 (30.1 ksi)
4WN31-3	9.80 (0.386)	355.6 (14.0)	"	FRACTURE	216.5 (31.4)	7.16 (0.282)	47.24 (1.86)	50.3 (45.8)	0.152	0.731						B.T. at 202.0 MN/m^2 (29.3 ksi)

TABLE 41: LIQUID HYDROGEN TEMPERATURE 2219 ALUMINUM WELD METAL TEST RESULTS (t = 3.18mm (0.125))

SPECIMEN NUMBER	GAGE THICKNESS, t mm (INCH)	GAGE WIDTH, W mm (INCH)	TEST TEMPERATURE °K (°F)	TEST TYPE	STRESS, σ MN/m² (KSI)	INITIAL FLAW DEPTH, a_i mm (INCH)	INITIAL FLAW LENGTH, $2c_i$ mm (INCH)	INITIAL STRESS INTENSITY, K_{I_i} MN/m^3/2 (KSI√IN)	$(a/2c)_i$	$(a/t)_i$	FINAL FLAW DEPTH, a_f mm (INCH)	FINAL FLAW LENGTH, $2c_f$ mm (INCH)	FINAL STRESS INTENSITY, K_{I_f} MN/m^3/2 (KSI√IN)	$(a/2C)_f$	$(a/t)_f$	REMARKS
2WH11-1	3.30 (0.130)	127.0 (5.00)	20 (-423)	LUL	203.4 (29.5)	2.39 (0.094)	16.26 (0.640)	26.7 (24.3)	0.147	0.723	2.59 (0.102)	16.26 (0.640)	28.5 (25.9)	0.159	0.785	
			"	CYCLIC	162.7 (23.6)	2.59 (0.102)	16.26 (0.640)	22.2 (20.2)	0.159	0.785	2.64 (0.104)	16.26 (0.640)	22.5 (20.5)	0.163	0.800	3 CPM, 250 Cycles Total
			295 (72)	FRACTURE	199.3 (28.9)	2.64 (0.104)	16.26 (0.640)	29.0 (26.4)	0.163	0.800						
2WH11-2	3.30 (0.130)	127.0 (5.00)	20 (-423)	LUL	183.4 (26.6)	2.34 (0.092)	16.26 (0.640)	23.3 (21.2)	0.144	0.708	2.49 (0.098)	16.26 (0.640)	24.5 (22.3)	0.153	0.754	
			295 (72)	FRACTURE	195.8 (28.4)	3.00 (0.118)	16.26 (0.640)	30.7 (27.9)	0.184	0.908						B.T. at 148.9 MN/m² (21.6 ksi)
3WH11-1	3.28 (0.129)	127.8 (5.03)	20 (-423)	FRACTURE	246.8 (35.8)	2.64 (0.104)	16.89 (0.665)	37.0 (33.7)	0.156	0.806						B.T. at 235.1 MN/m² (34.1 ksi)
4WH11-1	3.28 (0.129)	127.0 (5.00)	"	LUL	219.3 (31.8)	2.46 (0.097)	16.51 (0.650)	30.1 (27.4)	0.149	0.752	2.59 (0.102)	16.51 (0.650)	31.4 (28.6)	0.157	0.791	
			"	CYCLIC	197.2 (28.6)	2.59 (0.102)	16.51 (0.650)	27.8 (25.3)	0.157	0.791	2.79 (0.110)	16.51 (0.650)	29.5 (26.8)	0.169	0.853	1 CPM, 100 Cycles Total
			"	FRACTURE	250.3 (36.3)	2.79 (0.110)	16.51 (0.650)	39.0 (35.5)	0.169	0.853						B.T. at 235.8 MN/m² (34.2 ksi)

TABLE 42: LIQUID HYDROGEN TEMPERATURE 2219 ALUMINUM WELD METAL TEST RESULTS
(t = 6.35 mm (0.250 inch))

SPECIMEN NUMBER	GAGE THICKNESS, t mm (INCH)	GAGE WIDTH, W mm (INCH)	TEST TEMPERATURE °K (°F)	TEST TYPE	STRESS, σ MN/m^2 (KSI)	INITIAL FLAW DEPTH, a_i mm (INCH)	INITIAL FLAW LENGTH, $2c_i$ mm (INCH)	INITIAL STRESS INTENSITY, K_{I_i} $MN/m^{3/2}$ (KSI$\sqrt{IN}$)	$(a/2c)_i$	$(a/t)_i$	FINAL FLAW DEPTH, a_f mm (INCH)	FINAL FLAW LENGTH, $2c_f$ mm (INCH)	FINAL STRESS INTENSITY, K_{I_f} $MN/m^{3/2}$ (KSI$\sqrt{IN}$)	$(a/2C)_f$	$(a/t)_f$	REMARKS
2WH21-1	5.89 (0.232)	228.6 (9.00)	20 (-423)	LUL	203.4 (29.5)	4.27 (0.168)	30.23 (1.19)	36.0 (32.8)	0.141	0.724	4.83 (0.190)	30.23 (1.19)	39.9 (36.3)	0.160	0.819	
			"	CYCLIC	162.7 (23.6)	4.83 (0.190)	30.23 (1.19)	31.1 (28.3)	0.160	0.819	a = t	31.75 (1.25)	34.0 (30.9)	0.186	1.00	3 CPM, 232 Cycles to B.T.
			295 (72)	FRACTURE	189.6 (27.5)	a = t	31.75 (1.25)	41.5 (37.8)	0.186	1.00						
2WH21-2	5.82 (0.229)	228.6 (9.00)	20 (-423)	LUL	182.7 (26.5)	4.22 (0.166)	30.99 (1.22)	32.1 (29.2)	0.136	0.725	4.52 (0.178)	30.99 (1.22)	34.1 (31.0)	0.146	0.777	
			295 (72)	FRACTURE	163.4 (23.7)	a = t	54.36 (2.14)	42.4 (38.6)	0.107	1.00						
2WH21-3	5.77 (0.227)	228.6 (9.00)	20 (-423)	FRACTURE	241.3 (35.0)	4.37 (0.172)	30.48 (1.20)	45.6 (41.5)	0.143	0.758						B.T. at 209.6 MN/m^2 (30.4 ksi)
4WH21-1	6.05 (0.238)	228.6 (9.00)	"	LUL	212.4 (30.8)	4.42 (0.174)	30.48 (1.20)	38.6 (35.1)	0.145	0.731	4.98 (0.196)	30.48 (1.20)	42.4 (38.6)	0.163	0.824	
			"	CYCLIC	191.7 (27.8)	4.98 (0.190)	30.48 (1.20)	37.7 (34.3)	0.163	0.824						1 CPM, 35 Cycles to B.T. 42 to Fracture

TABLE 43: LIQUID HYDROGEN TEMPERATURE 2219 ALUMINUM WELD METAL TEST RESULTS (t = 9.53 mm (0.375 inch))

SPECIMEN NUMBER	GAGE THICKNESS, t mm (INCH)	GAGE WIDTH, W mm (INCH)	TEST TEMPERATURE °K (°F)	TEST TYPE	STRESS, σ MN/m^2 (KSI)	INITIAL FLAW DEPTH, a_i mm (INCH)	INITIAL FLAW LENGTH, $2c_i$ mm (INCH)	INITIAL STRESS INTENSITY, K_{I_i} $MN/m^{3/2}$ (KSI$\sqrt{IN}$)	$(a/2c)_i$	$(a/t)_i$	FINAL FLAW DEPTH, a_f mm (INCH)	FINAL FLAW LENGTH, $2c_f$ mm (INCH)	FINAL STRESS INTENSITY, K_{I_f} $MN/m^{3/2}$ (KSI$\sqrt{IN}$)	$(a/2C)_f$	$(a/t)_f$	REMARKS
2WH31-1	9.83 (0.387)	355.6 (14.0)	20 (-423)	LUL	203.4 (29.5)	6.40 (0.252)	44.42 (1.74)	41.2 (37.5)	0.145	0.651	6.96 (0.274)	44.42 (1.74)	44.0 (40.0)	0.157	0.708	
			"	CYCLIC	162.7 (23.6)	6.96 (0.274)	44.42 (1.74)	34.3 (31.2)	0.157	0.708	7.42 (0.292)	44.42 (1.74)	36.0 (32.8)	0.168	0.755	3 CPM, 200 Cycles Total
			295 (72)	FRACTURE	204.8 (29.7)	7.42 (0.292)	44.42 (1.74)	50.0 (45.5)	0.168	0.755						
2WH31-2	9.68 (0.381)	355.6 (14.0)	20 (-423)	LUL	182.7 (26.5)	6.35 (0.250)	44.45 (1.75)	36.7 (33.4)	0.143	0.656	6.86 (0.270)	44.45 (1.75)	38.9 (35.4)	0.154	0.709	
			295 (72)	FRACTURE	196.5 (28.5)	8.26 (0.325)	44.45 (1.75)	51.7 (47.0)	0.186	0.853						
4WH31-1	9.55 (0.376)	355.6 (14.0)	20 (-423)	LUL	203.4 (29.5)	6.55 (0.258)	44.20 (1.74)	42.6 (38.8)	0.148	0.686	7.19 (0.283)	44.20 (1.74)	45.9 (41.8)	0.163	0.753	
			"	CYCLIC	182.8 (26.5)	7.19 (0.283)	44.20 (1.74)	40.7 (37.0)	0.163	0.753	8.99 (0.354)	45.21 (1.78)	46.2 (42.0)	0.199	0.941	1 CPM, 100 Cycles Total
			"	FRACTURE	222.7 (32.3)	8.99 (0.354)	45.21 (1.78)	57.8 (52.6)	0.199	0.941						B.T. at 202.4 MN/m^2 (29.4 ksi)
3WH31-1	9.63 (0.379)	355.6 (14.0)	"	FRACTURE	224.8 (32.6)	6.60 (0.260)	44.96 (1.77)	48.2 (43.9)	0.147	0.686						B.T. at 216.5 MN/m^2 (31.4 ksi)

TABLE 44: 2219-T87 ALUMINUM BASE METAL STATIC FRACTURE TEST RESULTS

SPECIMEN NUMBER	TEST TEMP. °K (°F)	GAGE THICKNESS mm (INCH)	FLAW SHAPE a/2c	FRACTURE TOUGHNESS K_{IE} MN/m^2 (KSI $\sqrt{IN}$)	AVERAGE FRACTURE TOUGHNESS K_{IE} MN/m^2 (KSI $\sqrt{IN}$)
3BR21-1	295°K (72°F)	6.35 (0.250)	0.15	50.8 (46.2)	52.1 (47.4)
3BR31-1		9.53 (0.375)	0.15	53.5 (48.7)	
4BR31-1		9.53 (0.375)	0.15	52.1 (47.4)	
3BN21-1	75°K (-320°F)	6.35 (0.250)	0.15	55.9 (50.9)	55.8 (50.8)
3BN21-2		6.35 (0.250)	0.15	58.2 (53.0)	
2BN23-1		6.35 (0.250)	0.30	54.6 (49.7)	
3BN31-1		9.53 (0.375)	0.15	56.2 (51.1)	
3BN31-1		9.53 (0.375)	0.15	56.5 (51.4)	
3BN33-1		9.53 (0.375)	0.30	54.1 (49.2)	
3BN33-2		9.53 (0.375)	0.30	55.5 (50.5)	
2BH11-1	20°K (-423°F)	3.18 (0.125)	0.15	53.0 (48.2)	55.3 (50.3)
2BH11-4		3.18 (0.125)	0.15	54.0 (49.1)	
2BH21-1		6.35 (0.250)	0.15	56.0 (51.0)	
3BH21-1		6.35 (0.250)	0.15	58.3 (53.1)	
4BH31-1		9.53 (0.375)	0.15	55.0 (50.0)	

DISTRIBUTION LIST FOR FINAL REPORTS
NASA CR-135036 and CR-135037

CONTRACT NAS3-18906

	Copies
NASA-Lewis Research Center 21000 Brookpark Road Cleveland, OH 44135	
Attn: Contracting Officer, MS 500-313	1
Technical Report Control Office, MS 5-5	1
Technology Utilization Office, MS 3-16	1
AFSC Liaison Office, MS 501-3	1
Library, MS 60-3	1
R. H. Johns, MS 49-3	1
G. T. Smith, Project Manager, MS 49-3	18
R. H. Kemp, MS 49-3	1
W. F. Brown, MS 105-1	1
J. E. Srawley, MS 105-1	1
J. C. Freche, MS 49-1	1
J. A. Misencik, MS 49-3	1
National Aeronautics and Space Administration Washington, DC 20546	
Attn: RPX/Chief, Liquid Experimental Engineering	1
KT/Technology Utilization Office	1
Library	1
RWS / D.A. Gilstad	1
National Technical Information Service Springfield, VA 22151	16
Attn: NASA Representative, Box 333, College Park, MD 20740	2
NASA-Ames Research Center Moffett Field, CA 94035	
Attn: Library	1
D. Williams	1
NASA-Flight Research Center P.O. Box 273 Edwards, CA 93523	
Attn: Library	1

	Copies
NASA-Goddard Space Flight Center Greenbelt, MD 20771 Attn: Library	 1
NASA-John F. Kennedy Space Center Kennedy Space Center, FL 32931 Attn: Library	 1
NASA-Langley Research Center Hampton, VA 23365 Attn: Library R. W. Leonard H. Hardrath W. Elber	 1 1 1 1
NASA-Manned Spacecraft Center Houston, TX 77001 Attn: Library R. G. Forman, ES-5 S. V. Glorioso, ES-5	 1 1 1
NASA-Marshall Space Flight Center Marshall Space Flight Center, AL 35812 Attn: Library S&E-ASTN/AA/C. Lifer S&E-ASTN/ASR/C. Crockett S&E-ASTN-AS/H. Coldwater	 1 1 1 1
Air Force Office of Scientific Research Washington, DC 20333 Attn: Library	 1
Air Force Rocket Propulsion Laboratory (RPM) Edwards, CA 93523 Attn: Library	 1
Air Force Systems Command Aeronautical Systems Division Wright-Patterson AFB, OH 45433 Attn: Library C. F. Tiffany, Code ENF	 1 1

	Copies
Air Force Systems Command Andrews Air Force Base Washington, DC 20332 Attn: Library	1
Air Force Systems Command Arnold Engineering Development Center Tellahoma, TN 37389 Attn: Library	1
Wright-Patterson Air Force Base Wright-Patterson Air Force Base, OH 45433 Attn: AFML	1
D. M. Forney	1
Wright-Patterson Air Force Base Wright-Patterson Air Force Base, OH 45433 Attn: AFFDL	1
H. A. Wood	1
Frankford Arsenal Philadelphia, PA 19137 Attn: 1320/Library	1
C. Carman	1
Department of the Army U.S. Army Material Command Washington, DC 20315 Attn: AMCRD-RC	1
U.S. Army Missile Command Redstone Scientific Information Center Redstone Arsenal, AL 35808 Attn: Document Section	1
Commanding Officer U.S. Army Research Office (Durham) Box CM, Duke Station Durham, NC 27706 Attn: Library	1
Bureau of Naval Weapons Department of the Navy Washington, DC 20360 Attn: RRRE-6	1

Copies

Commander U.S. Naval Ordnance Laboratory White Oak Silver Springs, MD 20910	
Attn: Library	1
Director, Code 6180 U.S. Naval Research Laboratory Washington, DC 20390	
Attn: Library	1
H. W. Carhart	1
J. M. Krafft	1
Atomic Energy Commission Division of Reactor Development and Technology Washington, DC 20767	1
National Science Foundation Engineering Division 1800 G Street, NW Washington, DC 20540	
Attn: Library	1
Battelle Memorial Institute 505 King Avenue Columbus, OH 43201	
Attn: Library	1
E. Hulbert	1
G. Hahn	1
C. Federson	1
IIT Research Institute Technology Center Chicago, IL 60616	
Attn: Library	1
Stanford Research Institute 3333 Ravenswood Ave. Menlo Park, CA 94025	
Attn: Library	1
Brown University Providence, RI	
Attn: Technical Library	1
J. R. Rice	1

	Copies
Case Western Reserve University 10090 Euclid Ave. Cleveland, OH 44115 Attn: Technical Library	1
Carnegie Institute of Technology Department of Civil Engineering Pittsburgh, PA 15213 Attn: Library	1
Colorado State University Dept. of Mechanical Engineering Ft. Collins, CO 80521 Attn: F. Smith	1
Cornell University Dept. of Materials Science and Engineering Ithaca, NY 14830 Attn: Library	1
Massachusetts Institute of Technology Cambridge, MA Attn: Library	1
Pennsylvania State University State College, PA Attn: Library	1
University of Denver Denver Research Institute P.O. Box 10126 Denver, CO 80210 Attn: Security Office	1
Aerojet Liquid Rocket Company P.O. Box 15847 Sacramento, CA 95813 Attn: Technical Library, 2484-2115A	1

	Copies
Aerospace Corp. 2400 E. El Segundo Blvd. Los Angeles, CA 90045 Attn: Library-Documents	1
Bell Aerosystems, Inc. Box 1 Buffalo, NY 14240 Attn: J. Davis	1
Brunswick Corp. Defense Products Division P.O. Box 4594 43000 Industrial Ave. Lincoln, NE Attn: Library	1
Chrysler Corp. Space Division P.O. Box 29200 New Orleans, LA 70129 Attn: P. Munafo	1
Library	1
Del Research Corp. 427 Main St. Hellertown, PA 18055 Attn: P. Paris	1
Del West Associates, Inc. 6324 Variel Ave. Suite C Woodland Hill, CA 91364 Attn: M. Creager	1
Garrett Corp. Air Research Manufacturing Division 2525 West 190th St. Torrence, CA 90509	1

	Copies
General American Transportation Corp. General American Research Division 7449 N. Natchez Ave. Niles, IL 60648	
Attn: R. N. Johnson	1
General Dynamics P.O. Box 748 Ft. Worth, TX 76101	
Attn: Library	1
C. D. Little	1
Genral Dynamics/Convair Aerospace P.O. Box 1128 San Diego, CA 92112	
Attn: Library	1
J. Jensen	1
W. Witzel	1
J. Haskins	1
General Electric Co. Missiles and Space Systems Center Valley Forge Space Technology Center P.O. Box 8555 Philadelphia, PA 19101	
Attn: Library	1
Grumman Aircraft Engineering Corp. Bethpage, Long Island, NY	
Attn: Library	1
W. Lundwig	1
Jet Propulsion Laboratory 4800 Oak Grove Dr. Pasadena, CA 91103	
Attn: Library	1
J. Lewis	1
Ling-Temco-Vought Corp. P.O. Box 5907 Dallas, TX 75222	
Attn: Library	1

	Copies
Lockheed Missiles and Space Co. P.O. Box 504 Sunnyvale, CA 94087	
Attn: Library	1
R. E. Lewis	1
Martin-Marietta Corp. Denver Division P.O. Box 179 Denver, CO 80201	
Attn: F. Schwartzberg, MS 0430	1
A. Holsten	1
Martin-Marietta Corp. P.O. Box 29304 New Orleans, LA 70189	
Attn: D. Bolstad	1
McDonnell Douglas Aircraft Corp. P.O. Box 516 Lambert Field, MO 63166	
Attn: Library	1
McDonnell Douglas Astronautics Western Division 5301 Bolsa Ave. Huntington Beach, CA 92647	
Attn: Library	1
H. Babel	1
R. Rawe	1
G. Bockrath	1
Northrop Space Laboratories 3401 West Broadway Hawthorne, CA	
Attn: Library	1
North American Rockwell, Inc. Rocketdyne Division 6633 Canoga Ave. Canoga Park, CA 91304	
Attn: Library, Dept. 596-306	1
G. Vorman	1

	Copies
North American Rockwell, Inc. Space and Information Systems Division 12214 Lakewood Blvd. Downey, CA	
Attn: Library	1
J. Colipriest	1
Republic Aviation Fairchild Hiller Corp. Farmington, Long Island, NY	
Attn: Library	1
Thiokol Chemical Corp. Wasatch Division P.O. Box 524 Brigham City, UT 84302	
Attn: Library Section	1
TRW Systems, Inc. One Space Park Redondo Beach, CA 90278	
Attn: Technical Library, Document Acquisition	1
United Aircraft Corp. Corporate Library 400 Main St. East Hartford, CT 06108	
Attn: Library	1
United Aircraft Corp. Pratt and Whitney Division Florida Research and Development Center P.O. Box 2691 West Palm Beach, FL 33402	
Attn: Library	1
Westinghouse Research Laboratories Beulah Rd., Churchhill Borough Pittsburgh, PA 15235	
Attn: Library	1
W. K. Wilson	1
G. T. Wessel	1

	Copies
Aluminum Company of America 1200 Ring Bldg. Washington, DC 20036 Attn: G. B. Bauthold	1

APR 1982 B
B. Ballag E457/2TOE/E14/28408

12 00 6 OCT 1976